Identification and Characterization of Developmental Genes in *Streptomyces*

PROEFSCHRIFT

ter verkrijging van de graad van Doctor
aan de Universiteit Leiden,
op gezag van Rector Magnificus prof. mr. C.J.J.M. Stolker,
voorzitter van het College voor Promoties
in het openbaar te verdedigen op
woensdag 27 mei 2015
klokke 16:15 uur

door
Le Zhang
geboren te Xi'an, China
19 december 1983

PROMOTIECOMMISSIE

Promotor:	Prof. dr. G.P. van Wezel
Overige leden:	Prof. dr. H.P. Spaink
	Prof. dr. J. Brouwer
	Prof. dr. P. Hooykaas
	Dr. P.R. Herron
	Dr. L.W. Hamoen

Nieuwe technologie
mogelijk maken

This research was supported by the Dutch Technology Foundation STW, which is part of the Netherlands Organization for Scientific Research (NWO).

"It's always morning somewhere in the world."

Richard Henry Horne

I

Control of cell division and nucleoid segregation in *Streptomyces*

Le Zhang and Gilles P. van Wezel

THE LIFE CYCLE OF *STREPTOMYCES*

Streptomycetes are Gram-positive mycelial bacteria that belong to the actinobacteria, and are of great importance for the medical and biotechnological industry for their ability to produce many natural products, including antibiotics, anticancer agents and immunosuppressants, as well as industrial enzymes (Hopwood, 2007). The life cycle of *Streptomyces* starts with a single spore that germinates and grows out to form vegetative hyphae, and a process of hyphal growth and branching then results in an intricately branched vegetative mycelium (Chater and Losick, 1997). A prominent feature of the vegetative hyphae of *Streptomyces* is that they grow by tip extension rather than extension of the lateral wall (Flärdh, 2003b). This in contrast to unicellular bacteria like *Bacillus subtilis* and *Escherichia coli*, where cell elongation is achieved by incorporation of new cell-wall material in the lateral wall (Donachie, 1993). Exponential growth of the vegetative hyphae is achieved by a combination of tip growth and branching, rather than by cell fission. The fact that cell division during vegetative growth does not lead to physical cell fission but rather leads to cross walls that separate the hyphae into connected compartments make streptomycetes a rare example of a multicellular bacterium, whereby each compartment contains multiple copies of the chromosome (Claessen *et al.*, 2014). The spacing of the vegetative cross walls varies significantly, both between different *Streptomyces* and within the same species between different growth conditions as well as age of the mycelium.

Under adverse conditions such as nutrient depletion, the vegetative mycelium differentiates to form erected sporogenic structures called aerial hyphae. The production of antibiotics is temporally correlated to this phase of the *Streptomyces* life cycle (Bibb, 2005; van Wezel and McDowall, 2011). Two rounds of programmed cell death (PCD) occur during the *Streptomyces* life cycle (Manteca *et al.*, 2011). After spore germination, a compartmentalized mycelium grows and then undergoes a first round of PCD, formed during early vegetative growth, followed by a second round of PCD that is initiated during the onset of development (Manteca *et al.*, 2005). At this stage, the vegetative or substrate hyphae are lysed, so as to provide nutrients for the next round of biomass formation, *i.e.* growth of the aerial mycelium. The aerial hyphae give the colonies their characteristic white and fluffy appearance and the aerial hyphae eventually differentiate to form chains of unigenomic spores (Flärdh and Buttner, 2009). Genes that are required for the formation of aerial hyphae are referred to as *bld*, referring to the bald ('hairless') phenotype of the mutants lacking the fluffy aerial hyphae (Merrick, 1976), while mutants that

are blocked at a stage prior to sporulation are called *whi* (white), due to their failure to produce the grey spore pigment (Chater, 1972).

Aerial hyphae differ substantially from vegetative hyphae. One major difference is that aerial hyphae of wild-type cells do not branch, are nearly twice as wide as vegetative hyphae and undergo rapid growth and concomitant chromosome replication. The process of cell division is also completely different: while cross walls divide the vegetative hyphae into multi-genomic compartments, during sporulation-specific cell division in aerial hyphae many septa are formed nearly simultaneously, followed by formation of spore compartments and cell fission, which then results in chains of spores that each contain a single copy of the chromosome (discussed below). Whereas the process of chromosome segregation and cell division in aerial hyphae involves similar machinery as found in other bacteria, in particular the control of sporulation requires *Streptomyces*-specific mechanisms, including the Whi regulatory proteins and the SsgA-like proteins.

CELL DIVISION IN *STREPTOMYCES*

Many of the genes involved in cell division were first identified by the isolation of conditional mutations in unicellular bacteria such as *E. coli* or *B. subtilis* causing the formation of long filamentous cells devoid of division septa at a non-permissive temperature. For this reason many of the division genes were termed *fts*, for filamentous temperature-sensitive phenotype (Van De Putte *et al.*, 1964). FtsZ is the key cell division protein in virtually all bacteria and many eukaryotic organelles. FtsZ is highly similar to eukaryotic tubulins, both with regard to protein structure and biochemistry, and forms a cytokinetic ring at the division site, generally referred to as the Z ring (Bi and Lutkenhaus, 1991; de Boer *et al.*, 1992; Erickson, 1995). The Z-ring then mediates the recruitment of the other components of the cell-division machinery, thus forming the so-called divisome, a contractile ring that divides the cells (de Boer, 2010; Margolin, 2005; Errington *et al.*, 2003).

The study of cell division in streptomycetes is particularly interesting for several reasons. As mentioned above, the switch from vegetative to aerial division is a crucial step in the developmental pathway leading to sporulation. A landmark discovery was that *ftsZ* null mutants of *S. coelicolor* were viable (McCormick *et al.*, 1994). With that, *S. coelicolor* is so far the only organism that can grow after *ftsZ* has been deleted. Consistent with a central role of FtsZ in cell division, the null mutant did not form any detectable septa. Interestingly,

the fact that *ftsZ* null mutants can still grow exponentially and form a mycelium means that FtsZ and cell division are not required for hyphal branching (McCormick *et al.*, 1994). The small membrane protein FtsQ, which is encoded by a gene immediately upstream of *ftsZ*, is also required for cell division and viability in most bacteria, although its precise function is still not clear. In *S. coelicolor*, *ftsQ* is not absolutely required for septation, but cross-wall formation is reduced by some 95%, producing few cross walls in the vegetative hyphae (McCormick and Losick, 1996). This gave rise to a similar but somewhat less severe phenotype than that of *ftsZ* null mutants, with small colonies that failed to develop, and overproduction of the blue-pigmented antibiotic actinorhodin. Interestingly, suppressors of *ftsQ* null mutants could be isolated, which showed partially restored sporulation septation. However, these suppressor mutations had no clear effects on cell division in cells harboring *ftsQ* and the basis for suppression remains unclear (Bennett and McCormick, 2001). Besides *ftsZ* and *ftsQ*, other cell division genes are also dispensable for growth, and null mutants have been made for among others *divIC, ftsL* (Bennett *et al.*, 2007), *ftsI, ftsW* (Bennett *et al.*, 2009; Mistry *et al.*, 2008), and *ftsE* and *ftsX* (McCormick, 2009; Noens, 2007).

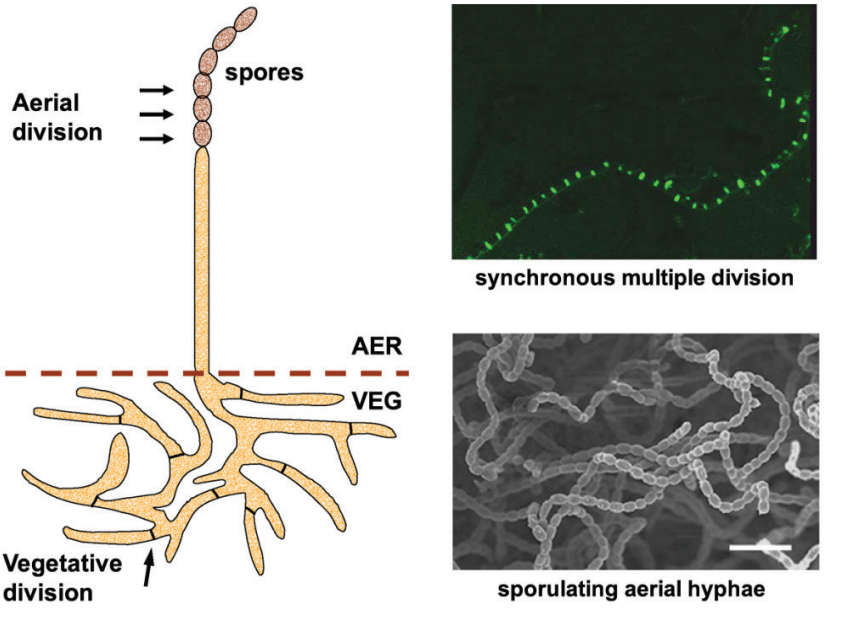

Figure 1. Unique aspects of multiple cell division of streptomycetes. **Left,** schematic drawing of the life cycle with two types of cell division; **Right,** multiple cell division (FtsZ-GFP reveals septa, top) and spores (cryo-scanning electron microscopy; bottom). Bar=5 μm.

Importantly, while *ftsZ* null mutants are completely devoid of septa, deletion of other cell division genes primarily affects sporulation-specific cell division, with normal cross walls produced by mutants lacking *e.g. ftsW* or *ftsI* (Mistry *et al.*, 2008) or the *ssgB* gene that is required for recruitment of FtsZ during sporulation-specific cell division ((Willemse *et al.*, 2011); see below). This means that while FtsZ is required for cross-wall formation, the other divisome components are not. Perhaps this can be explained by the physical differences between the two modes of cell division: the bacterial divisome is directed at cell fission, with activation of Z-ring contraction, while such Z-ring contraction is in fact undesirable during cross-wall formation.

Features of cell division that are unique to streptomycetes, like the dispensability of cell division for growth and the striking developmental phenotypes, make them useful model organisms for analysis of fundamental properties of the bacterial cell division machinery and how it can be regulated. From a biotechnological perspective, improved understanding of how cell division can be manipulated, and how it relates to growth and branching, may also be useful from the perspective of engineering new production strains with altered morphological properties, to circumvent some of the growth-related problems.

NUCLEOID REPLICATION

Bacterial development requires accurate scheduling of the expression of different sets of genes for among others metabolism, morphogenesis, cell division and DNA replication. Chromosome replication needs to be synchronized with cytokinesis to guarantee that each daughter cell obtains a copy of the chromosome. The initiation of chromosome replication is tightly controlled with the life cycle. In bacteria, chromosome replication starts with binding of DnaA (*trans*-acting element) to DnaA boxes (*cis*-regulatory element) in the *oriC* region (Fuller *et al.*, 1984; Kaguni, 2006; Katayama *et al.*, 2010; Leonard and Grimwade, 2010). Streptomycetes have a large linear and GC-rich chromosome and the *oriC* region has 19 DnaA boxes instead of the five found in *E. coli* (Majka *et al.*, 1999; Majka *et al.*, 2001; Jakimowicz *et al.*, 1998). The spacing, orientation and position of these 19 DnaA boxes are conserved among *Streptomyces* spp (Wolański *et al.*, 2014). In contrast to DnaA of *E. coli*, the DnaA protein-mediated unwinding of *Streptomyces oriC* has not been detected (Jakimowicz *et al.*, 1998), perhaps due to the absence of an AT-rich region within the *oriC* region (Jakimowicz *et al.*, 1998).

To make sure that chromosome replication only occur once per cell cycle, the availability and activity of both *oriC* region and DnaA need to be tightly controlled. ATP hydrolysis is the most common strategy to inactivate ATP-DnaA (the active form of DnaA) (Zakrzewska-Czerwińska *et al*., 2007). However, titration of DnaA by positioning clusters of DnaA boxes outside the *oriC* region is another widely occurring phenomenon to control the initiation of chromosome replication (Zakrzewska-Czerwińska *et al.*, 2007). Additional levels of control occur, and in *Streptomyces* the A-factor responsive regulator AdpA, a key transcription regulator of development and antibiotic production in this organism, directly binds to the *oriC* region to decrease the accessibility of the DnaA boxes, consequently inhibiting chromosome replication (Wolánski *et al.*, 2011a; Wolánski *et al.*, 2012; Ohnishi *et al*., 2005). This is a typical example of how in the bacterial life cycle, additional regulatory networks are in place to coordinate chromosome replication with other key developmental processes.

In *Streptomyces* hyphal compartments, multiple chromosomes remain uncondensed until the final stages of sporulation, and replication in both vegetative and aerial hyphae seems asynchronous (Ruban-Ośmiałowska *et al.*, 2006). Little is known of DNA segregation during normal growth, but replicating chromosomes follow the growing hyphal tip (Wolánski *et al.*, 2011b). ParA and ParB protein likely play a role in the control of chromosome replication. Indeed, ParA directly affects DnaA function in *B. subtilis* (Murray and Errington, 2008; Scholefield *et al.*, 2012). It is yet unclear if similar interactions occur in *Streptomyces*.

NUCLEOID SEGREGATION AND CONDENSATION

One of the earliest hypotheses of chromosome segregation was proposed in 1963 by François Jacob and co-workers (Jacob *et al.*, 1963). They proposed that the newly replicated *oriC* regions attached to the cytoplasmic membrane, whereby growth and elongation of the cell would cause separation of the sister chromosomes. However, cell elongation in rod-shaped bacteria happens in a cell-cylinder pattern, not restricted to midcell (Scheffers and Pinho, 2005). Additionally, the *ori* moves at a speed of 0.1-0.3 μm/min while the rate of cell elongation is much slower (Fiebig *et al.*, 2006; Viollier *et al.*, 2004; Webb *et al.*, 1998; Misra *et al.*, 2013). This suggests that the elegant and simple model originally proposed by Jacob may not reflect the real situation.

Indeed, a dynamic *oriC* partitioning system was identified, called the Par

system (Abeles *et al.*, 1985). This system is widely distributed, since over 70% of all bacteria contain *par* loci on their genomes (Livny *et al.*, 2007). Par includes the ParA and ParB proteins, and the *cis*-acting centromere-like site(s) *parS* sites. In *S. coelicolor*, *parA* and *parB* form an operon and in total 24 *parS* sites were found in the region near *oriC* (Jakimowicz *et al.*, 2002). ParB specifically recognizes *parS* sites, and ParA is a Walker-type ATPase, which likely provides the energy required for ParB-mediated chromosome segregation (Jakimowicz *et al.*, 2005; Jakimowicz *et al.*, 2002; Leonard *et al.*, 2005a; Leonard *et al.*, 2005b). Surprisingly, deletion of *parAB* does not cause major defects in chromosome segregation during vegetative growth of *Streptomyces*, which may be explained by the fact that the large multinucleoid hyphal compartments contain many non-segregated chromosomes (Jakimowicz *et al.*, 2005). However, in the absence of *parAB*, aberrant chromosome segregation was observed in the spores (Dedrick *et al.*, 2009; Jakimowicz *et al.*, 2005). Unlike in rod-shaped bacteria, where ParB drives origin regions to the poles of the dividing cell, in *Streptomyces* ParB complexes align the chromosomes regularly along the aerial hyphae to ensure that each of the many prespore compartments receives a single copy of the chromosome (Jakimowicz *et al.*, 2005; Jakimowicz and van Wezel, 2012; Dedrick *et al.*, 2009).

Another protein that plays a major role in chromosome segregation is FtsK (Wang *et al.*, 2007). In *E. coli* and *B. subtilis*, FtsK (SpoIIIE in *Bacillus*) function as a DNA translocase, transporting the chromosome through the closing septum to the daughter cells (Bigot *et al.*, 2005; Yu *et al.*, 1998; Burton *et al.*, 2007). In *B. subtilis*, SpoIIIE is required for sporulation (Burton *et al.*, 2007; Fleming *et al.*, 2010). Deletion of *ftsK* in *S. coelicolor* did not cause a major sporulation defect, but rather resulted in reduction of genetic stability (Wang *et al.*, 2007). Progeny spores of the *ftsK* mutant frequently lost larger parts of the chromosome, predominantly close to the chromosomal ends (Wang *et al.*, 2007).

Noncondensed bacterial chromosomes would occupy much more space than the volume of bacterial cell itself (Trun and Marko, 1998) and therefore the chromosome must be tightly compacted. SMC (for structural maintenance of chromosome) proteins are widely distributed from prokaryotes to eukaryotes, and function as condensins or cohesins for dynamic chromatin organization (Graumann, 2001; Strunnikov, 2006; Hirano, 2006; Hirano, 2002). As in other bacteria, SMC in *Streptomyces* is also involved in chromosome condensation and segregation (Dedrick *et al.*, 2009; Kois *et al.*, 2009). Besides SMC, several other proteins were found to be involved in chromosome condensation in bacteria. These include sIHF (integration host factor), which

plays an important role in site-specific recombination, DNA replication, transcription and genome organization (Goosen and Putte, 1995), Fis (factor for inversion stimulation), which trans-activates among others the transcription of stable RNA operons (Nilsson *et al.*, 1990); the histone-like protein HU and H-NS, which are antagonists of each other and play implementing roles in DNA structure, site-specific recombination and global control of gene expression (Dame, 2005; Murphy and Zimmerman, 1997; Varshavsky *et al.*, 1977; Johnson *et al.*, 1986; Drlica and Rouviere-Yaniv, 1987; Anuchin *et al.*, 2011); and Dps proteins (for DNA-binding proteins from starved cells), which function to protect DNA from oxidative damage and are involved in DNA condensation (Ceci *et al.*, 2004; Grant *et al.*, 1998; Wolf *et al.*, 1999; Chiancone and Ceci, 2010). *Streptomyces* have two HU-like proteins, HupA and HupS. HupA is the conventional HU protein and binds to ssDNA, affecting growth of *Streptomyces* in submerged culture with an unknown mechanism (Yokoyama *et al.*, 2001). HupS is an actinomycete-specific HU protein, involved in spore maturation by affecting chromosome condensation, while deletion of *hupS* led to an increase in the nucleoid size within the spores (Salerno *et al.*, 2009). Three IHF homologs occur in streptomycetes. One of these, sIHF, belongs to an actinomycete-specific type of IHF proteins that was first identified in mycobacteria (Pedulla and Hatfull, 1998; Pedulla *et al.*, 1996). *S. coelicolor sihf* mutants have strongly reduced viability, which may be explained by defective DNA segregation during sporulation (Yang *et al.*, 2012). Chromosome condensation is controlled by Dps-like nucleoid-associated proteins, which control nucleoid structure during stationary phase in bacteria and form large nucleoprotein complexes with the DNA (Nair and Finkel, 2004). In *Streptomyces*, DpsA and DpsC affect spore nucleoids and positioning of the sporulation septa (Facey *et al.*, 2009), and are thus actinomycete-specific architectural proteins that control organization of the nucleoid.

DIVISION SITE SELECTION

In rod-shaped bacteria, the positioning and timing of cell division assembly are negatively controlled by two distinct systems, controlled by the Min and Noc systems (Adams and Errington, 2009; Harry *et al.*, 2006; Barák and Wilkinson, 2007; Wu and Errington, 2012). The Min proteins prevent cell division away from the midcell position by inhibiting FtsZ polymerization near the cell poles (Barák and Wilkinson, 2007; Lutkenhaus, 2007; Bramkamp and van Baarle, 2009). MinC, the FtsZ polymerization inhibitor, forms a complex with the membrane-associated ATPase MinD. In *E. coli* this block of cell di-

vision is suppressed by the action of MinE, which oscillates from pole to pole (Hale *et al.*, 2001). As a result, MinE localization is biased towards midcell so as to allow FtsZ polymerization (Hale *et al.*, 2001). By contrast, in *B. subtilis*, the MinCD complex is recruited to the cell poles by DivIVA, the ortholog of MinE (Marston *et al.*, 1998; Marston and Errington, 1999). The second system is nucleoid occlusion, which inhibits septum formation over non-segregated chromosomes; this process is governed by Noc in *B. subtilis* and by SlmA in *E. coli* (Wu and Errington, 2004; Bernhardt and de Boer, 2005). SlmA inhibits cell division via affecting FtsZ polymerization or its higher-ordered assembly (Cho *et al.*, 2011; Tonthat *et al.*, 2011), while the precise mechanism by which Noc functions is still unclear (Wu and Errington, 2012). Once FtsZ is directed to midcell, Z-ring assembly and tethering to the membrane depends on specific membrane proteins. Z-ring assembly, attachment and stabilization is mediated by a number of proteins including FtsA and ZipA (RayChaudhuri, 1999; Hale and de Boer, 1997; Pichoff and Lutkenhaus, 2002), ZapA (Gueiros-Filho and Losick, 2002)and SepF (Ishikawa *et al.*, 2006; Hamoen *et al.*, 2006). Though deletion of *sepF* alone had a mild phenotype, *sepF* became essential in the absence of *ftsA*, and overexpression of SepF could restore cell division to an *ftsA* null mutant (Ishikawa *et al.*, 2006).

The cell division machinery itself is generally well conserved in streptomycetes, but the control of division-site selection and FtsZ recruitment in the long and multinucleoid hyphae is entirely different. No direct homologs of MinC occur in *Streptomyces*, and two distant relatives of *minD* do not play a role in the control of cell division but instead are likely components of a tight adhesion system (Jakimowicz and van Wezel, 2012). DivIVA is present in *Streptomyces*, but instead of playing a role in the control of cell division, the protein is required to drive tip growth, and is therefore essential for viability (Flärdh, 2003a). In terms of nucleoid occlusion, no homologs of either Noc or SlmA are found in *Streptomyces*. And finally, of all the proteins that are involved in Z-ring assembly and stabilization, only SepF is present in *Streptomyces* (see Chapter III). This raises the question as to division site selection is controlled in *Streptomyces* in the absence of the canonical control systems.

Streptomyces have a mycelial life cycle and grow as long hyphae instead of single cells, and these hyphae by definition lack a defined midcell position. This likely explains the absence of control systems such as Min and Noc and the requirement of a different way of cell division control. Instead, actinomycete-specific protein families have been identified that play a role in the control of cell division, and in particular the CrgA family and SsgA family proteins are relevant for the control of cell division. CrgA-like proteins are a

family of small membrane integral proteins, also thought to be part of time control system via inhibiting FtsZ-ring formation during development (Del Sol *et al.*, 2006). Deletion of *crgA* caused notable increase of Z-ring formation (Del Sol *et al.*, 2006). However, CrgA also occurs in nonsporulating actinomycetes, and in mycobacteria the protein is a divisome component that interacts with the cell division proteins FtsZ, FtsI and FtsQ (Plocinski *et al.*, 2011). The precise role of CrgA is unknown.

The SsgA-like proteins are a family of proteins that control sporulation of actinomycetes, with seven paralogs occurring in *S. coelicolor* (Traag and van Wezel, 2008; Jakimowicz and van Wezel, 2012). SsgA was originally identified as a suppressor of a hyper-sporulating *S. griseus* mutant (designated SY1) and was shown to be essential for submerged sporulation (Kawamoto and Ensign, 1995; Kawamoto *et al.*, 1997). Over-expression of *S. griseus* SsgA in liquid-grown mycelium of *S. coelicolor* induced mycelial fragmentation and spore formation (van Wezel *et al.*, 2000b). There is a suggestive correlation between the number of SALPs in an actinomycete and the complexity of sporulation. Indeed, species producing single spores (*e.g. Micromonospora, Salinispora*) typically have a single SALP, those producing short spore chains (*e.g. Saccharopolyspora*) typically have two SALPs and those forming spore chains (*Streptomyces*) or sporangia (*Frankia*) have multiple SALPs (Girard *et al.*, 2013; Traag and van Wezel, 2008). Members of the SALP family of proteins are on average 130-145 aa long, with 30-50% aa identity between the different family members. SsgB is most likely the archetypal SALP, because if a single SALP is present in an actinomycete, it is invariably SsgB based on gene synteny evidence. Its crystal structure was resolved and revealed a bell-shaped trimer with strong similarity to mitochondrial guide RNA-binding proteins, although direct nucleic-acid binding by SALPs is unlikely, based on structural and experimental data (Xu *et al.*, 2009).

Of the SALPs, SsgA, SsgB and SsgG control the selection of sites of septation in *S. coelicolor*. On solid media, *ssgA* null mutants display a conditional "white" (non-sporulating) phenotype, producing spores on agar-based media containing mannitol as the sole carbon source, but not in the presence of glucose (van Wezel *et al.*, 2000b; Jiang and Kendrick, 2000). Although many early developmental (*bld*) mutants are carbon-source dependent (Merrick, 1976; Pope *et al.*, 1996), such dependence is rare among *whi* mutants. *ssgB* is required for sporulation under all growth conditions (Keijser *et al.*, 2003; Sevcikova and Kormanec, 2003; van Wezel *et al.*, 2000b), while in *ssgG* mutants septa are frequently skipped, resulting in large spores containing multiple chromosomes that are well segregated (Noens *et al.*, 2005).

SsgA and SsgB together control the process of septum-site localization during sporulation-specific cell division. SsgB is required for recruiting FtsZ to septum sites during the onset of sporulation-specific cell division (Willemse *et al.*, 2011). In turn, SsgA dynamically controls the localization SsgB. SsgB is a member of the divisome, where it colocalizes with FtsZ during the entire process of sporulation-specific cell division (Willemse *et al.*, 2011). However, at a time prior to the onset of sporulation-specific cell division, when FtsZ is not yet localized, SsgB forms foci at septum sites and only later does FtsZ localize specifically to the same sites as SsgB. *Förster* resonance energy transfer combined with fluorescence lifetime imaging (FRET-FLIM) revealed that SsgB directly recruits FtsZ (Willemse *et al.*, 2011). This rare example of positive control of cell division by SsgB in an SsgA-dependent manner, explains the importance of SsgAB for sporulation. SsgB also actively stimulates the polymerization of FtsZ protofilaments (Willemse *et al.*, 2011). The mode of action of SsgB is similar to that of ZipA, which also stimulates the formation of filament networks (RayChaudhuri, 1999).

One major question to be answered is how SsgB itself is localized. Also, SsgA and SsgB lack a membrane binding domain, so it is logical to propose that an additional membrane component exists that tethers the SsgB-FtsZ complex to the membrane. As shown in this thesis, a major candidate is SepG which lies close to *ftsZ* on the genome of firmicutes and actinobacteria.

OUTLINE OF THE THESIS

Many of the genes involved in cell division and cell-wall synthesis are located in the *dcw* (division and cell wall biosynthesis) cluster (Fig. 2). The gene order and many of the components of the *dcw* cluster are quite well conserved in different bacteria, whereby the genes can be classified into those encoding components of the divisome and those that encode cell-wall biosynthetic enzymes (Mur complex) (Mingorance *et al.*, 2004; Tamames *et al.*, 2001). Several of the genes in the *dcw* cluster in Gram-positive bacteria still have unknown functions, despite their location in-between the pivotal genes *divIVA* (SCO2077) and *ftsZ* (SCO2082). These are in particular *ylmD* and *ylmE* which are in operon with *ftsZ*, and *sepG*, which lies between *sepF* and *divIVA*. Considering this location, important roles in (the control of) cell division or cell-wall synthesis were anticipated.

SepG is studied in **Chapter II**, where we show that this membrane protein likely acts as the missing membrane anchor for SsgB, to allow the protein to dock to future septum sites. In the absence of *sepG*, SsgB fails to remain at the

future septum sites and thus Z-ring formation is prohibited. This suggests that SepG tethers SsgB to division sites, followed by the recruitment of FtsZ by SsgB to initiate sporulation-specific cell division.

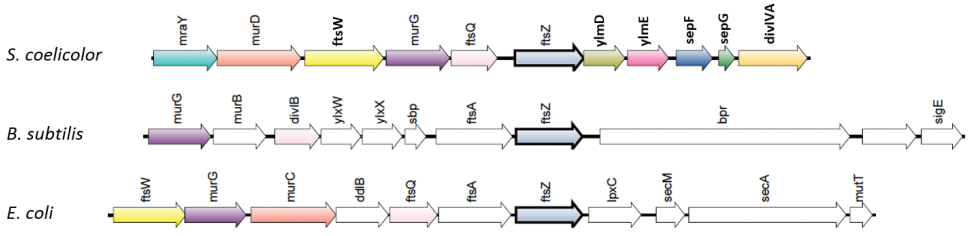

Figure 2. Organizations of part of *dcw* gene cluster of *Streptomyces coelicolor*, *Bacillus subtilis* and *Escherichia coli*. These gene maps were generated by SyntTax (Oberto, 2013). Genes *ylmD*, *ylmE*, *sepF*, *sepG* of *Streptomyces* were renamed according to the nomenclature used in the thesis.

Two SepF-like proteins, SflA and SflB, were shown to relate to branching of aerial hyphae and attachment of *Streptomyces* colonies to solid surfaces **(Chapter III)**. SflA and SflB are paralogs of the cell division protein SepF. Deletion of *sflA* and/or *sflB* led to a 'fluffy' colony phenotype likely due to more extensive branching of the (aerial) hyphae, which was confirmed by high resolution imaging (by electron microscopy), while over-expression of these genes led to reduced adherence to the agar surface.

The *ylmD* and *ylmE* genes, which are downstream of and in the same operon with *ftsZ*, play important roles in septum synthesis (**Chapter IV**). Deletion of *ylmD* or *ylmE* led to mis-placement of cell-wall material and membrane during sporulation, but had no apparent effect on vegetative growth. The pentapeptide bridge that connects the peptidoglycan strands contains two consecutive D-alanine (D-Ala) residues at the end, and a correlation was found between YlmE and the intracellular D-Ala pool.

Another cluster of cell division-related genes is studied in **Chapter V**. *lcmA* was discovered after sequencing and SNP analysis of a mutant of *S. griseus* SY1, which is a hyper-fragmenting strain in submerged culture that has enhanced levels of the cell division activator SsgA (Kawamoto and Ensign, 1995). The seventh codon of *lcmA* was changed to a stop codon, and work in this thesis shows that Lcm proteins are membrane proteins that localize to the septum during sporulation, and are required for correct sporulation and spore wall integrity.

Sequencing and SNP analysis of another spontaneous mutant, in this case nonsporulating mutant AFN of *Streptomyces griseus*, revealed a mutation in the *afsR* gene (**Chapter VI)**. The mutation changed codon 881 to a stop codon, leading to the synthesis of a truncated AfsR protein. While we failed to not find conclusive evidence that this mutation alone caused the AFN phenotype, the expression level of AfsR affected *S. griseus* development. Introducing of extra copies of *afsR* or truncated *afsR** increased streptomycin production and enlarged colony size.

The data and their implications for the control of sporulation and cell division of *Streptomyces* are discussed and summarized in **Chapter VII**.

II

SepG acts as a membrane anchor for SsgB to allow recruitment of FtsZ to division sites in *Streptomyces coelicolor*

Le Zhang, Joost Willemse, Dennis Claessen and Gilles P. van Wezel

Submitted for publication

ABSTRACT

In bacteria that divide by binary fission, a single septum is formed at midcell. Landmark events are the localization of the cell-division scaffold protein FtsZ, and the timely segregation of the nucleoids. Here we show that SepG acts as membrane anchor for SsgB, which is a determining step for the recruitment of FtsZ in *Streptomyces*. FRET imaging revealed direct interaction between SepG and SsgB. Without SepG, SsgB briefly localizes in foci but then rapidly disperses along the membrane, consistent with SepG anchoring the SsgB-FtsZ complex. While SsgB remains associated with FtsZ, SepG re-localizes to sites of active spore-wall synthesis. Expanded doughnut-shaped nucleoids are formed in *sepG* null mutants, suggesting that SepG acts to prevent DNA damage during spore-wall synthesis. Thus, our data provide the first insights into the function of *sepG*, which is one of the last genes in the *dcw* cluster of Gram-positive bacteria whose function was still unresolved.

INTRODUCTION

Most unicellular bacteria grow and divide by binary fission, which involves an increase in cell length, chromosome replication and segregation and septum formation, eventually resulting in two daughter cells that each inherits a single copy of the chromosome. Chromosome organization and segregation are tightly coordinated with the spatial and temporal initiation of cell division. The prokaryotic cell division scaffold is formed by the tubulin homolog FtsZ (Bi and Lutkenhaus, 1991), which forms a contractile ring (or Z ring) that mediates recruitment of the cell division machinery to the mid-cell position (reviewed (Goehring and Beckwith, 2005; Adams and Errington, 2009)). In unicellular bacteria, septum-site localization and Z-ring stabilization is mediated by a number of proteins including FtsA and ZipA (Hale and de Boer, 1997; RayChaudhuri, 1999; Pichoff and Lutkenhaus, 2002), ZapA (Gueiros-Filho and Losick, 2002) and SepF (Hamoen *et al.*, 2006; Ishikawa *et al.*, 2006). The process of Z-ring (dis-)assembly during division is actively controlled (reviewed in (Romberg and Levin, 2003)).

Streptomycetes are filamentous Gram-positive soil bacteria that have a complex multicellular life cycle (Claessen *et al.*, 2014; Flärdh and Buttner, 2009) and produce over 60% of all known antibiotics and many other bioactive natural products (Hopwood, 2007). Expression of these natural products is typically coordinated with the onset of spore development (van Wezel and McDowall, 2011). The vegetative mycelium consists of syncytial cells separated by widely spaced crosswalls (Wildermuth and Hopwood, 1970). During sporulation-specific cell division, FtsZ initially assembles in long filaments in the aerial hyphae, then as regular foci, to finally form a ladder of Z rings (Schwedock *et al.*, 1997). Eventually, cytokinesis results in long chains of spores, following a complex process of coordinated cell division and DNA segregation (Jakimowicz and van Wezel, 2012; McCormick and Losick, 1996)). Cell division is not essential for growth of *Streptomyces*, which provides a unique system for the study of this process (McCormick *et al.*, 1994; McCormick and Losick, 1996).

The mycelial life style of streptomycetes imposes specific requirements for cell division control, in particular due to the lack of a defined midcell position and the synchronous formation of multiple septa. The canonical model for the control of Z-ring formation involves the action of negative control systems such as Min, which prevents Z-ring assembly at the cell poles (Marston *et al.*, 1998; Raskin and de Boer, 1997), and nucleoid occlusion that prevents formation of the Z ring over non-segregated chromosomes (Bernhardt and

de Boer, 2005; Woldringh *et al.*, 1991; Wu and Errington, 2004; Wu and Errington, 2012). However, in *Streptomyces* septum-site localization is positively controlled, via the recruitment of FtsZ by SsgB, which in turn depends on the action of SsgA (Willemse *et al.*, 2011). The SsgA-like proteins (SALPs) are proteins that uniquely occur in actinomycetes (Girard *et al.*, 2013). This different mode of division control most likely explains the absence of direct homologs of Min and Noc proteins and of the canonical Z-ring anchoring proteins. SepF and DivIVA are rare examples of cell division control proteins shared between *Streptomyces* and other bacteria, and of these, DivIVA is not involved in the control of division, but is instead required for driving apical (tip) extension and growth (Flärdh, 2003a). The concept of positive control of cell division is more widespread in bacteria, as it was also found in *Myxococcus xanthus* where the ParA-like protein PomZ recruits FtsZ (Treuner-Lange *et al.*, 2013), while the recent discovery that *Bacillus* cells divide at midcell in the absence of Min and Noc may be explained by a positive control-like mechanism, although there the mechanism of septum positioning is unknown (Rodrigues and Harry, 2012).

With the recruitment of FtsZ by SsgB, another important question is left unaddressed, namely how the highly symmetrical spacing between the sporulation septa is achieved; in other words, how is the localization of SsgB itself orchestrated? We previously suggested that the regularly spaced nucleoids might provide the boundaries for Z-ring assembly, in analogy with a nucleoid-occlusion mechanism (Willemse *et al.*, 2011). One possible candidate is the conserved *ylmG* gene, which lies between *sepF* and *divIVA* in the *dcw* cluster (division and cell-wall synthesis), in particular in actinobacteria, firmicutes and cyanobacteria, as well as in chloroplasts of photosynthetic eukaryotes. The YlmG ortholog AtYLMG1-1 of the plant *Arabidopsis thaliana* is a membrane protein that controls nucleoid morphology (Kabeya *et al.*, 2010). Knock-down of the gene via expression of an anti-sense RNA impaired nucleoid partitioning and changed the morphology of nucleoids in *A. thaliana*. Similar results were obtained in the cyanobacterium *Synechococcus elongates* (Kabeya *et al.*, 2010). However, deletion of *ylmG* in *Streptococcus* did not result in any noticeable defects in cell division or nucleoid segregation (Marbouty *et al.*, 2009).

In this work, we show that after the initial localization of SsgB by SsgA at a central location in the hyphae, YlmG is required for the subsequent membrane anchoring of SsgB and consequentially also for the recruitment of FtsZ. The protein was therefore renamed SepG. The SepG protein localizes to the periphery of the future spore compartments, where it contributes to main-

tenance of chromosome compaction. In the absence of SepG, the nucleoid expands to the outer limits of the spore compartments, compromising septum synthesis. Taken together, our data provide the first insights into the function of SepG that is well conserved in Gram-positive bacteria, and show that SepG is required for positive control of cell division as well as for nucleoid morphogenesis in *Streptomyces*.

MATERIALS AND METHODS

Bacterial strains and media

The bacterial strains used in this work are listed in Table 1. *E. coli* strains JM109 (Sambrook *et al.*, 1989) and ET12567 (MacNeil *et al.*, 1992) were used for routine cloning and for isolation of non-methylated DNA, respectively. *E. coli* transformants were selected on LB agar media containing the relevant antibiotics and grown O/N at 37°C. *Streptomyces coelicolor* A3(2) M145 was used as parental strain to construct mutants. All media and routine *Streptomyces* techniques are described in the *Streptomyces* manual (Kieser *et al.*, 2000). Yeast extract-malt extract (YEME) and tryptone soy broth with 10% sucrose (TSBS) were the liquid media for standard cultivation. Regeneration agar with yeast extract (R2YE) was used for regeneration of protoplasts and with appropriate antibiotics for selection of recombinants (Kieser *et al.*, 2000). Soy flour mannitol (SFM) agar plates were used to grow *Streptomyces* strains for preparing spore suspensions and for morphological characterization and microscopy.

Table 1. Bacterial strains.

Bacterial strains	Genotype	Reference
E. coli JM109	See reference	(Sambrook *et al.*, 1989)
E. coli ET12567	See reference	(MacNeil *et al.*, 1992)
M145	*S. coelicolor* A3(2) SCP1- SCP2-	(Kieser *et al.*, 2000)
K202	M145 + KF41	(Grantcharova *et al.*, 2005)
JSC2	FM145 + genomic ssgB-egfp fusion + pGWS523	(Willemse *et al.*, 2011)
JSC3	FM145 + genomic SsgB-mCherry fusion + pKF41	(Willemse *et al.*, 2011)
GAL1	M145Δ*ylmG*	This work
GAL2	M145 + pGWS755	This work
GAL3	GAL1 + KF41	This work
GAL4	GAL1 + pGWS116	This work
GAL5	GAL1 + pGWS526	This work
GAL7	GAL1 + pGWS755	This work
GSA3	M145Δ*ssgA*(::*aadA*)	(van Wezel *et al.*, 2000b)
GSB1	M145Δ*ssgB*(::*aac(3)IV*)	(Keijser *et al.*, 2003)
GAL93	GAL1 + pGWS771	This work
GAL94	M145 + pGWS791 + pGWS116	This work
GAL95	M145 + pGWS791 + pGWS526	This work
GAL96	M145 + pGWS755 + pGWS529	This work

Plasmids and constructs

All plasmids and constructs described in this work are summarized in Table 2 and oligonucleotides are listed in Table 3. PCRs were carried out with Phusion enzyme (Finnzymes, Bioké, Leiden, the Netherlands) as previously described (Colson *et al.*, 2007).

Table 2. Plasmids and constructs.

Plasmid and constructs	Description	Reference
pWHM3	*E. coli*/*Streptomyces* shuttle vector, around 100 copies per chromosome in both *E. coli* and *Streptomyces*.	(Vara *et al.*, 1989)
pGWS725	pWHM3 with deleted XbaI site from multiple cloning sites region.	This work
pSET152	*E. coli*/*Streptomyces* shuttle vector, around 100 copies per chromosome in *E. coli* and integrative in the φC31 attachment site in *Streptomyces*	(Bierman *et al.*, 1992)
pGWS523	FtsZ-mCherry from its native promoter in pSET152-derivative vector, containing the neomycin resistance cassette	(Willemse et al., 2011)
pHJL401	*E. coli*/*Streptomyces* shuttle vector, around five per chromosome copies in *Streptomyces* and around 100 copies per chromosome in *E. coli*	(Larson and Hershberger, 1986)
pGWS731	pWHM3 containing flanking regions of *S. coelicolor* SCO2078 with apra-*loxP* inserted in between	This work
pUWL-Cre	Plasmid expressing Cre-recombinase	(Fedoryshyn *et al.*, 2008)
pKF41	integrative construct expressing *ftsZ-egfp* from the natural *ftsZ* promoter region	(Grantcharova *et al.*, 2005)
pGWS755	pSET152 harboring the *ylmG-egfp* under the control of the *ftsZ* promoter of *S. coelicolor*	This work
pGWS771	pSET152 harboring the +1/+294 region of *ylmG* under the control of the *ftsZ* promoter of *S. coelicolor*	This work
pGWS116	pHJL401 expressing SsgA-eGFP	(Noens *et al.*, 2007)
pGWS526	pHJL401 expressing SsgB-eGFP	(Willemse *et al.*, 2011)
pGWS791	pSET152 with *ylmG-mCherry* under the control of the *ftsZ* promoter of *S. coelicolor*	This work
pGWS529	pHJL401 expressing FtsZ-mCherry from its native promoter	This work

The strategy for creating knock-out mutants is based on the unstable multi-copy vector pWHM3 (Vara et al., 1989), essentially as described previously (Świątek *et al.*, 2012). The -1442/+6 and +277/+1521 regions relative to the translational start of *ylmG* (SCO2078) were amplified by PCR from the *S. coelicolor* M145 genome using primer pairs ylmG_LF_1442 and ylmG_LR+6 and ylmG_RF+277 and ylmG_RR+1521, respectively (Table 3). Fragments were then cloned into EcoRI/BamHI-digested pGWS725, with the oligonucleotides designed such as to create a unique XbaI site in-between the flanking regions. The apramycin resistance cassette *aac(3)IV* flanked by *loxP* sites was then cloned via the engineered XbaI site to generate knock-out construct pGWS731. The presence of *loxP* sites allows the efficient removal of the apramycin resistance cassette from the chromosome following the introduction of plasmid pUWL-Cre that expresses the Cre recombinase (Fedoryshyn *et al.*, 2008). For complementation of the *ylmG* null mutant the integrative vector pSET152 harboring the coding sequence (+1/+294 region) of *ylmG* under control of the *ftsZ* promoter (pGWS771) was used.

To obtain a construct expressing YlmG-eGFP, we used plasmid pKF41 which expresses FtsZ-eGFP from the native *ftsZ* promoter region (Grantcharova et al., 2005). The insert was excised using restriction enzymes BglII and NotI, cloned into the integrative vector pSET152. To replace the *ftsZ* coding region by that of *ylmG*, the construct was digested with StuI and BamHI, and the *ylmG* gene was PCR-amplified from the genome of *S. coelicolor* using primer pair ylmG_F+1 and ylmG_R+282. The PCR product was subsequently cloned as a StuI-BamHI fragment in between *ftsZ*p and *egfp* to generate pGWS755. To generate a similar construct expressing YlmG-mCherry, the *egfp* gene in pGWS755 was removed by digestion with BamHI and NotI and replaced by *mCherry* to generate pGWS791.

Table 3. Oligonucleotides.

Name	**5'-3' sequence** [#]
ylmG_LF-1442	GTCA**GAATTC**GCGGACGATGTGCGCATTCTCTCG
ylmG_LR+6	GTCAGAAGTTATCCATCACC**TCTAGA**GCTCATGACCTGTGCTTCCCTCTC
ylmG_RF+277	GTCAGAAGTTATCGCGCATC**TCTAGA**CAGCTGTGAGCGATGAGAGAGATAC
ylmG_RR+1521	GTCA**GGATCC**TCGATCAGGAACCCGCGCATCGGC
ylmG_F+1	GTCAGAATTC**AGGCCT**TCGACATGAGCGTGGTCCTGGATGTC
ylmG_R+282	GTCAAAGCTT**GGATCC**AGCTGGCTCACGATCGAGAT
ylmG_R+294	GCTA**GGATCC**TCTCATCGCTCACAGCTGGCT

[#] Restriction sites used for cloning are underlined and in bold face. GGATCC, BamHI; GAATTC, EcoRI; AGGCCT stuI; TCTAGA, XbaI.

Microscopy

Sterile cover slips were inserted at an angle of 45 degrees into SFM agar plates, and spores of *S. coelicolor* and derivatives were carefully inoculated at the intersection angle. After incubation at 30°C for 3 to 5 days, cover slips were positioned on a microscope slide prewetted with 5 µl of 1x PBS. Fluorescence and corresponding light micrographs were obtained with a Zeiss Axioscope A1 upright fluorescence microscope (with an Axiocam Mrc5 camera at a resolution of 37.5 nm/pixel). The green fluorescent images were created using 470/40 nm band pass excitation and 525/50 band pass detection, while for the red channel 550/25 nm band pass excitation and 625/70 nm band pass detection was used (Willemse and van Wezel, 2009). DAPI was detected using 370/40 nm excitation with 445/50 nm emission band filter. For membrane staining FM5-95 was used and for DNA staining DAPI (all obtained from Molecular Probes). To obtain a sufficiently dark background, all images were corrected by setting the signal outside the hyphae to zero. These corrections were made using Adobe Photoshop CS4.

Chromosome distribution in spores of *S. coelicolor* strains was studied using stimulated emission depletion (STED) microscopy. For this, patches of the different *Streptomyces* strains were grown on SFM agar plates and incubated at 30°C for 5 days. Live cells were stained with Syto 9 (0.5 mM) for 5 minutes, after which STED was performed with a Leica TCS STED CW system with 488 nm excitation (5% laser power) and depletion at 592 nm (30% laser power).

Morphological studies on surface grown aerial hyphae and/or spores by cryo-scanning electron microscopy were performed using a JEOL JSM6700F scanning electron microscope as described previously (Colson et al., 2008). Transmission electron microscopy (TEM) for the analysis of cross-sections of hyphae and spores was performed with a FEI Tecnai 12 BioTwin transmission electron microscope as described (Noens et al., 2005).

Acceptor photobleaching was performed with a Zeiss Imager. eGFP was excited with a 488 nm laser (5% intensity) and emission was detected from 505-530 nm. mCherry was excited with 543nm laser (5% intensity) and detected with a 560 long-pass. Both channels were recorded sequentially to prevent signal cross-bleeding. Bleaching was performed with the 543 nm laser at maximum intensity for 25 iterations. For all experiments, the original intensity was determined as the average of three pre-bleach frames and the post bleaching intensity was set as the average of the first three post-bleach frames. For SsgA-eGFP with YlmG-mCherry (no interaction) eleven independent experiments were carried out, for the combination of FtsZ-mCherry and

YlmG-eGFP eighteen and for SsgB-eGFP and YlmG-mCherry twenty four. The average post-bleach intensity was calculated relative to the pre-bleach intensity, including standard error. All images were collected in a 512x512 pixel format with a 63x 1.4 NA oil objective.

Computer analysis

Analysis of *Streptomyces* genes and proteins was done at the StrepDB database (http://strepdb.streptomyces.org.uk/). For phylogenetic analysis and correlations the String engine (http://string.embl.de) was used, while putative transmembrane domains were identified using transmembrane prediction server DAS (http://www.sbc.su.se/~miklos/DAS/).

RESULTS

SsgB shows exceptional evolutionary conservation, whereby a maximum of one amino acid (aa) change is seen in orthologs from the same genus, while conversely, conservation is low between different actinomycete genera, even if they are closely related (Girard et al., 2013). During recruitment of FtsZ, SsgB docks to the membrane, but the lack of a predicted membrane domain suggests that another protein ensures its membrane attachment. To search for candidate membrane docking proteins, an *in silico* analysis of the estimated 1850 membrane proteins of *S. coelicolor* was performed. Considering the peculiar conservation of SsgB, we narrowed down the number by searching for proteins with >90% aa identity between the *Streptomyces* orthologs, and lower conservation (<70% aa identity) between orthologs in other actinomycete genera. The 20 best hits are listed in Table 4. Of these, *ylmG* (SCO2078) stood out. Its genomic location in-between *sepF* (controls the polymerization of FtsZ) and *divIVA* (controls the septum site in *B. subtilis*) suggests a role in the earliest phase of cell division. Furthermore, the predicted cytoplasmic domain consisting of aa residues 30-69 shows a very similar conservation as SsgB, with near complete conservation between the *Streptomyces* orthologs (99-100%), but low conservation (50-60% aa identity) between *Streptomyces* and other actinomycetes. Interestingly, the TM domain is less well conserved, consisting with possible covariation of especially the YlmG cytoplasmic domain and SsgB.

The *ylmG* gene encodes a 95 aa protein and lies upstream of *divIVA* (SCO2077) and downstream *sepF* (SCO2079) in the *dcw* cluster of *S. coelicolor*, whereby *sepF* and *ylmG* are likely cotranscribed. YlmG has an N-terminal and a C-terminal transmembrane domain, with the central part of the protein predicted to reside intracellularly. The distribution of *ylmG* includes the phylum of the Actinobacteria (high G+C Gram positives), which encompasses both sporulating and nonsporulating genera, several Firmicutes (low G+C Gram positives), including *Bacillus* and *Streptococcus*, as well as Cyanobacteria and chloroplasts. A detailed phylogenetic tree was presented by Kabeya and colleagues (Kabeya *et al.*, 2010). The wide distribution of YlmG suggests an ancient common ancestor.

Table 4. Membrane proteins with high conservation in streptomycetes but lower conservation between different actinomycete genera. The 20 best hits are listed.

SCO #	Protein	Function	Conservation ^
SCO1541	SsgB [a]	Cell division protein	99
SCO4609	HtpX	Metallopeptidase	97
SCO2155	Cox1	Cytochrome C oxidase subunit I	96
SCO2151	Cox3	Cytochrome C oxidase subunit III	96
SCO2078	YlmG	Membrane protein	96
SCO2944		Sugar permease subunit	95
SCO4602	NuoH2	NADH dehydrogenase subunit	95
SCO1389	ClsA	Cardiolipin synthase	95
SCO5118	OppB	oligopeptide permease subunit	95
SCO3404	FtsH2 [b]	metalloprotease	95
SCO1527		Alcohol phosphatidyl transferase	94
SCO2534		hemolysin-like protein	93
SCO1796		Stomatin-like protein	93
SCO2150	QcrC	Cytochrome C heme-binding subunit	93
SCO5670		putative polyamine permease subunit	93
SCO2945		Sugar permease subunit	93
SCO2148	QcrB	Cytochrome B subunit	93
SCO4722	SecY	Preprotein translocase subunit	92
SCO1215	CtaG	Cytochrome c oxidase assembly factor	92
SCO3945	CydA	Cytochrome ubiquinol oxidase subunit	92
SCO2087	MurX	phospho-N-acetylmuramoyl-pentapeptide-transferase	92

according to the *Streptomyces coelicolor* database numbering.

^ average aa identity (in %) between streptomycetes. For this comparison the eight genomes of the streptomycetes in StrepDB were used. The value is on average 2-3% lower if *S. lividans* is not included.

[a] included for reference purposes.

[b] does not occur in all streptomycetes.

ylmG null mutants are defective in sporulation

To study the function of *ylmG* in *Streptomyces*, an in-frame deletion mutant was created in *S. coelicolor* M145. For this, gene replacement construct pGWS731 (see Materials and Methods section) was introduced into *S. coelicolor* M145 and colonies selected for apramycin resistance (marker for *ylmG* disruption) and sensitivity to thiostrepton (marker for the vector). These colonies presumably had *ylmG* replaced by the apramycin resistance cassette on the genome. Expression of the Cre recombinase in these cells resulted in a number of markerless deletion mutants, which all had very similar pheno-

types with impaired sporulation as judged by the lack of grey pigmentation. After PCR verification of the deletion of *ylmG* in these colonies, one representative colony was then selected and designated GAL1.

Growth on SFM agar plates showed that *ylmG* mutants were impaired in development. While the parental strain *S. coelicolor* M145 developed normal grey-pigmented colonies indicative of sporulation, the *ylmG* null mutant GAL1 had a nearly white phenotype, eventually showing light-grey pigmentation (Fig. 1A). The sporulation defect was confirmed by phase-contrast light microscopy of impression prints of surface-grown colonies, which demonstrated that GAL1 produced only very few spore chains (Fig. 1B). Introduction of plasmid pGWS771, which is a low-copy number vectors expressing *ylmG* behind the *ftsZ* promoter (see below), restored sporulation to the mutant, indicating that the sporulation deficiency was indeed due to the deletion of *ylmG*.

Closer inspection of the aerial hyphae and spores by cryo-scanning electron microscopy (SEM) showed that where the parental strain *S. coelicolor* M145 produced abundant spiraling hyphae and well-developed chains of spores, the *ylmG* null mutant predominantly produced straight aerial hyphae, whereby only very few chains of irregularly shaped spores could be identified (Fig. 2A). To quantify the size distribution, approximately 130 spores from the *ylmG* mutant and the wild-type strain *S. coelicolor* M145 were measured. While wild-type spores showed the typical Gaussian distribution centered around 0.8-1.2 μm in length, *ylmG* mutant spores showed a broader distribution, with an average size (1.3 μm) of around 0.2 μm larger than wild-type spores (1.1 μm). These data identify *ylmG* as a novel sporulation gene involved in sporulation-specific cell division and the gene was therefore renamed *sepG*.

1A

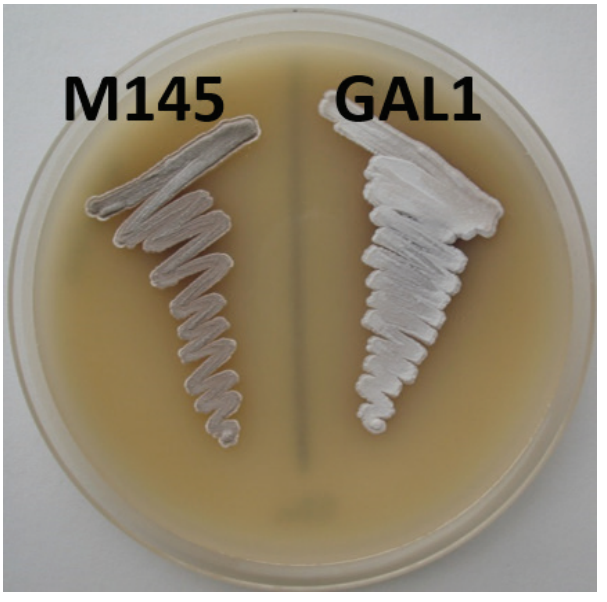

1B

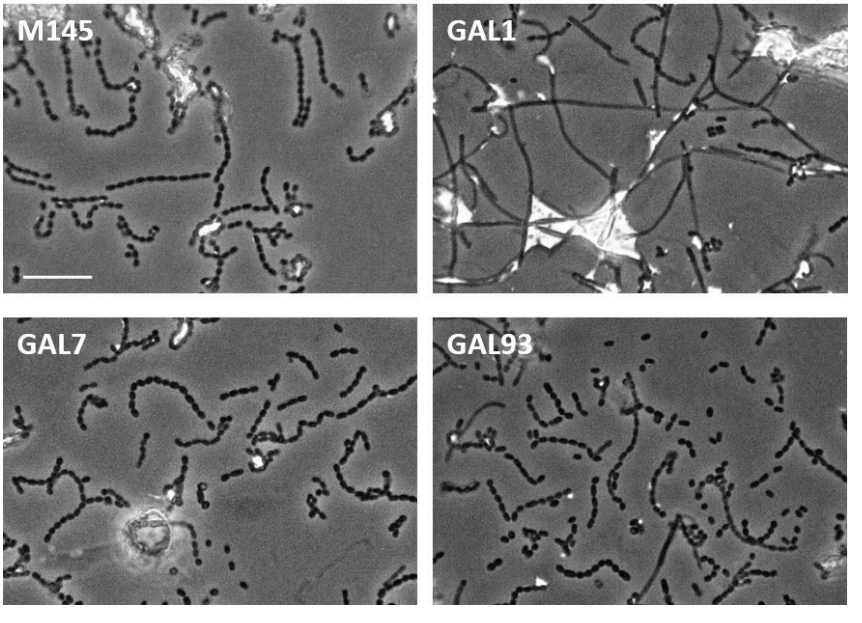

Figure 1. Light micrographs of the *ylmG* null mutant of *S. coelicolor*. **(A)** Comparison of *S. coelicolor* M145 and its *ylmG* null mutant GAL1. Note the lack of grey pigmentation of the *ylmG* mutant due to failure to produce the grey spore pigment. **(B)** Phase-contrast light micrographs of impression prints from cultures grown on SFM agar. Note that expression of wild-type YlmG (GAL93) or YlmG-eGFP (GAL7) restores sporulation to the *ylmG* mutant. All cultures were grown on SFM agar plates for 5 days at 30^0C. Bar, 10 μm.

2A

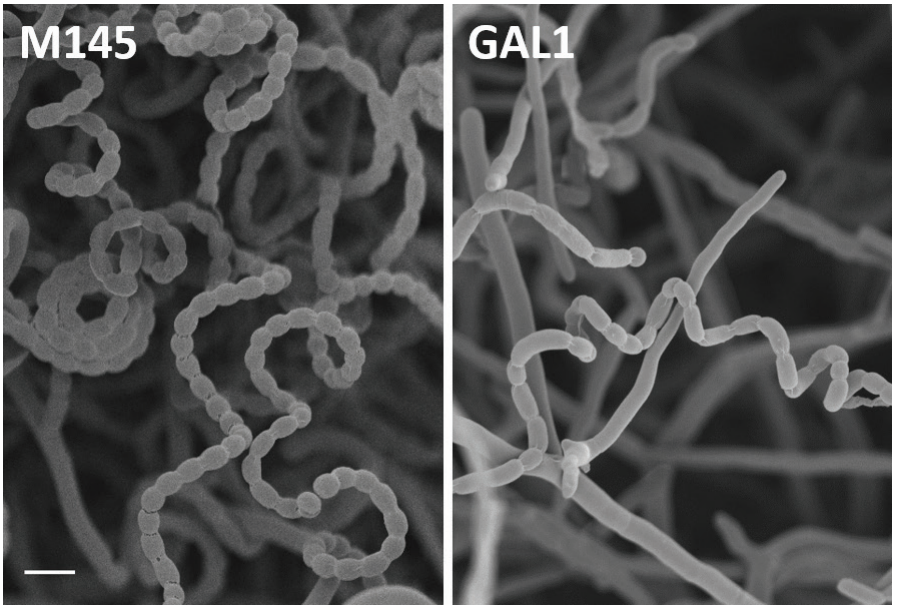

2B

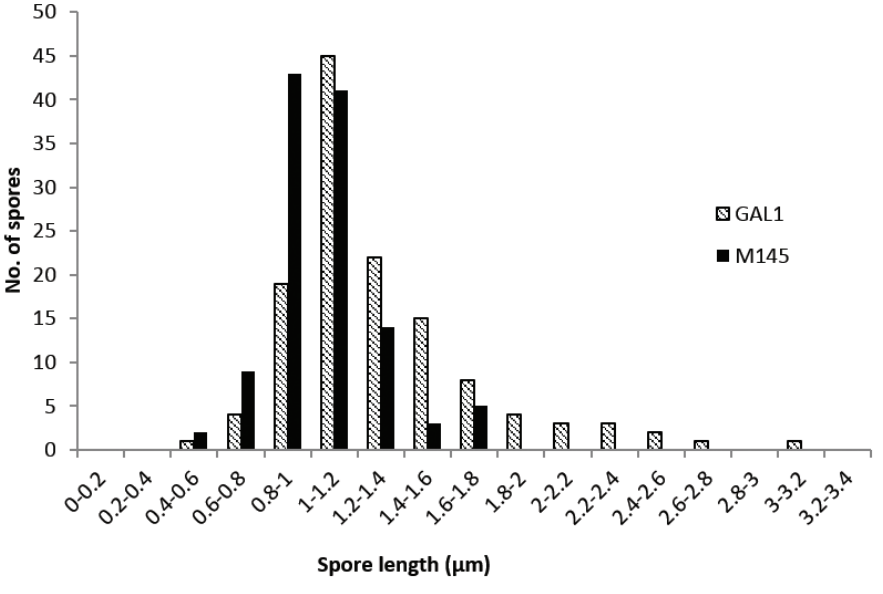

Figure 2. Comparison of spores produced by wild-type *S. coelicolor* M145 and its *ylmG* null mutant. (A) Cryo-scanning electron micrographs of wild-type and *ylmG* mutant aerial hyphae. Wild-type sporulated abundantly, while occasional chains of irregularly sized spores were produced by the *ylmG* mutant. Cultures were grown on SFM agar plates for 5 days at 30^{0}C. Bar, 2 µm. **(B)** Size distribution of wild-type and *ylmG* mutant spores. Spores were measured from a representative number of cryo-scanning electron micrographs, so that around 130 spores were measured for each strain. Note that a significant number of *ylmG* mutant spores were unusually long.

SepG is required for proper spore-wall synthesis and nucleoid morphology

To obtain more detailed insight into spore morphology and spore-wall thickness, we performed high-resolution imaging using transmission electron microscopy (TEM) on thin sections. This again revealed the irregular sporulation of the *sepG* mutant. Furthermore, *sepG* mutant spores contained a considerably thinner and more electron-lucent cell wall, indicative of altered spore-wall synthesis (Fig. 3). Another major alteration observed in *sepG* mutant spores was the shape of the spore nucleoid. Rather than a well-condensed nucleoid in the center of the spores as seen in wild-type spores, the *sepG* mutant spores show a less well condensed nucleoid that primarily localized close to the edge of the spores, with a pattern suggesting an unusual toroidal or doughnut shape (Fig. 3). Notably, such a doughnut shape is found routinely for nucleoids in developing or germinating spores of *Bacillus*.

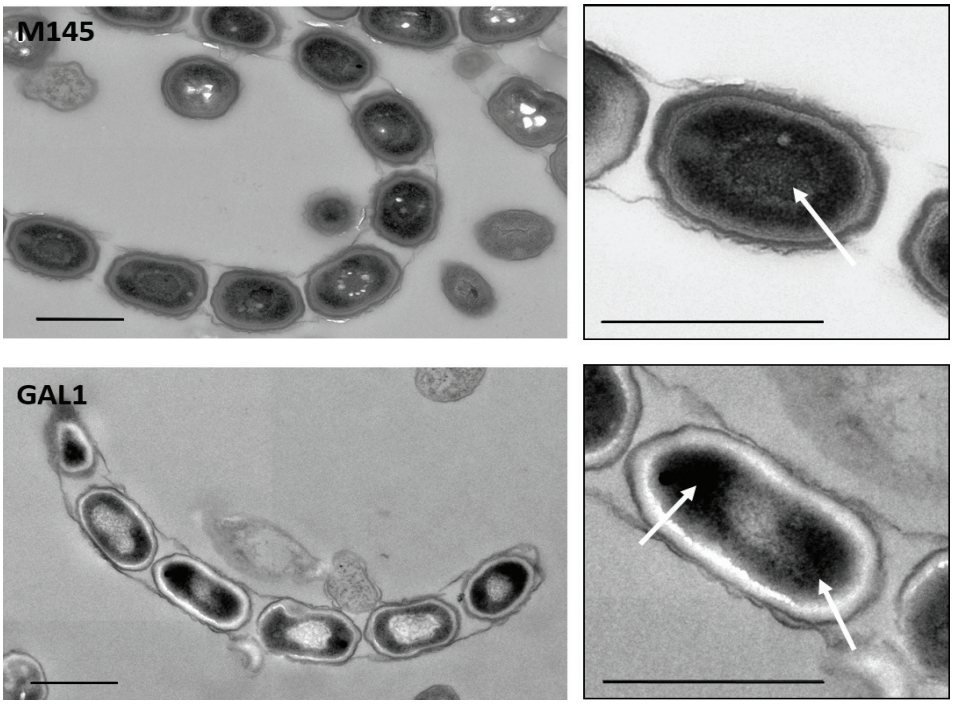

Figure 3. Transmission electron micrographs of wild-type and *sepG* mutant spores. Both a representative overview (left) and close-up (right) are presented. Arrows indicate nucleoids. Note that whereas the wild-type (M145) nucleoid is well condensed and located at the center of the spores, that of the *sepG* mutant (GAL1) has an unusual distribution. Note the lighter appearance of the spore wall in the *sepG* mutant. Cultures were grown on SFM agar plates for 5 days at 30^0C. Bar, 1 µm.

Viability of the *sepG* mutant spores was tested by analyzing heat resistance. For this, spores were incubated for 10 minutes at 60°C and plated onto SFM agar plates. While 45% of the wild-type spores survived the heat treatment, survival of the *sepG* mutant spores was as low as 8%. The defect could be largely complemented by expressing SepG: 36% and 32% of spores of GAL93 and GAL7 survived the heat treatment, repectively. GAL93 is the *sepG* mutant transformed with pGWS771, which harbors wild-type *sepG*. GAL7 is the *sepG* mutant harboring localization construct pGWS755.

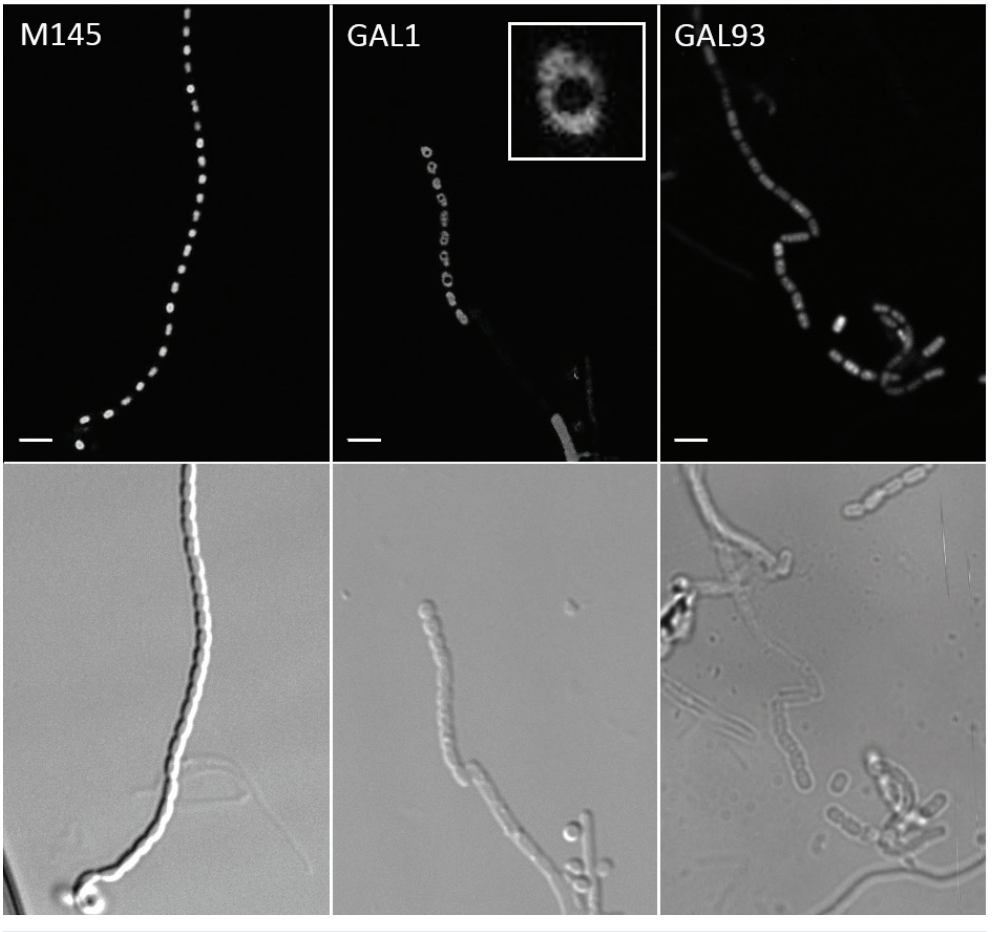

Figure 4. Fluorescence micrographs of nucleoid distribution in the spores by STED. Top, STED images; bottom, light images. DNA staining of wild-type spores (M145, left) shows normal spore lengths and proper nucleoid condensation. In contrast, nucleoids of *sepG* null mutants (GAL1, middle) appear doughnut shaped and less well condensed. The aberrant nucleoid shape is complemented by a clone expressing *sepG* (transformant GAL93, right), but DNA condensation is still affected. Inset: 7x magnification of one of the nucleoids. Cultures were grown on SFM agar plates for 5 days at 30^0C. Bar, 2 μm.

To visualize the nucleoid distribution in wild-type and *sepG* mutant spores, the nucleoids were stained with Syto 9 and imaged with stimulated emission depletion (STED) microscopy (Fig. 4). In wild-type spores, the nucleoids were seen as very bright dots that localized to the central part of the spores. Interestingly, in *sepG* null mutants the nucleoids were less condensed and more dispersed, whereby the centers of the spores were largely devoid of DNA. Spores of strain GAL93, which is the *sepG* null mutant containing plasmid pGWS771 expressing wild-type *sepG*, no longer showed such doughnut-shaped DNA structures, although the nucleoids appeared less well-condensed as compared to wild-type spores. Thus, TEM and STED data suggest that SepG is required for proper nucleoid compaction during sporulation.

Localization of SepG

To determine the localization of SepG in *S. coelicolor*, a C-terminal fusion with enhanced green fluorescent protein (eGFP) was constructed under the control of the *ftsZ* promoter (plasmid pGWS755). Introduction of pGWS755 into the *sepG* null mutant restored sporulation and spore viability, which shows that SepG-eGFP is functional *in vivo*. Confocal fluorescence microscopy was applied to investigate SepG-eGFP localization in wild type cells and the *sepG* mutant. The pattern of SepG-eGFP localization was dynamic and developmental stage-dependent. In young aerial hyphae, when the chromosomal DNA was still uncondensed and septal membrane synthesis had not yet initiated, SepG-eGFP formed distinct and widely spaced foci (Fig. 5A). Importantly, such a localization pattern is very similar to that of the initial stage of SsgB localization, prior to its septum-site localization ((Willemse *et al.*, 2011) and Fig. 6). During the subsequent spore maturation the nucleoids condensed, and at this stage SepG-eGFP relocalized to the intersection between the spores, which at this point in spore development is the only place where active cell-wall remodeling takes place (Fig. 5B). In the merged images, SepG-eGFP localized to the nucleoid-free zones in spores, with a ring of SepG surrounding the nucleoid (Fig. 5C). The fluorescence images strongly suggest that in *sepG* mutant spores, the nucleoid takes up the space normally occluded by a SepG-dependent mechanism, and it suggests that SepG and DNA may be mutually exclusive (Fig. 5D). In mature spores, which are physically separated, no GFP signal could be observed, suggesting that SepG eventually disappears (not illustrated).

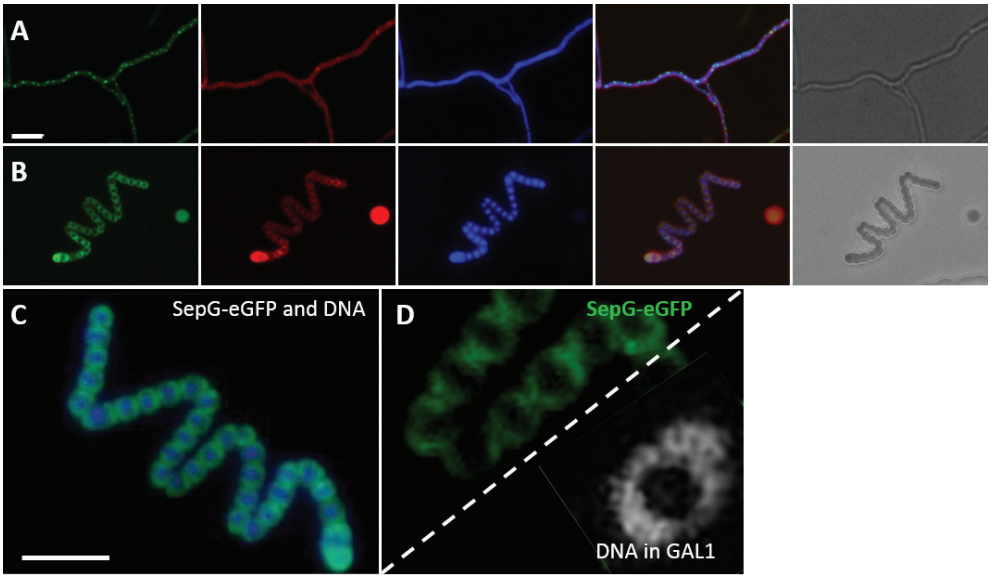

Figure 5. Localization of SepG-eGFP. Sporogenic aerial hyphae of *S. coelicolor* M145 were imaged by Fluorescence microscopy visualizing SepG-eGFP, membrane (stained with FM5-95), DNA (DAPI), the merged image and a light micrograph at the onset of sporulation in aerial hyphae **(A)** and during sporulation **(B)**. **C** represents a merged image of SepG-eGFP and the DNA taken from (B). Image **D** shows that SepG-eGFP in wild-type cells (left) has a similar localization in the spores as the DNA in the *sepG* null mutant (right), which suggests a model whereby SepG acts to condense the DNA in the center of the spores. Bar, 5 μm.

Localization of SsgB to septum sites depends on direct interaction with SepG

We previously showed that FtsZ is directly recruited by SsgB in an SsgA-dependent manner, followed by recruitment of the other divisome components (Willemse *et al.*, 2011). The phenotype of the *sepG* null mutants prompted us to investigate whether the localization of one or more of these proteins was affected by the absence of SepG. To address this question, pGWS116, pGWS526 or pKF41, expressing SsgA-eGFP, SsgB-eGFP or FtsZ-eGFP, respectively, were introduced into the *sepG* null mutant. While SsgA-eGFP localized normally in the mutant, SsgB-eGFP was mainly seen to localize diffusely along the hyphal membrane, instead of the focal pattern at future septum sites seen in sporogenic aerial hyphae of the parental strain M145. This is consistent with a model where SepG is required for the membrane docking of SsgB after its initial localization by SsgA (Fig. 6A). In line with the delocalized pattern of the FtsZ-recruiting SsgB protein, the *sepG* mutant also failed to produce the

typical ladder patterns of FtsZ-eGFP seen in wild-type hyphae (Fig. 6A). Only occasional septa were formed, a phenotype that is also observed in *ssgB* null mutants and other sporulation (*whi*) mutants (Willemse *et al.*, 2011). Interestingly, SsgB-eGFP still formed distinct foci in the middle of the hyphae, with around 1 μm spacing, typical of the first stage of SsgB localization (Fig. 6B). However, in contrast to SsgB in wild-type cells (Willemse *et al.*, 2011), in the *sepG* null mutant the foci subsequently disappeared, indicating that the stable localization of SsgB requires SepG. Thus, after SsgA ensures the initial localization of SsgB, SepG then acts to ensure the membrane association of SsgB at division sites, which is the first step in sporulation-specific cell division.

6A

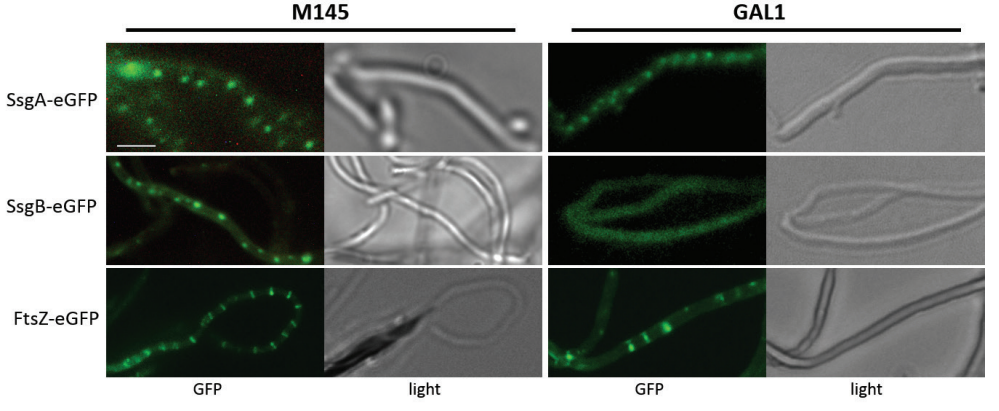

6B

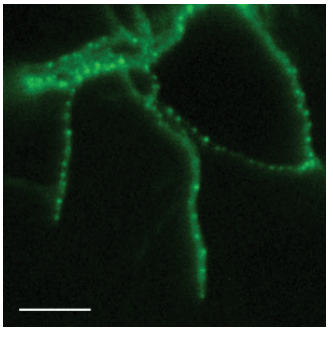

Figure 6. Effect of SepG on the localization of eGFP fusions of SsgA, SsgB and FtsZ. (A) all proteins localize correctly in wild-type cells (M145, left). In contrast, SepG is required for the formation of ladders of FtsZ or for the localization of SsgB at division sites. SsgA has a normal focal pattern in the *sepG* mutant. The occasional Z rings formed by *sepG* mutants are also seen in *ssgB* mutants of *S. coelicolor* (see the text for references). Bar, 2 μm. **(B)** SsgB temporarily forms foci in the central part of the aerial hyphae, but fails to localize to the membrane. Cultures were grown on SFM agar plates for 5 days at 30^0C. Bar, 5 μm.

This raised the question whether the mislocalization of SsgB and FtsZ could be explained by direct interaction between SepG and SsgB. To investigate this *in vivo*, we applied Förster resonance energy transfer (FRET), which allows the identification of direct molecular interactions. As low-wavelength fluorophore eGFP was used, and as longer-wavelength fluorophore mCherry. YlmG-mCherry was introduced into *S. coelicolor* M145 expressing either SsgA-eGFP or SsgB-eGFP to generate strains GAL94 and GAL95, respectively; YlmG-eGFP was introduced into *S. coelicolor* M145 expressing FtsZ-mCherry to generate strain GAL96. Strains JSC2 and JSC3, which are *S. coelicolor* FM145 co-expressing SsgB-eGFP with FtsZ-mCherry, and SsgB-mCherry with FtsZ-eGFP, respectively, were used as positive controls, based on the direct interaction between SsgB and FtsZ (Willemse *et al.*, 2011). As negative control we used *S. coelicolor* K202, which expresses FtsZ-eGFP alone.

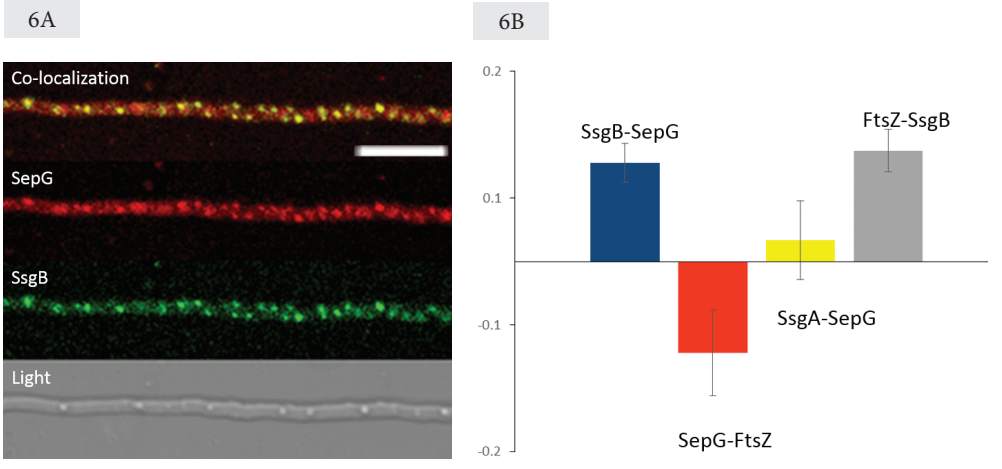

Figure 7. FRET imaging of the interaction between SepG and SsgB. (A) FM images showing the colocalization of SsgB and SepG. Bar, 5 μm. **(B)** Graphical representation of the FRET data. All efficiencies are represented relative to the control (which was set to zero). FRET data are summarized in Table 5.

Table 5. FRET efficiencies for different combinations of donor (eGFP) and acceptor (mCherry).

Strain	GAL95	GAL96	GAL94	JSC3	JSC2
Donor-acceptor	SsgB-SepG	SepG-FtsZ	SsgA-SepG	FtsZ-SsgB	SsgB-FtsZ[#]
Average FRET Efficiency	1.05	0.90	0.99	1.06	1.25
Standard deviation	0.02	0.03	0.03	0.02	0.21

[#] not included in Fig. 7B to allow better comparison.

JSC2 and JSC3 showed a FRET efficiency consistent with the short intermolecular distance between FtsZ and SsgB (Table 5). The molecular ratio between SsgB and FtsZ (approximately 1:3) explains why JSC2 yields a higher FRET efficiency as compared to JSC3, as the energy of one SsgB-eGFP can be transferred to multiple FtsZ-mCherry molecules while the energy of multiple FtsZ-eGFP molecules can only be transferred to one molecule of SsgB-mCherry. The negative control FtsZ-eGFP had a FRET efficiency of 0.97 ± 0.02, consistent with lack of interaction with an acceptor (Table 5). Interestingly, SepG and SsgB colocalized very well, with over 90% overlap of the foci (Fig. 7A). The two proteins also closely interact, as shown by the FRET efficiency of 1.05 ± 0.02 which suggests an intermolecular distance that is close to that between the known partners SsgB and FtsZ. No interaction was seen for SepG and SsgA (FRET efficiency of 0.99 ± 0.03) or SepG and FtsZ (0.90 ± 0.03). The data are summarized graphically in Fig. 7B, whereby the negative control was set to zero. These FRET data are consistent with direct interaction between SepG and SsgB *in vivo*, while no interaction was seen between SepG and either SsgA or FtsZ. Taken together, our data suggest that SepG and SsgB directly interact, whereby SepG is required for the septal localization of SsgB, which in turn recruits FtsZ to division sites to initiate sporulation-specific cell division in *S. coelicolor*. After cell division commences, SsgB remains on the divisome while SepG follows sites of active cell-wall remodeling, where it coordinates nucleoid compaction to keep the DNA away from the cell wall.

DISCUSSION

The control of cell division in the multicellular streptomycetes is very different from that in for example *E. coli* and *B. subtilis* (Claessen *et al.*, 2014). During sporulation, the aerial hyphae differentiate into long chains of spores, and the more or less simultaneous formation of many septa results in spectacular ladders of Z rings (Schwedock *et al.*, 1997). The canonical control systems and septum-localizing proteins (Min, Noc, FtsA, ZipA, ZapA, EzrA, etc.) found in bacteria that divide by binary fission are all absent in streptomycetes, and instead actinomycete-specific proteins control the localization of the septa. In streptomycetes cell division is positively controlled, whereby FtsZ is actively recruited to septum sites by the action of SsgB (Willemse *et al.*, 2011). SsgB is a member of the family of SsgA-like proteins, which exclusively occur in actinomycetes. While the role of SsgB explains how FtsZ is localized to the future septum sites, and the SsgA protein plays an active role in its localization (Willemse *et al.*, 2011), how the striking symmetry of the Z ladders is controlled, has so far remained unresolved.

In this work, we show that *ylmG,* which lies in-between *sepF* and *divIVA*, and is one of the last genes in the *dcw* cluster whose function had not yet been established, plays a major role in the control of sporulation-specific cell division in *S. coelicolor*. The gene was therefore renamed *sepG*. In streptomycetes, SepG apparently has two roles during sporulation-specific cell division. Firstly, SepG helps to orchestrate the earliest stage of sporulation-specific cell division, as it directly binds to SsgB and likely acts as a membrane anchor to ensure the localization of SsgB to future septum sites. After the initial localization of SsgB by SsgA to a central position in the aerial hyphae, this is the next crucial step in the positive control of cell division in *Streptomyces*, followed by the recruitment of FtsZ by SsgB. Secondly, at a later stage of spore development, SepG is required for synthesis of the mature spore wall as well as for maintaining nucleoid shape. In wild-type cells, SepG forms a ring that surrounds the nucleoid, while in *sepG* null mutants large doughnut-shaped nucleoids are formed accompanied by less dense spore wall, suggesting imperfect cell wall synthesis; the latter is consistent with the lower heat sensitivity of the spores. Taken together, these data suggest that during early sporulation, SepG allows SsgB to find the future sites of division, where after SepG continues to follow the spore-wall synthetic machinery, and ensures the coordination of spore-wall synthesis with nucleoid compaction by a mechanism that is yet unresolved.

FRET data revealed direct interaction between SepG and the FtsZ-recruit-

ing SsgB. Interestingly, the cytoplasmic domain of SepG shows a similar conservation as SsgB, with extremely high conservation in streptomycetes, but low conservation between different actinomycete genera. Such a conservation pattern is not evident in the transmembrane domains. The suggestive covariation in terms of aa conservation in different bacteria between the SepG cytoplasmic domain and SsgB provides supporting phylogenetic evidence consistent with direct interaction between SsgB and SepG. Furthermore, SsgB fails to localize specifically to the septum site in *sepG* null mutants, which also explains the mislocalization of FtsZ. The early co-localization of and direct interaction between SepG and SsgB implies that either SepG ensures the correct localization of SsgB, or *vice versa*. The fact that SepG localizes normally in *ssgB* mutants, while conversely, SsgB does not localize properly in *sepG* mutants, supports the former model. Interestingly, time-lapse imaging showed that in the absence of SepG, SsgB temporarily localizes to a central position in the hyphae, very similar to SsgA, but then rapidly disperses along the membrane rather than finding the future division sites. This strongly suggests a model whereby SsgA recruits SsgB to a central position in the hyphae, followed by the subsequent SepG-dependent docking of SsgB to the future division sites. It also suggests that SsgB has affinity for the membrane, which may be explained by the large hydrophobic patch in the SsgB trimeric structure (Xu *et al.*, 2009). SsgB then actively recruits FtsZ and assists in its polymerization, whereby SsgB remains part of the divisome and follows FtsZ throughout the process of cell division (forming the same ladders as FtsZ).

The joint movement of SepG and SsgB to the division sites also ensures that SepG arrives at the first site of peptidoglycan synthesis during sporulation, which is the septum. From there, the membrane protein SepG follows the spore-wall synthetic machinery, somehow ensuring that the DNA is kept away from this construction site and preventing lethal damage. It is yet unclear how SepG controls the nucleoid shape in *Streptomyces*. While relatively little is known of nucleoid dynamics in *Streptomyces*, we can try to glean information from the well-studied *B. subtilis*, although *Bacillus sepG* null mutants have no apparent phenotype (Hamoen et al., 2006). While during vegetative growth the nucleoid localizes close to mid-cell in *B. subtilis*, its shape changes during the onset of sporulation, and eventually a doughnut-shaped ring is formed similar to that found in *S. coelicolor sepG* mutants, with a diameter of around 1 μm (Pogliano *et al.*, 1995). During germination, these rings disappear and the nucleoids take up the diffuse lobular shape typical of vegetative cells (Ragkousi *et al.*, 2000). The nucleoid ring in *Bacillus* spores is maintained by the action of small acid soluble proteins (SASPs), encoded by the *sspA* genes. SASPs, which

are absent from streptomycetes, change the conformation of the DNA from B to A (Mohr et al., 1991) and also protect spores against heat, UV damage or oxidative stress (Mason and Setlow, 1987). Deletion of *sspA* genes results in collapse of the nucleoids towards the center of the spores (Setlow et al., 2000). In other words, the opposite occurs as compared to *Streptomyces*, where the wild-type nucleoid is condensed in the center of the spores, while deletion of *sepG* results in ring formation.

The expansion of the nucleoid towards the membrane likely contributes to disturbance of the cell cycle, as this is expected to trigger a nucleoid-occlusion like mechanism to prevent septum synthesis close to the nucleoid, even though such a mechanism has not yet been identified in streptomycetes. This includes various mutants disturbed in DNA partitioning, such as *parA* and *parB* mutants of *S. coelicolor*. We previously showed that the SsgA-like protein SsgC plays a role in nucleoid segregation, with highly disturbed distribution of DNA in *ssgC* null mutants (Noens et al., 2005). It is tempting to suggest that other SALPs may also interact with SepG, with SsgC as one of the candidates.

Since SsgB only occurs in actinomycetes, one may wonder how universal the function of SepG is. We expect that the principles shown in this work will translate to lower Gram-positives such as *Bacillus* and *Streptococcus*, which is among others based on strong phylogenetic evidence, since the location of *sepG* between *divIVA* and *sepF* was maintained during several hundred millions years of evolution, although *ylmH* was lost in actinomycetes. Therefore, functional overlap between the *Bacillus* and *Streptomyces* orthologs is to be expected. In this light, a key observation may well be that like in *Streptomyces*, a cell division control mechanism that is independent of the negative control systems Min and Noc has recently been identified in *B. subtilis*. It was shown that the Z ring can be positioned at division sites in the absence of Min and Noc, and that in Noc$^-$ cells the Z rings have a preference for the mid-cell position between the two nucleoids (Rodrigues and Harry 2012). Conceivably therefore, SepG may have a similar role in division-site selection in *B. subtilis* as in *Streptomyces*, but such a role would only be obvious if *sepG* were to be studied – and, if at all possible, mutated - in the absence of Noc. Further molecular insights into the function of SepG in streptomycetes will shed more light on the way the positive control of cell division is governed in these multicellular bacteria, as well as on the yet poorly understood mechanisms that prevent nucleoid damage during septum synthesis and cell-wall remodeling.

Acknowledgements

We are very grateful to Leendert Hamoen for discussions and for comments on the manuscript. The work was supported by ECHO and VICI grants from the Netherlands Organization for Scientific Research (NWO) to GPvW.

III

The SepF-like proteins SflA and SflB control hyphal branching and are required for proper spore maturation in *Streptomyces coelicolor*

Le Zhang, Joost Willemse and Gilles P. van Wezel

Manuscript in preparation

ABSTRACT

Cell division during the reproductive phase of the *Streptomyces* lifecycle requires tight coordination between synchronous formation of multiple septa and DNA segregation. One remarkable difference with most other bacterial systems is that cell division in *Streptomyces* is positively controlled by the recruitment of FtsZ by SsgB. In *Bacillus subtilis*, SepF tethers FtsZ to the membrane, and this is the only cell division protein from *Bacillus* that is conserved in *Streptomyces*. Uniquely, actinomycetes have multiple SepF paralogs, and we here show that the SepF-like proteins SflA and SflB control branching of the hyphae, with unusual branching spore chains in *sflA* and *sflB* mutants. Additionally, electron microscopy showed that spores of *sflA* and *sflB* mutants were irregular, with variation in sizes and in electron density. Bacterial two-hybrid analysis showed direct interaction of SflB with SepF, SflA, and with itself. SflB localizes to part of the sporulation septa but not close to the hyphal wall, suggesting that perhaps SflB inhibits SepF function. While SflA and SflB were not seen to localize specifically in vegetative hyphae, constitutive expression of SflA and SflB from the *ermE* promoter blocked development and resulted in detachment of the colonies from the agar surface, in line with a role in disturbing hyphal branching. Thus, SflA and SflB are novel sporulation proteins, that affect branching and cell division in aerial hyphae.

INTRODUCTION

The mycelial life style of streptomycetes imposes specific requirements for cell division control. One obvious difference between the mycelial *Streptomyces* and the unicellular *Bacillus subtilis*, the model system for cell division in Gram-positive bacteria, is the absence of a defined midcell position in the long hyphae of streptomycetes. Not surprisingly, the way cell division is controlled is very different between these bacteria. In rod-shaped bacteria, the control of cell division revolves around finding the midcell position. Several proteins are required to assist in septum-site localization, such as FtsA and ZipA (Hale and de Boer, 1997; Pichoff and Lutkenhaus, 2002; RayChaudhuri, 1999) and ZapA (Gueiros-Filho and Losick, 2002). Septum-site localization is negatively controlled, via the action of Min, which prevents Z-ring assembly at the cell poles (Marston *et al.*, 1998; Raskin and de Boer, 1997), and nucleoid occlusion that prevents formation of the Z-ring over non-segregated chromosomes (Bernhardt and de Boer, 2005; Woldringh *et al.*, 1991; Wu and Errington, 2004; Wu and Errington, 2012). Direct homologs of all of these control proteins are missing in streptomycetes. Cell division in *Streptomyces* is positively controlled, via the direct recruitment of FtsZ by the membrane-associated SsgB (Willemse *et al.*, 2011). SsgB is part of the divisome, and hence provides the first example of a divisome component that localizes prior to FtsZ. In turn, the localization of SsgB is mediated through the orthologous SsgA protein, a known activator of cell division (van Wezel *et al.*, 2000b; Kawamoto *et al.*, 1997). This system implies the evolution of an entirely new way of Z-ring control.

In Chapter II we presented evidence that SepG allows docking of SsgB to the membrane. Interestingly, one protein involved in early division control in *B. subtilis* is also conserved in streptomycetes, namely SepF, encoded by a gene that lies immediately upstream of *sepG*. SepF of *B. subtilis* assists in bundling of the FtsZ filaments, and polymerizes *in vitro*, forming large rings of around 50 nm in diameter (Ishikawa *et al.*, 2006; Hamoen *et al.*, 2006). Recently, it was shown that SepF also interacts with the membrane in *B. subtilis*, via its N-terminal domain (Duman *et al.*, 2013). This strongly suggests that besides a direct effect of Z-ring assembly, SepF also acts as a membrane anchor for FtsZ. This makes SepF an important protein required for the localization of FtsZ in bacteria that divide by binary fission, which is also found in *Streptomyces*.

In this chapter, we provide a functional analysis of two new *Streptomyces* developmental genes which are paralogs of *sepF*, and are designated as *sflA* and *sflB* (for *sepF* like). We show that deletion of either *sflA* or *sflB* results in branching of the aerial hyphae, and provide evidence that they may act via

interference with the function of *sepF*.

MATERIALS AND METHODS

Bacterial strains and media

The bacterial strains used in this work are listed in Table 1. *E. coli* strains JM109 (Sambrook *et al.*, 1989) and ET12567 (MacNeil *et al.*, 1992) were used for routine cloning and for isolation of non-methylated DNA, respectively. *E. coli* transformants were selected on LB agar media containing the relevant antibiotics and grown O/N at 37°C. *Streptomyces coelicolor* A3(2) M145 was used as parental strain to construct mutants. All media and routine *Streptomyces* techniques are described in the *Streptomyces* manual (Kieser *et al.*, 2000). Yeast extract-malt extract (YEME) and tryptone soy broth with 10% sucrose (TSBS) were the liquid media for standard cultivation. Regeneration agar with yeast extract (R2YE) was used for regeneration of protoplasts and with appropriate antibiotics for selection of recombinants (Kieser *et al.*, 2000). Soy flour mannitol (SFM) agar plates were used to grow *Streptomyces* strains for preparing spore suspensions and for morphological characterization and microscopy. *E. coli* strain BTH101, nonreverting adenylate cyclase-deficient (*cya*), was used for BATCH screening assay (Karimova *et al.*, 1998).

Table 1. Bacterial strains

Bacteria strains	Genotype	Reference
E. coli JM109	See reference	(Sambrook *et al.*, 1989)
E.coli ET12567	See reference	(MacNeil *et al.*, 1992)
E. coli BTH101	See reference	(Karimova *et al.*, 1998)
S. coelicolor M145	$SCP1^{-}$ $SCP2^{-}$	(Kieser *et al.*, 2000)
GAL14	M145Δ*sflA*	This work
GAL15	M145Δ*sflB*	This work
GAL16	M145Δ*sflA*Δ*sflB*	This work
GAL17	M145 + pGWS759	This work
GAL18	M145 + pGWS760	This work
GAL19	M145 + pGWS761	This work
GAL44	M145 + pGWS774	This work
GAL45	M145 + pGWS775	This work
GAL46	M145 + pGWS776	This work
GAL70	M145 + pWHM3	This work

Plasmids and constructs and oligonucleotides

All plasmids and constructs described in this chapter are summarized in Table

2. The oligonucleotides are listed in Table 3.

Table 2. Plasmids and Constructs

Plasmid and constructs	Description	Reference
pWHM3	*E. coli*/*Streptomyces* shuttle vector, multi-copy and very unstable in *Streptomyces*	(Vara *et al.*, 1989)
pSET152	*E. coli*/*Streptomyces* shuttle vector, high copy number in *E. coli* and integrative in *Streptomyces*	(Bierman *et al.*, 1992)
pHM10a	Conjugative *E. coli-Streptomyces* shuttle vector, harboring P*ermE* and RBS	(Motamedi *et al.*, 1995)
pGWS750	pWHM3 containing flanking regions of *S. coelicolor* SCO1749 with apraloxP-*Xba*I inserted between then in pWHM3 EcoRI-HindIII	This work
pGWS751	pWHM3 containing flanking regions of *S. coelicolor* SCO5967 with apraloxP-*Xba*I inserted between then in pWHM3 EcoRI-HindIII	This work
pUWL-Cre	Cre-recombinase expression plasmid	(Fedoryshyn *et al.*, 2008)
pGWS759	pSET152 harboring *sflA-egfp* under control of *ftsZ* promoter	This work
pGWS760	pSET152 harboring *sepF-egfp* under control of *ftsZ* promoter	This work
pGWS761	pSET152 harboring *sflB-egfp* under control of *ftsZ* promoter	This work
pGWS774	pWHM3 containing P*ermE*, RBS and *sflA*	This work
pGWS775	pWHM3 containing P*ermE,* RBS and *sepF*	This work
pGWS776	pWHM3 containing P*ermE,* RBS and *sflB*	This work
pBTH165	pUT18 harboring +1/+438 region of *sflA* from *S. coelicolor* fused behind the *cya* gene	This work
pBTH109	pUT18 harboring +1/+639 region of *sepF* from *S. coelicolor* fused behind the *cya* gene	This work
pBTH169	pUT18 harboring +1/+408 region of *sflB* from *S. coelicolor* fused behind the *cya* gene	This work
pBTH167	pKT25 harboring +1/+438 region of *sflA* from *S. coelicolor* fused behind the *cya* gene	This work
pBTH111	pKT25 harboring +1/+639 region of *sepF* from *S. coelicolor* fused behind the *cya* gene	This work
pBTH171	pKT25 harboring +1/+408 region of *sflB* from *S. coelicolor* fused behind the *cya* gene	This work

Constructs for creating deletion mutants

Construction for in-frame deletion were based on the instable vector pWHM3

(Vara *et al.*, 1989), essentially as described in Chapter II. For the deletion of *sflA*, its upstream region -1336/+9 (using primers sflA_LF-1339 and sflA_LR+9) and downstream region +427/+1702 (using primers sflA_RF_427 and sflA_RR+1702) were amplified by PCR from *S. coelicolor* M145 genomic DNA and cloned into pWHM3 as EcoRI-HindIII fragments, and the apramycin resistance cassette *aac(3)IV* flanked by *loxP* sites inserted in between. This resulted in plasmid pGWS750 that was used for deletion of *sflA* (SCO1749). The presence of *loxP* sites allows efficient removal of apramycin resistance cassette by Cre-recombinase (Fedoryshyn *et al.*, 2008). The same strategy was used to create construct pGWS751 for the deletion of *sflB* (SCO5967). This plasmid contained the -1258/+9 and +357/+1917 regions relative to *sflB*, and the apramycin resistance cassette inserted in-between. The *sflA* and *sflB* double mutant (GAL16) was constructed in the background of a *sflA* in-frame deletion mutant (GAL14) by deleting *sflB*.

Constructs for the expression of eGFP fusion proteins

The *ftsZ* gene with its own promoter and fused to *egfp* was excised from pKF41 as a BglII-NotI fragment, and cloned into pSET152 digested with BamHI-NotI. Subsequently, the *ftsZ* coding region was removed after digestion with StuI-BamHI and replaced by the coding region of *sflA* (amplified from *S. coelicolor* genomic DNA using primers sflA_F+1 and sflA_R+438), *sepF* (primers sepF_F+1 and sepF_R+639) or *sflB* (primers sflB_F+1 and sflB_R+408). This resulted in constructs pGWS759, pGWS760 and pGWS761, for the expression of SflA-eGFP, SepF-eGFP and SflB-eGFP, respectively.

Constructs for enhanced gene expression

To obtain enhanced expression of *sepF, sflA* and *sflB*, the genes were inserted behind the constitutive *ermE* promoter and an optimized ribosome binding site using plasmid pHM10a (Motamedi *et al.*, 1995). For this, DNA fragments harbouring the entire *sflA*, *sepF* or *sflB* coding region were amplified by PCR from *S. coelicolor* M145 genomic DNA using primer pairs sflA_F+4 and sflA_R+447, sepF_F+4 and sepF_R+648 and sflB_F+4 and sflB_R+417, respectively and cloned into pHM10a. The inserts of the pHM10a-based constructs were subsequently transferred to pWHM3 to generate pGWS774 (for expression of *sflA*), pGWS775 (for *sepF*) and pGWS776 (for *sflB*).

Constructs for BACTH screening

The entire coding region of *sflA* was amplified from *S. coelicolor* M145 genomic DNA using primer pair sflA-fw and sflA-rv, and cloned as an XbaI-KpnI

fragment into pUT18 and pKT25 to generate pBTH165 and pBTH167, respectively. *sepF* was amplified using primers sepF-fw and sepF-rv and cloned into pUT18 and pKT25 as an XbaI-XmaI fragment to generate pBTH109 and pBTH111, respectively. Finally, *sflB* was amplified from *S. coelicolor* M145 genomic DNA using primer pair sflB-fw and sflB-rv, cloned as an XbaI-KpnI fragment into pUT18 and pKT25, so as to generate pBTH169 and pBTH171, respectively.

Table 3. Oligonucleotides

Name	5'-3' sequence[#]
sflA_LF -1336	GTCA**GAATTC**GTTGAAGGTGCCGCAGCACATCTG
sflA_LR +9	GTCAGAAGTTATCCATCACC**TCTAGA**CGATCCCATGGACGCCTCCTCTCA
sflA_RF+427	GTCAGAAGTTATCGCGCATC**TCTAGA**TTCAACCAGAGCTGAGGCGGGGCC
sflA_RR +1702	GTCA**AAGCTT**CCCATGGCCGCGTCCCCGAAGTT
sflB_LF-1258	GTCA**GAATTC**GAACTGCACCATCAGGTAGGCGT
sflB_LR+9	GTCAGAAGTTATCCATCACC**TCTAGA**CGATTTCACTCGCCTTCATTGCCTGCA
sflB_RF +357	GTCAGAAGTTATCGCGCATC**TCTAGA**ACGTCTTCCTGCTGACCCCGGCG
sflB_RR+1917	GTCA**AAGCTT**CGGTCACGGGCTCAGGTGTACCA
sflA_F +1	GTCAGAATTC**AGGCCT**TCGACATGGGATCGGTACGCAAGGCG
sflA_R +438	GCTA**GGATCC**CTCTGGTTGAAGAATCCGTC
sepF_F +1	GTCAGAATTC**AGGCCT**TCGACATGGCCGGCGCGATGCGCAAG
sepF_R +639	GTCAAAGCTT**GGATCC**CTCTGGTTGAAGAACCCGCC
sflB_F +1	GTCAGAATTC**AGGCCT**TCGACGTGAAATCGGGGGAGCCGGTG
sflB_R +408	GTCA**AGATCT**ACTCCCGGCACCCCCGCCGC
sflA_F+4	GCTAGAATT**CATATG**GGATCGGTACGCAAGGCGAGT
sflA_R+447	GCTA**AAGCTT**CCCGCCTCAGCTCTGGTTGAA
sepF_F+4	GTCAGAATT**CATATG**GCCGGCGCGATGCGCAAGATG
sepF_R+648	GTCAAAGCTT**GGATCC**TAGTGCGTCTCAGCTCTGGTT
sflB_F+4	GTCAGAATT**CATATG**AAATCGGGGGAGCCGGTGAAC
sflB_R+417	GTCA**AAGCTT**GGACCGTCACACTCCCGGCAC
sflA-fw	CGC**TCTAGA**CATGGGATCGGTACGCAAGGC
sflA-rv	CGG**GGTACC**CAGCTCTGGTTGAAGAATCCG
sepF-fw	CG**TCTAGA**CATGGCCGGCGCGATGCGC
sepF-rv	CT**CCCGGG**AGCTCTGGTTGAAGAACCCGCC
sflB-fw	CGC**TCTAGA**AGTGAAATCGGGGGAGCCGGT
sflB-rv	CGG**GGTACC**CACACTCCCGGCACCCCCGCC

[#]Restriction sites used for cloning are underlined and in bold. GGATCC, BamHI; AGATCT, BglII; GAATTC, EcoRI; AAGCTT, HindIII; GGTACC, KpnI; CATATG, NdeI; AGGCCT, StuI; TCTAGA, XbaI; CCCGGG, XmaI.

Microscopy

Light microscopy

Sterile cover slips were inserted at an angle of 45 degrees into SFM agar plates, and spores of *Streptomyces* strains were carefully inoculated at the intersection angle. After incubation at 30°C for 3 to 5 days, cover slips were positioned on a microscope slide prewetted 5 µl of 1x PBS. Fluorescence and corresponding light micrographs were obtained with a Zeiss Axioscope A1 upright fluorescence microscope (with an Axiocam Mrc5 camera at a resolution of 37.5 nm/pixel). The green fluorescent images were created using 470/40 nm band pass (bp) excitation and 525/50 bp detection, for the red channel 550/25 nm bp excitation and 625/70 nm bp detection was used (Willemse and van Wezel, 2009). For membrane staining FM5-95 was used. For stereomicroscopy we used a Zeiss Lumar V12 stereomicroscope. All fluorescence images were background corrected setting the signal outside the hyphae to zero to obtain a sufficiently dark background. These corrections were made using Adobe Photoshop CS4.

Electron microscopy

Morphological studies on surface grown aerial hyphae and/or spores by cryo-scanning electron microscopy were performed using a JEOL JSM6700F scanning electron microscope as described previously (Colson *et al.*, 2008). Transmission electron microscopy (TEM) for the analysis of cross-sections of hyphae and spores was performed with a FEI Tecnai 12 BioTwin transmission electron microscope as described (Noens *et al.*, 2005).

BATCH complementation assay

For BACTH complementation assays, recombinant pKT25 and pUT18 harboring genes of interest were used in various combinations to co-transform *E. coli* BTH101 cells. The trans- formants were plated onto LB-X-Gal-IPTG medium containing ampicillin (100 mg/mL) and kanamycin (50 mg/mL), IPTG (0,5 mM) and X-gal (5-bromo-4-chloro-3-indolyl-β-D-galactopyranoside, 40 µg/mL) and were incubated for 24–36 h at 30°C.

Computer analysis

For DNA and protein searches we used StrepDB (http://strepdb.streptomyces.org.uk/). Phylogenetic analyses and gene synteny analysis were performed by using STRING (http://string.embl.de).

RESULTS

Three *sepF*-like genes in *Streptomyces*

Three genes with homology to *sepF* were found on the *S. coelicolor* genome. The *sepF* gene itself is SCO2079 and lies in the *dcw* cluster in close proximity to *ftsZ* (see also Chapter 1). Two *sepF*-like (*sfl*) genes, *sflA* (SCO1749) and *sflB* (SCO5967), are located elsewhere on the *S. coelicolor* chromosome. SepF is a predicted 213 aa protein, while SflA and SflB are 145 and 136 aa long, respectively. With that, SflA and SflB have lengths very similar to that of SepF of *Bacillus subtilis* (139 aa; accession number KFK80720). An alignment of the three proteins and their comparison to SepF of *B. subtilis* is presented in Figure 1. SepF of *S. coelicolor* has a 66 aa internal extension that runs from aa residues 45-110. The presence of three *sepF*-like genes is typical of streptomycetes, but *sflAB* are absent from many other actinomycetes.

Figure 1. Alignment of SepF proteins. Amino acid sequences of SepF proteins from *B. subtilis* (SepFbs) and *S. coelicolor* (SepFsc), and two SepF paralogs of *S. coelicolor* (SflA and SflB) were aligned using Boxshade program. Identical residues are shaded in black; conservative changes are shaded in grey.

Deletion of *sflA* and *sflB* affects colony morphology

Single mutants of *S. coelicolor* M145 in which either *sflA* or *sflB* was deleted or an *sflAB* double mutant were created using essentially the same strategy as described elsewhere in this thesis (see Chapters II and III; for constructs see

Materials and Methods section). The *sfl* single and double mutants sporulated well on SFM agar plates, developing abundant aerial mycelium and grey-pigmented spores (Fig. 2). However, when single colonies were analyzed in more detail, differences in colony morphology were observed. *S. coelicolor* M145 formed colonies with a smooth edge, while those of *sflA* or *sflB* mutants had a more 'fluffy' phenotype, and this was even more obvious in the *sflAB* double mutant (Fig. 2). First visual assessment of the vegetative hyphae showed that the hyphae of the *sfl* mutants had enhanced (around 50% increased) branching frequency as compared to wild-type hyphae.

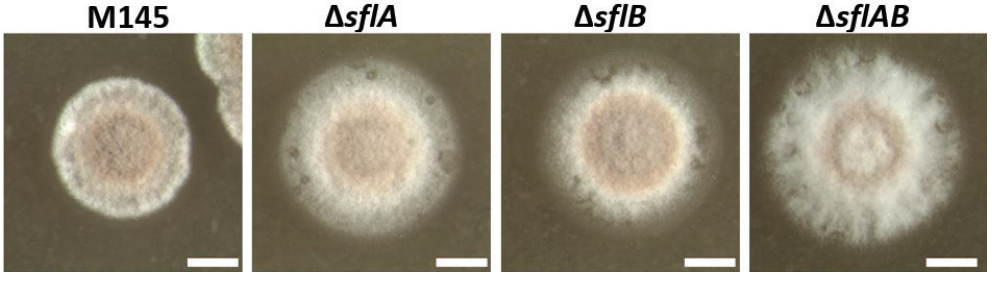

Figure 2. Phenotypic analysis of *sfl* mutants. Stereomicrographs show representative colonies of *S. coelicolor* M145 and its *sflA* and *sflB* null mutants. Strains were grown on SFM agar plates for three days at 30^{0}C. Colonies of *sfl* mutants were 'fluffier' than those of the parental strain M145. Bar, 2 mm.

sflA and *sflB* mutants have branching aerial hyphae

Surface-grown *S. coelicolor* M145, Δ*sflA*, Δ*sflB* and Δ*sflA*Δ*sflB* were analyzed in more detail by scanning electron microscopy (SEM). After three days of growth, *S. coelicolor* M145 produced abundant and regular spore chains (Fig. 3A). However, strains lacking *sflA* (*i.e.* both Δ*sflA* and Δ*sflA*Δ*sflB*) produced significantly fewer spore chains (Fig. 3B & 3D), while the *sflB* mutant produced a comparable amount of spore chains as the parental strain M145 (Fig. 3C). After prolonged incubation, sporulation of strains lacking *sflA* sporulated more abundantly, which suggests that sporulation was delayed in the mutants (data not shown). A more striking phenotype of *sflA* and *sflB* null mutants was that they frequently produced branching spore chains, which is never observed in the wild-type strain (Fig. 3E-G).

Transmission electron microscopy (TEM) allowed imaging of thin sections and this again revealed branching spore chains in *sflA* and *sflB* mutants (Fig. 4, arrows). Furthermore, variation in sizes within spore chains was frequently observed. Another obvious difference was that while wild-type spores had a

typical dark spore wall and well-condensed DNA, the spores of the mutants typically had lighter spore walls as well as less clearly visible DNA in many of the spores (Fig. 4). This suggests pleiotropic changes in spore maturation in the *sflA* and *sflB* mutants.

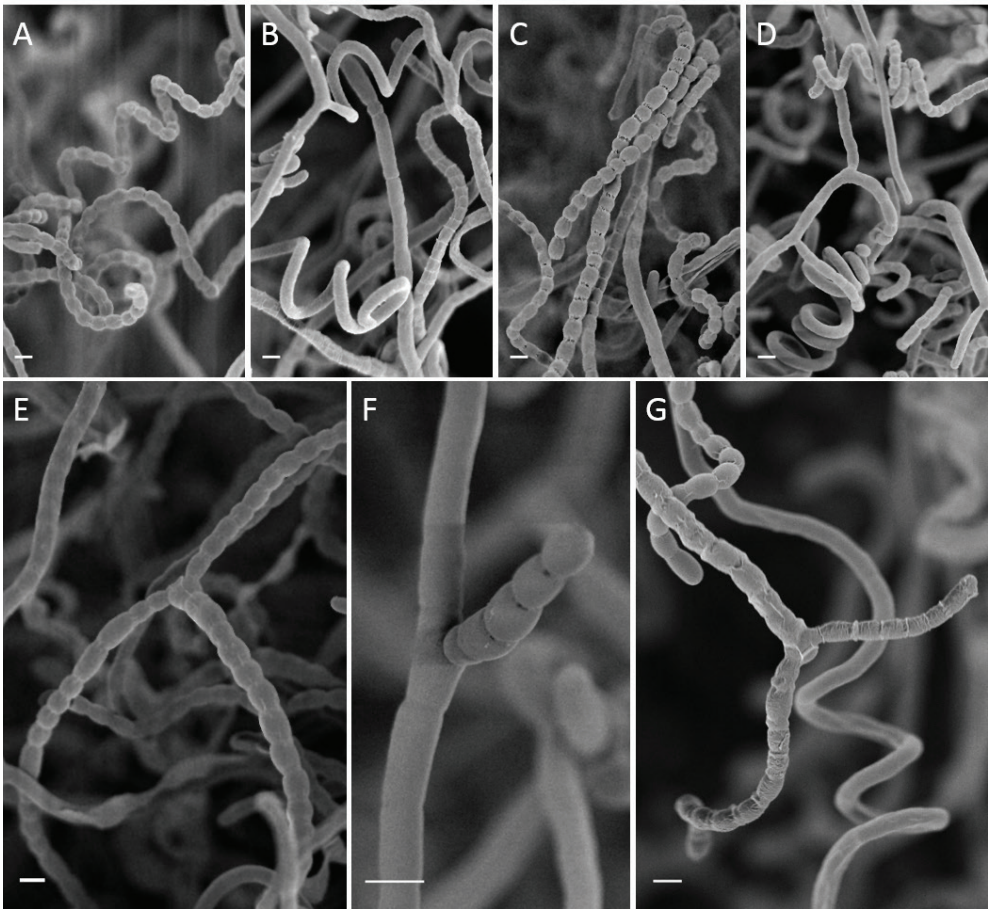

Figure 3. Cryo-scanning electron micrographs of spore chains of *S. coelicolor* M145 and its *sfl* mutants. Wild-type *S. coelicolor* M145 **(A)** sporulated abundantly after three days of incubation, while mutants lacking either *sflA* **(B & E)** or *sflAB* **(D & G)** showed reduced sporulation; the *sflB* null mutant **(C & F)** produced comparable amount of spores as the parental strain. Most notable change in all mutants was that the spore chains frequently branched. Bar, 1 μm.

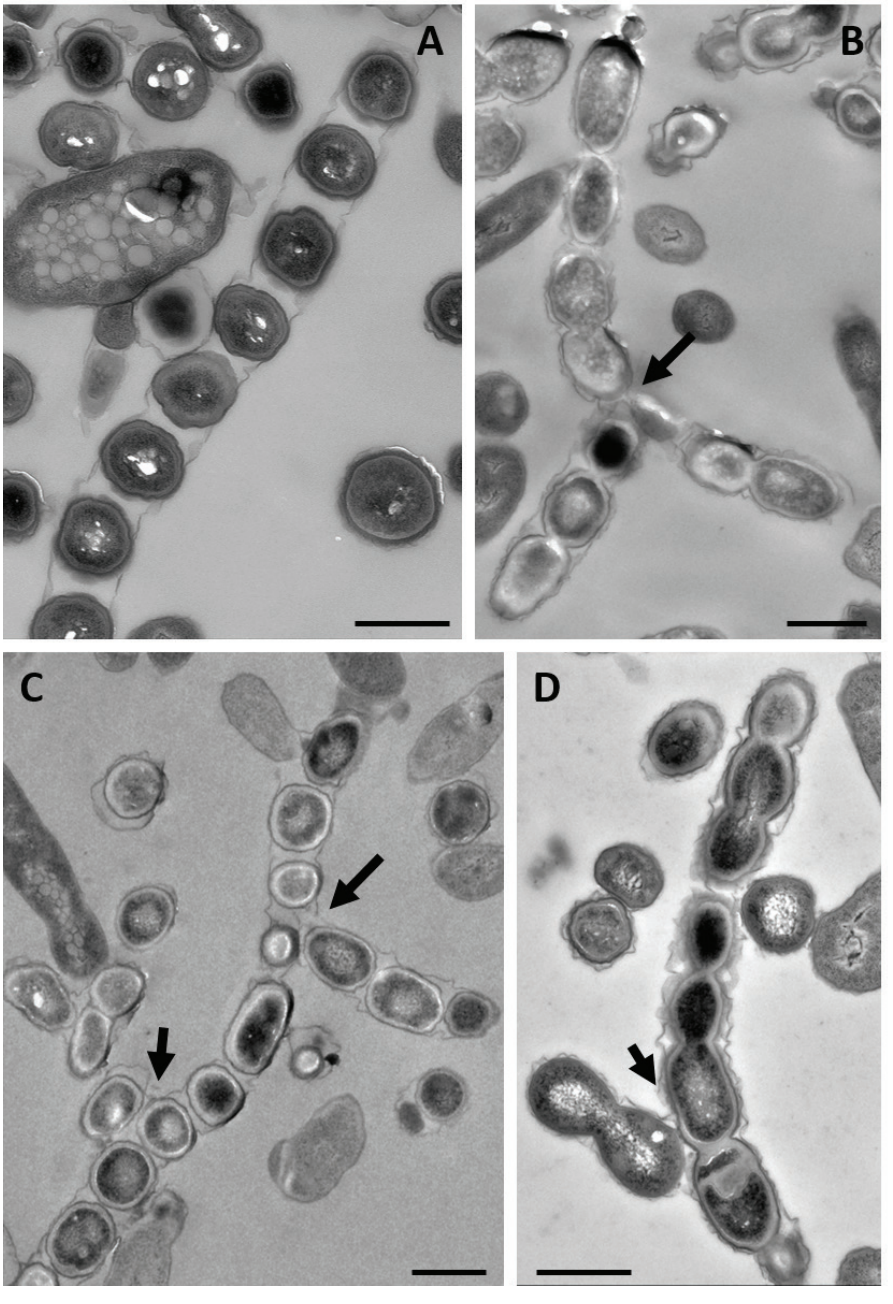

Figure 4. Transmission electron micrographs of spore chains of *S. coelicolor* M145 and its *sfl* mutants. While spore chains of wild type M145 **(A)** do not branch and contain regularly sized spores, mutant lacking either *sflA* **(B)**, *sflB* **(C)** or *sflAB* **(D)** produce irregular spores and spores chains frequently branch, in line with the SEM images (Figure 3). Cultures were grown on SFM agar plates for 5 days at 30^{0}C. Bar, 1 μm.

Localization of SflA and SflB *in S. coelicolor*

To analyze the localization of the SepF paralogs, constructs based on the integrative vector pSET152 were made containing in-frame fusion of *sepF* with *egfp* (for details see Materials and Methods section). These allow expression of *sflA-egfp*, *sepF-egfp* and *sflB-egfp* from the *ftsZ* promoter and were called pGWS759, pGWS760 and pGWS761 respectively. The constructs integrated at the ΦC31 attachment site on the *S. coelicolor* M145 chromosome.

In *B. subtilis*, $SepF^{Bs}$ localizes to division sites (Ishikawa *et al.*, 2006; Hamoen *et al.*, 2006). During vegetative growth of *S. coelicolor*, we failed to detect specific localization for SepF or SflAB (data not shown). In aerial hyphae, SepF localize to septum sites as $SepF^{Bs}$. It formed foci at either side of the hyphae, which most likely represented septum sites (Fig. 5A). And eventually, SepF-eGFP localized in a lader-like pattern, which co-stained with the septa as seen by membrane staining (Fig. 5A). The similar localization profiles of the SepF proteins from *B. subtilis* and *S. coelicolor* suggests that *Streptomyces* SepF plays a very similar role in cell division as *Bacillus* SepF.

SflA-eGFP formed foci at many positions along the entire lateral wall of the aerial hyphae, and often formed bright foci at apical sites (Fig. 5B, arrow). The pattern of SflA-eGFP localization varied, with foci that were widely spaced, distributed more symmetrically or clustered closely together (Fig. 5B, star). SflA-eGFP foci were only seen in aerial hyphae in which septum synthesis had not yet initiated (Fig. 5B). SflA-eGFP was not detected in mature spores. In early aerial hyphae, SflB-eGFP showed a similar localization pattern as SflA-eGFP, forming foci at hyphal tip and along the lateral wall of the aerial hyphae (Fig. 5C, **α**). SflB-eGFP localized in a ladder-like pattern prior to the initiation of septum synthesis (Fig. 5C, **β**). Interestingly, the 'sports' of the ladders formed by SflB were shorter than those formed by SepF or FtsZ, and did not span the entire width of the hyphae. Instead, they were biased towards the central part. This suggests that SflB stays away from the sites where cell division is initiated. At the time when septa were seen (with FM5-95 staining of membranes), ladder-like structure of SflB-eGFP largely disappeared (Fig. 5C, **γ**). This suggests that in contrast to SepF, SflB only localizes to the central part of the septum, and only during the onset of sporulation-specific cell division.

5A

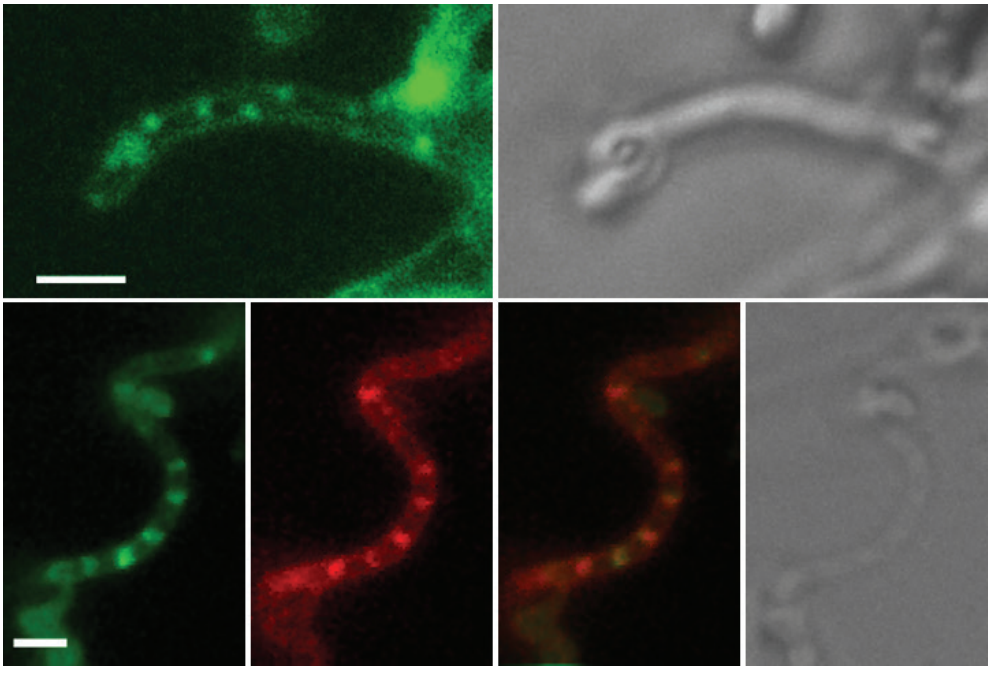

5B

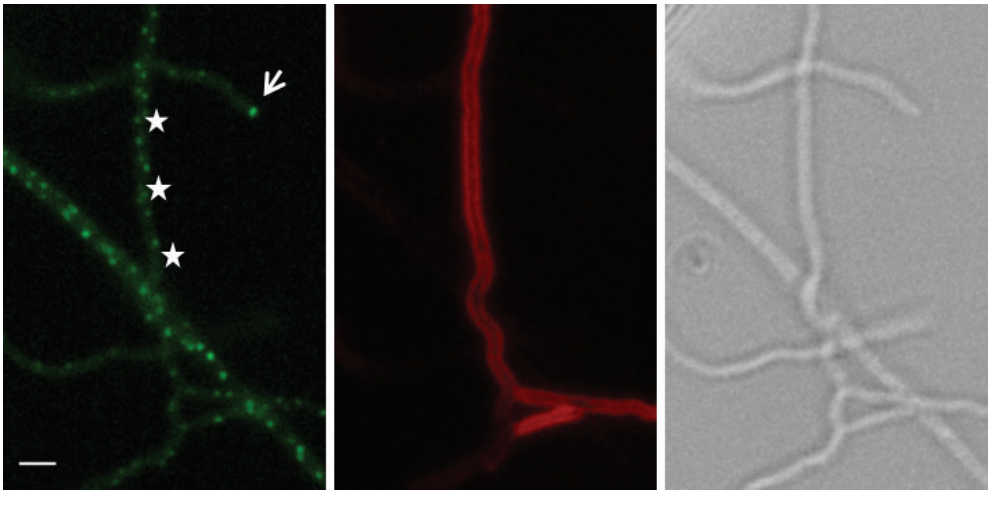

5C

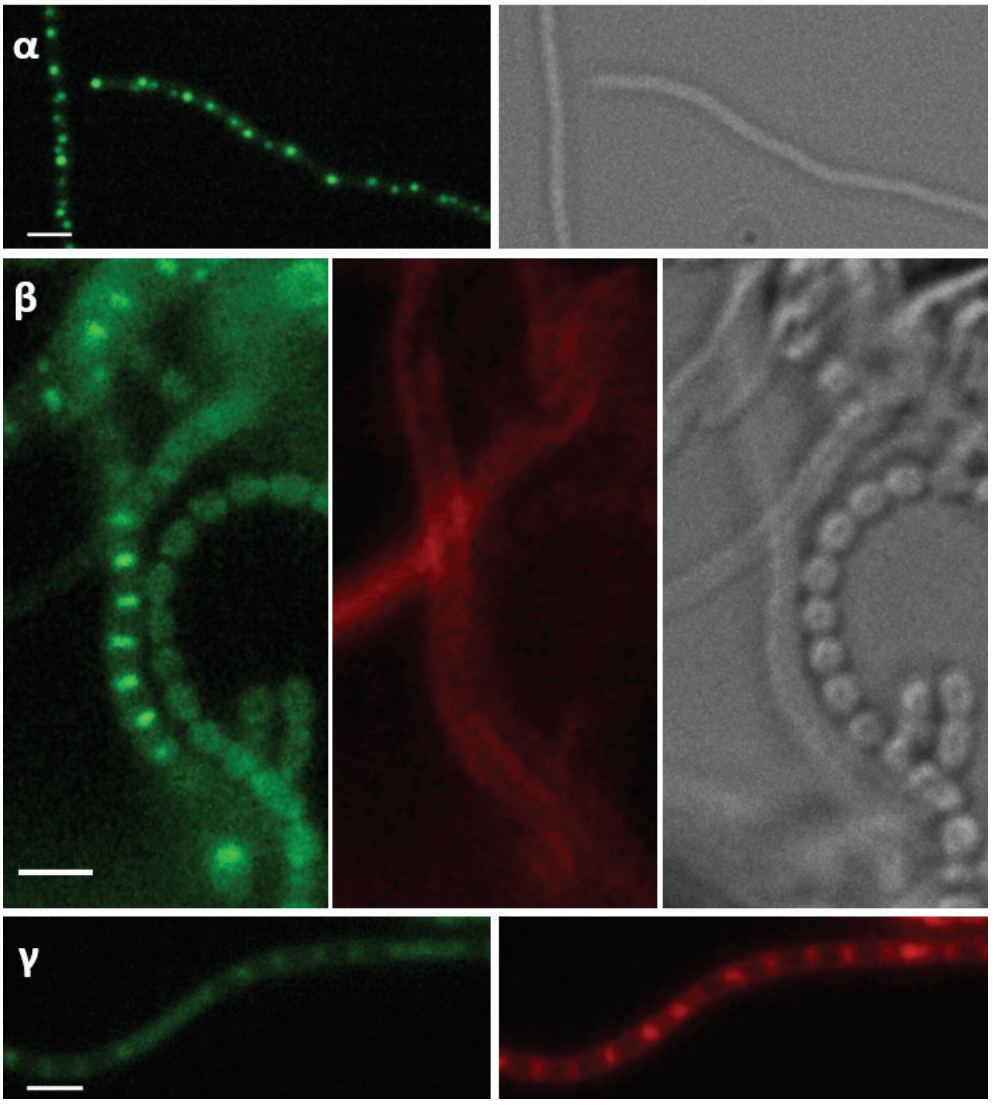

Figure 5. Localization of SepF-eGFP, SflA-eGFP and SflB-eGFP in *S. coelicolor*. Sporogenic aerial hyphae of *S. coelicolor* M145 were imaged by fluorescence microscopy visualizing the eGFP fusion proteins, membrane (stained with FM5-95; red), the merged image and corresponding light micrograph. **A.** SepF-eGFP localized in a ladder-like pattern that overlapped the sporulation septa. **B.** SflA-eGFP formed foci along aerial hyphae (star) and at apical tip (arrow) prior to septum synthesis. **C.** SflB-eGFP had similar localization pattern as SflA-eGFP in early aerial hyphae (α), while in sporogenic hyphae SflB-eGFP localized in a ladder-like pattern prior to septum synthesis (β), and SflB-eGFP ladders vanished septal membranes formed (γ). Bar, 2 μm.

Effect of enhanced expression of the *sepF* and *sfl* genes

To study the effect of overexpression of SepF paralogs in *S. coelicolor*, the *sflA*, *sepF* and *sflB* genes were all cloned individually behind the *ermE* promoter region with an optimized ribosome binding site (see Materials and Methods for details), and the expression cassettes were then inserted in the multi-copy shuttle vector pWHM3. The expression constructs were designated pGWS774, pGWS775 and pGWS776, respectively. Plasmid pWHM3 is unstable in *Streptomyces* and this is not only useful for gene disruption but also for varying the expression level. Indeed, the copy number of pWHM3 is largely dependent on the level of thiostrepton, and increasing the thiostrepton concentration allows the proportional increase of its copy number. Strains GAL44, GAL45, GAL46 and GAL70 (*S. coelicolor* M145 transformed with pGWS774, pGWS775, pGWS776 or control pWHM3) were plated onto R5 agar plates with different concentration of thiostrepton and the colony morphology was investigated after 5 days of incubation (Fig. 6).

On R5 agar plates without thiostrepton, all colonies had normal development and comparable colony size (Fig. 6). However, in the presence of thiostrepton (20 μg/ml), the colonies harboring the SflA and SflB expression constructs were blocked in development, while those expressing SepF produced aerial hyphae but formed significantly smaller colonies indicative of growth inhibition (Fig. 6). Interestingly, colonies of either GAL44 (expressing SflA) or GAL46 (expressing SflB) did not attach to the agar surface. This is shown clearly by touching colonies with a toothpick, which resulted in mashed up but fixed colonies for control plasmid (GAL70) as well as for colonies expressing SepF (GAL45), while colonies expressing SflA or SflB were moved easily over the plate. When the thiostrepton concentration was increased to 50 μg/mL, colonies of GAL44 and GAL46 more or less floated on the agar surface, while those of GAL70 and GAL45 were still firmly attached to the agar surface (not shown). Furthermore, in particular GAL44 produced very small colonies (Fig. 6). Taken together, this suggests that forced expression of SflA and SflB in the vegetative mycelium alters colony morphology and blocks development, while enhanced expression of SepF does not affect development, but also reduces colony size.

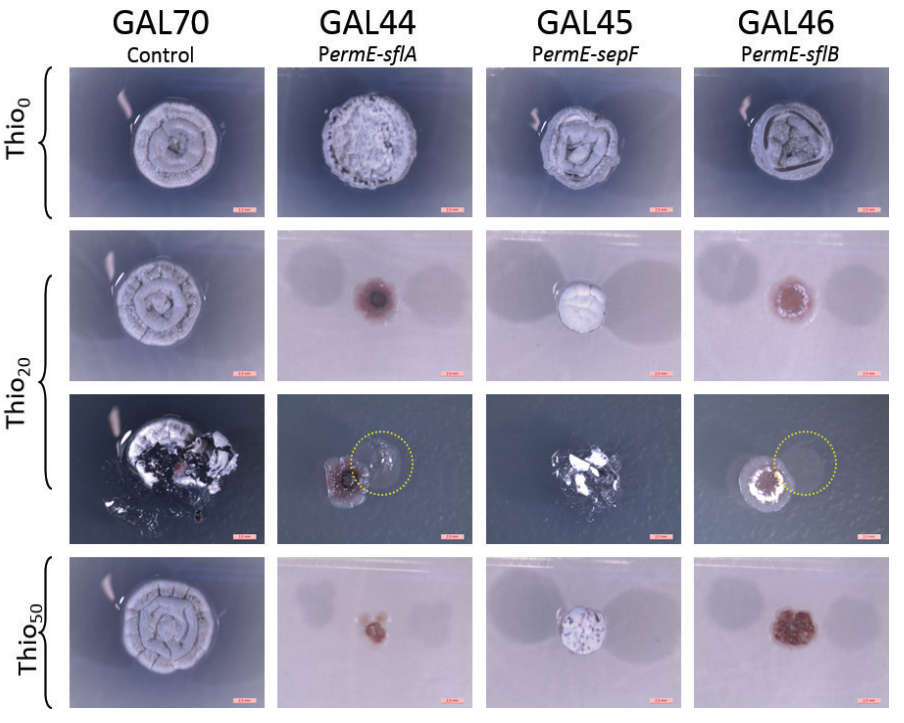

Figure 6. Effect of enhanced expression of *sepF* and *sfl* genes on colony morphology. Stereomicrographs showing the phenotype of GAL70 (*S. coelicolor* M145 + empty plasmid pWHM3 control), GAL44 (M145 + pGWS774, expressing *sflA*), GAL45 (M145 + pGWS775, expressing *sepF*) and GAL46 (M145 + pGWS776, expressing *sflB*) were grown on R5 agar plates containing different concentrations of thiostrepton (0-50 mg/ml). Plates were incubated for 5 days at 30^0C. Note that colonies overexpressing either *sflA* or *sflB* were blocked in development and had lost the ability to adhere to the agar surface, while overexpression of *sepF* primarily reduced colonial size while colonies adhered normally. Bar, 2 mm.

Direct interactions between the *sepF* paralogs

To examine possible interaction between the SepF and Sfl proteins, we performed two-hybrid screening using the bacterial two-hybrid system (see the Materials and Methods section for details). The result is displayed in Figure 7. The data showed that SflB directly interacts with SflA, SepF and also with itself, while no interaction was observed between SepF and SflA. Surprisingly, no self-interaction was seen for SepF. This indicates that the SepF-Cya fusion protein may not be entirely functional. Further biochemical and two-hybrid interaction studies are required to get more detailed insight into the way the SepF-like proteins interact with each other and with other (cell division) proteins.

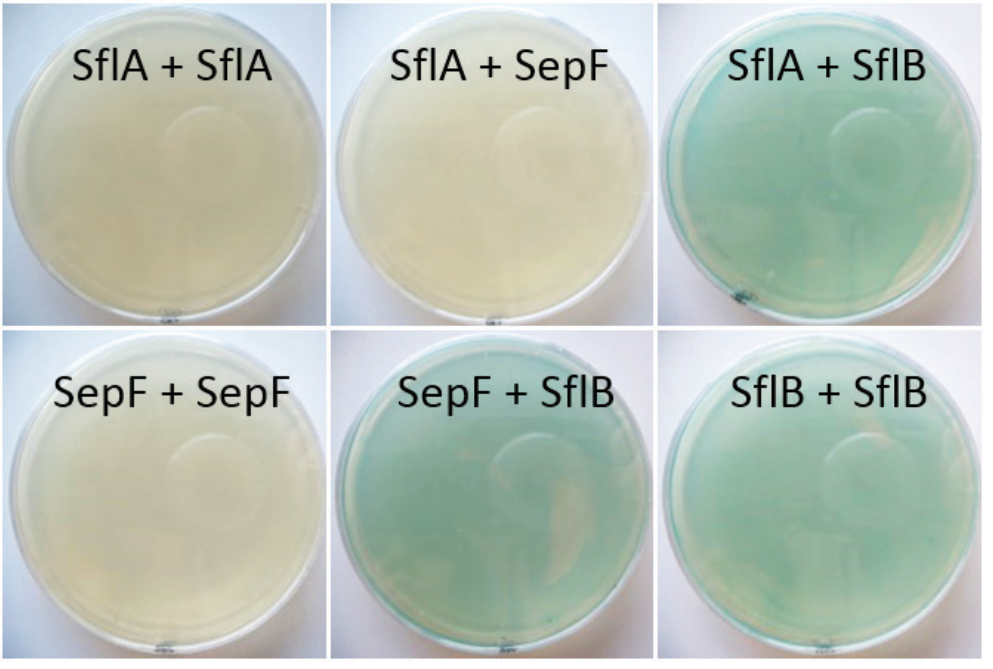

Figure 7. Analysis of protein interaction using the bacterial two-hybrid system. Possible interactions between SflA, SflB and SepF from *S. coelicolor* were assayed on LB agar plates containing X-Gal and IPTG. Blue pigmentation indicates interaction between the partners. SflB interacts with SlfA, SepF and itself. The lack of self-interaction of SepF is surprising and indicates that perhaps the protein is not fully functional.

DISCUSSION

A major question in the developmental biology of *Streptomyces* that we seek to address is, how do *Streptomyces* ensure that septa are controlled properly in time and space in the long and multinucleoid hyphae? We have shown previously that in streptomycetes the correct localization of FtsZ is governed by a rather unique system of positive control, whereby the actinomycete-specific SsgA and SsgB proteins recruit FtsZ to the septum sites to initiate sporulation-specific cell division (Willemse *et al.*, 2011). As a consequence, deletion of either *ssgA* or *ssgB* blocks sporulation (van Wezel *et al.*, 2000b; Keijser *et al.*, 2003). In Chapter 2 we added a new chapter to this story by providing evidence that SepG (YlmG in *B. subtilis*) is the protein that allows SsgB to dock to the membrane. Still, the question remains how the perfect spacing of the Z-rings in the aerial hyphae is governed, resulting in up to a 100 septa that are formed simultaneously, visualized as a spectacular ladder of FtsZ-GFP.

In this work we present another piece of the jigsaw, which points at the possible existence of a layer of negative control, which revolves around the SepF-like proteins SflA and SflB. Typical ladders of Z-rings were produced in both wild type *S. coelicolor* and in *sflA* or *sflB* null mutants, while the average distance between adjacent Z-rings in mutants was shorter compared to that of in wild-type *S. coelicolor*. The difference was most noteworthy in *slfA* null mutants. In wild-type hyphae, the average distance between neighboring Z-rings was 734 ± 146 nm, while it was reduced to 598 ± 134 nm and 672 ± 111 nm in *sflA*- and *sflB*-null mutants respectively, and 618 ± 135 nm in the *sflAB*-null mutant. It highlights the possibility that SflA plays a role in determining the (distance between the) septum sites.

In aerial hyphae, SflA and SflB localize primarily in young sporogenic aerial hyphae at the stage prior to septum formation, suggesting they start functioning in early aerial hyphae stage, possibly before FtsZ polymerization. An important observation is that SflB interacts with SepF as evidenced by two-hybrid studies, suggesting the protein may compete directly with SepF, *e.g.* by forming hetero-multimers. SflB also interacts with SflA and with itself. It should be noted that SflA and SepF share significant homology in particular in their C-terminal parts, with 74% aa identity (88% similarity) between residues 135-192 of SepF and residues 62-119 of SflA. The rest of the protein shows significantly lower homology. The C-terminal part of SepF is known to interact with FtsZ (Duman *et al.*, 2013), and the high degree of conservation suggests that SflA may also interact with FtsZ, although this remains to be proven. However, the fact that this domain is the only region that is well con-

served between SepF and SflA suggests that it also candidates for interaction with SflB.

Interestingly, SflA localized in many foci along the hyphal wall, while SflB localized at the middle of the septum, but away from the hyphal wall. While more extensive studies are required, these initial data suggest that as a net result, SflB leaves a gap at the intersection between the future septum and the lateral wall of the aerial hyphae. If indeed SflB interferes with SepF function by direct interaction, SepF will therefore be present precisely where it should be active, namely at the site where Z-ring formation is initiated following the recruitment by SsgB. We therefore hypothesize that SflB may function to block premature SepF polymerization away from the lateral wall. While localization of SflA-eGFP and SflB-eGFP fusion proteins was primarily seen in the aerial hyphae, it should be noted that many vegetative hyphae will have stopped growing, and only occasional septa occur in vegetative hyphae. Furthermore, enhanced expression of SflA and SflB has a distinct effect on colony morphology and surface attachment by the vegetative hyphae. Therefore, more extensive studies are required to establish what role SflAB play in branching of vegetative hyphae.

The most striking phenotype of *sflA* and *sflB* mutants is the extensive branching of the aerial hyphae. Furthermore, forced expression of SflA and SflB from a constitutive promoter largely blocked aerial growth and reduced adhesion of the colonies to the agar surface, indicating that branching is impaired in the vegetative mycelium. Conversely, deletion of *sflA* or *sflB* results in hyper-branching and in particular branching at non-canonical sites, as evidence by the branching aerial hyphae. These data strongly suggest an inverse correlation between the expression level of SflA and SflB and branching frequency. How can these data be explained if SepF controls cell division? The most obvious link is *divIVA*, which lies two genes downstream of *sepF* and next to the septum-localizing *sepG*. DivIVA is required for driving apical growth, and hence branching, and a high branching frequency is typical of strains over-expressing DivIVA (Flärdh, 2003a). Interestingly, initial experiments using two-hybrid studies revealed weak but significant interaction between SflB and DivIVA, which suggests that SflB may act via direct interaction with (and inhibition of) DivIVA which would indeed explain the inverse correlation between SflB expression and branching frequency (data not shown). SflA may compete indirectly with DivIVA through SflB, since clear interaction was observed between SflA and SflB in bacterial two-hybrid studies. The competition between SflA/SflB and DivIVA may serve to ensure that tip extension and branching are stopped at the right time to initiate development of the

sporogenic aerial hyphae into spore chains, but this speculative idea requires further substantiation by experiments.

IV

ylmD and *ylmE* are required for sporulation-specific cell division and control the flux of D-Ala in *Streptomyces coelicolor*

Le Zhang, Joost Willemse, Lizah van der Aart, Paul Hoskisson

and Gilles P. van Wezel

Manuscript in preparation

ABSTRACT

Streptomycetes are multicellular filamentous bacteria that undergo a complex developmental program resulting in sporulation. Many of the proteins that govern the complex process of multiple septation in the aerial hyphae are yet to be uncovered. Here we show that the genes *ylmD* (SCO2081) and *ylmE* (SCO2080), which lie in operon with the *ftsZ* in actinomycetes and firmicutes, are required for correct spore wall synthesis. YlmD and YlmE are not part of the divisome, but instead localize as foci with a regular spacing in young aerial hyphae, while during spore maturation YlmE forms distinct rings close to the spore wall. Electron and fluorescence microscopy demonstrated that in particular *ylmE* mutants display a highly aberrant phenotype with defective cell-wall synthesis, and produced very few spores that lack a thick spore wall. The sporulation defect of the *ylmE* mutant as well as its sensitivity to the antibiotic D-cycloserine could be rescued at least in part by the addition of D-alanine, consistent with a role of YlmE in maintaining the D-Ala pool. However, biochemical analysis showed that only Alr (SCO4745) acts as an alanine racemase *in vitro* and is essential for producing D-Ala *in vivo*, while no *in vitro* or *in vivo* racemase activity was observed for YlmE. We therefore propose that YlmE controls sporulation by tuning the flux of D-Ala.

INTRODUCTION

The major constituent of the bacterial cell wall is peptidoglycan, which consists of glycan strands composed of alternating N-acetylglucosamine (GlcNAc) and N-acetylmuramic acid (MurNAc) molecules, whereby the individual strands are linked together by a pentapeptide chain bridging the MurNAc residues. The composition of the pentapeptide varies between microorganisms, but contains both L- and D-amino acids, some of which are modified. In *Streptomyces*, the pentapeptide chain consists of L-alanine (L-Ala), D-glutamic acid (D-Glu), LL-diaminopimelic acid (Dap) and two consecutive D-alanine (D-Ala) residues at the end, of which the terminal D-amino acid can be cleaved off to create a glycine bridge. There is room for small changes in the pentapeptide chain, although the final D-Ala-D-Ala subunit is extremely well conserved. The final D-Ala is exchanged for a D-lactic acid (D-Lac) in the case of vancomycin resistance (Vollmer et al., 2008). Specific enzymes catalyze the transamination and racemization of L-amino acids to the D-enantiomer (Radkov and Moe, 2014). One of these is alanine racemase or Alr, which is essential for growth in most bacteria (Hols *et al.*, 1997; Milligan *et al.*, 2007).

During cell division, peptidoglycan synthesis needs to be coordinated with increase of the cell size, timely genome replication and segregation and septum synthesis followed by cell fission. The prokaryotic cell division scaffold is formed by the tubulin homolog FtsZ (Bi and Lutkenhaus, 1991), which forms a contractile ring (or Z-ring) that mediates the recruitment of the cell division machinery to the mid-cell position (reviewed in (Goehring and Beckwith, 2005; Adams and Errington, 2009)). In unicellular bacteria, cell division results in two identical daughter cells that each contain a single copy of the chromosome. Most of the genes in the *dcw* cluster for proteins involved in cell division and cell-wall biosynthesis have been studied extensively and their functions have been well characterized. Surprisingly however, little is known of the genes *ylmD* and *ylmE* that lie immediately downstream of, and likely in operon with, *ftsZ* (SCO2082) on the *S. coelicolor* genome. The operon structure is *ftsZ*-SCO2081-SCO2080, based on the very close proximity of the genes and on transcription data (Romero A *et al.*, 2014). The genes were previously implicated in the production of D-amino acids for cell-wall synthesis (Kolodkin-Gal *et al.*, 2010). Mutants of *E. coli* lacking the *ylmE* ortholog *yggS* had a radical change in the amino acid pool, with enhanced concentrations of the branched chain amino acids valine and leucine, as well as of α-ketoglutarate (Ito *et al.*, 2013). This most likely led to reduced levels of coenzyme A (CoA), which was supported by the full restoration of *yggS* mutants by the CoA pre-

cursor pantothenate (Vitamin B5). Interestingly, introduction of *ylmE* from *B. subtilis* also complemented the *yggS* null mutant. These data suggest a role for YlmE in amino acid metabolism.

In this chapter we demonstrate that YlmD and YlmE play a crucial role in cell-wall synthesis during sporulation, and probably affect the pool of D-Ala required for PG synthesis.

MATERIALS AND METHODS

Bacterial strains and media

All bacterial strains used in this study are listed in Table 1. *E. coli* JM109 was used for routine cloning and ET12567 to prepare nonmethylated DNA to bypass the methyl-specific restriction system of *S. coelicolor* (MacNeil *et al.*, 1992). *E.coli* strains were propagated in Luria broth, where appropriate supplemented with antibiotics for selection, namely ampicillin (100 μg/ml end concentration), apramycin (50 μg/ml) and/or chloramphenicol (25 μg/ml). *S. coelicolor* A3(2) M145 was obtained from the John Innes Centre strain collection. *S. coelicolor* strains were grown on soya flour medium (SFM) agar plates for phenotype characterization and on R5 agar plates for regeneration of protoplasts. Antibiotics used for screening Streptomyces were apramycin (20 μg/ml end concentration) and thiostrepton (10 μg/ml). Minimal media (MM) agar plates (Kieser *et al.*, 2000) with 1% carbon source (as indicated) was used to detect effect of amino acids on *Streptomyces* mutants growth. *E. coli* strain BL21 DE3 was used for expression of proteins in *E. coli* (Miroux and Walker, 1996).

Table 1. Bacterial strains.

Bacteria strains	Genotype	Reference
E. coli JM109	See reference	(Sambrook *et al.*, 1989)
E. coli ET12567	See reference	(MacNeil *et al.*, 1992)
E. coli BL21 DE3	See reference	(Miroux and Walker, 1996)
S.coelicolor M145	$SCP1^{-}$ $SCP2^{-}$	(Kieser *et al.*, 2000)
MreB-IFD	M145 Δ*mreB*	(Mazza *et al.*, 2006)
K202	M145 + KF41	(Grantcharova *et al.*, 2005)
GAL47	M145Δ*ylmD*	This work
GAL48	M145Δ*ylmE*	This work
GAL99	M145 *alr*:: *aac(3)IV*	This work
GAL100	M145 Δ*ylmE alr*::*aac(3)IV*	This work
GAL49	M145 + pGWS757	This work
GAL50	M145 + pGWS758	This work
GAL52	GAL47 + pKF41	This work
GAL53	GAL48 + pKF41	This work

Plasmids and constructs

All plasmids and constructs described in this chapter are summarized in Table 2. The oligonucleotides used for PCR are listed in Table 3. PCR reactions were performed using Pfu DNA polymerase as described (Colson *et al.*, 2007).

Constructs for the deletion of ylmD, ylmE and alr

The strategy for creating knock-out mutants is based on the unstable multi-copy vector pWHM3 (Vara *et al.*, 1989) as described previously (Świątek *et al.*, 2012). For each knock-out construct roughly 1.5 kb of upstream and downstream region of the respective genes were amplified by PCR from the *S. coelicolor* M145 genome. The upstream region was thereby cloned as an EcoRI-XbaI fragment, and the downstream part as an XbaI-BamHI fragment or XbaI-HindIII fragment, and these were ligated into EcoRI-BamHI- or EcoRI-HindIII-digested pWHM3 (for the precise location of the oligonucleotides see Table 3). In this way, an *XbaI* site was engineered in-between the flanking regions of the gene of interest. This was then used to insert the apramycin resistance cassette *aac(3)IV* flanked by *loxP* sites, using engineered XbaI sites. The presence of the *loxP* recognition sites allows the efficient removal of the apramycin resistance cassette following the introduction of a plasmid pUWL-Cre expressing the Cre recombinase (Fedoryshyn *et al.*, 2008; Khodakaramian *et al.*, 2006). Knock-out plasmids pGWS728, pGWS729 and pGWS1151 were created for the deletion of nucleotide positions +25/+696 of *ylmE* (SCO2080), +25/+705 of *ylmD* (SCO2081) and +11/+1167 of *alr* (SCO4745), whereby +1 refers to the translational start site of the respective genes. This allowed first the replacement by the apramycin resistance cassette. In the case of *ylmD* and *ylmE*, subsequently the apramycin resistance cassette was removed using expression of pUWL-Cre. For the *alr* null mutant the apramycin resistance cassette was not removed.

Constructs for the localization of YlmD and YlmE

The entire coding regions of SCO2080 and SCO2081 (without stop codons) were amplified from the *S. coelicolor* M145 chromosome using primer pairs ylmE_F+1 and ylmE_R+717 and ylmD_F+1 and ylmD_R+726, respectively. The PCR products were digested with StuI/BamHI, and inserted downstream of the native *ftsZ* promoter region and immediately upstream of *egfp* in pHJL401. The latter is a highly stable vector with low copy number that generally results in wild-type transcription levels and is well suited for among others complementation experiments (van Wezel *et al.*, 2000b). Thus con-

structs pGWS757 and pGWS758 were generated that express *ylmE-egfp* and *ylmD-egfp*, respectively, from the native *S. coelicolor ftsZ* promoter region. Plasmid pKF41 expresses *ftsZ-egfp* from its own promoter (Grantcharova *et al.*, 2005). Constructs pGWS757 and pGWS758 were also used to complement *ylmE*- and *ylmD*-null mutants, respectively.

Table 2. Plasmids and Constructs.

Plasmid and constructs	Description	Reference
pWHM3	*E. coli*/*Streptomyces* shuttle vector, high copy number and unstable in *Streptomyces*.	(Vara et al., 1989)
pSET152	*E. coli*/*Streptomyces* shuttle vector, high copy number in *E. coli* and integrative in *Streptomyces*.	(Bierman et al., 1992)
pET15b	*E.coli* vector, expressing N-terminally His_6-tagged proteins using the T7 RNA polymerase.	(Studier and Moffatt, 1986)
pGWS728	pWHM3 containing flanking regions of *S. coelicolor ylmE* (SCO2080), with the apramycin resistance cassette with *loxP* sites inserted as an XbaI fragment between the flanking regions.	This work
pGWS729	pWHM3 containing flanking regions of *S. coelicolor ylmD* (SCO2081), with the apramycin resistance cassette with *loxP* sites inserted as an XbaI fragment between the flanking regions.	This work
pGWS1151	pWHM3 containing flanking regions of *S. coelicolor alr* (SCO4745), with the apramycin resistance cassette with *loxP* sites inserted as an XbaI fragment between the flanking regions.	This work
pUWL-Cre	Plasmid expressing the Cre recombinase.	(Fedoryshyn et al., 2008)
pKF41	integrative construct expressing *ftsZ-egfp* from the natural *ftsZ* promoter region.	(Grantcharova et al., 2005)
pGWS757	pHJL401 harboring *ylmE-egfp* under control of the *ftsZ* promoter region.	This work
pGWS758	pHJL401 harboring *ylmD-egfp* under control of the *ftsZ* promoter region.	This work
pGWS1156	pET15b containing the coding region of *ylmE* inserted as NdeI-BamHI fragment.	This work
pGWS1157	pET15b containing the coding region of *alr* inserted as NdeI-BamHI fragment.	This work
*ermE*p-*ylmE*	pHJL401 harboring *ylmE* under control of the *ermE* promoter.	This work
*alr*p-*ylmE*	pHJL401 harboring *ylmE* under control of the *alr* promoter.	This work
*alr*p-*ylmDE*	pHJL401 harboring *ylmD-ylmE* under control of the *alr* promoter.	This work

Constructs for expression of ylmE during vegetative growth

Constructs were designed to express *ylmE* alone or the *ylmD-ylmE* gene cluster from the *alr* promoter, and *ylmE* from the strong and constitutive *ermE* promoter. Using gene synthesis (carried out by Genscript, La Jolla), the complete genes were positioned behind the -300/-1 region relative to *alr* (SCO4745) or the 300 bp *ermE** promoter (Bibb *et al.*, 1985) and the synthetic DNA fragments were then inserted as EcoRI-HindIII fragments into pHJL401, a stable low-copy shuttle vector (Larson and Hershberger, 1986). This resulted in the constructs *alr*P-*ylmE, alr*P-*ylmDE* and e*rmE*p-*ylmE.*

Table 3. Oligonucleotides.

Name	5'-3' sequence [#]
ylmE_LF-1455	GTCA**GAATTC**CGTCATCCCCAACGACCGGCTGCTG
ylmE_LR+24	GTCAGAAGTTATCCATCACC**TCTAGA**GAGTTCGTGCTTACGGTCCGTCAT
ylmE_RF+697	GTCAGAAGTTATCGCGCATC**TCTAGA**GGAGTCCGACCCAGGCTCGGGTAA
ylmE_RR+2145	GTCA**GGATCC**GTGCTGCTGATCCTGCGGAGGTTC
ylmD_LF-1452	GTCA**GAATTC**GCAGCGCTACGGCTGATCACATAG
ylmD_LR+24	GTCAGAAGTTATCCATCACC**TCTAGA**CACGGTGTCGCGCTGTCCTATCAC
ylmD_RF+706	GTCAGAAGTTATCGCGCATC**TCTAGA**GCGGGCTATGTGTGGCTGGACTGA
ylmD_RR+1951	GTCA**GGATCC**TAGGGCTCTCGTTCGGACACGACC
alr_LF-1238	GTCA**GAATTC**CGCTGTACGCAGTCCGCAT
alr_LR+10	GTCAGAAGTTATCCATCACC**TCTAGA**TCTCGCTCATCGT
alr_RF+1168	GTCAGAAGTTATCGCGCATC**TCTAGA**AACGAATGACGCTCAGC
alr_RR+2401	GTCA**AAGCTT**GTGCTCGCTCGGCGTCACCAGGT
ylmE_F+1	GTCAGAATTC**AGGCCT**TCGACATGACGGACCGTAAGCACGAACTC
ylmE_R+717	GTCAAAGCTT**GGATCC**CCGAGCCTGGGTCGGACTCCGAG
ylmD_F+1	GTCAGAATTC**AGGCCT**TCGACGTGATAGGACAGCGCGACACC
ylmD_R+726	GTCAAAGCTT**GGATCC**TCCAGCCACACATAGCCCGC
ylmE-FW	CTAGGAATT**CATATG**ACGGACCGTAAGCACGAACTC
ylmE-RV	GACT**GGATCC**TTACCCGAGCCTGGGTCGGACTC
alr-FW	CTAGGAATT**CATATG**AGCGAGACAACTGCTCGGC
alr-RV	CTAG**GGATCC**GCGTCATTCGTTGACGTA

[#] Restriction sites used for cloning are underlined, and in bold face. GGATCC, BamHI; GAATTC, EcoRI; AAGCTT, HindIII; CATATG, NdeI; AGGCCT, StuI; TCTAGA, XbaI.

Protein isolation

To obtain constructs for the expression of His_6-tagged YlmE and Alr, the genes were amplified from the *S. coelicolor* chromosome using primer pairs, ylmE-FW + ylmE-RV and alr-FW + alr-RV, respectively. The PCR fragments were digested with NdeI and BamHI and cloned into pET15b (Novagen, La Jolla) digested with the same enzymes, which generated constructs pGWS1156 and pGWS1157, respectively. These constructs were transformed to *E. coli* BL21 DE3 (Novagen, La Jolla), which was used as host for expression of the re-

combinant proteins. Proteins were expressed and purified using a Ni-NTA column as described previously (Mahr *et al.*, 2000). In brief, cells were grown at 37^0C until OD_{600} of 0.6, expression was induced by the addition of 0.5mM Isopropyl β-D-1-thiogalactopyranoside (IPTG) followed by growth for 4h or 16h at 16°C, for pGWS1156 and pGWS1157 transformants, respectively. Cells were resuspended in PBS, lysed by sonication, and an S30 extract prepared by centrifugation for 2 h at 30,000x g. The lysate was then transferred to a His-Pur Ni-NTA resin column (Thermo scientific 88221), the column was washed with washing buffer (PBS with 25 mM imidazole) and His_6-tagged proteins eluted with elution buffer (PBS with 250 mM imidazole) followed by dialysis to remove the imidazole.

Microscopy

Fluorescence and light microscopy were performed as described previously (Willemse *et al.*, 2011). For this, a Zeiss Axioscope A1 upright fluorescence microscope was used with an Axiocam Mrc5 camera (with a pixel size of 37.5 nm/pixel), with, for the blue channel, 360/60 nm excitation, and 445/50 detection. The green fluorescent images were created using 470/40-nm bandpass excitation and 525/50 bandpass detection; for the red channel, 550/25-nm band-pass excitation and 605/70 bandpass detection were used. For staining of the cell wall (peptidoglycan), we used FITC-WGA; for membrane staining, we used FM5-95 (all obtained from Molecular Probes). For DNA staining 4', 6-diamidino-2-phenylindole (DAPI) was used. All images were background-corrected, setting the signal outside the hyphae to 0 to obtain a sufficiently dark background. These corrections were made using Adobe Photoshop CS4. Cryo-scanning electron microscopy (cryo-SEM) and transmission electron microscopy (TEM) were performed as described previously (Colson *et al.*, 2007).

Computer analysis

DNA and protein database searches were completed by using StrepDB page (http://strepdb.streptomyces.org.uk/).

RESULTS

Phylogenetic analysis of SCO2080 and SCO2081

Many of the genes in the *dcw* (division and cell-wall synthesis) gene cluster have been extensively studied and their functions are well established. Perhaps surprisingly, for quite a few genes the functions have not yet been elucidated, and two notable examples are *ylmD* and *ylmE*, which lie immediately downstream of - and most likely in operon with - *ftsZ* in many bacteria (Fig. 1). In all *Streptomyces* genomes analysed, *ftsZ* (SCO2082), *ylmD* (SCO2081) and *ylmE* (SCO2080) most likely form an operon, with translational fusion between *ftsZ* and *ylmD* (overlapping start and stop codons) and only 6 nt spacing between *ylmD* and *ylmE*, suggesting these genes may play a prominent role in cell division. Genome-wide transcript analysis of wild-type *S. coelicolor* by DNA microarrays indeed showed that transcript levels of *ftsZ* are similar to those of *ylmD* and *ylmE* during vegetative growth on MM agar plates; however, *ftsZ* was transcribed at significantly higher levels during sporulation(Świątek *et al.*, 2013; Świątek, 2012). SCO2081 and SCO2080 share 32% aa identity with YlmD and YlmE of *B. subtilis*, respectively.

ylmD and *ylmE* are wide spread in Gram-positive bacteria, and particularly in firmicutes (*Bacillus, Staphylococcus*) and in actinobacteria, but are also occasionally found in Gram-negative bacteria. The direct genetic linkage to *ftsZ* is almost exclusively seen in firmicutes and actinobacteria (Fig. 1A). Phylogenetic analysis of the YlmD and YlmE proteins in actinobacteria shows that while YlmE is widespread, YlmD is often absent in actinobacteria, including sporulating genera, *e.g.* in *Stackebrandtia, Catenulispora, Salinispora, Micromonospora, Amycolatopsis* and *Mycobacterium tuberculosis* (Fig. 1B). The reverse situation, with *ylmD* present and not *ylmE*, does not occur. This suggests that the function of YlmD is becoming redundant.

YlmE is a YBL036c-like protein, and the structure of YBL036c from *Saccharomyces cerevisiae* was resolved at 2.0 Å resolution (PDB 1CT5). The protein folds as a triose phosphate isomerase (TIM) barrel with a long N-terminal helix, in contrast to the classic TIM proteins, which have a β-strand at their N-terminus. Pyridoxal 5'-phosphate is bound near the C-terminal end of the barrel, which constitutes the active site in TIM-barrel folds (Eswaramoorthy *et al.*, 2002). The majority of the type III PLP-dependent enzymes has a TIM barrel domain followed by a C-terminal β-sandwich domain. The protein resembles the N-terminal part of alanine racemases and the lack of the β-sandwich domain is expected to limit the activity of YBL036c as alanine or non-specific racemase (Percudani and Peracchi, 2003).

1A

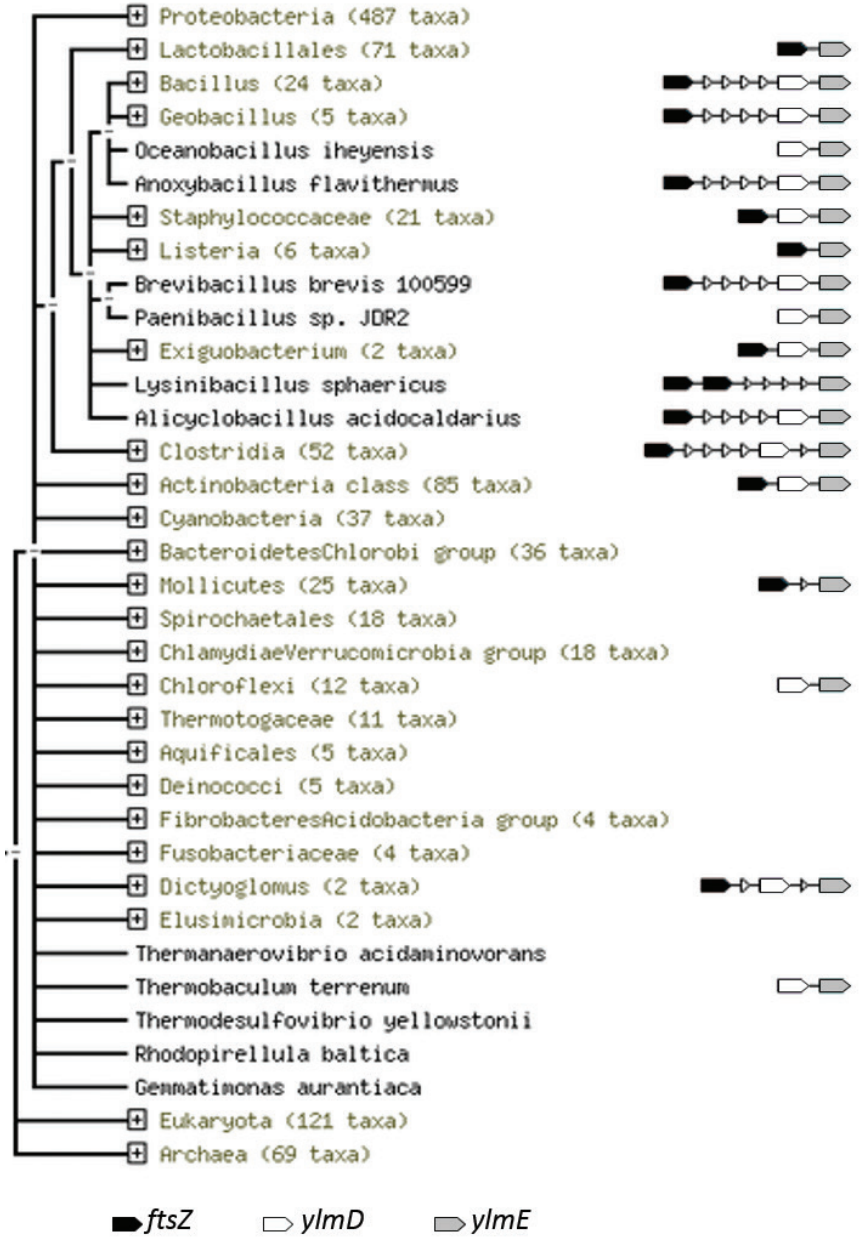
Proteobacteria (487 taxa)
Lactobacillales (71 taxa)
Bacillus (24 taxa)
Geobacillus (5 taxa)
Oceanobacillus iheyensis
Anoxybacillus flavithermus
Staphylococcaceae (21 taxa)
Listeria (6 taxa)
Brevibacillus brevis 100599
Paenibacillus sp. JDR2
Exiguobacterium (2 taxa)
Lysinibacillus sphaericus
Alicyclobacillus acidocaldarius
Clostridia (52 taxa)
Actinobacteria class (85 taxa)
Cyanobacteria (37 taxa)
BacteroidetesChlorobi group (36 taxa)
Mollicutes (25 taxa)
Spirochaetales (18 taxa)
ChlamydiaeVerrucomicrobia group (18 taxa)
Chloroflexi (12 taxa)
Thermotogaceae (11 taxa)
Aquificales (5 taxa)
Deinococci (5 taxa)
FibrobacteresAcidobacteria group (4 taxa)
Fusobacteriaceae (4 taxa)
Dictyoglomus (2 taxa)
Elusimicrobia (2 taxa)
Thermanaerovibrio acidaminovorans
Thermobaculum terrenum
Thermodesulfovibrio yellowstonii
Rhodopirellula baltica
Gemmatimonas aurantiaca
Eukaryota (121 taxa)
Archaea (69 taxa)
ftsZ
ylmD
ylmE

1B

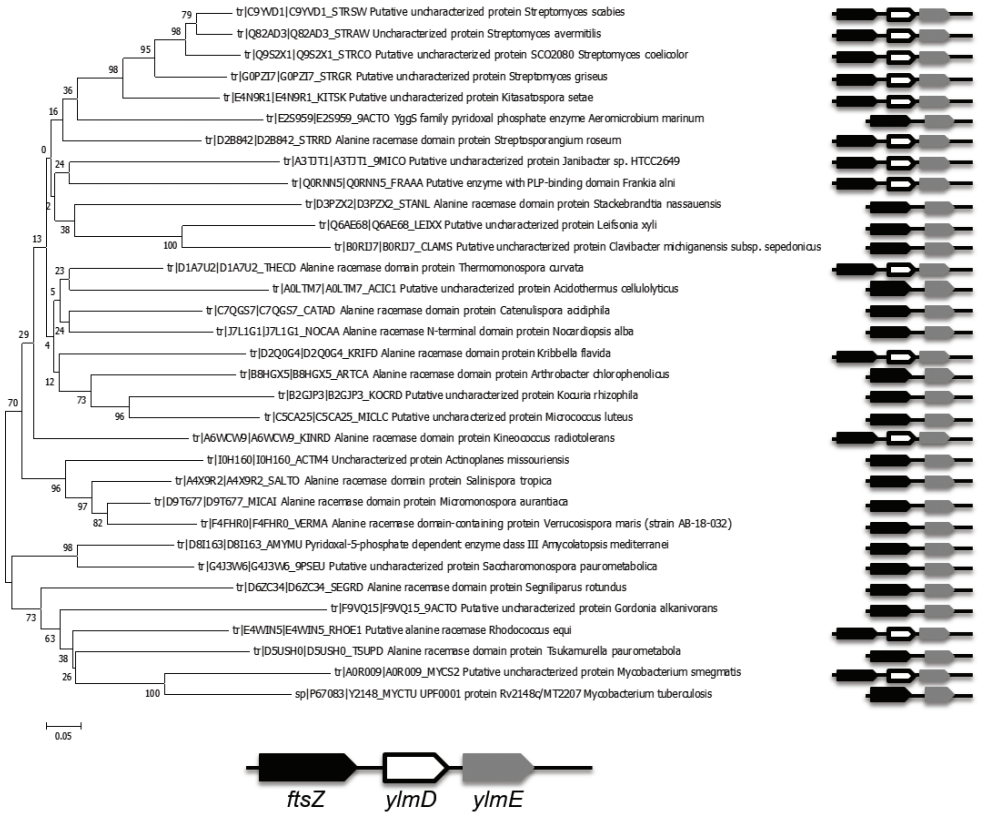

Figure 1. Phylogenetic analysis of YlmD and YlmE in actinobacteria. A. Neighborhood analysis for *ftsZ*, *ylmD* and *ylmE* using the String engine. **B.** Phylogenetic tree of YlmE proteins in Actinobacteria and genetic linkage of *ylmE* (grey) to *ftsZ* (black) and *ylmD* (white).

YlmD has a domain that belongs to multiple-copper polyphenol oxidoreductase laccases, which are oxidoreductases that are widely distributed in both prokaryotes and eukaryotes (Claus, 2003). Typically, laccases are secreted proteins, but such a domain is lacking in YlmD. YlmD belongs to the same protein family (Pfam PF02578; DUF152) as YfiH from *Shigella flexneri*. This is a Zinc binding protein of unknown function, and its crystal structure (PDB 1XAF; 2.0 Å resolution) revealed a dimeric protein with an α/β/α fold (Kim *et al.*, 2006). There is structural similarity between YfiH and cytosine/cytidine deaminases and in *S. flexneri*, the gene lies adjacent to *sfhB*, encoding pseudouridine synthase that suppresses the *ftsH* cell division defect (Ray-

chaudhuri *et al.*, 1998). Notably, String analysis of *ylmD* shows rather strong phylogenetic linkage to nucleotide/nucleoside-related enzymes, including tyrosyl tRNA synthetase (SCO1818) and a putative xanthosine/inosine triphosphatase (SCO2902), that protects cells from DNA damage by removing non-canonical purine homologs, which otherwise cause chromosomal lesions (Burgis and Cunningham, 2007).

ylmD and y*lmE* are required for proper sporulation

To analyze the role of *ylmD* and *ylmE*, deletion mutants were created in *S. coelicolor* M145 as detailed in the Materials and Methods section. The +25 to +696 region of *ylmE* (SCO2080) or the +25 to +705 region of *ylmD* (SCO2081) were replaced by the apramycin resistance cassette, followed by deletion of the cassette using the Cre recombinase so as to avoid polar effects. This resulted in *ylmD* null mutant GAL47 (*S. coelicolor* M145 ΔSCO2081) and *ylmE* null mutant GAL48 (*S. coelicolor* M145 ΔSCO2080).

The *ylmD* null mutant GAL47 had a light grey appearance, while *ylmE* null mutant GAL48 hardly produced any grey pigment after 6 days incubation, indicative of lack of grey-pigmented spores (Fig. 2A). Phase-contrast light microscopy of impression prints of the top of the colonies demonstrated that while the parent produced typical long spore chains, the *ylmD* null mutant produced many aberrantly sized (in particular large) spores, while the *ylmE* null mutant hardly produced any spores. The same delay in sporulation was observed on R5 and MM mannitol agar plates. The mutants produced wild-type levels of the pigmented antibiotics actinorhodin and undecylprodigiosin. To establish whether the sporulation defects were indeed solely due to the deletion of the respective genes, we introduced plasmids expressing either *ylmD* or *ylmE* from the native *ftsZ* promoter in the respective null mutants. This resulted in partial restoration of sporulation, whereby sporulation was restored to the *ylmE* mutants, while the majority of the spores of the complemented *ylmD* mutant had a regular appearance (Fig. 2B).

2A

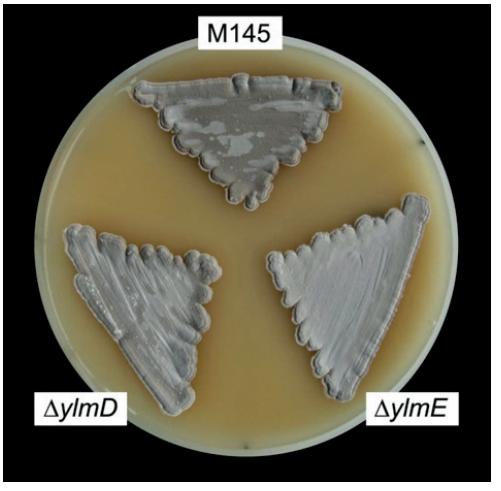

2B

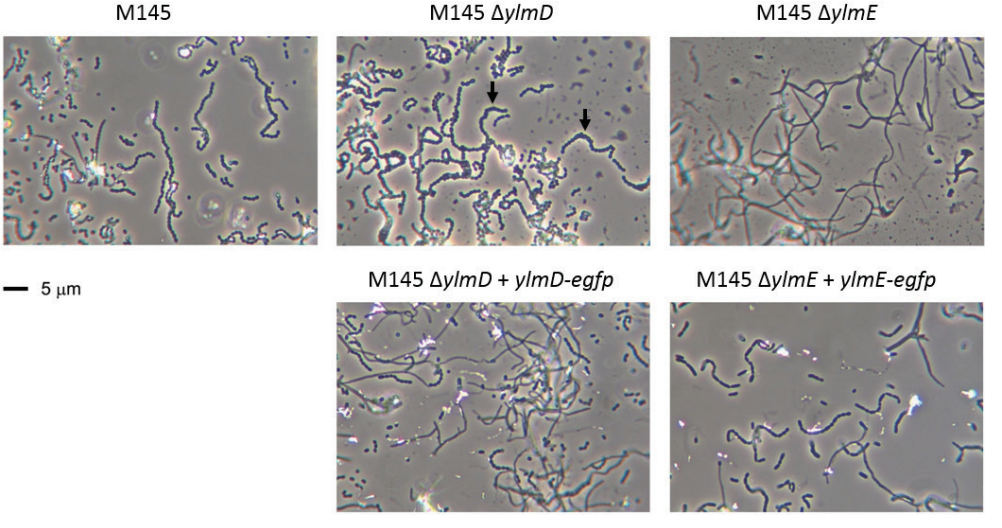

Figure 2. Phenotype of the *S. coelicolor ylmD* and *ylmE* mutants. A. Sporulation of M145 and its *ylmD* and *ylmE* mutants on SFM agar. **B.** Phase-contrast micrographs of impression prints of the strains shown in (A) as well as the complemented mutants. Arrows point at irregularly shaped spores in the *ylmD* mutant. The sporulation defect of the *ylmD* mutant could be complemented by introduction of wild-type *ylmD*, while complementation of the *ylmE* mutant restored sporulation, although irregularly sized spores were often produced. Bar, 5 µm.

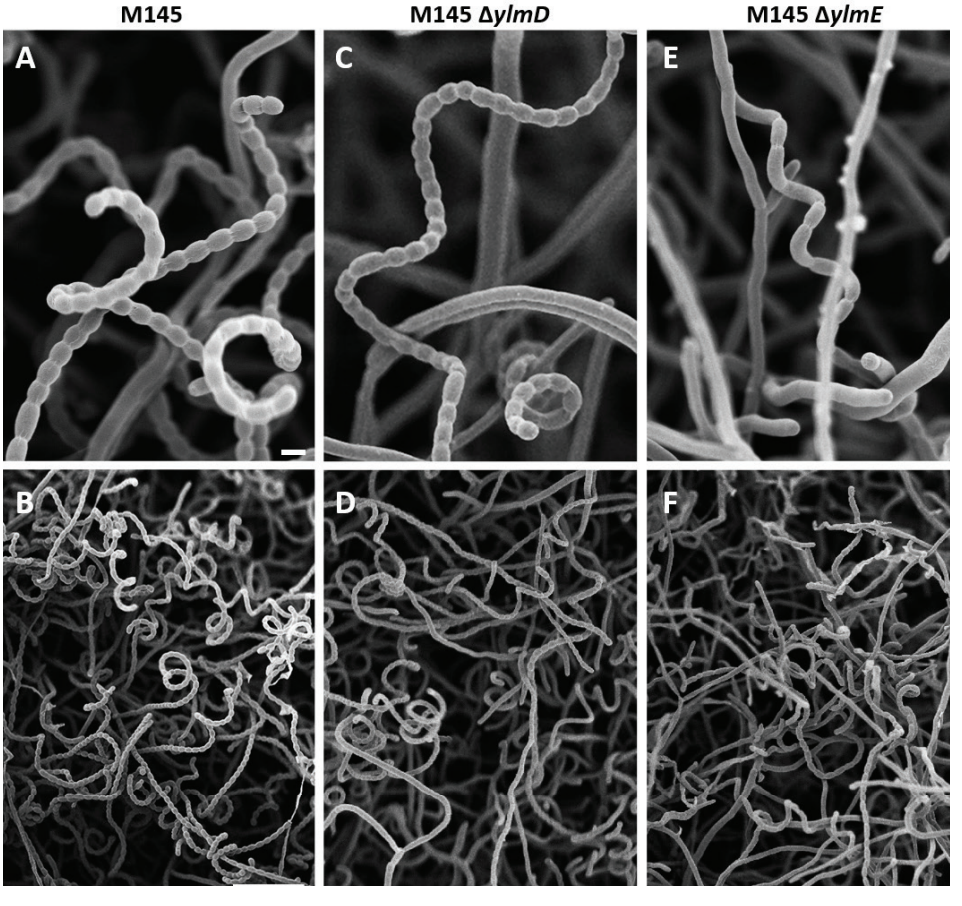

Figure 3. Cryo-scanning electron micrographs of aerial hyphae of *S. coelicolor* M145 and its *ylmD* and *ylmE* mutants. Wild-type sporulated abundantly, ylmD mutant spores showed irregular features while the *ylmE* null mutant produced occasional spores with highly irregular sizes. Cultures were grown on SFM agar plates for 5 days at 30^0C. Bars: top row, 1 μm; bottom row, 10 μm.

To scrutinize the spores at high resolution, cryo-scanning electron microscopy (SEM) was performed, which again demonstrated the sporulation defects of the *ylmD* and *ylmE* mutants of *S. coelicolor*. The parental strain *S. coelicolor* M145 produced abundant spore chains, with nearly all hyphae fully developed into mature spore chains (Fig.3AB). In GAL48, precious few and often aberrant spores were identified, while GAL47 produced many highly aberrantly sized spores (Fig 3C-F). Deletion of the genes in the related strain *Streptomyces lividans* 1326 gave essentially the same phenotype on all media tested (data not illustrated). The highly similar phenotypes of the mutants in

S. coelicolor M145 and *S. lividans* 1326 were consistent with the notion of a conserved function of the genes in sporulation-specific cell division in *Streptomyces*.

Aberrant morphology and reduced viability of *ylmD* and *ylmE* mutant spores

Viability of the spores was tested by plating around 100 and 1000 colony forming units (cfu) - as determined by counting in a haemocytometer - of M145, GAL48 (Δ*ylmE*) and GAL47 (Δ*ylm*D) onto SFM agar plates. While the wild-type strain had close to 100% viability, spores of the *ylmD* and *ylmE* mutants had reduced viability, with 60% and 50% of the spores, respectively, giving rise to a colony. Introduction of the genes resulted in partial restoration of viable counts, namely to 79% for *ylmD* mutant and 75% for the *ylmE* mutant. Spores of in particular the *ylmE* mutant were also more heat sensitive, with 24% viability after 5 min incubation at 60^0C, while for the *ylmD* null mutant 44% survived this heat treatment, and 50% of the wild-type spores.

To analyze the possible defects in the cell wall in more detail, all strains were grown on SFM agar plates for 5 days and analyzed by Transmission Electron Microscopy (TEM). The parent produced typical spore chains and thick-walled mature spores (Fig. 4A, D), while *ylmD* and *ylmE* mutants produced aberrant spores (Fig 4B and 4C). The mutant spores were deformed and highly irregular, and in particular the *ylmE* mutant had a thin wall indicative of complete lack of spore wall synthesis (Fig 4C). Considering the pleiotropic defect in spore morphology, we compared the spores of the *ylmE* mutant with those produced by *mreB* mutants. While both mutants produced spores with aberrant shapes, the morphology of the spores of the *ylmE* null mutant was significantly different from that of the spores of the *mreB* mutant (Fig. 4D).

YlmD and YlmE are required for cell-wall synthesis

To analyze cell wall, nucleoid and membrane distribution in *ylmD* and *ylmE* mutants, fluorescence microscopy was done on three days old SFM-grown cultures of mutants GAL48 (M145 Δ*ylmE*) and GAL47 (M145 Δ*ylmD*) and their parent M145. Peptidoglycan precursors were stained with FITC-labeled wheat germ agglutinin (FITC-WGA), membranes were visualized by staining with FM 5-95, and chromosomes with DAPI.

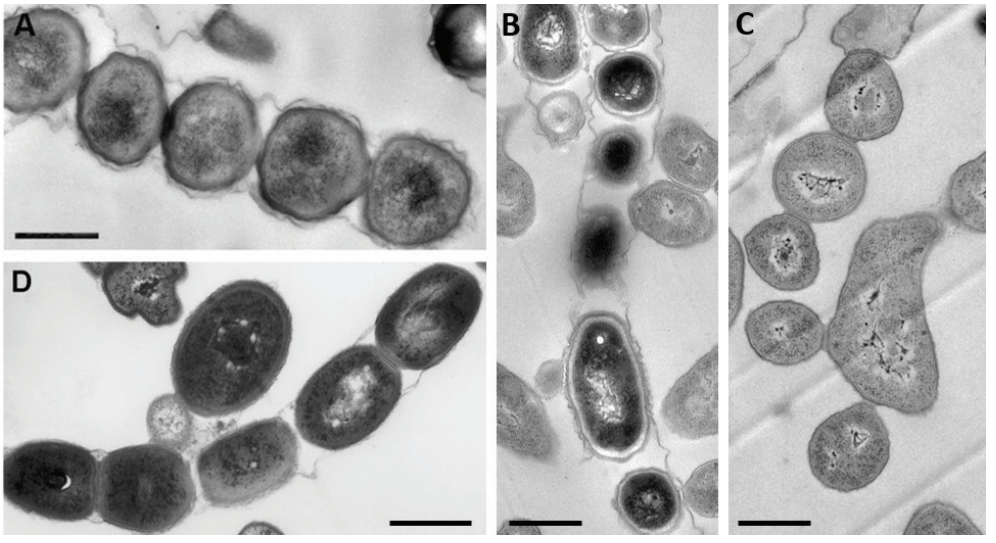

Figure 4. Transmission electron micrographs of spores of *S. coelicolor* M145 and its *ylmD* and *ylmE* mutants. While the wild-type (M145) spores are of similar size and appearance **(A)**, *ylmD* **(B)** and *ylmE* **(C)** null mutants produce irregular spores. Note the lighter appearance of the spore wall in the *ylmD* null mutant and the lack of the thick spore wall in *ylmE* mutants. A TEM micrograph of spores of an *mreB* in-frame deletion mutant (Mazza *et al.*, 2006) has been added for reference purposes **(D)**. Cultures were grown on SFM agar plates for 5 days at 30^0C. Bar, 500 nm.

In wild-type pre-division aerial hyphae, chromosome condensation had finished and long symmetrical septal ladders were observed when stained for cell wall or membranes (Fig. 5A). In contrast to the wild-type strain, in most aerial hyphae of the mutants, and in particular *ylmE* mutants, cell wall and membrane placement were highly disturbed, and most of these hyphae failed to produce septa (Fig. 5A). As shown by the overlays, there was hardly any overlap between cell wall and DNA synthesis in the two mutants (Fig. 5B). Re-introduction of *ylmD* in the *ylmD* mutant or *ylmE* in the *ylmE* mutant restored sporulation to near wild-type levels (Fig. 5C). Taken together, these data suggest an important role for YlmD and YlmE in cell-wall synthesis during sporulation.

5A

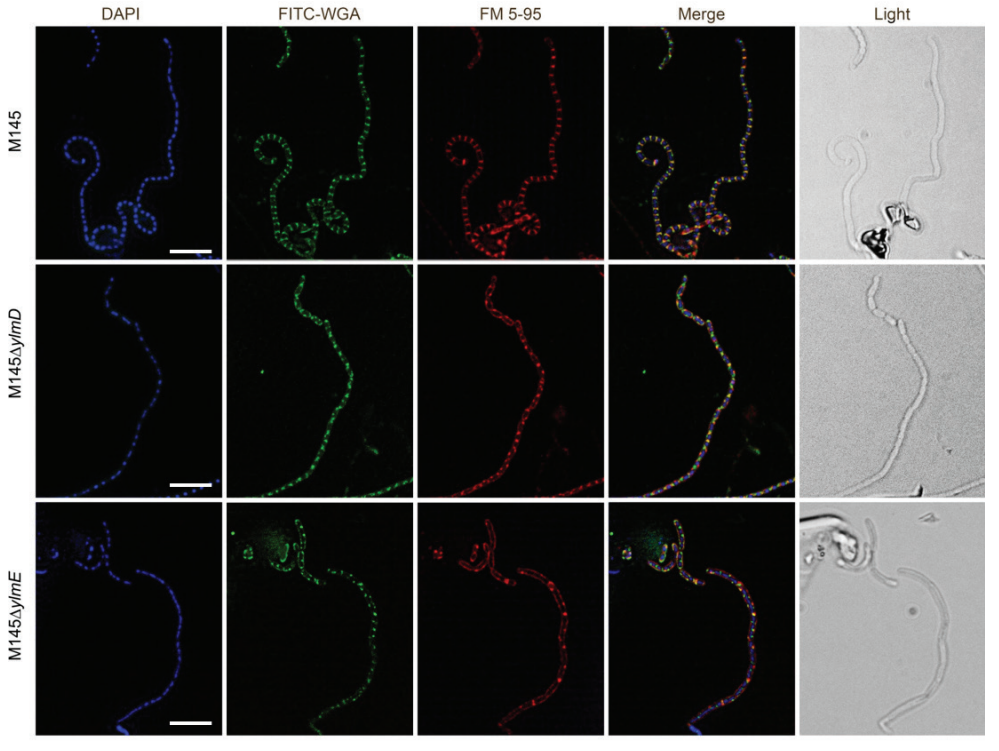
DAPI
FITC-WGA
FM 5-95
Merge
Light
M145
M145ΔylmD
M145ΔylmE

5B

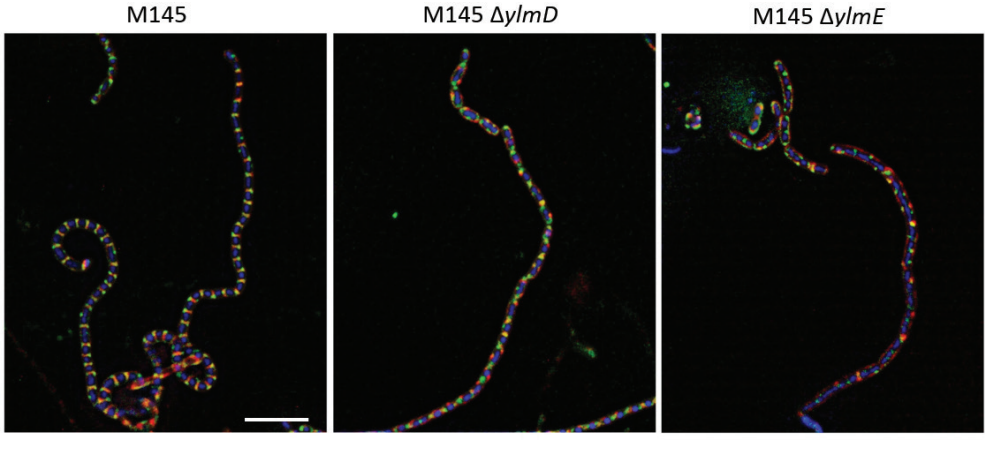
M145
M145 ΔylmD
M145 ΔylmE

5C

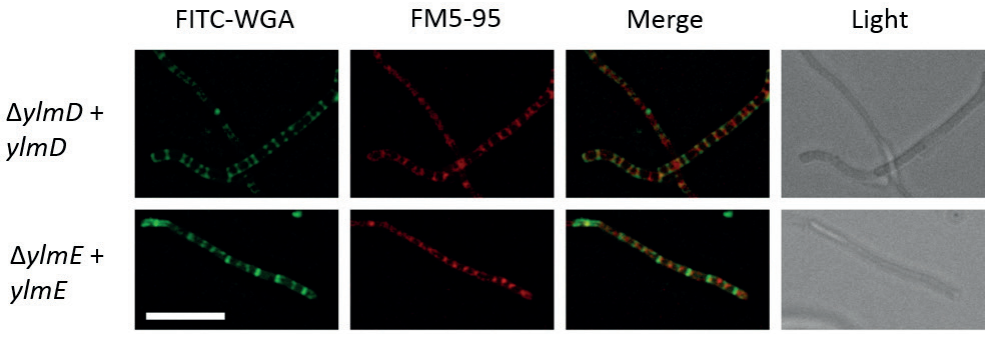

Figure 5. Fluorescence microscopy of cell wall, DNA and membranes.
(A) Fluorescent micrographs show hyphae stained for DNA (DAPI), cell-wall synthesis (FITC-WGA) or membranes (FM5-95). An overlay of these images is presented in the fourth column, and the corresponding light image in the last column. Bar, 5 μm. **(B)** close up of the composite images of 5A. Bar, 5 μm. **(C)** Fluorescence micrographs showing DNA and cell-wall distribution in the complemented *ylmD* and *ylmE* mutants. While typical ladders of septa were formed in both strains, indicative that sporulation was restored to the mutants, in particular the complemented *ylmE* mutant formed imperfect septa. Bar, 10 μm.

Localization of YlmD and YlmE

We then wondered how YlmD and YlmE localized in the hyphae of *Streptomyces*. For this, constructs based on the low-copy number vector pHJL401 were prepared so as to allow the expression of YlmD-eGFP and YlmE-eGFP fusion proteins, which were expressed from the natural *ftsZ* promoter region (see Materials and Methods section). These constructs were then introduced into *S. coelicolor* M145 and (as a control for functionality) in the mutants. The constructs restored development, with significant reduction in the number of aberrant spores in the *ylmD* mutant, and many spore chains produced by the *ylmE* mutant (Fig. 2B).

During early aerial development, both YlmD-eGFP and YlmE-eGFP formed foci along the aerial hyphae, with an approximately 1 μm spacing similar to the spacing between septa during sporulation-specific cell division (Fig. 6). In premature spores, YlmD apparently formed a helical pattern, while YlmE-eGFP localized as a ring inside the spores, consistent with a putative role in the cell-wall synthetic machinery. During spore maturation, YlmE localized to the spore poles, where cell-wall remodelling takes place, while YlmD produced an irregular pattern of bright foci and patches (Fig 6).

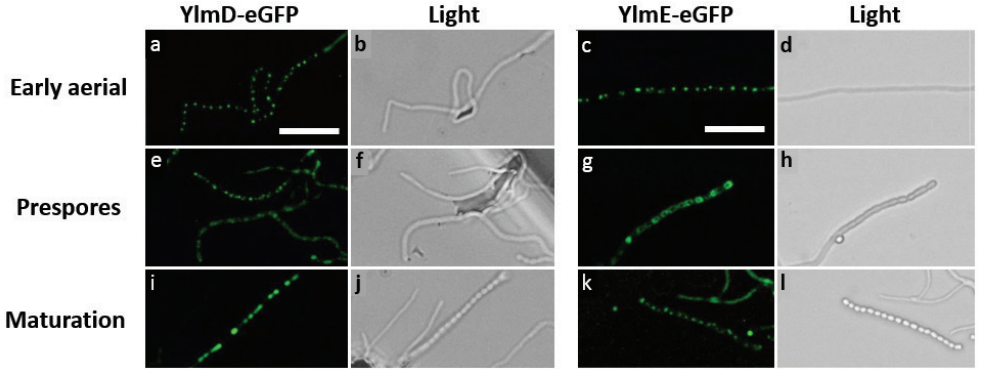

Figure 6. Localization of YlmD-eGFP and YlmE-eGFP. Sporogenic aerial hyphae of *S. coelicolor* M145 at different stages of development were imaged by fluorescence microscopy visualizing YlmD-eGFP (a,b,e,f,I,j) and YlmE-eGFP (c,d,g,h,k,l). Stages were: early aerial development (a-d), prespores (e-h) and spore maturation (i-l). YlmD and YlmE localized in foci with approximately 1 μm spacing during early development of the aerial hyphae. During later stage of sporulation, YlmD had a 'patchy' localization, while YlmE was frequently seen to localize in a ring-like fashion inside the spores, suggesting that at this stage YlmE may co-localize with the cell-wall synthetic machinery. Bar, 5 μm.

Localization of FtsZ in Δ*ylmD* and Δ*ylmE*

To investigate whether YlmD and YlmE affect the localization of FtsZ, integrative plasmid pKF41 harboring *ftsZ-egfp* under control of native *ftsZ* promoter (Grantcharova *et al.*, 2005), was introduced into the *ylmD* and *ylmE* mutants to generate strain GAL52 and GAL53, respectively. Prior to sporulation, typical ladders of Z-rings were observed in the parental strain *S. coelicolor* M145, while *ylmD* and *ylmE* null mutants showed abnormal ladders of FtsZ rings (Fig. 7). In the absence of YlmD, ladders were still observed, but the spacing between the individual rings was far less regular, with many neighboring Z-rings either close together or widely spaced. Consistent with the sporulation defect, *ylmE* null mutants produced very few Z-rings, and the few that where formed were highly irregular and a lot shorter than in the parental strain. Thus, FtsZ localization is irregular in *ylmD* mutants and highly compromised in *ylmE* mutants, consistent with the defects in cell-wall synthesis and morphogenesis seen in the mutants.

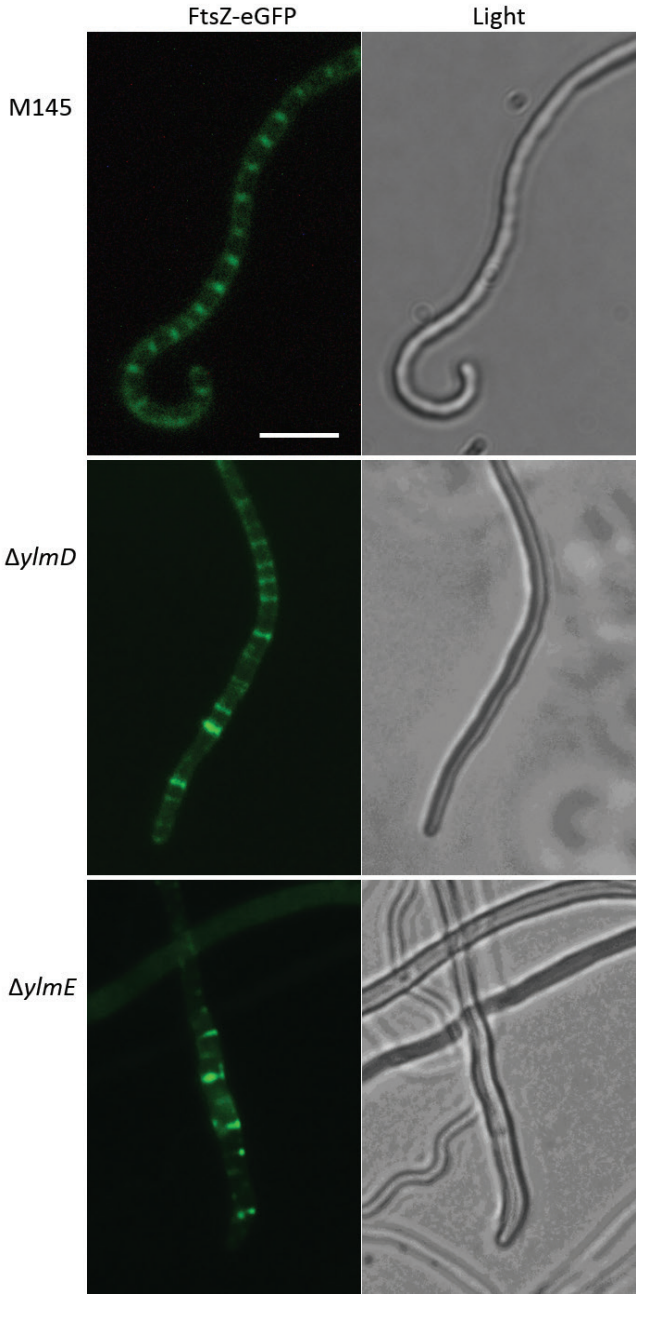

Figure 7. Localization of FtsZ-eGFP in *S. coelicolor* M145 and its *ylmD* and *ylmE* mutants. FtsZ-eGFP formed typical ladders in wild-type cells (M145). In contrast, YlmE is required for the formation of ladders of FtsZ, while the absence of YlmD caused irregular spacing between the septa. Cultures were grown on SFM agar plates for 5 days at 30^0C. Bar, 5 μm.

Alanine racemase assays for YlmE

As mentioned above, YlmE bears significant similarity to alanine racemases, the question is whether YlmE indeed functions as an alanine racemase *in vivo*. Previous work by Ito and coworkers (Ito *et al.*, 2013) showed that at least the *E. coli* homolog YggS did not bind any of the 20 amino acids and a regulatory instead of enzymatic function was proposed for YlmE-like proteins. The main alanine racemase in *S. coelicolor* is likely encoded by *alr* (SCO4745), which lies elsewhere on the chromosome. *S. coelicolor* Alr is 45% identical at the aa level to Alr from *Mycobacterium tuberculosis*, which was previously shown to be essential for providing D-Ala to the cells (Milligan *et al.*, 2007). To establish if *alr* is the only alanine racemase, and hence essential for D-Ala synthesis during normal growth, an *alr* null mutant of *S. coelicolor* was generated using essentially the same strategy as described for *ylmD* and *ylmE*. Gene deletion construct pGWS1151 allows replacement of the entire coding region of *alr* (SCO4745) by the apramycin resistance cassette. The construct was introduced in both *S. coelicolor* M145 and in its *ylmE* null mutant GAL48, and propagated on agar plates supplemented with D-Ala to ensure that a possible auxotrophy would not prevent growth of the double recombinants. Mutants were selected on the basis of apramycin resistance and thiostrepton sensitivity (due to loss of the plasmid) and were readily obtained, resulting in *alr* null mutant GAL99 and *alr-ylmE* double mutant GAL100. Both mutants were verified by PCR. Neither mutant was able to grow in the absence of D-Ala, and this auxotrophy confirmed that indeed the *alr* gene is essential for supplying D-Ala for PG synthesis in *S. coelicolor*. This also implies that YlmE cannot produce sufficient D-Ala to compensate for the absence of Alr *in vivo* (Fig. 8A).

Considering *ylmE* likely under control of *ftsZ* promoter, which is only up regulated since the beginning of sporulation stage, the failure of YlmE to compensate deletion of *alr* might due to its late expression level, even though the transcript level of *alr* and *ylmDE* are comparable during vegetative growth as shown by microarray analysis (Świątek *et al.*, 2013; Świątek, 2012).

Therefore, we designed constructs wherein either *ylmE* alone or the *ylmD-ylmE* gene cluster was expressed from the *alr* promoter. Additionally, a construct was designed that expressed *ylmE* alone from the strong and constitutive *ermE* promoter. As plasmid we used the low-copy shuttle vector pHJL401. The constructs were produced by gene synthesis, resulting in the constructs: *alr*p-*ylmE, alr*p-*ylmDE* and e*rmE*p-*ylmE.* These constructs were then introduced in *S. coelicolor* M145 and its *alr* null mutant. However, the *alr* null mutant failed to grow in the absence of D-Ala, regardless of which construct was introduced. This again suggests that YlmE does not function as an alanine

racemase *in vivo*.

To see if Alr and YlmE could function as alanine racemase *in vitro*, the enzymes were purified to homogeneity. For this, the coding regions of *alr* and *ylmE* were cloned into pET15b, which allows the expression of N-terminally His_6-tagged proteins in *E. coli* (see Materials and Methods section). The purified Alr-His_6 and YlmE-His_6 proteins were used as enzymes in an alanine racemase activity assay. For this, we made use of the fact that the *alr* null mutant fails to grow in the absence of D-Ala (Fig.8A). Addition of D-Ala but not L-Ala restores growth, and if Alr or YlmE would convert L-Ala to D-Ala in an *in vitro* assay, the reaction mixture should supply the *alr* mutant with sufficient D-Ala to grow. The principle is presented in Fig. 8B (left). 1 M L-Ala was incubated with either Alr or YlmE for various times ranging from 0 to 16 hr followed by heat inactivation of the enzyme. Supplementing media devoid of D-Ala with the reaction mixture of L-Ala with purified Alr protein that had been incubated for 30 min or longer, was sufficient to allow the *alr* null mutant to grow; this clearly shows that indeed Alr is a functional alanine racemase, and efficiently converted L-Ala into its enantiomer D-Ala (Fig.8B, right). However, a similar experiment with YlmE failed to rescue the *alr* mutant, indicating that YlmE was not able to efficiently convert L-Ala into D-Ala *in vitro* (Fig. 8B).

8A

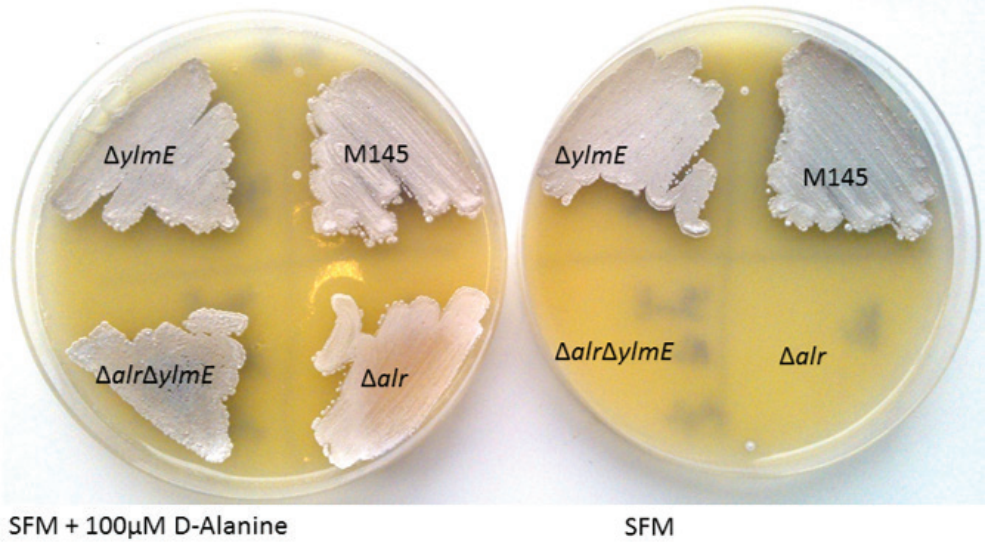

8B

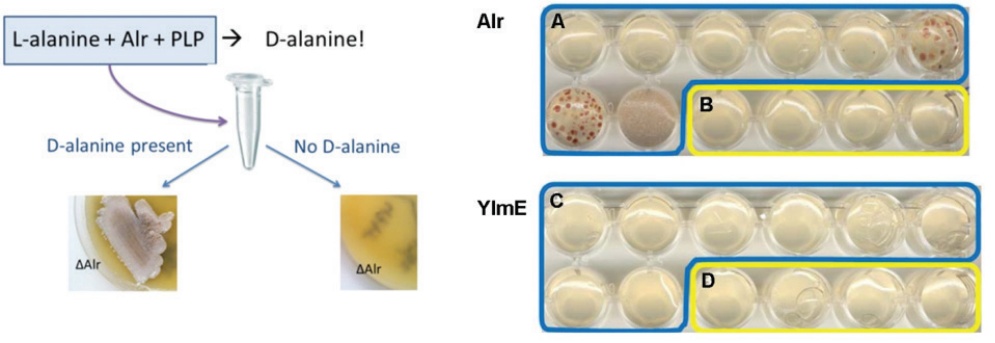

8C

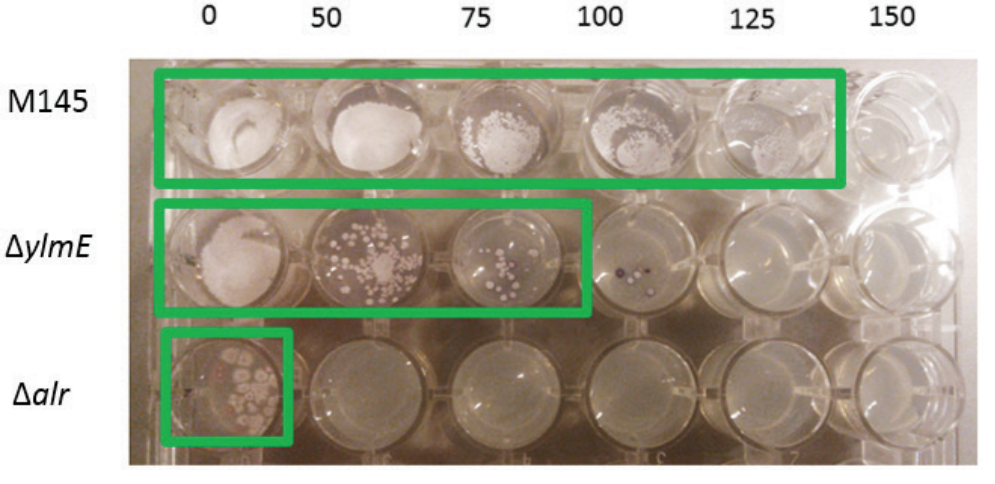

Figure 8. Alanine racemase activity assays for Alr and YlmE.
(A) Lack of *alr* results in D-Ala auxotrophy. *S. coelicolor* M145 and its *alr, ylmE and alr/ylmE* null mutants were grown on SFM agar plates with (left) or without (right) 100 μM D-Ala. Mutants lacking *alr* were auxotrophic for D-Ala, while the *ylmE* mutant showed better sporulation in the presence of added D-Ala as shown by the enhanced pigmentation.

(B) Enzymatic assay for alanine racemase activity. **Left,** schematic representation of the assay. Purified Alr or YlmE were added to L-Ala, incubated for up to 16 hr and the reaction mixture was then spotted onto an agar plate and overlayed with the D-Ala auxotrophic mutant *S. coelicolor* M145 Δ*alr*Δ*ylmE*. If D-Ala is produced by an enzyme *in vitro*, this should allow growth of the D-Ala dependent mutant. **Right,** *in vivo* tests of the enzyme reactions. Alr (A) or YlmE (C) or heat-inactivated Alr (B) or YlmE (D) was added to 0.5 M L-Ala in the presence of 25 μg/ml pyridoxal 5' phosphate (PLP), and incubated for various times at 30'C. Incubation times were (from left to right) 0, 5, 15, 30, 60, 120, 240 minutes or overnight for Alr and YlmE, and 60, 120, 240 min and overnight for reactions with heat-inactivated enzymes. 20 μl of the mixture was heat-inactivated, spotted onto a well

containing MM mannitol and overlayed with soft agar containing M145 Δ*alr*Δ*ylmE*. Reaction mixtures with Alr incubated for 120 min or longer were able to restore growth of the D-Ala auxotroph, while control mixtures with heat-inactivated Alr failed to enable growth of the auxotroph. YlmE was not able to produce sufficient levels of D-Ala regardless of the incubation time.

(C) Sensitivity of *alr* and *ylmE* mutants to D-cycloserine (DCS). All strains were grown on MM agar plates with mannitol (1% w/v) and 100 μM D-Ala to support growth of the *alr* null mutant. The parental strain *S. coelicolor* M145 grew up to 125 μg/ml DCS, *ylmE* mutants up to 75 μg/ml and *alr* mutants failed to grow at the lowest tested concentration of DCS (50 μg/ml). This shows that lack of either *alr* or *ylmE* results in enhanced sensitivity to DCS.

YlmE potentially controls the pool of D-Ala

To further analyze the effect on D-Ala, we made use of the antibiotic D-cycloserine (DCS), a cyclic analogue of D-Ala which targets alanine racemase (Alr) as well as the D-Ala-D-Ala ligase (Ddl). The MIC of DCS is inversely correlated to the level of D-Ala, and overproduction of Alr is a well-known mechanism to gain resistance to DCS (Caceres et al., 1997). Earlier research has shown that a knockout of alr results in hypersensitivity to DCS (Peteroy et al., 2000; Noda et al., 2004; Caceres et al., 1997). Interestingly, our experiments showed that the MIC of DCS was reduced not only in alr mutants but also in ylmE mutants (Fig. 8C). This suggests that the pool of D-Ala is reduced in the ylmE mutant. Indeed, supplying additional D-Ala rescued the DCS sensitivity of the mutants (not shown). In summary, the high sensitivity of the ylmE null mutant to DCS but the failure of YlmE of being alanine racemase suggest that YlmE may be involved in D-alanine maintaining for sporulation (at future septum sites) but not D-alanine production.

Considering the relationship between YlmE and cell-wall synthesis, we tested the effect of adding D-Ala to ylmE null mutants. Interestingly, when grown on MM agar plates with mannitol (1% w/v) supplemented with D-Ala (0.5% w/v), sporulation of ylmE mutant GAL48 was largely restored, while L-Ala had no effect (Fig. 9). However, when grown on SFM agar plates, addition of D-Ala failed to restore sporulation to the ylmE mutant. This suggests that deletion of ylmE affects the pool of D-Ala or a derivative thereof in a culture-condition dependent manner, during sporulation.

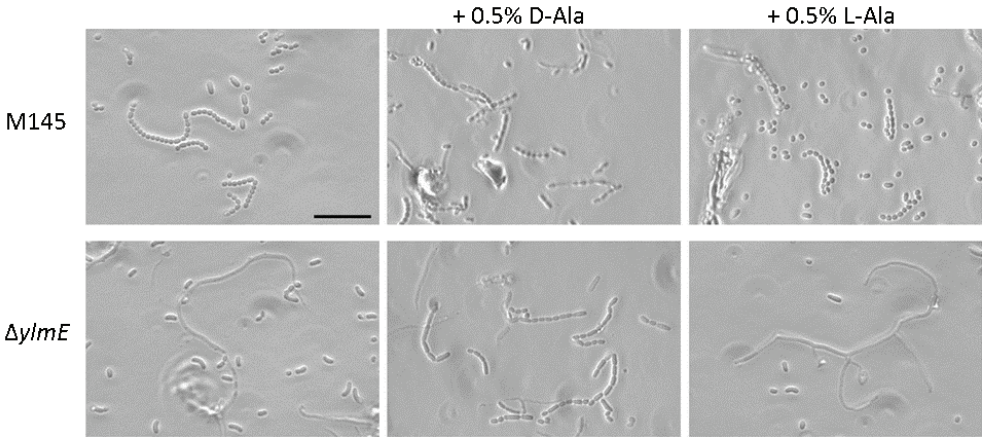

Figure 9. D-Ala restores sporulation to *ylmE* null mutants. Phase contrast micrographs of *S. coelicolor* M145 (top) and its *ylmE* null mutant (bottom) grown on MM agar with mannitol (left) or the same media supplemented with 0.5 % (w/v) of either D-Ala (middle) or L-Ala (right). Note that supplementing with D-Ala promotes sporulation by the *ylmE* mutant while supplementing L-Ala has no effect.

DISCUSSION

In unicellular bacteria a single septum is formed at mid-cell, and the control of cell division is directed at the correct timing of this event in time and space. In contrast, during sporulation-specific cell division of *Streptomyces*, up to a hundred septa are formed simultaneously, which is seen as spectacular ladders of FtsZ rings. Eventually, cytokinesis results in long chains of spores, following a complex process of coordinated cell division, cell-wall synthesis and DNA segregation. We recently discovered that the correct positioning of the sporulation septa depends on the SsgA and SsgB proteins, which are unique to actinomycetes, whereby SepG (YlmG) ensures that SsgB is tethered to the membrane (Chapter II).

Relatively little is known of the way spore-wall synthesis is governed. Peptidoglycan is a major constituent of the bacterial cell wall, and consists of glycan strands that consist of alternating N-acetylglucosamine (GlcNAc) and N-acetyl muramic acid (MurNAc) residues, connected by a pentapeptide chain between the MurNAc residues. In *Streptomyces*, the pentapeptide chain consists of L-Ala, D-Glu, LL-diaminopimelic acid (Dap) and two D-Ala residues, of which the terminal D-Ala can be cleaved off to create a glycine bridge. D-Ala is an important element in the bacterial cell matrix, and is among others also required for the stability of cell-wall teichoic acid in *Bacillus* (Wecke *et al.*, 2009). Many genes involved in cell division and cell-wall synthesis, such as most *fts* and *mur* genes, lie in the *dcw* cluster. Our focus lies on the genes between *ftsZ* (SCO2082) and *divIVA* (SCO2077), which *ylmD-G*, for which orthologs exist in many low and high G+C Gram-positive bacteria, including *Bacillus*. Until recently, only the function of *ylmF* (*sepF*) was elucidated, which assists in Z-ring assembly (Hamoen *et al.*, 2006; Ishikawa *et al.*, 2006) and in this thesis we propose a function for YlmG in attaching the FtsZ-recruiting SsgB to the membrane (Chapter II).

The two remaining genes are *ylmD* and *ylmE*, which lie immediately downstream of, and most likely in operon with, *ftsZ*. In this work we show that YlmE, which is a protein with an annotated amino acid racemase domain, is required for sporulation of *S. coelicolor*, since many aberrant spores formed in *ylmD* mutants. However, YlmE failed to catalyze conservation of L-Ala to D-Ala *in vitro* and *in vivo*, suggesting it plays role in sporulation through other mechanism rather than alanine racemase.

Phylogenetic analysis shows strong linkage between *ylmE* and the structural cell division gene *ftsZ*, and the genes are often in operon, which sug-

gests that YlmE plays a major role in (the control of) cell division. YlmD and YlmE are both expressed in a sporulation-specific manner, as shown by the localization in aerial hyphae. At a later stage of sporulaiton, YlmE forms rings inside the prespores, consistent with a role in spore-wall synthesis. Mutants lacking *ylmD* and *ylmE* both show deficiencies in sporulation, although *ylmE* mutants have a much more severe phenotype than strains mutated for *ylmD*, with major rearrangements of cell-wall synthesis in *ylmE* null mutants. High resolution imaging by TEM as well as fluorescence microscopy showed that *ylmE* mutants are highly defective in cell-wall synthesis, depositing cell wall and membrane at seemingly random positions in the aerial hyphae. Cell-wall synthesis was also defective in *ylmD* mutants, but eventually this strain produces relatively normal spore chains, albeit that many spores have aberrant shapes. This difference in the impact on cell division was corroborated by the fact that the typical FtsZ-ladders in sporogenic aerial hyphae were formed in *ylmD* mutants, although with imperfect symmetry, while FtsZ failed to localize properly in *ylmE* mutants. Therefore, YlmE plays a more important role than YlmD during sporulation-specific cell division. Indeed, many bacteria that have *ylmE* lack *ylmD* and this makes it unlikely that YlmE functionally depends on the activity of YlmD. Considering the relatively mild (though by no means irrelevant) sporulation defect of *ylmD* mutants, we primarily focused on unravelling the function of *ylmE*.

The major question to answer is, how does YlmE (and YlmD) contribute to sporulation of *Streptomyces*? Previous work by others showed that the YlmE ortholog in *E. coli*, YggS, somehow controls the levels of the branched chain amino acids Val and Ile, and is required for supplying Coenzyme A to the cells (Ito *et al.*, 2013). Expression of YlmE from *B. subtilis* in *E. coli yggS* mutants could overcome this defect. The same authors also showed that purified YlmE did not act as a racemase despite its racemase domain, and failed to bind any of the amino acids. We recently initiated extensive metabolite binding experiments to compare alanine racemase Alr with YlmE, using a calorimetric assay (ITC) (Rafaella Tassoni, , Lizah van der Aart, Gilles P. van Wezel and Marcellus Ubbink, unpublished data). This revealed strong affinity of Alr for L-Ala and D-Ala as well as for D-cycloserine (DCS), an antibiotic which inhibits cell-wall biosynthesis by blocking the function of Alr and Ddl. The binding of DCS was further supported by a ^{15}N-HSQC titration experiment. However, the same experiments showed that YlmE not only fails to bind D-Ala, L-Ala or DCS, but also L-Glu and D-Glu, L-Gln, pyruvate, L-Val, α-ketoglutarate and γ-aminobutyrate (GABA) (Rafaella Tassoni, Lizah van der Aart, Gilles P. van Wezel and Marcellus Ubbink, unpublished data). Still, our data demonstrated

that deletion of *ylmE* makes the cells much more sensitive to the antibiotic D-cycloserine, which is a feature typical of alanine racemase mutants and strains with reduced D-Ala levels.

At present the data on YlmE are hard to reconcile. While the purified YlmE bound to its cofactor PLP (as shown by the yellow color of the protein solution), we cannot rule out that YlmE was not active *in vitro*, either due to incorrect folding or because it requires another protein or molecule for its activity. To establish if YlmE could act as a true alanine racemase *in vivo*, we attempted to complement the D-Ala auxotrophy of *alr* null mutants of *S. coelicolor* by introducing clones expressing *ylmE* from the strong constitutive *ermE* promoter or from the *alr* promoter. This should allow expression of *ylmE* during vegetative growth. However, the transformants failed to grow in the absence of D-Ala, in other words Alr was still required to produce sufficient D-Ala for growth. Taken together, this suggests that YlmE is not an alanine racemase, but instead controls the flux of D-Ala, *e.g.* by producing a metabolite whose biosynthesis relates directly to D-Ala and will lead to depletion of the D-Ala pool in the absence of YlmE. Still, such a compound should directly relate to sporulation-specific cell division, considering the transcriptional linkage between *ylmE* and *ftsZ* and the major defects in cell-wall synthesis caused by the deletion of *ylmE*. Conceivably, YlmE may produce a cell wall-related metabolite, which in the absence of YlmE failed to keep D-Ala at cell division sites, resulting in a drain of the D-Ala pool specifically for sporulation.

In summary, we have shown that the cell division-related *ylmD* and *ylmE* play an important role in the early stages of sporulation-specific cell division, whereby *ylmE* is required for sporulation. Thought YlmE contains the alanine racemase domain and *ylmE* mutant is hyper sensitive to D-cycloserin which is typical phenotype caused by D-alanine reduction. However, our experiments failed to establish such a racemase activity *in vitro* or *in vivo*, and the precise way that YlmE controls the flux of D-Ala remains to be elucidated.

ACKNOWLEDGEMENTS

We are very grateful to Raffaella Tassoni and Marcellus Ubbink for sharing unpublished data and for discussions.

V

The Lcm proteins control spore wall integrity of *Streptomyces*

Le Zhang, Joost Willemse, Changsheng Wu, Young H. Choi and Gilles P. van Wezel

ABSTRACT

Streptomycetes are mycelial microorganisms that reproduce by sporulation. Studying spontaneous mutants with defects in morphogenesis is a promising approach to find novel genes that control growth and/or development. Here we show that the spontaneous mutant *Streptomyces griseus* SY1, which hyper-sporulates in submerged cultures, has a nonsense mutation in the first gene of the *lcmABC* operon, which is widely distributed among the actinobacteria and was previously implicated in cell division in *Bacillus*. Deletion of the *lcmABC* gene cluster or recreating the nonsense mutation in *lcmA* in *S. griseus* or our model strain *Streptomyces coelicolor* resulted in accelerated growth and development on solid media, with longer spores with a thinner spore wall, which were sensitive to heat. Defective septum synthesis was frequently observed in the mutants. LcmA, LcmB and LcmC localized as a regular pattern of foci in young aerial hyphae, and then localized at the septum during sporulation-specific cell division, whereby LcmB overlapped the entire septum, while LcmA and LcmC crossed the septum at a 45º angle, perhaps forming a complex at the site of septum closure. NMR-based metabolomic analysis showed significant changes in terms of primary metabolite composition in *lcmABC* and *lcmA** mutants. Our data show that LcmA, LcmB and LcmC are novel cell division-related proteins in *Streptomyces* that are required for spore integrity.

INTRODUCTION

Actinomycetes are important industrial microorganisms as producers of a wide variety of natural products, including antibiotics, anticancer agents and immunosuppressants (Hopwood, 2007), as well as many industrially relevant enzymes (Vrancken and Anné, 2009). Of the actinomycetes, the streptomycetes produce around half of all known antibiotics. Streptomycetes are mycelial microorganisms not dissimilar to filamentous fungi in their morphology, and undergo a complex multicellular life cycle (Claessen *et al.*, 2014). After germination of a spore, a branched vegetative mycelium is formed that consists of multinucleoid compartments separated by cross-walls (Chater and Losick, 1997). In the reproductive phase, triggered by adverse conditions such as nutrient depletion, aerial hyphae are formed that eventually differentiate into long chains of spores.

In submerged cultures streptomycetes grow as mycelial networks, and often form large mycelial pellets. However, a number of streptomycetes, including the streptomycin producer *Streptomyces griseus* and the chloramphenicol producer *Streptomyces venezuelae*, show more dispersed growth and can sporulate in submerged culture (Girard *et al.*, 2013). The process of submerged sporulation has not been studied extensively, but is important for our understanding of sporulation-specific cell division; it allows the identification of genes that affect sporulation-specific cell division but not aerial hyphae formation (Reviewed in (van Dissel *et al.*, 2014)). Besides the important fundamental implications, knowledge of the genes that control liquid-culture morphogenesis can also be exploited for directed strain evolution at the molecular level for industrial application.

To obtain more information on genes that play a role in submerged sporulation and cell division of streptomycetes, studying spontaneous mutants is an attractive approach, in particular now genome sequencing and comparison has become feasible. One such mutant is strain SY1 of *Streptomyces griseus*, which was derived as a fragmenting variant of *S. griseus* NRRL B2682 by random mutagenesis (Kawamoto and Ensign, 1995). While the parental strain only sporulates after nutritional shift-down from rich to poor media, its derivative SY1 also sporulates in rich cultures, similarly to *S. venezuelae*. On studying *S. griseus* SY1 in more detail, we previously reported that the strain produces enhanced levels of the cell division activator protein SsgA, which is important for sporulation in surface- and liquid-grown cultures (van Wezel *et al.*, 2000b). Members of the family of SsgA-like proteins exclusively occur in actinomycetes, and the number of paralogs in an organism directly relates to

the morphogenesis (Jakimowicz and van Wezel, 2012; Traag and van Wezel, 2008). Overexpression of SsgA from *S. griseus* in *S. coelicolor* induces mycelial fragmentation and spore formation in submerged cultures (van Wezel *et al.*, 2000b). This was applied in industrial fermentations to obtain improved growth and enzyme production during fermentation (van Wezel *et al.*, 2006). Of the SALPs, *ssgA, ssgB* and *ssgG* control septum-site localization in streptomycetes, whereby *ssgA* and *ssgB* are essential for sporulation (Keijser *et al.*, 2003; Sevcikova and Kormanec, 2003; van Wezel *et al.*, 2000b).

Understanding the nature of the mutation in *S. griseus* SY1, could better our understanding of the control of submerged sporulation and cell division in streptomycetes. In this work compared the genomes of *S. griseus* SY1 with its parent B2682, which identified several SNPs, including a mutation in a putative sporulation-related gene SCO1387 that resulted in a premature stop codon after the sixth codon position. SCO1387 is the first gene of a likely operon of three genes encoding membrane proteins of unknown function, which we renamed *lcmABC* (for liquid culture morphology). LcmB was previously implicated as a sporulation-related protein in *Bacillus subtilis* (Beall and Lutkenhaus, 1989). In this work, we show that the Lcm proteins play a role in morphogenesis probably via affecting spores composition.

MATERIALS AND METHODS

Bacterial strains and media

Bacterial strains used in this work are listed in Table 1. *Escherichia coli* strains JM109 (Sambrook *et al.*, 1989) was used for routine cloning procedures, *E. coli* ET12567 (MacNeil *et al.*, 1992; Kieser *et al.*, 2000) was used for obtaining non-methylated DNA isolation for efficient *S. coelicolor* transformation and *E. coli* IR539 (Suzuki *et al.*, 2011) for preparing DNA for efficient transformation of *S. griseus*. *E.coli* transformants were selected on LB agar containing the appropriate antibiotics and grown O/N at 37°C (Sambrook *et al.*, 1989). *Streptomyces coelicolor* A3(2) M145 and *Streptomyces griseus* IFO13350 were the parents for the mutants. YMPD (Ohnishi *et al.*, 1999) or TSBS (tryptone soy broth (Difco) containing 10% (w/v) sucrose) were used for standard cultivation as described (Kieser *et al.*, 2000). R5 agar plates were used for regeneration of protoplasts and - after addition of antibiotics - to select recombinants, and SFM (soy flour mannitol) and MM (minimal media) agar plates for preparing spores suspensions, and for morphological characterization and microscopy of all strains (Kieser *et al.*, 2000).

Plasmids and constructs

Plasmids and constructs used in this work are summarized in Table 2, all oligonucleotides are listed in Table 3.

Constructs for creating mutants and for complementation

The strategy for creating knock-out mutants was described previously (Świątek *et al.*, 2012). The method is based on the multi-copy shuttle vector pWHM3 (Vara *et al.*, 1989), which is an unstable multi-copy vector that is easily lost when selection is relieved (van Wezel *et al.*, 2005). For the deletion of *lcmA*, plasmid pGWS736 was created. For this, the -1496/+6 upstream region (nt numbering relative to the start of *lcmA*) was amplified by PCR from *S. coelicolor* M145 genomic DNA using primer pairs lcmA_LF-1496 and lcmA_LR+6, and the downstream region +832/+2232 was amplified using primer pair lcmA_RF+832 and lcmA_RR+2232. The PCR-amplified upstream and downstream regions were digested with EcoRI and XbaI, and with XbaI and HindIII, respectively, and ligated in a three-fragment ligation into EcoRI/HindIII-digested vector pWHM3. The unique XbaI site engineered in-between the flanking regions allows insertion of the apramycin resistance cassette *aac(3)IV* flanked by *loxP* recognition sites. The presence of *loxP* sites allows

efficient removal of the apramycin resistance cassette by expression of the Cre-recombinase by introducing plasmid pUWL-Cre, which then generates a marker-less deletion mutant (Fedoryshyn *et al.*, 2008). Essentially the same strategy was used to create gene deletion constructs pGW738, pGWS739, and pGWS740 for the gene replacement of *lcmB*, *lcmC*, and the whole *lcmABC* gene cluster, respectively. pGWS738 contains the -1483/+60 and +274/+1832 regions relative to the start of *lcmB*, pGWS739 contains the -1396/+45 and +847/+2177 regions relative to the start of *lcmC*, and pGWS740 contains the -1496/+6 region relative to *lcmA* and the downstream +847/+2177 region relative to *lcmC*. All constructs contained the apramycin resistance cassette flanked by *loxP* sites for selection of mutants and subsequent removal to create markerless deletion mutants.

Construct pWGS737 was designed to replace the 7th codon position of *lcmA* by a stop codon, corresponding to the spontaneous mutation found in *S. griseus* SY1. pGWS737 contains -1496/+21 and +22/+2232 regions relative to *lcmA,* with the apramycin resistance cassette flanked by *loxP* sites inserted in-between. Regions -1496/+21 and +22/+2232 relative to *lcmA* were amplified using primer pairs lcmA_LF-1496 and lcmA_LR+21 and lcmA_RF+22 and lcmA_RR+2232, respectively. Primers lcmA_LR+21 contains mutation at amino acid position 7 of *lcmA*; CCA was changed to TGA (proline was changed to stop codon). Using a similar approach, plasmids pGWS741, pGWS742 and pGWS743 were created, for the deletion of *lcmA*, to create a non-sense mutation at the 7th codon position in *lcmA* and to delete *lcmABC*, respectively, in strain *S. griseus* IFO13350.

For complementation of the mutants of *S.coelicolor* M145 construct pGWS778 was made which is based on the integrative vector pSET152 (Bierman *et al.*, 1992). For this, the entire *lcmABC* gene cluster (including promoter region) was amplified by PCR using primer pair lcmB_LF-1483 and lcmB_R+1326, and inserted into EcoRI/XbaI-digested pSET152. The construct harbors the entire *lcmABC* gene cluster including 580 bp of upstream and 140 nt downstream region and expresses *lcmABC* from the natural promoter.

Constructs for translational fusion of LcmABC with eGFP

To obtain a construct expressing LcmA-eGFP, we used plasmid pKF41 which expresses FtsZ-eGFP from the native *ftsZ* promoter region (Grantcharova *et al.*, 2005). The insert was excised with BglII and NotI, cloned into the integrative vector pSET152 and the coding region of *ftsZ* was replaced by that of *lcmA*. For this, the vector was digested with StuI and BamHI, the *lcmA*

gene was PCR-amplified from the genome of *S. coelicolor* using primer pair lcmA_F+1 and lcmA_R+903, and cloned as a StuI-BglII fragment in-between *ftsZ*p and *egfp* to generate pGWS768. Using the same strategy, pGWS769 and pGWS770 were constructed for in frame fusion of *lcmB-egfp* and *lcmC-egfp* using primer pairs lcmB_F+1 and lcmB_R+330 and lcmC_F+1 and lcmC_R+852, respectively.

Table 1. Bacterial strains

Bacteria strains	Genotype	Reference
E. coli JM109	See reference	(Sambrook *et al.*, 1989)
E. coli ET12567	See reference	(MacNeil *et al.*, 1992)
E. coli IR539	See reference	(Suzuki *et al.*, 2011)
S. coelicolor M145	$SCP1^{-}$ $SCP2^{-}$	(Kieser *et al.*, 2000)
S. griseus IFO13350	See reference	(Ohnishi *et al.*, 2008)
GAL56	M145 Δ*lcmA*	This work
GAL57	M145 Δ*lcmB*	This work
GAL58	M145 Δ*lcmC*	This work
GAL59	M145 *lcmA** (7^{th} AA changed to stop codon)	This work
GAL60	M145 Δ*lcmABC*	This work
GAL61	M145 Δ*gcvP* (::*aac(3)IV*)	This work
GAL56-sg	IFO13350 Δ*lcmA*	This work
GAL59-sg	IFO13350 Δ*lcmA**	This work
GAL60-sg	IFO13350 Δ*lcmABC*	This work
GAL64	M145 + pGWS768	This work
GAL65	M145 + pGWS769	This work
GAL66	M145 + pGWS770	This work
GAL68	GAL59 + pGWS778	This work
GAL69	GAL60 + pGWS778	This work
ΔUTR-T	*S. griseus* IFO13350 with deletion of 5'-untranslated region of *gcvTH*	(Tezuka and Ohnishi, 2014)
ΔUTR-P	*S. griseus* IFO13350 with deletion of 5'-untranslated region of *gcvP*	(Tezuka and Ohnishi, 2014)
ΔUTR-PΔUTR-T	*S. griseus* IFO13350 with deletion of 5'-untranslated regions of *gcvP* and *gcvTH*	(Tezuka and Ohnishi, 2014)

Table 2. Plasmids and Constructs

Plasmid and constructs	Description	Reference
pWHM3	*E. coli*/*Streptomyces* shuttle vector, high copy number but unstable in *Streptomyces*	(Vara *et al.*, 1989)
pSET152	*E. coli*/*Streptomyces* shuttle vector, high copy number in E. coli and integrative in Streptomyces	(Bierman *et al.*, 1992)
pUWL-Cre	plasmid expressing Cre-recombinase	(Fedoryshyn *et al.*, 2008)
pGWS736	pWHM3 containing flanking regions of *S. coelicolor* SCO1387 with apra*loxP* inserted in-between	This work
pGWS737	pWHM3 containing regions -1496/+21 and +22/+2232 relative to SCO1387 with apraloxP-XbaI inserted between and with non-sense mutation at 7th amino acid position of SCO1387	This work
pGWS738	pWHM3 containing flanking regions of *S. coelicolor* SCO1386 with apra*loxP* inserted in-between	This work
pGWS739	pWHM3 containing flanking regions of *S. coelicolor* SCO1385 with apra*loxP* inserted in-between	This work
pGWS740	pWHM3 containing upstream region of *S. coelicolor* SCO1387 and downstream region of *S. coelicolor* SCO1385 with apra*loxP* inserted in-between in pWHM3	This work
pGWS752	pWHM3 containing flanking regions of *S. coelicolor* SCO1378 with apra*loxP* inserted in-between	This work
pGWS741	pWHM3 containing flanking regions of *S. griseus* SGR_6142 with apra*loxP* inserted in-between	This work
pGWS742	pWHM3 containing Regions -1473/+21 and +22/+2312 relative to SGR_6142 apra*loxP* inserted in-between and with non-sense mutation at 7th amino acid position of SGR_6142	This work
pGWS743	pWHM3 containing upstream region of *S. griseus* SGR_6142 and downstream region of *S. griseus* SGR_6144 with apra*loxP* inserted in-between	This work
pGWS768	pSET152 harboring *lcmA* and *egfp* under control of the *ftsZ* promoter	This work
pGWS769	pSET152 harboring *lcmB* and *egfp* under control of the *ftsZ* promoter	This work
pGWS770	pSET152 harboring *lcmC* and *egfp* under control of the *ftsZ* promoter	This work
pGWS778	pSET152 with 2.8kb fragment harboring *lcmABC* cluster and its native promoter region	This work

Table 3. Oligonucleotides

Name	5'-3' sequence[#]
lcmA_LF-1496	GTCA**GAATTC**GCGCGTTCGTCAACACCTCGGTG
lcmA_LR+6	GTCAGAAGTTATCCATCACC**TCTAGA**GCACATCGTCGCACGCCACCGCCA
lcmA_RF+832	GTCAGAAGTTATCGCGCATC**TCTAGA**GACCTCAAGCTGCCGGCCGCACCG
lcmA_RR+2232	GTCA**AAGCTT**AACGCACTGGCCGACCCGGACAC
lcmA_LR+21	GTCAGAAGTTATCCATCACC**TCTAGA**TCACTGCGGCATGCCGCACATCGT
lcmA_RF+22	GTCAGAAGTTATCGCGCATC**TCTAGA**CCCCCCGTTCGGAGCACACCCGGG
lcmB_LF-1483	GTCA**GAATTC**GTACCACGGCACGCAGGTCGAG
lcmB_LR+60	GTCAGAAGTTATCCATCACC**TCTAGA**CTCGGGCCGGACCAGCAATCCGGC
lcmB_RF+274	GTCAGAAGTTATCGCGCATC**TCTAGA**CTCGGCATCCGTATCTTCTCCAAC
lcmB_RR+1832	GTCA**AAGCTT**ATCGCCGTCTGGCCGGTGACCTC
lcmC_LF-1396	GTCA**GAATTC**TCCGCACAGGCGCTGCTGGA
lcmC_LR+45	GTCAGAAGTTATCCATCACC**TCTAGA**CAGCTCCTTGCGCAGCCTGTTCGC
lcmC_RF+847	GTCAGAAGTTATCGCGCATC**TCTAGA**TCCCAGTGAACCGGCGGTGCATGG
lcmC_RR+2177	GTCA**AAGCTT**ACGGCGTCCAGATGCTCACG
lcmB_R+1326	GTCA**TCTAGA**ACGCACTGGCCGACCCGGACAC
gcvP_LF-1309	GTCA**GAATTC**ACTGTCCGGGCGGACCATCG
gcvP_LR+9	GTCAGAAGTTATCCATCACC**TCTAGA**GGCGGTCATTGCGGAGGCCTC
gcvP_RF+2881	GTCAGAAGTTATCGCGCATC**TCTAGA**GACTGAGTCCCGCCAAGAAGG
gcvP_RR+4232	GTCA**AAGCTT**CGACGCCCGTCAGTGGATGC
lcmA-sg_LF-1473	GTCA**GGATCC**ACGTCGAGATCACCCCCGAACTG
lcmA-sg_LR+6	GTCAGAAGTTATCCATCACC**TCTAGA**GCACATCGTCGCACGTCATCACGG
lcmA-sg_RF+850	GTCAGAAGTTATCGCGCATC**TCTAGA**GCCTGATCGTCCGTACAGCAGAG
lcmA-sg_RR+2312	GTCA**AAGCTT**ACTGTTGCTGTCCTCGCGTGCAC
lcmA-sg_LR+21	GTCAGAAGTTATCCATCACC**TCTAGA**CTACTGCGACATGCCGCACATCGT
lcmA-sg_RF+22	GTCAGAAGTTATCGCGCATC**TCTAGA**TCCCCCGATCGGAGCACCGCCCCG
lcmC-sg_RF+811	GTCAGAAGTTATCGCGCATC**TCTAGA**TCCCCGTGAGCCGGCCGAGCGTGA
lcmC-sg _RR+2100	GTCA**AAGCTT**CCCTGATGACCTTCAGCGGCAG
lcmA_F+1	GTCAGAATTC**AGGCCT**TCGACATGTGCGGCATGCCGCAGCCA
lcmA_R+903	GCTAAAGCTT**AGATCT**GATGTGCCCTTCTCGGTTAT
lcmB_ F+1	GTCAGAATTC**AGGCCT**TCGACGTGATCGCCGTACTGGGCCTC
lcmB_R+330	GCTAAAGCTT**GGATCC**GCCCGGAAGACGTGGCGTCG
lcmC_F+1	GTCAGAATTC**AGGCCT**TCGACATGAGCGACGACGAGCAGCCG
lcmC_R+852	GCTAAAGCTT**GGATCC**TGGGAGGACGACCGAGCGTA

[#] Restriction sites are underlined and in bold face. GGATCC, BamHI; AGATCT, BglII; GAATTC, EcoRI; AAGCTT, HindIII; AGGCTT, StuI; TCTAGA, XbaI.

Microscopy

S. coelicolor M145 and its mutant derivatives were grown on SFM agar plates and incubated at 30°C for 5-6 days. Aerial hyphae/ spores of *S. coelicolor* and derivatives were studied by cryo-scanning electron microscopy (SEM) using a JEOL JSM6700F cryo-scanning electron microscope as described (Colson *et al.*, 2008). Thin sections of hyphae and spores were imaged at high resolution by Transmission electron microscopy (TEM) using a FEI Tecnai 12 BioTwin transmission electron microscope (Noens *et al.*, 2005).

Sterile cover slips were inserted into SFM agar plates under a 45 degree angle and *S. coelicolor* strains grown at the intersection angle for 3-5 days at 30°C. Then the cover slips were placed on a microscope slide with 5 µl of PBS for fluorescence and corresponding light micrographs, which were taken with an Axiocam Mrc5 camera at a resolution of 37.5 nm/pixel. FITC-WGA, FM5-95 and DAPI were used for staining of cell wall (peptidoglycan), membrane and DNA respectively. The green fluorescence was imaged using 470/40 nm band pass (bp) excitation and 525/50 bp detection; the red images were created using 550/25 nm bp excitation and 625/70 nm bp detection; DNA staining with DAPI was visualized using 370/40 nm excitation with 445/50 nm emission band filter (Willemse and van Wezel, 2009). Images were processed using Adobe Photoshop CS4.

Computer analysis

DNA and protein database searches were done using StrepDB (http://strepdb.streptomyces.org.uk). Phylogenetic relationship analyses and homology searched were performed using STRING (http://string.embl.de). Putative transmembrane domains were identified using transmembrane prediction server DAS (http://www.sbc.su.se/~miklos/DAS).

NMR measurement of spores

For the preparation of cultures, approximately 10^7 spores were inoculated onto 25 ml SFM agar and incubated at 30 °C for 7 days. For each strain, spores from three SFM agar plates were collected in 15 ml H_2O, spores harvested by centrifugation at 3000 rpm for 15 min and supernatant and pellet separated. Spores and spore washout samples were frozen at -80 °C and dehydrated in a freeze dryer for two days. 20 mg of each sample was then re-dissolved in 500 µl D_2O-phosphate buffer and 500 µl CD_3OD, sonicated for 30 minutes for NMR analysis. 0.03% of 3-(trimethylsilyl) propionic acid-d4 sodium salt (TSP) was added to D_2O-phosphate buffer as internal marker. All experiments

were carried out in quintuplicate.

NMR was performed on a 600 MHz Bruker DMX-600 spectrometer (Bruker, Karlsruhe, Germany) operating at a proton NMR frequency of 600.13 MHz. Detailed NMR parameters were used as previously described (Kim *et al.*, 2010). Methanol-*d4* was used as the internal lock. Each ^{1}H NMR spectrum consisted of 128 scans requiring 10 min and 26 sec acquisition time with the following parameters: 0.16 Hz/point, pulse width (PW) = 30° (11.3 μsec), and relaxation delay (RD) = 1.5 sec. A pre-saturation sequence was used to suppress the residual H_2O signal with low power selective irradiation at the H_2O frequency during the recycle delay. FIDs were Fourier transformed with LB = 0.3 Hz. The resulting spectra were manually phased and baseline corrected, and calibrated to MeOH- *d*4 at 3.3 ppm, using XWIN NMR (version 3.5, Bruker).

^{1}H NMR spectra were manually phased, baseline corrected and calibrated. ^{1}H-NMR spectra were further automatically converted to ASCII files using AMIX (v. 3.7, Bruker Biospin). Spectral intensities were scaled to total intensity and the region of δ_H 0.3-10.0 was reduced to integrated regions of width (0.04 ppm). The regions δ_H 4.7 - 5.0 and δ_H 3.30 - 3.34 were excluded from the analysis because of the residual signal of H_2O and methanol-*d4*, respectively. Data were extracted after acquiring the spectra by "binning" or "bucketing", in which spectra are split into discrete regions and integrated (Jellema *et al.*, 2009). Principal component analysis (PCA) was performed with the SIMCA-P software (v. 13.0, Umetrics, Umeå, Sweden) with scaling methods (Kim *et al.*, 2010).

RESULTS

SNP analysis of *S. griseus* SY1 reveals a mutation in a novel cell division-related gene

To identify the mutations in *S. griseus* SY1 relative to its parent *S. griseus* NRRL B2682, both strains were sequenced by Illumina paired end sequencing, and compared to the wild-type strain *S. griseus* IFO13350 (Ohnishi *et al.*, 2008). This revealed around 100 single nucleotide permutations (SNPs) between SY1 and the published sequence of the wild-type strain (not shown). A single SNP stood out, which was a nonsense mutation in gene SGR_6142, the first gene of a likely operon of hypothetical genes encoding membrane proteins; the mutation results in a premature translational stop, whereby Gln7 codon CAG was changed into a TAG stop codon. This will most likely also affect the expression of the downstream genes SGR_6143 and SGR_6144. The orthologs of this gene cluster in *S. coelicolor* are SCO1387-1385. Considering their correlation to the morphology in liquid-grown cultures, the genes SGR_6142-6144 and SCO1387-1385 were renamed *lcmA-C* (for liquid culture morphology) (Fig. 1A).

1A

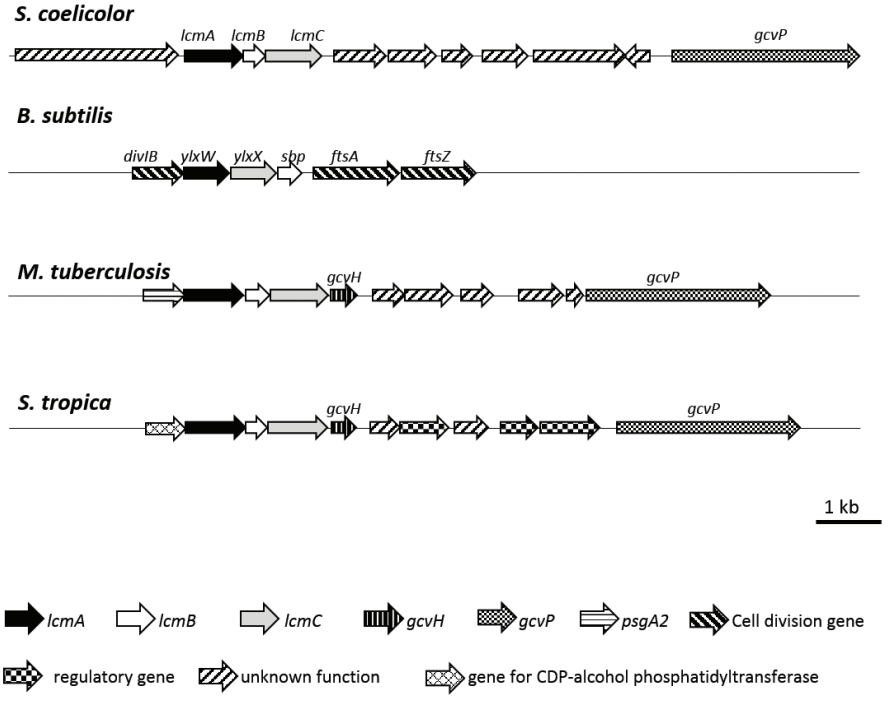

1B

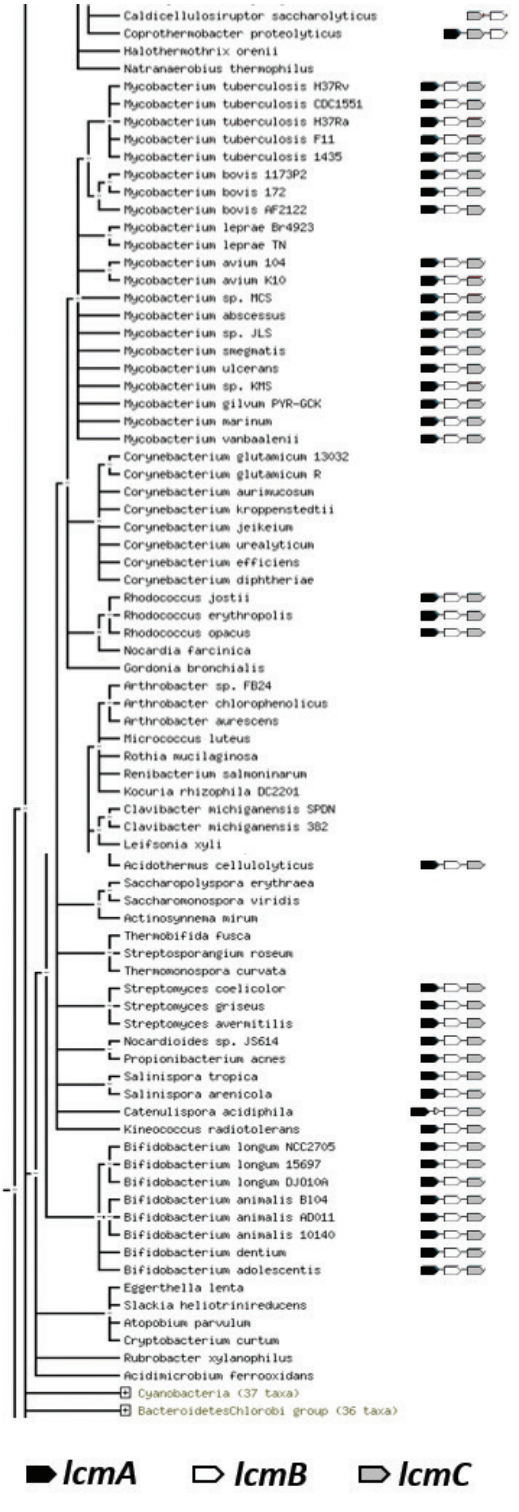

Figure. 1 Gene organization and conservation of *lcm* genes.
(A) Gene organization around the *lcm* genes. The genetic context in *Streptomyces coelicolor* is compared to that in *Bacillus subtilis*, *Mycobacterium tuberculosis* and *Salinispora tropica*. **(B)** Phylogenetic distribution of *lcm* genes in Actinobacteria (output from String engine)

The *lcm* gene cluster

The *lcm* genes are widely conserved among actinobacteria, in a pattern of "all or none", in other words when present they always occur as a cluster (Fig. 1B). With four nucleotides overlap between *lcmA* and *lcmB* and only five nucleotides spacing between *lcmB* and *lcmC*, the three genes most likely form an operon (Romero A *et al.*, 2014). LcmA (301 aa) and LcmC (284 aa) are paralogs based on the significant homology of 30% aa identity and 50% aa similarity between them, in both *S. coelicolor* and *S. griseus*. LcmA and LcmC have a predicted N-terminal transmembrane domain of unknown function (DUF881). Interestingly, LcmC also contains an additional FliH domain, belonging to flagellar assembly proteins. LcmB (110 aa) is a basic protein with four predicted transmembrane domains.

The orthologs of *lcmA*, *lcmB* and *lcmC* in *B. subtilis* are *ylxX*, *sbp* and *ylxW*, respectively, which are located downstream of *divIB* in the *dcw* cluster with genes involved in cell division and cell-wall synthesis (Rowland *et al.*, 1995; Cha and Stewart, 1997) (Fig. 1A). Temperature-sensitive mutant *B. subtilis tms-12* has a sporulation defect at elevated temperatures (Breakefield and Landman, 1973; Miyakawa and Komano, 1981). The *tms-12* mutation in *B. subtilis* mutates *divIB*, and surprisingly, like the mutation in *lcmA*, was also a nonsense mutation close to the start of the gene, resulting in elimination of 93 residues of the DivIB protein (Beall and Lutkenhaus, 1989). *divIB* lies immediately upstream of *ylxX*, and considering the translational coupling between *divIB* and *ylmX*, with overlapping stop and start codons (ATGA arrangement, whereby ATG is the start codon for *ylmX* and TGA the stop codon for *divIB*), the nonsense mutation in *divIB* most likely affects the expression of the downstream genes *ylxX*, *ylxW* and *sbp*. These data suggest that the *Streptomyces lcm* locus may play a role in cell division, apparently correlating with the observed fragmenting phenotype of spontaneous mutant SY1 of *S. griseus*.

Deletion of the *lcm* genes accelerates development in *S. coelicolor*

To investigate the effect of the mutation in *lcmA* on growth and development of wild-type *S. griseus* IFO13350 and of *S. coelicolor* M145, mutants of the *lcmABC* operon were created, so as to obtain single mutants and a cluster deletion. The strategy and plasmids used for gene replacements and mutations are described in detail in the Materials and Methods section. To introduce the corresponding nonsense mutation found in SY1 in *S. coelicolor lcmA*, the CCA codon for amino acid residue Pro7 was changed to a TGA stop codon, resulting in strain GAL59. Deletion mutants GAL56 (*S. coelicolor* M145 Δ*lcmA*),

GAL57 (*S. coelicolor* M145 Δ*lcmB*) and GAL58 (*S. coelicolor* M145 Δ*lcmC*) were also obtained, as well as cluster deletion mutant GAL60. Similarly, the CAG codon for amino acid residue Gln7 of *S. griseus lcmA* was changed to a TAG stop codon, resulting in strain GAL59-sg. Mutants GAL56-sg (*S. griseus* IFO13350 Δ*lcmA*) and GAL60-sg (*S. griseus* IFO13350 Δ*lcmABC*) were created using *S. griseus* IFO13350 as the parental strain.

The morphology all mutants and their parental strains were studied in submerged culture. Despite the strong phenotype of *S. griseus* SY1, none of the mutants of *S. coelicolor* or *S. griseus* showed mycelial fragmentation under the conditions tested (Fig. 2A). Dense clumps were produced by all mutants, similar as the parents *S. griseus* IFO13350 or *S. coelicolor* M145. Light microscopy did not identify major changes in development in any of the *lcm* mutants in *S. coelicolor* or *S. griseus*, producing abundant grey-pigmented spores, very similar to the parental strains, although some mutants consistently sporulated earlier than the parent. Further studies on the effect of the *lcm* mutations were done only in *S. coelicolor*.

2A

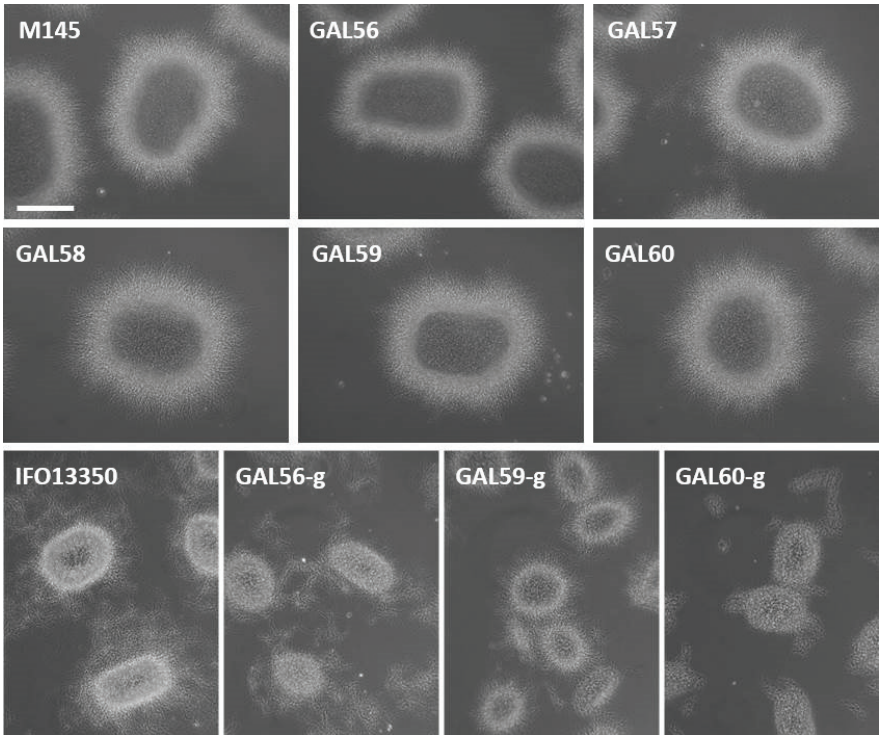

2B

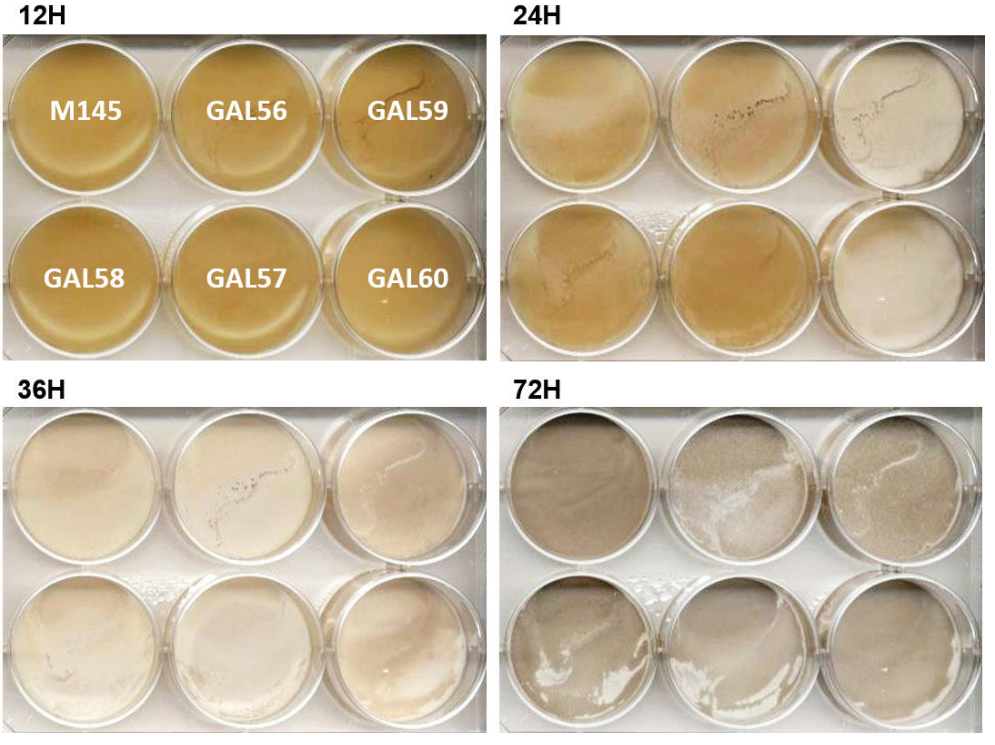

Figure. 2 Morphology of *S. coelicolor* and *S. griseus* and their *lcm* mutants.
(A) phase-contrast micrographs of liquid-grown cultures of wild-type *S. coelicolor* M45, and its mutant derivatives GAL56 (Δ*lcmA*), GAL57 (Δ*lcmB*), GAL58 (Δ*lcmC*), GAL59 (*lcmA**, nonsense mutation) and GAL60 (Δ*lcmABC*), and wild-type *S. griseus* IFO13350 and its mutants GAL56-g (Δ*lcmA-sg*), GAL59-g (*lcmA*-sg* and GA60-g (Δ*lcmABC-sg*). Bar, 50 μm. **(B)** Growth of *S. coelicolor* M145 and its *lcm* mutants of M145 on SFM medium at different time points.

To investigate whether timing of development was indeed affected in these mutants, spores of *S. coelicolor* mutants were counted using a haemocytometer, and the titer in terms of colony forming units (cfu/ml) determined. The same amount of viable spores was then taken for each strain and plated onto SFM agar plates at 30^0C. The plates were photographed in the incubator at 30 min intervals. Interestingly, strains GAL59 (M145 *lcmA**) and GAL60 (M145 Δ*lcmABC*) produced abundant white-pigmented aerial hyphae after only 24 h of growth, which is much earlier than the wild-type strain (Fig. 2B). After 36 h, GAL59 and GAL60 already entered sporulation, as indicated by the grey pigmentation, while the parent and the other mutants had now initiated aerial growth. After 72 h all strains had completed development (Fig. 2B). On R5 agar media, all mutants produced comparable amount of the pigmented

antibiotics undecylprodigiosin (red) and actinorhodin (blue) as the wild-type strain, but again strains GAL59 and GAL60 developed much earlier than the other strains, consistent with the results obtained for growth on SFM agar (data not shown). Taken together, the *lcmA** and *lcmABC* mutants had accelerated development by at least half a day. However, since none of the single deletion mutants was affected, the accelerated sporulation was most likely due to the absence or altered expression of at least two of the genes.

The *lcm* locus is involved in sporulation

Cryo-scanning electron microscopy (SEM) was used to examine the spores in detail. Wild type *S. coelicolor* M145 produced typical chains of uniform spores. All *lcm* mutants also sporulated abundantly, in line with the light microscopy. However, variations in spore sizes were seen in all mutants (Fig. 3). To quantify this, the average spore length was calculated based on a hundred spores per strain (Table 4). The average length of wild-type spores was 0.97 ± 0.13 μm, while spores of single *lcm* gene deletion mutants GAL56, GAL57 and GAL59 were around 80-110 nm longer. However, the *lcmA** and the *lcmABC* cluster deletion mutants produced significantly larger spores, namely on average 1.12 ± 0.20 μm.

In an attempt to complement the mutants, construct pGWS778, which is a low-copy number vector harboring the entire *lcmABC* cluster and its native promoter region, was introduced into GAL59 and GAL60, generating strains GAL68 (GAL59 + pGWS778) and GAL69 (GAL60 + pGWS778). In line with the notion that the sporulation defect was due only to mutations in the *lcm* cluster, the average spore length of the transformants was reduced to values close to those of the wild-type strain M145, namely to 0.99 ± 0.15 μm and 1.03 ± 0.14 μm, respectively. This established that the genes in the *lcm* locus are involved in sporulation.

Table 4. Spore length of *S. coelicolor* M145, its *lcm* mutants and complemented strains.

	M145	GAL56	GAL57	GAL58	GAL59	GAL60	GAL68	GAL69
Spore length (μm)	0,97 ± 0.13	1.05 ± 0,15	1.08 ± 0.17	1.08 ± 0.23	1.12 ± 0,20	1.12 ± 0.20	0.99 ± 0,15	1.03 ± 0,14

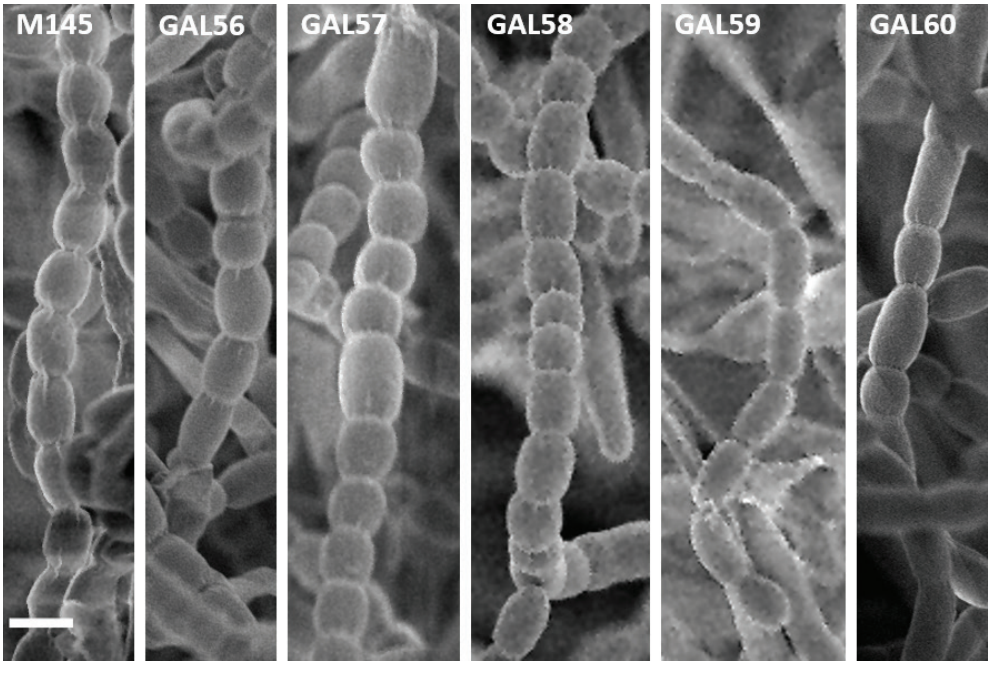

Figure 3. Scanning electron micrographs of spores of wild type *S. coelicolor* M145 and its *lcm* mutants. For strains see legend to Fig. 2A. Cultures were grown on SFM agar plates for 5 days at 30^0C. Bar, 1 μm.

lcm mutants produce heat-sensitive spores

Considering the changes to sporulation seen in the mutants, we examined the stress resistance of the spores. To test heat resistance, around 400 cfu were incubated at 60°C for 10 minutes and plated onto SFM agar plates. Approximately 47% of the wild-type spores survived the heat treatment (Fig. 4A). The survival rates for spores of single deletion mutants GAL56 (Δ*lcmA*), GAL57(Δ*lcmB*) and GAL58 (Δ*lcmC*) were 43%, 40% and 42%, which indicates slightly lower heat resistance as compared to spores of the parent. The *lcmA** and *lcmABC* mutants were less resistant to the heat treatment, with 35% and 36% of spores surviving the heat treatment, respectively. Spores of GAL68 and GAL69, which are GAL59 and GAL60 complemented with pGWS778, showed very similar heat survival rate as wild-type spores (Fig. 4A). This suggests that the increased sensitivity to heat treatment was most likely due to changes in the *lcm* locus.

Transmission electron microscopy (TEM) was applied to study the spores in more detail. Again, the TEM confirmed the large variation in spore sizes in

some of the *lcm* mutants (Fig. 4B). Furthermore, a white crystalline material was often seen to accumulate near the wall of mutant spores (Fig. 4B, arrows). This may be explained as accumulation of the fixative inside the mutant spores (with weaker and hence more easily penetrated spore walls) used for sample fixation prior to TEM imaging. Additionally, while the spores of M145 and of single mutants GAL56, GAL57 and GAL58 had a typical thick cell wall, strain GAL59 that carries non-sense mutation *lcmA** and the *lcm* cluster mutant GAL60 had a thinner cell wall (Fig. 4B). Such a thinner cell wall could explain the increased heat sensitivity, the penetration of fixative and the accelerated germination. The latter corresponds to previous observations that germination efficiency correlates to cell-wall thickness (Piette *et al.*, 2005).

4A

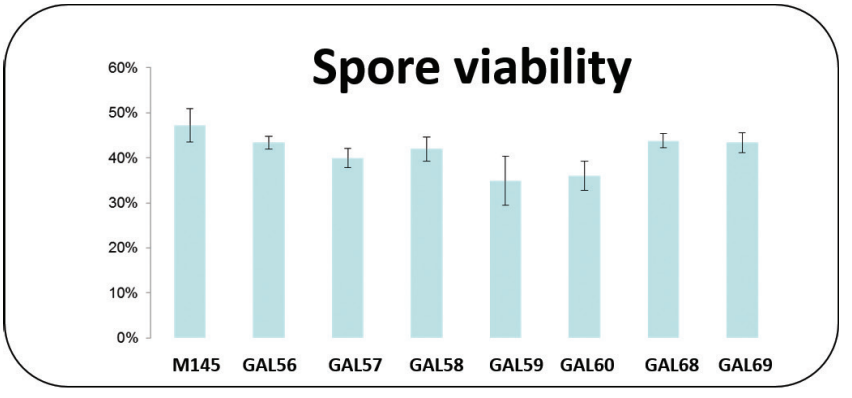

4B

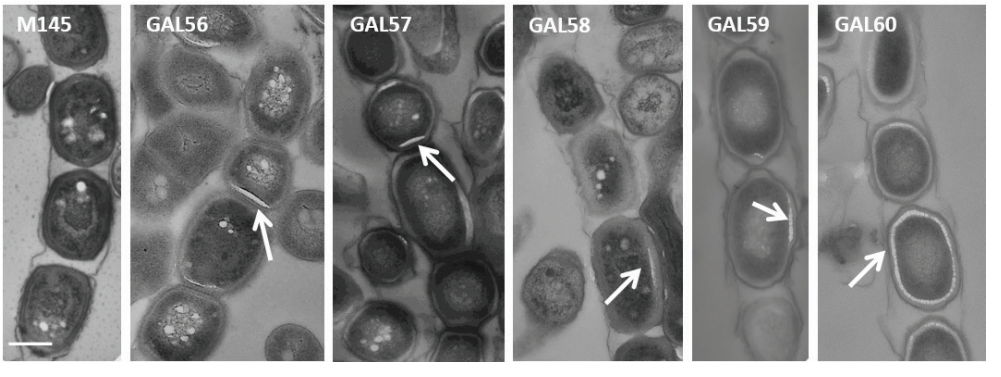

Figure 4. Spore viability after heat shock (A) and transmission electron micrographs (B) of spores of *S. coelicolor* M145 and its *lcm* mutants. For transmission electron microscopy, strains were grown on SFM agar plates for 5 days at 30^{0}C. White crystalline material in *lcm* mutants are indicated by arrows. For strains see legend to Fig. 2A. Bar, 500 nm.

lcm genes and cell-wall assembly

To further study the *lcm* mutants *in vivo*, fluorescence microscopy was applied on 72 hr old SFM-grown strains GAL56, GAL57, GAL58, GAL59, GAL60 and M145 to analyze cell wall, membrane and nucleoid distribution. Peptidoglycan precursors were stained with FITC-WGA, membranes with FM5-95, and DNA with DAPI. Mutants GAL56, GAL57 and GAL58 showed a very similar pattern of cell wall and membrane distribution as the wild type strain, although some variation in spore sizes was observed (Fig. 5A). Conversely, mutants GAL59 (Fig. 5B) and GAL60 (Fig. 5B) produced much larger spores, consistent with the SEM and TEM analysis. Interestingly, the large spores sometimes contained mis-localized cell-wall material, perhaps as a result of incomplete septation; this suggests that the *lcm* gene cluster may play a role in spore maturation and completion of septation. Indeed, we regularly observed incomplete septa in both the *lcmA** mutant and the *lcmABC* deletion mutant (arrows in Fig. 5B).

5A

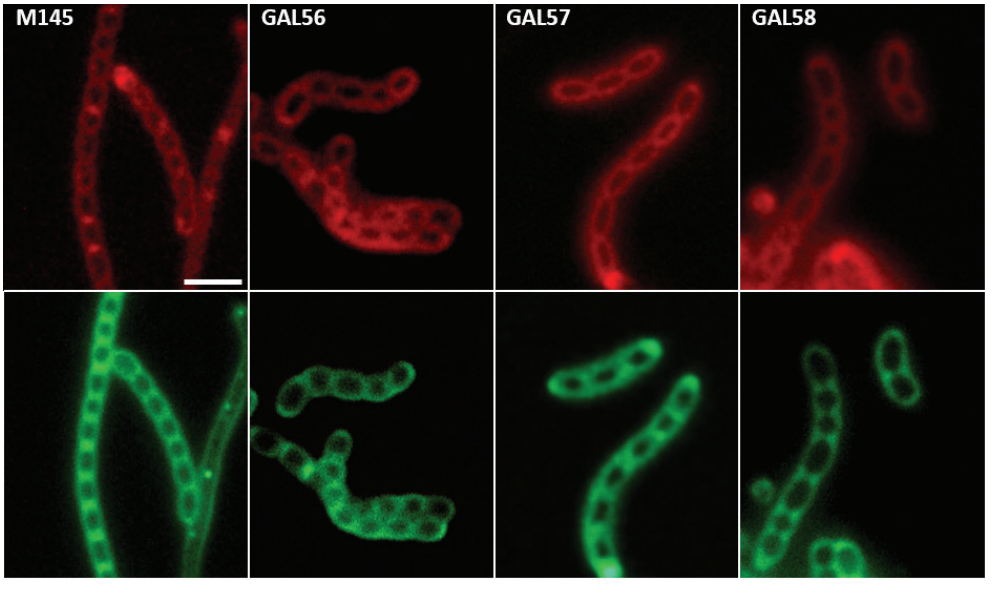

5B

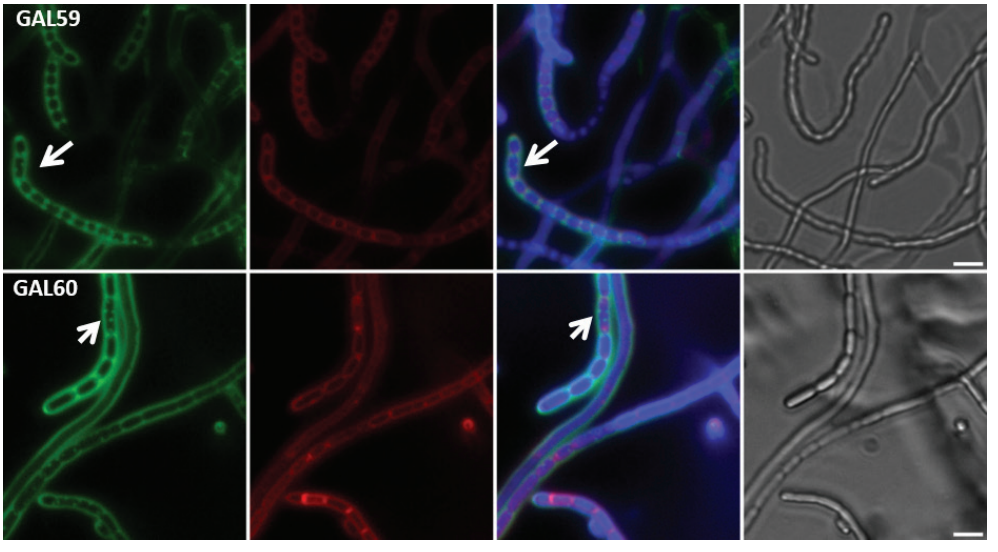

Figure 5. Fluorescence micrographs of *S. coelicolor* M145, and its *lcm* mutants. The samples were stained for cell wall (FITC-WGA, green), membrane (FM5-95, red), or DNA (DAPI, blue; co-stained with FITC-WGA and FM5-95) and corresponding light images. Incomplete septation in GAL59 and GAL60 is indicated by arrows. For strains see legend to Fig. 2A. Bar is 3 μm.

Localization of the Lcm proteins

To examine the localization of the Lcm proteins in the hyphae of *S. coelicolor*, integrative plasmids were constructed, harboring *lcmA, lcmB* or *lcmC* under the control of the *ftsZ* promoter, and fused immediately upstream of *egfp* so as to create translational fusions (see Materials and Methods section). Constructs pGWS768, pGWS769 and pGWS770, which express LcmA-eGFP, LcmB-eGFP and LcmC-eGFP, respectively, were then introduced into *S. coelicolor* M145.

We failed to detect specific localization of LcmA, LcmB or LcmC foci in vegetative hyphae (not shown). However, in aerial hyphae LcmA-eGFP either formed distinct foci, including one at the tip (Fig. 6A), or was more dispersed (Fig. 6A). This indicates that LcmA localizes in a stage-specific manner, and perhaps that the 'random' localization precedes the focal localization, but to determine the precise order requires live imaging. A similar localization pattern as seen for LcmA-eGFP was also observed for LcmB-eGFP and LcmC-eGFP at the stage prior to sporulation (Fig. 6A). Once sporulation had started, and septa ladders became visible, LcmA-eGFP, LcmB-eGFP and LcmC-eGFP localized in a ladder-like pattern close to the septa (Fig. 6B). Interestingly, the

paralogous proteins LcmA and LcmC localized in foci at either side of the center of the septum and in an oblique arrangement, with an imaginary line through the foci forming an approximately 45° angle with the septum (Fig. 6B). However, LcmB-eGFP overlapped the septum (Fig. 6B). The localization of the Lcm proteins could be classified in three groups: overlap with septum staining, no overlap with septum staining and cross-septum staining (*i.e.* foci at either side of the septum). LcmA-eGFP (92%) and LcmC-eGFP (79%) primarily formed foci across the septum, while LcmB-eGFP (89%) dominantly overlapped septum staining (Table 5). This suggests that perhaps the membrane protein LcmB assembles at the septum site, and interacts with LcmA and LcmC at the centre of the septum. No localization of LcmA, LcmB and LcmC was detected in mature spores.

6A

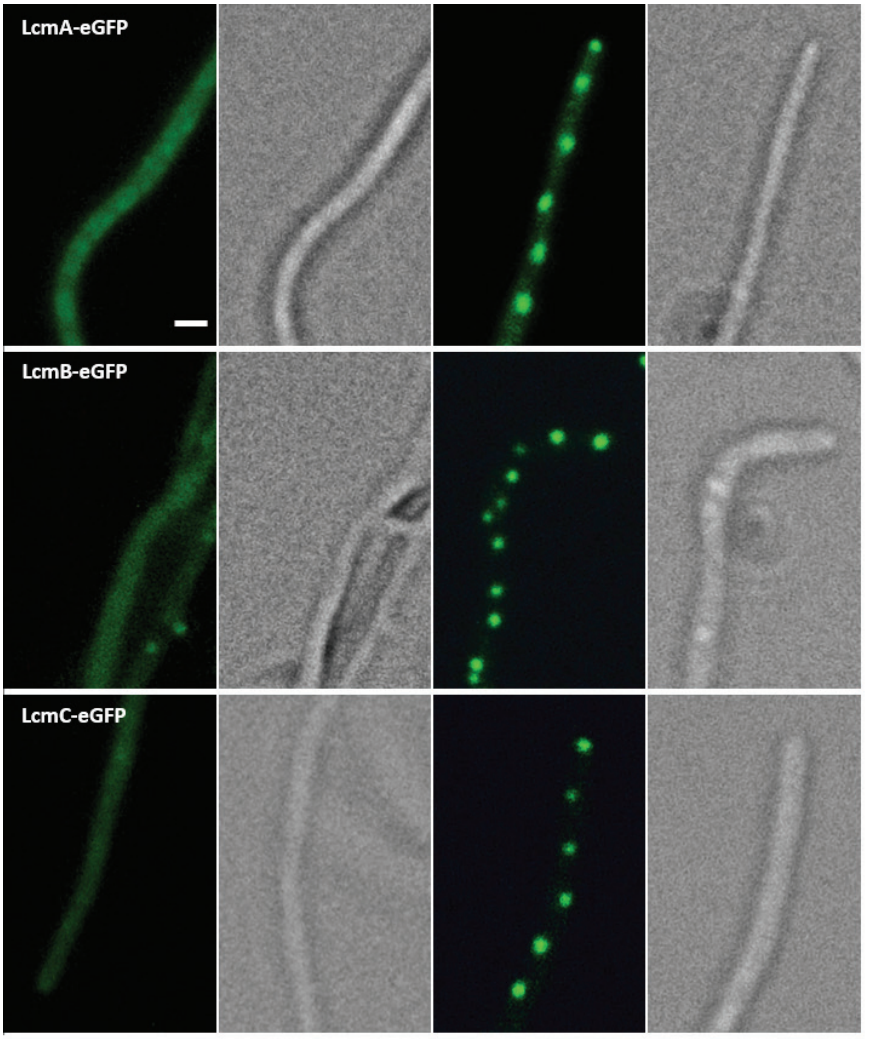

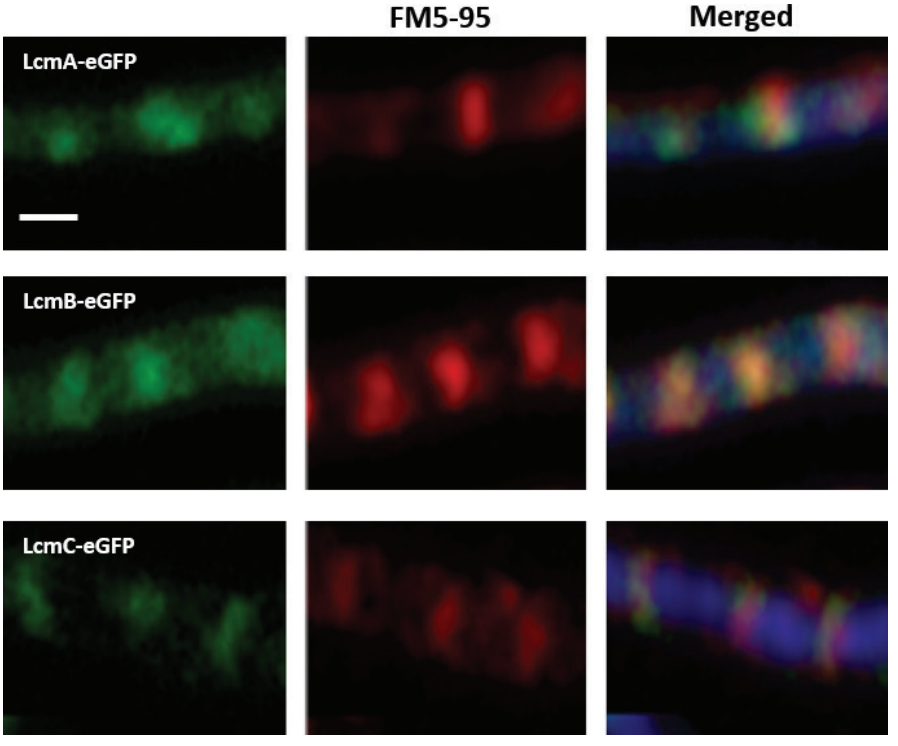

Figure 6. Localization of LcmA-eGFP, LcmB-eGFP and LcmC-eGFP at the septa. Aerial hyphae of *S. coelicolor* M145 were imaged by fluorescence microscopy visualizing eGFP fusion proteins of LcmA, LcmB and LcmC. **(A)** FM of the eGFP fusion protein in young aerial hyphae (diffuse localization; left) and in pre-mature spores (right). For each image both FM and light micrographs are presented. Bar, 1 μm. **(B)** Close-ups of eGFP fusions (left) and membrane staining (FM5-95; middle), together with the merged images (right), showing localization of Lcm proteins at the septa.

Table 5. Statistical analysis of the localization of Lcm proteins relative to the sporulation septa.

Position of foci	LcmA-eGFP	LcmB-eGFP	LcmC-eGFP
Overlap with septum	**2%**	**89%**	**5%**
Not at the septa	7%	4%	17%
Cross septum	**92%**	8%	**79%**

Phylogenetic linkage to *gcv* genes

In actinomycetes the *lcm* cluster is typically associated with genes of the glycine cleavage system, and in particular *gcvP* or *gcvH* (Fig. 1A). In several actinomycetes, including *Salinispora*, *Kineococcus* and *Catenulispora*, *gcvH* lies immediately downstream of *lcmC*, while *gcvP* (SCO1378) lies 7 genes downstream of *lcmC* in *S. coelicolor*. This suggests possible functional linkage be-

tween the *lcm* and *gcv* genes. The glycine cleavage system (GCS) is expressed in response to high concentration of the amino acid glycine, to recycle glycine (Kikuchi *et al.*, 2008). This is important as glycine is toxic for many microorganisms at higher concentrations (Hishinuma *et al.*, 1969). Considering that glycine is an important part of the cell wall, forming glycine bridges between the peptidoglycan strands, and also affects pellet morphology of streptomycetes, we analyzed if the *lcm* genes played a role in glycine-related metabolism. Therefore, a null mutant of *S. coelicolor gcvP* (called GAL61) was obtained by replacing the gene with the apramycin resistance cassette *aac(3)IV* (see Materials and Methods section). Expectedly, this mutant was inhibited by higher glycine concentrations, as described previously for *gcv* mutants ΔUTR-T and ΔUTR-P of *S. griseus* IFO13350 (Tezuka and Ohnishi, 2014) (Fig. 7). However, none of the *lcm* mutants of *S. coelicolor* or *S. griseus* showed significant changes in terms of glycine sensitivity as compared to the parental strains (Fig. 7), suggesting that the *lcm* genes are not required for glycine catabolism.

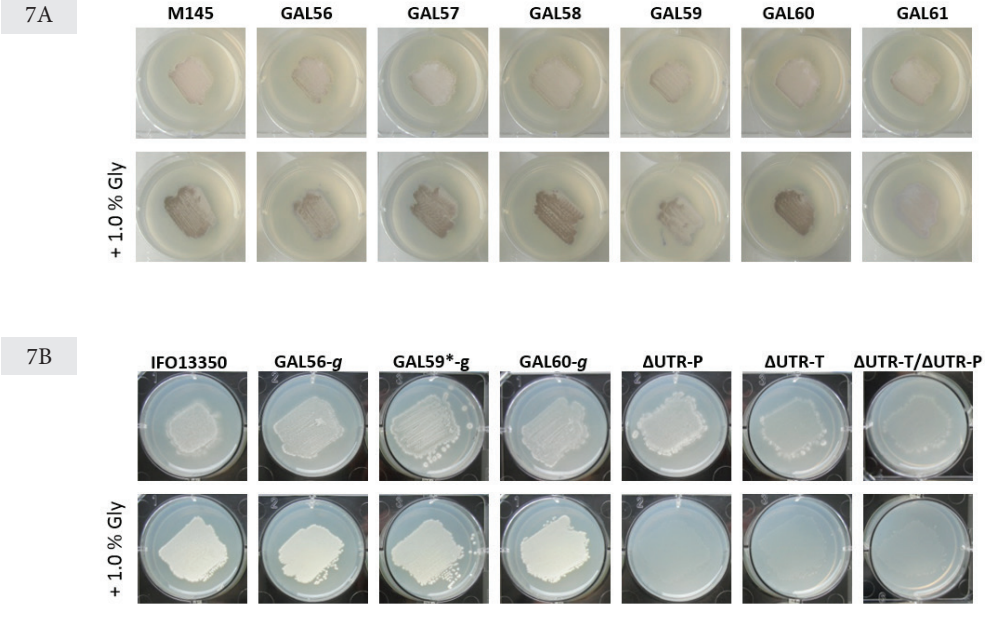

Figure 7. Effect of glycine on growth. (A) *S. coelicolor* M145 and its *lcm* and *gcvP*-null mutants on MM agar (with only agar as carbon source) or on MM agar containing additional 1% (w/v) glycine. **(B)** Growth of *S. griseus* IFO13350, its *lcm* mutants and a glycine riboswitch-null mutants on SMM agar (with only agar as carbon source) or on SMM agar containing additional 1% (w/v) glycine. Photos were taken after 4 days incubation at 30°C.

PCA analysis of metabolic profiles by proton NMR

NMR was applied to metabolically investigate spores of the *lcm* mutants. Strains GAL59 (*lcmA**) and GAL60 (Δ*lcmABC*) were selected since these two strains exhibited the most obvious changes as compared to the wild-type strain. Strain GAL61 (M145 Δ*gcvP* (::*aac(3)IV*)) was also included in NMR experiment as a control. To get full metabolic profiles for each strain, the spore pellet and supernatant were prepared as described in the Materials and Methods, followed by NMR spectroscopy. Five replicates were used for each experiment, so as to guarantee good statistical value of the data. Metabolite variations of samples from different strains were identified by principal component analysis (PCA). PCA is an unbiased and unsupervised method which is able to reduce the dimensionality of datasets. All NMR signals of the data sets were simplified to Principal Component 1 (PC1) and Principal Component 2 (PC2). Via this method, most NMR information was covered and spread out into a two-dimensional diagram (Kim *et al.*, 2010; Jellema *et al.*, 2009).

In the PCA score plot of spores, mutant strains and wild type were mainly separated by PC1 (Fig. 8A). Metabolites from the parental strain *S. coelicolor* M145 were predominantly found in the neutral part of the plot, *gcv* mutant GAL61 was at the negative side of PC1, while *lcm* mutants GAL59 and GAL60 were mostly at the positive side of PC1. The column loading plot of PC1 clearly showed large accumulation of glycine in GAL61 spores, in line with the mutation of the glycine cleavage system (Fig. 8A). The level of trehalose was also sharply increased in GAL61 spores. The accumulation of trehalose in *Streptomyces* spores enhanced the resistance to heat and postponed time of germination (McBride and Ensign, 1987). GAL59 and GAL60 showed a wide range of changes in the metabolic profiles, with 2-phosphoglycerate as a striking example. 2-phosphoglyceric acid is the intermediate product in the conversion of glucose to pyruvate, and the observed accumulation of 2-phosphoglycerate suggests a major change in glucose metabolism in the mutants.

In the PCA score plot of the supernatants, again mutants and wild-type were well separated, this time by PC2. Wild-type and GAL61 were at the positive side of PC2, while wild-type supernatants were close to the neural region; supernatants of GAL59 and GAL60 were both at the negative side of PC2 (Fig. 8B). A large amount of glycine was found in the supernatant of *gcv* mutant GAL61, and also of lactic acid (Fig. 8B). Consistent with the column loading plot for the spores, GAL59 and GAL60 once more showed significant changes in the metabolite profiles than *gcv* mutant GAL61. Among others, higher concentrations of the sugars mannitol and raffinose were found in the supernatant of GAL59 and GAL60 as compared to supernatants of the wild-

type strain, while the level of 2-phosphoglycerate was also higher in the supernatant of GAL59 and GAL60. This was in line with the changes seen in the spore fractions. The distinct spore and supernatant profiles observed in the PCA score plot strongly suggests that mutation or deletion of the entire *lcm* cluster causes major metabolic changes. The PCA loading plots showed that in particular the profiles of sugars and amino acids (but not glycine) were altered in GAL59 and GAL60.

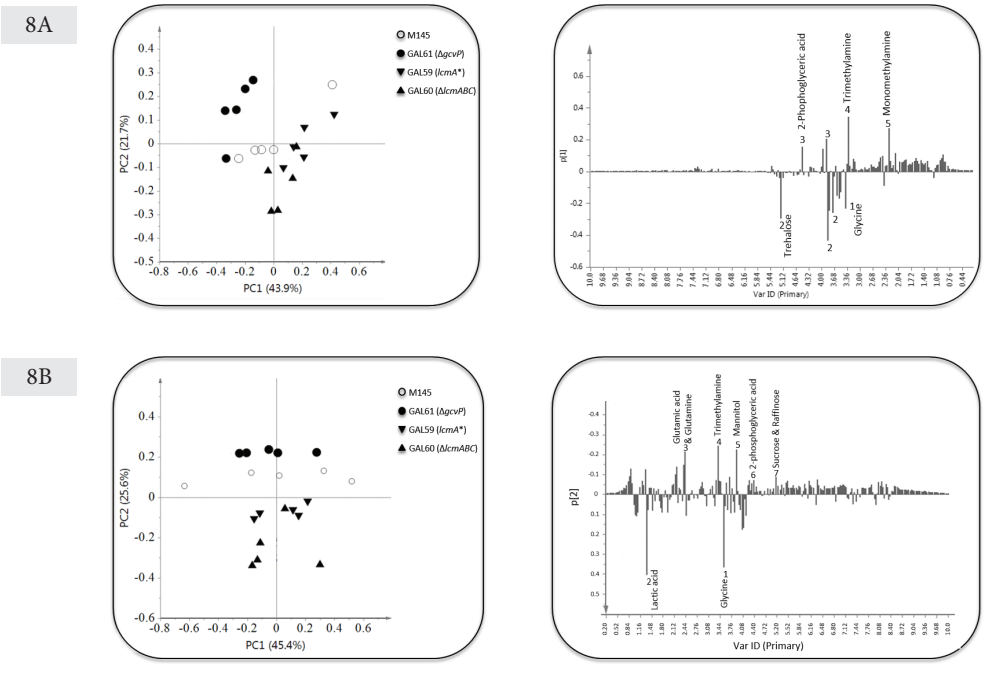

Figure 8. Metabolome analysis of spore metabolites by PCA. PCA analysis and corresponding loading plots are shown for **(A)** spores and **(B)** supernatants from spore preps. Extracts and supernatants from spores of wild type *S. coelicolor* M145, GAL59 (*lcmA**), GAL60 (Δ*lcmABC*) and GAL61 (Δ*gcvP*) were analyzed.

DISCUSSION

Streptomycetes are mycelial microorganisms that reproduce via sporulation on solid media. In addition, a significant number of the streptomycetes can also sporulate in submerged culture (Girard *et al.*, 2013). The factors that determine mycelial morphogenesis in submerged cultures are still largely unknown, although altering the expression of the cell division activator SsgA or deletion of cell matrix genes like *cslA* for cellulose synthase-like protein CslA or *chp* for the chaplin spore-coat proteins results in fragmentation of the mycelia and in some cases even submerged sporulation (van Dissel *et al.*, 2014). Important clues could come from the analysis of spontaneous mutants with altered morphology. One such mutant is *S. griseus* strain SY1, which was derived from wild-type *S. griseus* by random mutagenesis (Kawamoto and Ensign, 1995), and fragments and sporulates in rich liquid media, while wild-type *S. griseus* only produces spores after nutritional shift-down. SNP analysis showed that *S. griseus* SY1 contains among others a non-sense mutation in the gene *lcmA,* which is the first gene of an operon of three genes (*lcmABC*). This change probably has a detrimental effect on the expression of all three genes in the cluster, as the genes likely form an operon, with *lcmA* and *lcmB* translationally coupled. To establish the role of the *lcmABC* gene cluster in the medium-dependent submerged sporulation of *S. griseus*, a series of mutants was created in both *S. griseus* and in our model system *S. coelicolor*. These mutants were gene deletion mutants for either *lcmA*, *lcmB* or *lcmC*, or a complete cluster deletion mutant, as well as a mutant (designated *lcmA**) with the same non-sense mutation found in SY1 (replacing codon 7 by a stop codon). While the *lcmA** strain containing the nonsense mutation and the *lcmABC* deletion strain showed altered sporulation on solid cultures, with larger spores, thinner spore walls and accelerated development, none of the mutants had significantly altered morphology in submerged cultures, regardless of whether the *lcm* mutants were created in *S. coelicolor* or in *S. griseus*. This suggests that at least one other mutation sustained after random chemical mutagenesis was responsible for the hypersporulating phenotype of *S. griseus* SY1. Considering that some 100 SNPs were found in SY1 relative to the parental strain *S. griseus* NRRL B2682 (a derivative of the wild-type strain), and the fact that the phenotype may have been the result of multiple mutations, the search for the responsible gene(s) was abandoned. However, based on the strong connection between the *lcm* genes and sporulation, we expect that the *lcmA** mutation will at least have contributed to the hyper-sporulating phenotype of *S. griseus* SY1.

What then is the role of *lcmABC* in sporulation? All three genes encode predicted membrane proteins, and suggestively, in *Bacillus* the genes lie downstream of the cell division gene *divIB* in the *dcw* cluster of genes for division and cell-wall synthesis. Interestingly, localization studies on eGFP fusion protein showed that all three proteins localize close to or at the septum, whereby LcmB-eGFP overlaps the sporulation septa, while LcmA-eGFP and LcmC-eGFP produce foci on either side of the center of the septa. This localization suggests that perhaps LcmABC play a role in septum closure, although more data are required to establish their precise roles in cell division. Also, the sequence of their localization pattern in younger aerial hyphae requires more extensive imaging, and in particular live imaging, as it is very difficult to judge the exact stage of development of aerial hyphae where indentation (*i.e.* sporulation) has not yet started.

The observed accelerated growth for the *lcm*A* and *lcmABC* mutants on solid media may among others be explained by the altered (and somewhat thinner) spore wall of the mutants, since this would facilitate more rapid germination (Piette *et al.*, 2005). Phylogenetic evidence shows strong correlation between the *lcm* genes with the *gcv* genes that encode components of the glycine cleavage system, although in contrast to *gcv* mutants, *lcm* mutants did not show enhanced sensitivity to glycine. However, analysis of the spores and spore supernatants of the lcmA* and *lcmABC* mutants by NMR-based metabolomics did reveal major changes in metabolic composition, as shown by the PCA analysis of five independent replicates. In particular, the mutants showed altered in sugar and amino acid metabolism. Further analysis of the Lcm proteins, such as identification of possible interaction partners as well as elucidation of the molecular basis for the metabolic changes observed in the mutants, should shed further light on their role during sporulation of streptomycetes.

VI

The SARP-family regulator AfsR controls colony size and streptomycin production in *S. griseus* IFO13350

Le Zhang, Erica G. Wilson, Changsheng Wu, Young Hae Choi, Hiroshi Otani, Yasuo Ohnishi and Gilles P. van Wezel

ABSTRACT

AfsR is a regulatory protein that has been implicated in the control of development and/or secondary metabolism in streptomycetes. The proposed model is that it may influence the production of the γ-butyrolactone A-factor, which acts as a signal for the onset of development and antibiotic production in *S. griseus*. The spontaneous mutant AFN of *Streptomyces griseus* fails to develop or produce streptomycin due to almost complete block of A-factor production. Sequencing of this mutant suggestively revealed a truncation of the *afsR* gene, by mutation of Trp codon 881 (TGG) to a TAG stop codon. An *afsR* mutant was created, which showed accelerated development when grown as single colonies. Introduction of additional copies of either *afsR* or truncated mutant *afsR** led to increased streptomycin production and much larger colonies. However, we failed to see a correlation between A-factor production level and the presence or absence of *afsR* or *afsR**. Since introduction of *afsR** into the *afsR* null mutant developed normally, we conclude that the *afsR** mutation was not the (only) cause of the AFN phenotype.

INTRODUCTION

Streptomycetes and other actinobacteria are a predominant source of natural products for agricultural, biotechnological and medical applications (Hopwood, 2007). The production of natural products is closely correlated with the developmental program, and the signals that control development therefore also affect the secondary metabolism (Liu *et al.*, 2013; van Wezel and McDowall, 2011). The mycelial streptomycetes produce a branching network of hyphae in their habitat, the soil. These vegetative or substrate hyphae are divided by crosswalls, and hence *Streptomyces* are a rare example of a multicellular bacterium (Claessen *et al.*, 2014). On nutrient depletion, streptomycetes initiate a complex developmental program, whereby the vegetative mycelium serves as a substrate to build a second mycelium consisting of so-called aerial hyphae. Eventually these aerial hyphae differentiate to produce chains of spores. Mutants that fail to develop aerial hyphae are called bald or *bld* mutants (reflecting the lack the fluffy white aerial mycelium), and mutants that fail to sporulate are called white or *whi* mutants, as they do not produce the grey spore pigment.

A-factor (2-isocapryloyl-3R-hydroxymethyl-gamma-butyrolactone) is a hormone-like autoregulatory molecule that acts as a trigger of differentiation and streptomycin production in *Streptomyces griseus* (Horinouchi and Beppu, 2007). A-factor binds to the A-factor receptor protein ArpA, thus relieving inhibition by ArpA of transcription of the global regulatory gene *adpA* (Ohnishi *et al.*, 1999; Ohnishi *et al.*, 2005). AdpA directly activates transcription of a whole range of genes involved in development and secondary metabolism (Ohnishi *et al.*, 1999; Ohnishi *et al.*, 2005). Upon reaching a threshold level, A-factor synchronizes the activities of individual cells within a mycelium and likely also nearby cells (Horinouchi, 2002). The enzyme that synthesizes A-factor is AfsA (Kato *et al.*, 2007). An intriguing A-factor related regulatory system is formed by the sensory kinase AfsK and its cognate regulator AfsR, first discovered as a system that controls development in response to glucose (Umeyama *et al.*, 1999). AfsK is a serine/threonine kinase, which phosphorylates AfsR as well as itself (Hempel *et al.*, 2012; Umeyama *et al.*, 1999). AfsR is a member of the so-called SARP regulators, to which also many pathway specific activators of antibiotic production belong (Wietzorrek and Bibb, 1997), but has additional domains ATPase activity and a phosphorylation receiver domain (Hong *et al.*, 1991). AfsR binds to the promoter of *afsS*, a small gene located immediately downstream of *afsR* (Lee *et al.*, 2002), thereby activating its transcription (Tanaka *et al.*, 2007). The precise function of AfsS is unclear,

but it shows similarity to σ factors (Lee *et al.*, 2002) and its enhanced expression stimulates antibiotic production in *S. coelicolor, S. lividans* and *S. griseus* (Atsushi *et al.*, 1994; Floriano and Bibb, 1996; Vögtil *et al.*, 1994).

Previous research identified a spontaneous A-factor non-producing mutant (AFN) of *S. griseus* NRRL B2682 (Biró *et al.*, 2000). Mutant AFN is unable to form aerial hyphae or to produce streptomycin, likely due to its very limited A-factor production, and sporulation could be restored to *S. griseus* AFN by supplementing cultures with A-factor (Birkó *et al.*, 2009). Interestingly, the transcription of the key A-factor synthesis gene *afsA* was significantly up-regulated in *S. griseus* AFN as compared to its parental strain, which suggests that the defect in production was downstream of *afsA* (Birkó *et al.*, 2007). We have now sequenced the genome of *S. griseus* AFN, which revealed a non-sense mutation in the *afsR* gene, whereby the codon for Trp881 was changed to a stop codon. In this study, we introduced this so-called *afsR** mutation into a newly created *afsR* null mutant of the model strain *S. griseus* IFO13350. This showed that the *afsR** mutation could not explain the AFN phenotype as it did not cause any defect in development or streptomycin production, and that A-factor production was not affected. However, increasing the *c*opy number of *afsR* and flanking region resulted in a large colony phenotype and enhanced streptomycin production.

MATERIALS AND METHODS

Bacterial strains and media

Bacterial strains used in this work are listed in Table 1. *Escherichia coli* strains JM109 (Sambrook *et al.*, 1989) and IR539 (Suzuki *et al.*, 2011) were used for routine cloning procedure and specific sites-methylated DNA isolation respectively. Transformations in *E.coli* were selected in L broth (LB) media containing proper antibiotics at 37°C (Sambrook *et al.*, 1989). *Streptomyces griseus* IFO13350 was used as parental strain to construct mutants described in this work. YEME (yeast extract - malt extract (Kieser *et al.*, 2000)) or TSBS (tryptone soy broth (Difco) containing 10% (w/v) sucrose) were used for standard cultivation. R5 agar plates (Kieser *et al.*, 2000) were used for regeneration of protoplast and with appropriate antibiotics for selection of recombinants. Spore suspensions, morphological characterization and all microscopy analysis were performed on R5 and YMPD (1.5% glucose) agar plates as described (Colson *et al.*, 2008; Umeyama *et al.*, 1999). Bennett maltose agar plates (Hirano *et al.*, 2008) were used to detect streptomycin production.

Table 1. Bacteria strains.

Bacteria strains	Genotype	Reference
E. coli JM109	See reference	(Sambrook *et al.*, 1989)
E. coli IR539	See reference	(Suzuki *et al.*, 2011)
S. griseus IFO13350	See reference	(Ohnishi *et al.*, 2008)
GAL74	IFO13350 Δ*afsR*	This work
GAL75	IFO13350 + pHJL401	This work
GAL76	IFO13350 + pGWS781	This work
GAL77	IFO13350 + pGWS782	This work
GAL78	GAL74 + pHJL401	This work
GAL79	GAL74 + pGWS781	This work
GAL80	GAL74 + pGWS782	This work

Plasmids and constructs

All plasmids and constructs are summarized in Table 2 and oligonucleotides in Table 3.

Table 2. Plasmids and Constructs

Plasmid and constructs	Description	Reference
pWHM3	*E. coli*/*Streptomyces* shuttle vector, multi-copy and very unstable in *Streptomyces*	(Vara *et al.*, 1989)
pHJL401	*E. coli*/*Streptomyces* shuttle vector, 5-10 copies in *Streptomyces* and around 100 copies in *E. coli*	(Larson and Hershberger, 1986)
pUWL-Cre	Plasmid expressing Cre-recombinase	(Fedoryshyn *et al.*, 2008)
pGWS753	pWHM3 containing flanking regions of *S. griseus* IFO13350 SGR_3012 with apraloxP-*Xba*I inserted between them in pWHM3 EcoRI-HindIII	This work
pGWS781	pHJL401 with 3.9kb fragment harboring *afsR* and *orf4* (SGR_3012) behind native promoter of *afsR*	This work
pGWS782	pHJL401 with 3.1kb fragment harboring truncated *afsR* (*afsR**) and its native promoter region	This work

Table 3. Oligonucleotides.

Name	**5'-3' sequence**[#]
afsR_LF-1383	GTCA**GAATTC**GAGCACGTTGCCGACGCCGATC
afsR_LR+6	GTCAGAAGTTATCCATCACC**TCTAGA**GTCCATTGATGCCCCCTGTCCTG
afsR_RF+2920	GTCAGAAGTTATCGCGCATC**TCTAGA**GGCTGACCGCCGCGGAGGCGTTC
afsR_RR+4367	GTCA**AAGCTT**CTGATGCGGGGGGCCACGATG
afsR_F-153	AGACAAGGCAGACTGTTGAG
afsR_R+2964	AGTGCGCCGATAAACGATTG
afsR_F-480	CATGGAATTCGAACTTGCCGCCCAGGAAGGTCA
afsR_R+1576	CATGAAGCTTCG**AGATCT**CCCGCCTGGAGCTCGTC[a]
afsR_F+1562	CATGGAATTCAGGCGGGAGATCTCGCGGTGAAGGC[a]
afsR_R+3390	CATG**AAGCTT**CACACATTCCCCCGTACCGCGA
afsR_R+2649	CATG**AAGCTT**CCCGTGCTACAGCTGCTGCCGGCTC[b]

[#]Restriction sites used in oligos are underlined and in bold. GAATTC, EcoRI; AGATCT, BglII; AAGCTT, HindIII; TCTAGA, XbaI;

[a] A in black shade of oligo afsR_F+1562 was designed to replace C on wild type sequence, to create restriction site BglII with silent mutation. T in black shade of oligo afsR_R+1576 has the same designation.

[b] Stop codon (CTA) in black shade of oligo afsR_R+2649 was designed to replace Trp codon (TGG) on wild type sequence, to create non-sense mutation.

Constructs for creating in-frame deletion mutant

Creation of knock-out mutants is based on pWHM3, which is a multi-copy and unstable *Streptomyces* vector (Vara *et al.*, 1989). See Chapter II and III for details. For the deletion of *afsR*, its upstream region -1383/+6 (using primer pair afsR_LF-1383 and afsR_LR+6) and downstream region +2920/+4367 (using primer pair afsR_RF+2920 and afsR_RR+4367) were amplified by PCR on *S. griseus* IFO13350 genomic DNA. DNA fragments harboring flanking regions were cloned into pWHM3, and subsequently the engineered XbaI site in-between the inserts was used to insert the apramycin resistance cassette *aac(3)IV* flanked by *loxP* recognition sites. The resulting plasmid was called pGWS753. The presence of *loxP* sites allows efficient removal of apramycin resistance cassette by Cre-recombinase, expressed from plasmid pUWL-Cre, to generate a marker-less deletion mutant (Fedoryshyn *et al.*, 2008). To analyze the correctness of the mutant, PCR was done on genomic DNA of strain GAL74, using primer pair afsR_F-153 and afsR_R+2964.

Cloning and expression of afsR, truncated afsR (afsR) from S. griseus*

Primer pairs afsR_F-480 and afsR_R+1576 and afsR_F+1562 and afsR_R+3390 were used to amplify -480/+1576 region and +1562/+3390 region relative to *afsR* from *S. griseus* IFO13350 genomic DNA. The PCR-engineered BglII site allowed cloning of *afsR* and its upstream and downstream sequences as two parts, with introduction of a C → A mutation at nt position +1569 of *afsR*. A 3.9 kb DNA fragment encompassing the entire coding region of *afsR* as well as its putative promoter region and downstream gene *orf4*, was cloned into pHJL401 to generate pGWS781. To express *afsR**, the truncated *afsR*, primers afsR_F+1562 and afsR_R+2649 were used to amplify the +1562/+2649 region relative to *afsR* from *S. griseus* IFO13350 genomic DNA. Primer afsR_R+2649 was designed to introduce replace codon 881 of *afsR* by a stop codon. The approximately 1 kb fragment was cloned as a BglII-HindIII fragment into pGWS781 to replace the terminal part of *afsR* and downstream sequences, to generate pGWS782.

Streptomycin activity assay

To assess the level of streptomycin production, wild-type *S. griseus* IFO13350 and its derivatives were grown on Bennett's maltose agar plates (Hirano *et al.*, 2008) for 5 days, then overlaid with culture of *B. subtilis* as an indicator as described previously (Horinouchi *et al.*, 1984).

Stereo microscopy

Strains were grown on SFM plates for four days at 30°C. The strains were imaged using a Zeiss Lumar V12 stereomicroscope.

HPLC-Q_TOF

Approximately 100 colonies for each strain were spread out on 6,25 ml R5 agar solid medium containing thiostrepton (20 μg/ml), and incubated at 30°C for seven days. Then the spent medium was soaked into 30 ml ethyl acetate overnight. The liquid phase was evaporated, and the extracted compounds re-dissolved in 300 μl ethanol for UHPLC-TOF-MS. UHPLC-TOF-MS analyses were performed on a UHPLC system (Ultimate 3000, ThermoScientific, Germany) coupled to an ESI-Q-TOF spectrometer (micrOTOF-QII, Bruker Daltonics, Germany). Detection was done in the negative mode. The *m/z* range was set to be 100–600mz. The ESI conditions were as follows: capillary voltage of 3500V, source temperature of 250°C, dry gas flow 10 ml min^{-1}. For internal calibration, a 10 mM solution of sodium formate (Fluka, Steinheim, Germany) was infused. UHPLC-TOF-MS chromatograms were obtained using a 150mm× 2.1 mm i.d., 2.6 micron Kinetex C18 UPLC column (Phenomenex, USA) in gradient mode at a flow rate of 0.3 ml min^{-1} with the following solvent system: (A) 0.1 vol% FA(formic acid) in water; (B) 0.1 vol% FA in methanol. Analysis began with gradient of 5% to 95% B over 14 min, followed by an isocratic step of 95 B from 14 to 15 min and a re-equilibration step of 5% B from 15 to 17 minutes. The temperature was maintained at 30 °C, and the injection volume was 3 μl.

Computer analyses

DNA and protein databank searches were performed using and StrepDB page services (http://strepdb.streptomyces.org.uk/).

RESULTS AND DISCUSSION

S. griseus AFN contains a mutation in *afsR*

The genome of the spontaneous A-factor nonproducer strain *S. griseus* AFN (Biró *et al.*, 2000) was sequenced by Illumina paired end sequencing and compared to wild-type *S. griseus* IFO13350 (Ohnishi *et al.*, 2008) to identify the mutations in *S. griseus* AFN relative to its parent strain *S. griseus* NRRL B2682. Around 100 single nucleotide permutations (SNPs) were found between AFN and the published sequence of wild-type *S. griseus* IFO13350. Of these, most were also found in *S.* griseus NRRL B2682. Importantly, one mutation that was specific to *S.* griseus mutant AFN was a nonsense mutation in *afsR*, which caused a premature translational stop by mutating the Trp881 codon TGG to a TAG stop codon. AfsR is a DNA binding protein that is conditionally needed for development and antibiotic production of *S. griseus* and *S. coelicolor* (Umeyama *et al.*, 1999; Floriano and Bibb, 1996).

Gene organization around *afsR* region in *S. griseus* and *S. coelicolor*

AfsR is phosphorylated by phosphokinase AfsK at Ser and Thr residues in various *Streptomyces* spp., including *S. coelicolor*, *S. lividans* and *S. griseus* (Atsushi *et al.*, 1994; Hong *et al.*, 1991; Umeyama *et al.*, 1999). AfsR contains a DNA-binding and an ATPase domain, which are both required for AfsR function (Lee *et al.*, 2002) (Fig. 1A). The C-terminal domain of AfsR contains three so-called tetratricopeptide repeats (TPR) (Fig. 1A), which are important for mediating protein-protein interactions (Blatch and Lässle, 1999). The gene organization around *afsR* in *S .coelicolor* and *S. griseus* is very different (Fig. 1B). In both species, a small ORF lies downstream of *afsR*. In *S. coelicolor* this *afsS*, for a 63 aa activator of secondary metabolism (Tanaka *et al.*, 2007), while the function of the putative 58 aa protein encoded by the downstream ORF in *S. griseus* is unknown. Furthermore, while in *S. coelicolor afsK* and *afsR* lie 1 kb away from each other, in *S. griseus* these genes are spaced by some 6 kb.

1A

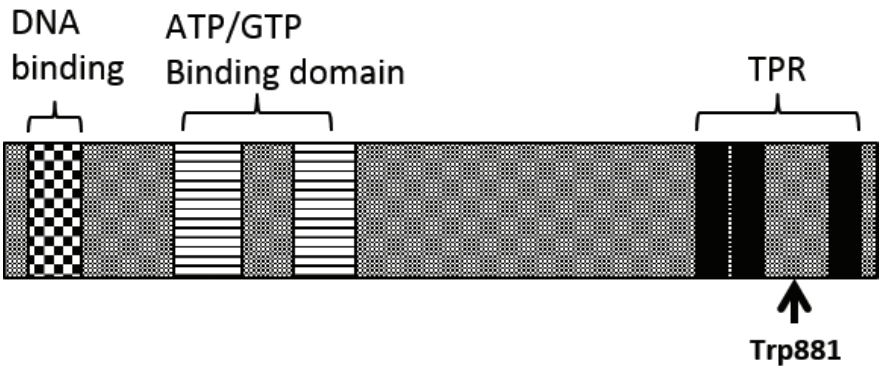

1B

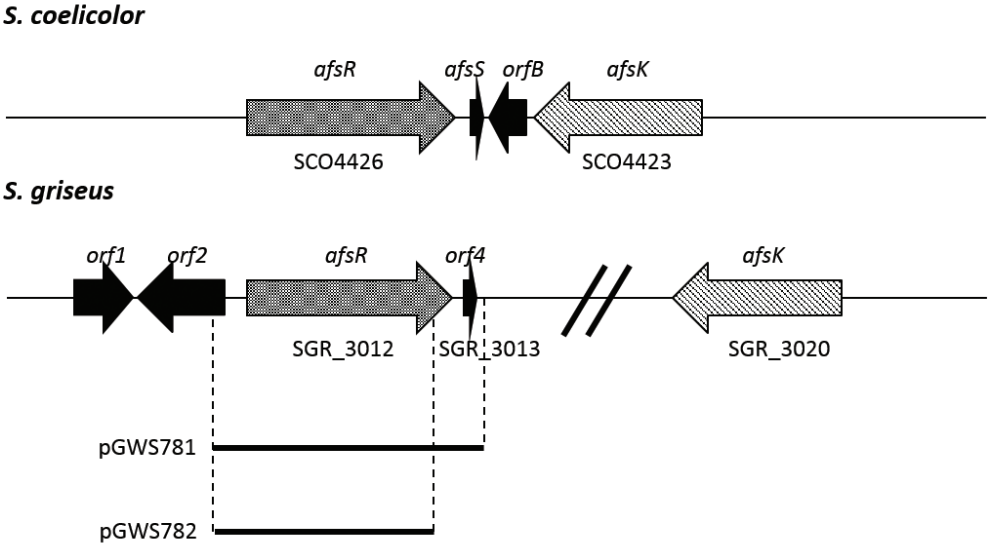

Figure 1. Protein domain structure of AfsR and gene organization of the *afsR* locus.
(A) Domain structure of the AfsR protein. AfsR is a SARP-family regulator, with an N-terminal DNA binding domain, an ATP binding motif in the middle, and three tetratricopeptide repeats at the C-terminal end of the protein. The non-sense mutation at position of Trp881 is indicated. **(B)** Genetic organization of the region around *afsR* and *afsK* in *S. coelicolor* and *S. griseus*. Note that in *S. coelicolor afsR* and *afsK* are closer (spacing 1 kb encompassing two ORFs between the genes) than in *S. griseus* (6 kb spacing encompassing six ORFs). The inserts of plasmids pGWS781 (harboring *S. griseus afsR* and the small downstream ORF) and pGWS782 (harboring truncated *afsR**) are indicated by a horizontal line.

Deletion of *afsR* conditionally accelerates development of *S. griseus*

An *afsR* null mutant was created in *S. griseus* IFO13350 by deleting the +7/+2919 bp region relative to *afsR* (see Materials and Methods section). After replacement of the *afsR* gene by the apramycin resistance cassette using knock-out construct pGWS753, the apramycin resistance cassette was excised following expression of the Cre recombinase from plasmid pUWL-Cre. The resulting marker-less deletion mutant was designated GAL74. Previously, it was published that an *afsR* null mutant of *S. griseus* had a bald phenotype on YMPD media containing 1.5% glucose (Umeyama *et al.*, 1999). However, this mutant is not available any more. In contrast, at least in our hands, deletion of *afsR* in *S. griseus* IFO13350 did not cause major developmental defects when the strain was grown on YMPD media containing 1.5% glucose, and the mutant sporulated as well as the parental strain after 7 days of incubation (Data not shown).

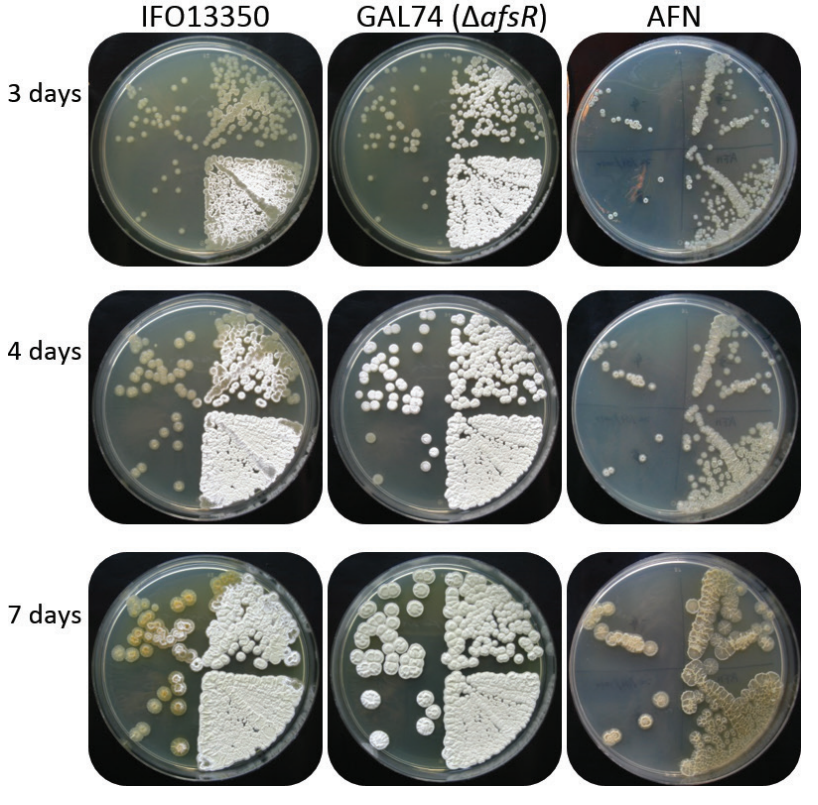

Figure 2. Growth of wild type *S. griseus* IFO13350, its *afsR*-null mutant (GAL74) and *S. griseus* B2682 AFN on R5 medium. Dilutions of spore suspensions (for *S. griseus* IFO13350 and *afsR* null mutant GAL74) or liquid-grown mycelium (for nonsporulating mutant *S. griseus* AFN) were plated onto R5 agar plates. Plates were photographed after 3 days, 4 days or 7 days of growth at 30 °C.

Interestingly, when the same dilutions were plated on R5 agar plates, ranging from a density of a few to some 1000 colonies per quarter agar plate, significant differences were observed between GAL74 and the parental strain. Consistent with previous observations (Biró et al. 2000), *S. griseus* mutant AFN failed to form aerial hyphae irrespective of incubation time and density of inoculation (Fig. 2, right column). After three days of growth, at high density both wild-type *S. griseus* and its *afsR* null mutant produced aerial hyphae. However, at lower densities, single colonies of GAL74 formed aerial hyphae much earlier than the parental strain, and at the lowest dilution in fact the parental strain produced very few aerial hyphae even after 7 days, while those of GAL74 had fully developed. Taken together, these data show that the absence of *afsR* conditionally accelerates the developmental program in *S. griseus*, in a cell density-dependent manner.

Expression level of AfsR affects growth and development of *S. griseus*

To study the effect of AfsR on development, construct pGWS781 (Fig. 1B), which harbors *afsR* with 480 bp promoter region and downstream sequences including the downstream located ORF4 (see Fig. 1B), was transformed to *S. griseus* IFO13350 and its *afsR* null mutant GAL74, resulting in strains GAL76 and GAL79, respectively. Similarly, construct pGWS782 (Fig. 1B), which expresses truncated AfsR* (which has codon Trp881 changed to a stop codon), was also introduced into *S. griseus* IFO13350 and GAL74 to generate strains GAL77 and GAL80, respectively. *S. griseus* IFO13350 and GAL74 containing empty plasmid were used as controls. Thiostrepton (20 μg/ml) was added to the media to maintain constructs in transformants. All constructs were based on plasmid pHJL401, which is a low-copy number vector (around 5-10 copies per chromosome) in *Streptomyces*.

On YMPD plates with glucose (1.5% w/v) and with thiostrepton as selective marker for the plasmids, all strains fully developed when grown at high density. Differences in growth were mainly observed in the quadrants with fewer colonies. Introduction of additional copies of *afsR* or *afsR** into wild-type *S. griseus* IFO13350 (GAL76 and GAL77, respectively) promoted aerial hyphae formation in the quadrant with around a hundred colonies, while strains harboring the control plasmid showed very limited aerial hyphae formation (Fig. 3A). At the next lowest dilution, GAL76 and GAL77 entered aerial growth where the control strain grew vegetatively (Fig. 3A). However, no effect of the introduction of pHJL401/*afsR* or pHJL401/*afsR** was seen in the *afsR* null mutant. Similarly, on R5 agar plates with thiostrepton, in the quadrant with

around a hundred colonies, and around the edges of the high density patches, introduction of *afsR* or to a lesser extent *afsR** into wild-type cells accelerated aerial hyphae formation in colonies grown in close proximity (Fig. 3B). Again, this effect was far less strong in *afsR* mutant colonies.

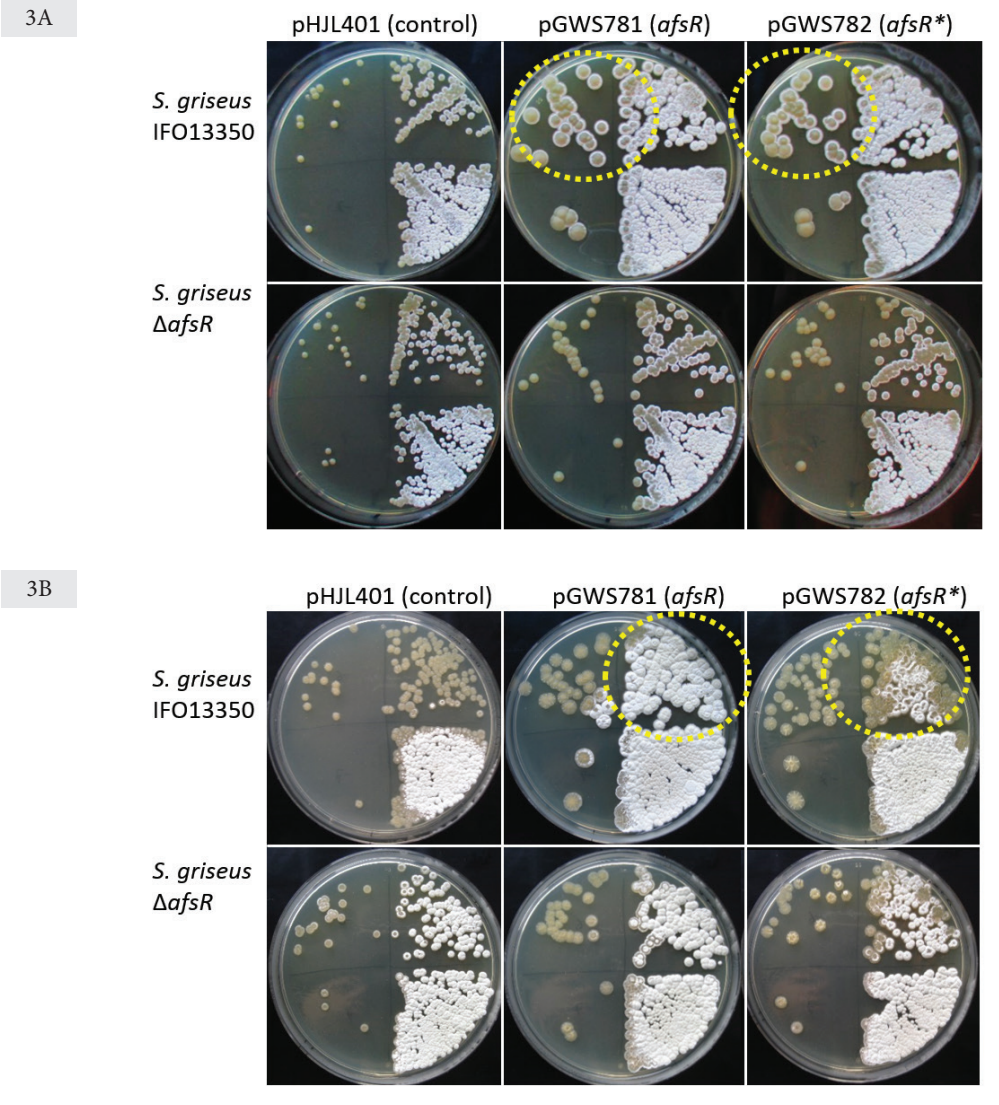

Figure 3. Effect of *afsR* and *afsR on development of *S. griseus* IFO13350.** Overview of whole plates on YMPD (1.5% glucose) agar plates **(A)** and on R5 agar plates **(B)**. Dilutions of spore-preps of *S. griseus* IFO13350 or its *afsR* null mutant with either control plasmid (pHJL401), plasmid pGWS781 (pHJL401 + *afsR*) or pGWS782 (pHJL401 with *afsR**) were plated onto YMPD (1.5% glucose) and R5 agar plates with thiostrepton (20 µg/ml). Photos were taken after 7 days incubation at 30 °C.

Correlation between AfsR and colony size

While differences in the timing of development were significant yet relatively small, a striking difference was observed in terms of colony size irrespective of culturing conditions. Colonies harboring control plasmid pHJL401 were very similar in size. However, introduction of pGWS781, which harbors *afsR*, in wild-type cells led to an approximately 10-fold increase in colony size, and a similar increase was seen for pGWS782 harboring *afsR** (Fig. 4A). Interestingly, introduction of either plasmid in the *afsR* null mutant GAL74 had a very small effect on colony size (Fig. 4A). This suggests that the copy number of *afsR* and/or that of the downstream gene, which is higher in the wild-type strain than in the *afsR* mutant, plays an important role in determining colony size, and that *afsR** is equally active in this respect as wild-type *afsR*. Since the downstream gene (SGR_3013; Fig. 1B) is absent from the construct expressing *afsR**, it is unlikely that this gene plays a major role in determining colony size.

To test the stability of the plasmids, all transformants were grown as a confluent lawn on agar plates in the absence of thiostrepton, replicated twice to nonselective media, and then spores were harvested and plated for single colonies on agar plates with or without thiostrepton, and resistance to thiostrepton assessed. Interestingly, control plasmid pHJL401 was lost almost completely by wild-type cells after two rounds of nonselective growth. However, the plasmid harboring *afsR* or *afsR** was maintained by around 70% and 27% of the cells, respectively (Fig. 4B). When the same experiment was done for *afsR* null mutant GAL74, all three plasmids were rapidly lost (Fig. 4B). These data are consistent with growth promotion by additional copies of *afsR* and to a lesser extent *afsR**, as this would select for maintenance of the plasmid. The lack of such an effect in *afsR* null mutants (see Fig. 3) explains the loss of the pHJL401/*afsR* and pHJL401/*afsR** plasmids in this genetic background.

4A

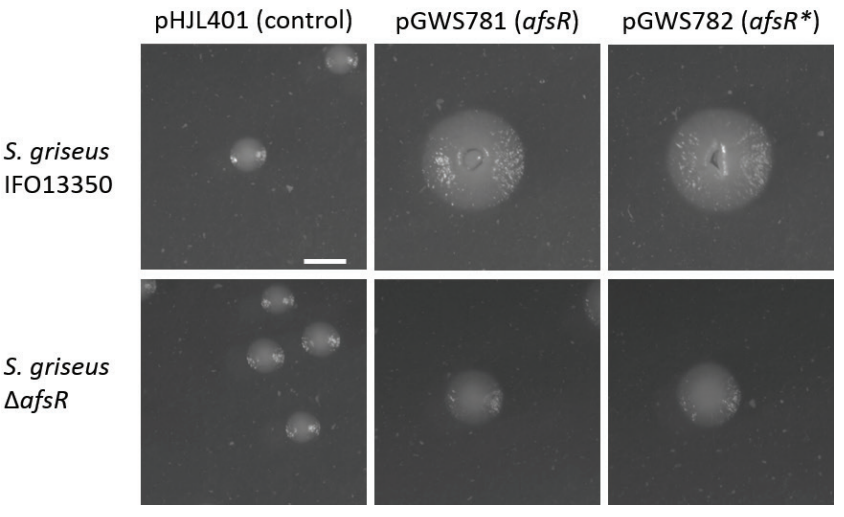

4B

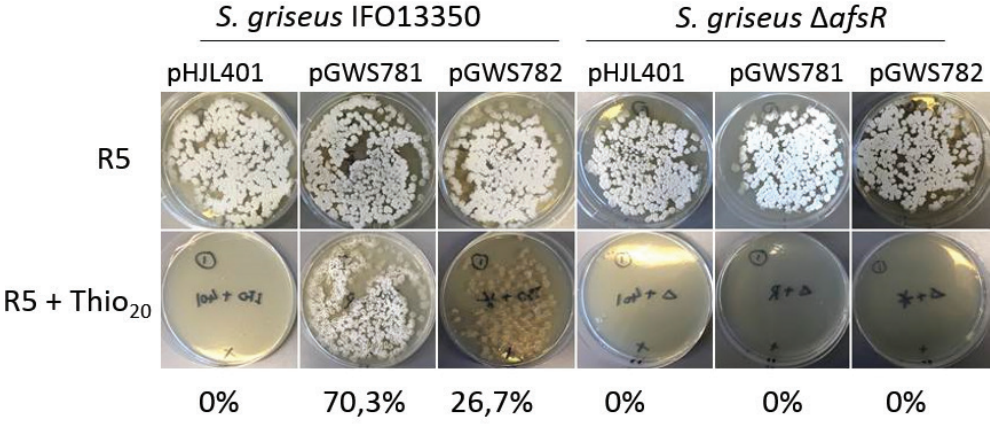

Figure 4. Effect of *afsR* and *afsR on colony size and plasmid stability of *S. griseus* IFO13350.** **(A)** Stereomicrographs of representative colonies to show the effect on colony size. Dilutions of spore-preps of *S. griseus* IFO13350 or its *afsR* null mutant with either control plasmid (pHJL401), plasmid pGWS781 (pHJL401 + *afsR*) or pGWS782 (pHJL401 with *afsR**) were plated onto R5 agar plates with thiostrepton (20 μg/ml). Photos were taken after 7 days incubation at 30 °C. Bar, 2 mm. **(B)** Detection of plasmid maintaining in transformants of wild type *S. griseus* IFO13350 and in *afsR* null mutants. Percentage of cells still containing plasmid after two rounds of non-selective growth were indicated at bottom.

AfsR enhances streptomycin production

It was shown previously that over-expression of *afsR* in different Streptomyces species promotes antibiotic production (Kim *et al.*, 2012; Stutzman-Engwall *et al.*, 1992; Floriano and Bibb, 1996). Therefore, we compared the effect of *afsR* copy number on streptomycin production in solid-grown cultures, using *Bacillus subtilis* as the indicator strain. Streptomycin production was measured as the size of the inhibition zones around the colonies. Consistent with such a stimulation of antibiotic production, extra copies of either *afsR* or *afsR** enhanced streptomycin production in *S. griseus* IFO13350 (Fig. 4). Interestingly, introduction of a plasmid with *afsR** (which also lacks the downstream gene SGR_3013) stimulated streptomycin production more strongly than a plasmid with wild-type *afsR* (Fig. 4). Deletion of *afsR* did not cause a noticeable change in streptomycin production, with the size of the inhibition zones of strain GAL78 (*afsR*-null mutant with empty plasmid) being comparable to that of wild-type *S. griseus* IFO13350 with empty plasmid (Fig.5). This is in line with earlier observations (Umeyama *et al.*, 1999). Complementation of the *afsR* null mutant with *afsR* or *afsR** only slightly enhanced streptomycin production (Fig. 5).

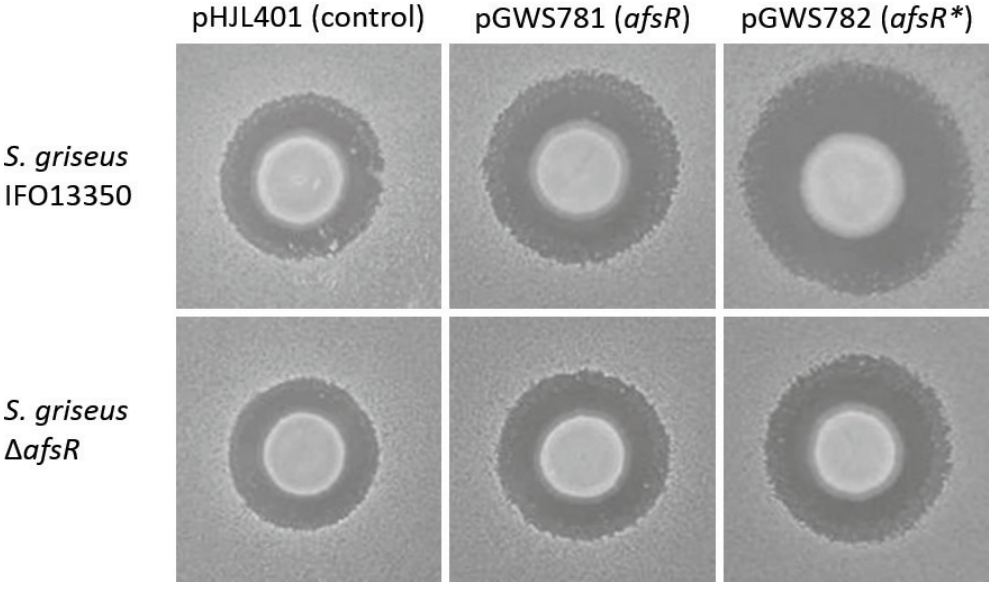

Figure 5. Effect of *afsR* and *afsR on streptomycin production.** Strains of *S. griseus* were inoculated on Bennett maltose agar using a toothpick and overlaid with soft agar containing *B. subtilis* after 5 days. For details on strains see Figure 3.

A-factor production is apparently not influenced by *afsR*

S. griseus B2682 AFN, which is a spontaneous A-factor non-producer, has a bald phenotype and fails to produce streptomycin, in accordance with a role of A-factor in signaling the onset of morphological and chemical differentiation (Birkó *et al.*, 2007). To establish whether the *afsR** mutation is the cause of the reduced A-factor production, the amount of A-factor produced by the different strains was determined using HPLC-Q-TOF. The acquisition time of A-factor was at approximately 11.5 min, giving a peak with an m/z of 241 Da in negative ion mode (Fig. 6). Perhaps surprisingly, we failed to detect major differences in A-factor production, although the peak in the sample corresponding to the largest inhibition zones (strain GAL77, IFO13350 + *afsR**) was somewhat larger than those for other strains. These data suggest that *afsR* or its mutant version *afsR** does not have a major impact on A-factor production (Fig. 6).

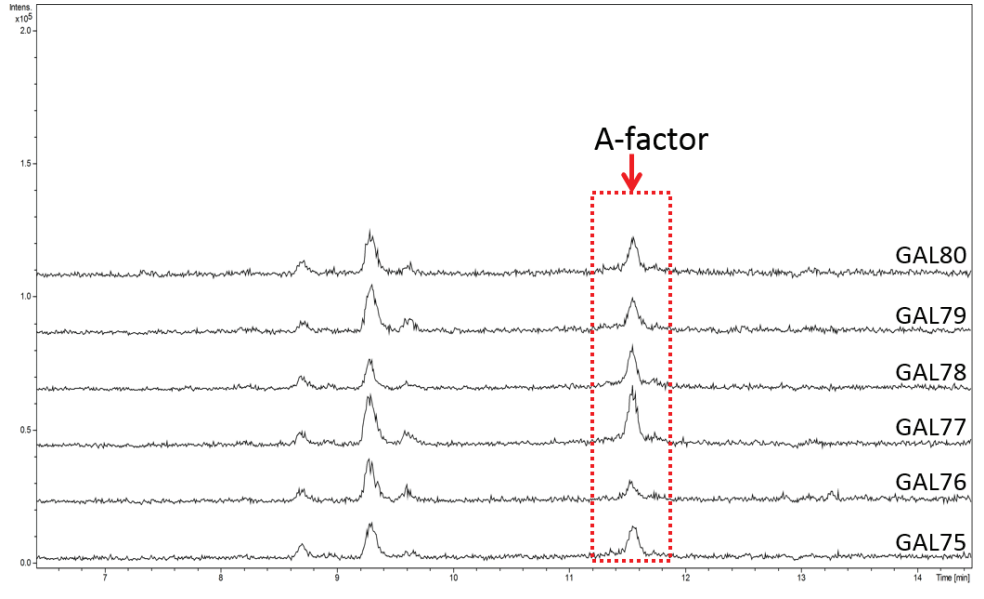

Figure 6. UHPLC-TOF mass spectra of A-factor produced by strains of *S. griseus*. GAL75, GAL76 and GAL77 are *S. griseus* IFO13350 harboring pHJL401, pHJL401/afsR and pHJL401/afsR*, respectively; GAL78, GAL79 and GAL80 are the *afsR* null mutant harboring pHJL401, pHJL401/*afsR* and pHJL401/*afsR**, respectively.

DISCUSSION

AdpA is a master transcriptional activator in *Streptomyces*, which controls many genes involved development and secondary metabolite production (Higo *et al.*, 2012; Ohnishi *et al.*, 2005). The autoregulatory hormone-like molecule A-factor binds to the ArpA protein, so as to allow activation of the AdpA-dependent regulatory network (Ohnishi *et al.*, 2005). An unsolved mystery is a spontaneous mutant of *S. griseus* NRRL B2682 that has the ability to produce A-factor, but fails to produce enough of the molecule to allow development and antibiotic production to proceed. None of the genes relating to A-factor production carries a mutation. In fact, surprisingly, expression of the large signaling protein Factor C, restored development to the *S. griseus* AFN mutant. This suggested that the AFN mutation should be located in a novel gene of the A-factor pathway. Thus, identification of the mutation that causes the AFN mutation should provide new insight in the very important A-factor regulatory cascade.

This work shows that one of the mutations in fact causes truncation of AfsR, a regulator of development and antibiotic production. But is the nonsense mutation in *afsR* really the main cause of the non-sporulating phenotype of *S. griseus* AFN? The answer is probably negative. While the AFN mutant produced minute amounts of A-factor, and failed to produce aerial hyphae or streptomycin, strain GAL80 (which essentially has wild-type *afsR* replaced by the truncated *afsR** variant found in AFN) showed normal development and streptomycin production. This was explained by the fact that A-factor production in GAL80 was comparable to that of the wild-type strain. Therefore, it is highly unlikely that the nonsense mutation in *afsR* is the (sole) cause of the AFN phenotype. The many mutations in the AFN mutant, and the fact that it was made in a background of *S. griseus* NRRL B2682 and not of the sequenced IFO13350, make looking for the AFN mutation looking for the proverbial needle in the haystack.

Nevertheless, our data did establish a role of AfsR in the control of development, colony size and streptomycin production in *S. griseus*. The *afsR* expression level positively correlates to colony size, which in turn is directly proportional to streptomycin production. However, in *S. coelicolor*, AfsR has been shown to have a negative effect on colony size, with extra copies of *afsR* reducing colony size on various solid media (Floriano and Bibb, 1996).

Mutants of *S. coelicolor* that lack the *ssgB* gene, which encodes a positive regulator of *Streptomyces* cell division during sporulation (see *e.g.* Chapter II),

have a large colony variant (LCV) phenotype, with colonies more than twice the size of wild-type colonies (Keijser *et al.*, 2003). The *ssgB* mutant colonies produce a very large aerial mycelium, and these mutants apparently lack the signal that enforces aerial hyphae to stop growing, which is a prerequisite for the onset of sporulation-specific cell division (Jakimowicz and van Wezel, 2012). In terms of a correlation between colony size and antibiotic production, deletion or mutation of the antibiotic regulatory gene *absB* resulted in an SCV phenotype in *S. coelicolor* (Price *et al.*, 1999; Adamidis and Champness, 1992), while microcystin production by *Microcystis* positively correlated to colony size (Kurmayer *et al.*, 2003). Small colony variants (SCV) also occur in other bacteria, including *Brucella, Burkholderia*, *Escherichia, Lactobacillus, Neisseria, Pseudomonas* and *Salmonella* (Proctor *et al.*, 2006; Morris *et al.*, 1943; Rohde, 1999; Morton and Shoemaker, 1945; Kopeloff, 1934; Colwell, 1946; Häussler *et al.*, 2003; Hall and Spink, 1947). Changing to SCV allows pathogens to escape the host defense system from antibiotics and persistence in mammalian cells (Proctor *et al.*, 2006; von Eiff *et al.*, 2001). Elucidation of the molecular background of the LCV (and SCV) phenotype of colonies, and the role of *afsR* in this phenomenon, should allow us to better understand the factors that control growth and antibiotic production of streptomycetes.

In terms of development, it has been observed previously that deletion or enhanced expression of *afsR* blocks development of *S. griseus* on media containing glucose as sole carbon source (Umeyama *et al.*, 1999). However, in our hands, deletion of *afsR* did not have a major effect on growth or development, while introduction of additional copies of *afsR* in wild-type cells accelerated development. Unfortunately, the original *afsR* mutant is lost and we cannot compare our mutant with those produced by Umeyama and colleagues. Our study revealed that AfsR plays a role in the control of growth and streptomycin production, with a promising stimulation of streptomycin levels by AfsR and particularly of AfsR*. Clearly, more extensive system biology approaches are required to decipher the AfsR regulon and analyze its yet ambiguous role in the control of growth and antibiotic production in streptomycetes.

VII

Summary and Discussion
&
Samenvatting en Discussie

SUMMARY AND DISCUSSION

Cell division in *Streptomyces* differs a lot from the situation in most bacteria, which is due to the mycelial instead of planktonic life style. Firstly, two different types of cell division occur: cytokinesis and cell fission only occur during sporulation, while in the vegetative stage cell division results in the formation of cross walls which dissect the hyphae into large compartments (for an overview see Chapter I). Therefore, streptomycetes are multicellular, which is again in contrast to most bacteria (Claessen *et al.*, 2014). In fact, the concept of multicellularity was first mentioned only some 25 years ago (Shapiro, 1988). Secondly, the way cell division is controlled is also very different. In the model organisms *E. coli* and *B. subtilis*, cell division is primarily negatively controlled, aiming at preventing cell division at places away from midcell, and avoiding damage to the nucleoid. In other words, cell division is controlled such that the septum is formed only at the middle of the cell and when the DNA is duplicated and safely out of the way. This immediately highlights a major conceptual difference, as the long hyphae of streptomycetes do not have a clear midcell position. Instead, during *Streptomyces* sporulation, the actinomycete-specific protein SsgA marks future septation sites and somehow ensures the localization of SsgB to the septum sites, which then in turn recruits the cell division scaffold protein FtsZ (Willemse *et al.*, 2011); subsequently FtsZ then forms a characteristic pattern that is seen as spectacular ladders in the sporogenic hyphae (Schwedock *et al.*, 1997). During cell division, SsgB remains at the septum and keeps interacting with and stabilizing FtsZ, forming the same ladder-like pattern. Thus, SsgB is a unique example of a divisome component that localizes prior to FtsZ.

All data suggest that SsgA is mainly responsible for the initial activation of cell division, and indeed overexpression of the protein during early growth results in what can only be described as metamorphosis of the vegetative hyphae, which then resemble sporogenic aerial hyphae and even at times sporulate (notably in liquid-grown cultures; (van Wezel *et al.*, 2000b; van Wezel *et al.*, 2000a)). However, many of the components required for proper sporulation are missing - including the sporulation-specific SsgB protein - and the process is at best erratic. SsgA-like proteins (SALPs) do not show significant sequence similarity to other proteins in the databases to give away clues as to how they may function, but structural analysis revealed strong structural similarity of SsgB to mitochondrial guide RNA binding proteins (Xu *et al.*, 2009). However, interaction with FtsZ, the structural model and experimental evidence suggest that SsgB does not interact with nucleic acids. Instead, it lo-

calizes close to the membrane.

At the start of this PhD work, major questions we sought to address were, how does SsgB interact with the membrane, and what other actinomycete-specific proteins are there to control the localization of the septum in time and space in aerial hyphae? And how is damage to the chromosomes prevented during synchronous multiple cell division in multinucleoid hyphae? One obvious place to look is in the *dcw* cluster which contains primarily genes related to cell wall synthesis and cell division. The function of several of the genes between *ftsZ* (SCO2082) and *divIVA* (SCO2077) was unknown, despite the fact that for example *ylmD* and *ylmE* are downstream of - and most likely in operon with *ftsZ* in many Gram positive bacteria, including *Streptomyces*. All four genes in this region, namely *ylmD, ylmE, sepF* and *ylmG* (SCO2081-SCO2078), were therefore analyzed in more detail.

YlmG is a relatively small 95 aa protein with transmembrane domains at the N- and C-terminus. Deletion of *sepG* caused largely delayed and also impaired sporulation, pointing out its role in sporulation-specific cell division (Chapter II). Due to its clear role in the control of septum formation, *ylmG* was renamed *sepG*. Strikingly, in the absence of *sepG*, SsgB localized temporarily in foci, with foci formed in a 'flash'-like manner, similarly to SsgA (Joost Willemse & Gilles van Wezel, unpublished data). This suggests that the initial SsgB localization can occur in the absence of SepG, but that it failed to localize to septum sites. FRET imaging data showed direct interaction between SepG and SsgB, which strongly suggests a model whereby SepG forms the membrane anchor for SsgB to ensure the localization of SsgB to future septum sites. Therefore, SepG was identified as a new member of the positive cell division control system in *Streptomyces*. However, SepG did not remain at the septum and is therefore not a component of the divisome. Instead, the protein follows the spore-wall synthetic machinery. There it most likely plays a second role, namely in ensuring that the nucleoid is compacted to avoid DNA damage by spore wall (and septum) synthesis. Indeed, during spore maturation, SepG forms a ring structure close to the spore wall, enveloping the chromosomes. Conversely, deletion of *sepG* led to doughnut-shaped chromosomes, suggesting that SepG plays a role in nucleoid compaction during sporulation. The precise role of SepG in a nucleoid-occlusion-like mechanism requires further investigation.

SepF, encoded by the gene upstream of *sepG*, was previously shown to tether the Z-ring to the membrane in *B. subtilis* and promote FtsZ protofilament formation (Hamoen *et al.*, 2006; Ishikawa *et al.*, 2006). Like in *B. subtilis*, in *S. coelicolor* SepF also localized to septum sites and formed the septal ladder-like

pattern typical of *Streptomyces* divisome proteins (Chapter III). We failed to delete the *sepF* gene, despite many different attempts, but work by the group of Joe McCormick showed that in their genetic background such mutants were viable, displaying a sporulation-deficient phenotype very similar to that of *ftsZ* null mutants (Joe McCormick, unpublished data). This suggests that SepF is required for FtsZ localization but also its polymerization, as the phenotype is more destructive than that of *ssgB* mutants (which still form occasional septa). In other words, while SsgB recruits FtsZ and also stimulates FtsZ filament formation (Willemse *et al.*, 2011), SepF is essential for FtsZ polymerization.

Besides *sepF* itself, *Streptomyces* have two *sepF*-like genes, SCO1749 and SCO5967, encoding SflA and SflB (for SepF-like proteins), respectively. Our study showed that SflA and SflB play different roles than SepF, with deletion of *sflAB* leading to extensive branching of the spore chains. Conversely, over-expression of SflA or SflB largely blocked aerial hyphae formation, suggesting they act as negative regulators of *Streptomyces* development. The data can perhaps be reconciled by a repressing effect on apical growth of the aerial hyphae: deletion then results in more tips, while overexpression reduces tip growth altogether. Furthermore, the colonies of *sflA*- or *sflB*-overexpressing strains lost the ability to adhere to the agar surface, again suggesting an effect on hyphal branching, albeit in this case of the vegetative hyphae (no aerial hyphae were formed by these colonies). It should thereby be noted that *divIVA*, which is essential for tip growth of vegetative hyphae (Flärdh, 2003a), lies only two genes downstream of *sepF*. Taken together, our data suggest that SflA and SflB control branching of *Streptomyces* hyphae. Still, we cannot rule out that these effects are mediated directly or indirectly via the control of SepF. SflB directly interacts with SepF in two-hybrid studies, and surprisingly localized in a ladder-like pattern except close to the cell wall, where septum formation is initiated. This implies that SflB and SepF form heterocomplexes, aimed perhaps at inhibition of SepF function. Additionally, SflA localizes along the lateral membrane of the aerial hyphae. More detailed imaging analysis is required, but a model wherein SflA and SflB together inhibit premature polymerization of SepF at all sites other than the site of septum initiation - and therefore inhibit premature division - is feasible. That would imply the existence of a negative control system besides the SsgAB-mediated positive control. Finally, the roles of SflAB on both division and branching may be explained by a single activity if SepF controls the localization and/or function of DivIVA. However, no data are currently available to support this highly speculative concept.

Once the septum is formed by the divisome, which is highly conserved also in *Streptomyces* (Flärdh and van Wezel, 2003; Jakimowicz and van Wezel,

2012; McCormick, 2009), sporulation progresses and eventually a thick spore wall is produced. Peptidoglycan synthesis includes several stages (recently reviewed in (Pinho *et al.*, 2013)): the biosynthesis of the cell-wall precursors UDP-*N*-acetylmuramic acid (UDP-MurNAc) and UDP-*N*-acetylglucosamine (UDP-GlcNAc); addition of the pentapeptide chain to UDP-MurNAc to produce UDP-MurNAc-pentapeptide; coupling of MurNAc-pentapeptide to bactoprenol to form lipid I followed by further addition of GlcNAc to form lipid II; and transport over the cytoplasmic membrane by FtsW (Mohammadi *et al.*, 2011) followed by polymerization through cross-bridges to form mature peptidoglycan. In terms of peptidoglycan (PG) synthesis, a challenging issue for streptomycetes is to ensure the timely accumulation of large amounts of PG precursors that are required for septum and spore-wall synthesis. Considering the amount of PG precursors required, synthesis most likely has to occur *in situ* in the aerial hyphae rather than through long-distance transport. Our data suggest that YlmD and YlmE, which show similarity to alanine racemase and laccase, respectively, plays a role in such precursor supply (Chapter IV). D-Ala-D-Ala produced by the enzyme D-Ala-D-Ala ligase (Ddl) is the final unit of the pentapeptide chain of UDP-MurNAc-pentapeptide and the racemase domain in YlmE suggested a possible role in precursor synthesis. However, YlmE failed to show alanine racemase activity *in vitro* and could not take over the function of alanine racemase (Alr) during vegetative growth *in vivo*, suggesting that it either has a different function or requires a co-factor for function. Still, deletion of either *ylmD* or *ylmE* resulted in a sporulation defect, with defective and mislocalized peptidoglycan and cell membrane synthesis in *ylmD* and in particular in *ylmE* mutants during sporulation. Furthermore, higher concentrations of D-Ala partially restored sporulation to *ylmE* mutants, and the sensitivity of *ylmE* mutant cells to D-cycloserine increased. Earlier research showed similar hypersensitivity to DCS in *alr* mutants (Caceres *et al.*, 1997; Noda *et al.*, 2004; Peteroy *et al.*, 2000). Therefore, the sporulation defect of *ylmE* mutants may indeed be attributed at least in part to the lack of D-Ala precursor supply.

Another cell division-related gene cluster was discovered by genome sequencing of a hypersporulating mutant of *Streptomyces griseus*, whereby SNP analysis identified a mutation that changed the 7th codon of *lcmA* to a stop codon, thereby affecting the entire *lcmABC* operon (Chapter V). The orthologs in *S. coelicolor* are SCO1385-SCO1387, and suggestively, those in *B. subtilis* lie immediately adjacent to *divIB* in the *dcw* cluster. Mutation or deletion of *lcm* genes, which all encode membrane proteins, led to production of thin-walled spores with increased sensitivity to heat treatment, especially in mutants with

either the nonsense mutation *lcmA** or lacking the entire *lcmABC* cluster. The mutants also showed accelerated growth and development on solid media, perhaps due to the fact that the thinner spore-wall allows faster germination. Such a correlation between spore-wall thickness and germination had been seen previously for *crp* mutants (Piette *et al.*, 2005). LcmA, LcmB and LcmC all localize to the septum at sites of septum closure, and mutants frequently produce unfinished septa. This is consistent with a function of the Lcm proteins in the last stages of spore maturation. Interestingly, the phylogenetic linkage of the *lcm* genes to genes of the glycine cleavage (*gcv*) system in many bacteria prompted NMR-based metabolome analysis of spore content; this indeed showed significant changes in primary metabolism in *lcmABC* null mutants as compared to wild-type spores, although not in glycine accumulation, which was however seen for a *gcv* mutant that was used as the control. The precise implications of the altered metabolic profile in the spores are as yet unclear.

Finally, the genetic cause was examined of another exciting and long-known spontaneous mutant of *S. griseus* NRRL B2682, namely the A-factor nonproducer AFN (Biró *et al.*, 2000). For more than 40 years now, *S. griseus* has been a model strain for γ-butyrolactone (GBL)-mediated extracellular signaling via the GBL A-factor (Khokhlov *et al.*, 1973). A-factor acts by binding to the A-factor receptor protein ArpA, which results in the release of the repression by ArpA of the transcription of the global regulatory gene *adpA* (Ohnishi *et al.*, 1999; Ohnishi *et al.*, 2005). AdpA then directly activates the transcription of genes involved in development and secondary metabolism (Ohnishi *et al.*, 1999; Ohnishi *et al.*, 2005). Sequence analysis of *S. griseus* AFN revealed that in this mutant, the codon for Trp881 of the gene *afsR* was changed to a stop codon (Chapter VI). AfsR, which is phosphorylated by the important cell cycle serine/threonine kinase AfsK, was previously studied and likely involved in the response of development and antibiotic production to glucose (Umeyama *et al.*, 1999). We noticed a strong direct correlation between AfsR expression and colony size and streptomycin production in *S. griseus*, with a large colony phenotype and accelerated aerial hyphae formation as well as enhanced streptomycin production for colonies with extra copies of *afsR*. This is in apparent contrast to the data published previously (Umeyama *et al.*, 1999). Unfortunately the original *afsR* mutant of *S. griseus* was lost and could therefore not be compared. However, A-factor production was not affected in either a full deletion mutant of *afsR* or in strains in which the AFN-derived nonsense mutation was introduced, which suggests that AfsR may play its role independent of the A-factor cascade.

Future work

Many new cell division-related genes have been identified in this work, and deletion resulted in often pleiotropic defects in sporulation or spore maturation. This offers a lot of potential for future research. However, while the phenotypic changes are sometimes drastic, it is not always easy to understand the underlying molecular basis for the defects, in other words, to find out what precisely these genes do. SepG controls sporulation-specific cell division, most likely by tethering SsgB to the membrane, while the role of SepG in nucleoid compaction is yet unexplained. *In vivo* and *in vitro* interaction studies, such as FRET interaction studies to establish the interaction with the membrane, and bacterial two-hybrid screening or pull-down assays to find interaction partners, should provide further functional insights into the function of SepG and in the control of division. The surprising and yet unexplained effect of the SepF-like proteins on apical growth and branching is also something that needs to be pursued, and colocalization studies and live imaging of SepF, SflA, SflB, DivIVA and FtsZ would shed light on their role in balancing apical growth and sporulation. Biochemical studies on ring formation by SepF and the Sfl proteins should establish whether heterocomplexes are formed and what the affinities are, to validate the model wherein the Sfl proteins serve to curb the activity of SepF.

Despite many cell biological and biochemical experiments, and their crucial roles in cell-wall synthesis, it is yet unclear how precisely the enzymes YlmD and YlmE contribute to sporulation-specific peptidoglycan synthesis. Currently, in collaboration with Raffaella Tassoni and Marcellus Ubbink (Department of Chemistry, Leiden University), extensive ligand-interaction studies are being performed using purified YlmD and YlmE proteins, in an attempt to identify the substrate for these enzymes. Live imaging techniques, including FRET studies, should provide insights into how the Lcm proteins function and interact, and what their roles are in septum synthesis and/or closure during sporulation-specific cell division. How the Lcm proteins relate to the observed changes in the spore metabolome remains to be elucidated. Finally, the observed relationship between AfsR expression level, colony size and secondary metabolism (streptomycin production) is surprising. Reverse engineering of the *afsR** mutation into wild-type *S. griseus* did not result in an AFN phenotype, and to find the responsible mutation perhaps more extensive SNP analysis, or genetic complementation with a genomic library should be attempted, both in a wild-type and *afsR** background.

This PhD study started out from the perspective that, besides the clear fundamental importance, the study of novel cell division-related genes may also

offer new leads for strain-engineering approaches, similar to earlier applications of the cell division activator SsgA. So far however, the major valorization of the work lies in generating functional insights on several well-conserved genes near *ftsZ* in the *dcw* cluster and also elsewhere on the genome. This has further deepened our understanding of how positive control of cell division is governed in *Streptomyces*, but since many of the targets are conserved in Gram-positive bacteria, will also have an impact in the broad field of bacterial cell division.

SAMENVATTING EN DISCUSSIE

Celdeling in *Streptomyces* is wezenlijk anders dan in de meeste bacteriën, wat vooral wordt veroorzaakt door hun multicellulaire levensstijl via groei als mycelia tegenover de ééncellige levensstijl van de meeste bacteriën. Ten eerste zijn er twee verschillende vormen van celdeling: cytokinese en binaire deling vinden alleen plaats tijdens de sporulatie, terwijl vegetatieve celdeling resulteert in grote compartimenten die geschieden worden door op onregelmatige afstand geplaatste tussenschotten (voor een overzicht zie Hoofdstuk I). Daardoor zijn streptomyceten multicellulair (Claessen *et al.*, 2014). Het concept dat bacteriën ook meercellig kunnen zijn is pas zo'n 25 jaar geleden voor het eerst genoemd (Shapiro, 1988). Ten tweede is de manier waarop celdeling geregeld wordt heel anders. In de modelorganismen *E. coli* en *B. subtilis* is de celdeling voornamelijk negatief gereguleerd, gericht op het voorkomen van celdeling op andere plekken dan in het midden van de cel en op het voorkomen van schade aan het DNA. Met andere woorden, celdeling is zo gereguleerd dat het septum alleen wordt gevormd in het midden van de cel als het DNA gedupliceerd en veilig uit de weg is. Dit is een belangrijk conceptueel verschil, aangezien de lange hyfen van streptomyceten geen duidelijk aanwijsbaar middelpunt hebben. In plaats daarvan geeft het eiwit SsgA - wat net als de andere SsgA-achtige eiwitten alleen in actinomyceten voorkomt - de toekomstige plekken voor de celdeling aan en zorgt het voor de lokalisatie van SsgB op deze posities. SsgB rekruteert dan het celdelingseiwit FtsZ (Willemse *et al.*, 2011) en FtsZ vormt vervolgens een karakteristiek ladderachtig patroon in de sporenvormende hyfen (Schwedock *et al.*, 1997). Tijdens de celdeling vormt SsgB een vergelijkbaar ladderpatroon waar het FtsZ stabiliseert. Dit maakt SsgB een uniek voorbeeld van een onderdeel van het divisoom (oftewel het celdelingsapparaat) dat op de toekomstige plaats van het septum lokaliseert voordat FtsZ aanwezig is.

Gebaseerd op deze data lijkt het erop dat SsgA primair verantwoordelijk is voor de initiatie van de celdeling en inderdaad zorgt overexpressie van het eiwit tijdens de vroege groei voor een metamorfose van de vegetatieve hyfe die dan op sporulerende luchthyfen gaan lijken (van Wezel *et al.*, 2000b; van Wezel *et al.*, 2000a). Soms kunnen de hyfen zelfs in vloeibare culturen gaan sporuleren, wat in onze modelstam *Streptomyces coelicolor* normaal niet gebeurt. Echter, veel onderdelen die nodig zijn voor sporulatie ontbreken – zoals het sporulatiespecifieke SsgB eiwit – en de sporulatie is op zijn best grillig. SsgA-achtige eiwitten (SALPs) hebben geen significante sequentie-overeenkomsten met welk ander eiwit dan ook zodat het lastig is iets te kunnen zeggen over hun functie, maar er is op structureel niveau veel overeenkomst tussen

SsgB en mitochondriale guide-RNA bindende eiwitten (Xu *et al.*, 2009). De interactie met FtsZ, de structuur en ander experimenteel bewijs doen echter vermoeden dat SsgB niet met nucleïnezuren interactie aangaat. In plaats daarvan lokaliseert het dicht bij het membraan.

Aan het begin van dit promotieonderzoek, waren de belangrijkste vragen die we wilden beantwoorden. Hoe interacteert SsgB met de membraan en welke andere actinomyceet-specifieke eiwitten zijn er betrokken bij het lokaliseren van het septum in tijd en ruimte in luchthyfen? En hoe wordt schade aan de chromosomen voorkomen tijdens de gelijktijdige vorming van meerdere septa tegelijkertijd in een lange hyfe met vele nucleoïden? Een voor de hand liggende plaats om te gaan zoeken was het *dcw* cluster dat voornamelijk genen bevat die gerelateerd zijn aan celwandsynthese en celdeling. De functie van een aantal genen tussen *ftsZ* (SCO2082) en *divIVA* (SCO2077) was nog onbekend, ondanks het feit dat bijvoorbeeld *ylmD* en *YlmE* stroomafwaarts van – en waarschijnlijk in een operon met – *ftsZ* liggen in veel Gram positieve bacteriën, inclusief *Streptomyces.* Alle vier genen in deze regio, namelijk *ylmD, ylmE, sepF* en *ylmG* (SCO2081-SCO2078), zijn daarom in meer detail bekeken.

YlmG is een relatief klein 95 aminozuren groot eiwit met transmembraan domeinen aan zowel de N- als de C- terminus. Deletie van *sepG* veroorzaakt een vertraagde en verzwakte sporulatie dat op een rol in de sporulatie-specifieke celdeling duidt (Hoofdstuk II). Door de duidelijke rol tijdens de septumvorming hebben we de naam van *ylmG* in *sepG* veranderd. Opvallend is dat in de afwezigheid van *sepG,* foci van SsgB slechts heel kort te zien zijn. Ze worden daarbij in een 'flits' gevormd, vergelijkbaar met SsgA (Joost Willemse & Gilles van Wezel, ongepubliceerde resultaten). Dit doet vermoeden dat de initiële lokalisatie van SsgB plaatsvindt onafhankelijk van SepG, maar dat het niet bij de septum sites aankomt. FRET experiment laat een directe interactie tussen SepG en SsgB zien, wat sterk wijst op een model waar SepG het membraananker vormt voor SsgB lokalisatie op toekomstige septa. Daarom is SepG geïdentificeerd als nieuw onderdeel van de positieve controle van celdeling in *Streptomyces*. Echter, SepG blijft niet op het septum tijdens de deling en is daarom in tegenstelling tot bijvoorbeeld SsgB en FtsZ geen onderdeel van het divisoom. In plaats daarvan volgt SepG de eiwitmachinerie die betrokken is bij de synthese van de celwand van sporen. Daar heeft het waarschijnlijk een tweede rol, namelijk het condenseren van DNA om schade door de celwandsynthese te voorkomen. Tijdens sporenrijping vormt SepG ringen vlakbij de sporenwand, om de chromosomen heen. Omgekeerd leidt het weghalen van *sepG* tot donutvormige chromosomen, wat suggereert dat

SepG een rol heeft bij nucleoïdecondensatie tijdens sporulatie. De precieze rol van SepG in een nucleoïde beschermingsmechanisme moet nog verder worden onderzocht.

Van SepF, gecodeerd door het gen dat voor *sepG* in de *dcw* cluster ligt, was al eerder aangetoond dat het de Z-ring aan het membraan verankert in *B. subtilis* en dat het de vorming van FtsZ protofilamenten stimuleert (Hamoen *et al.*, 2006; Ishikawa *et al.*, 2006). Net als in *B. subtilis*, lokaliseert SepF in *S. coelicolor* ook op het septum en vormt een ladderachtig patroon wat typerend is voor divisoomeiwitten van streptomyceten (Hoofdstuk III). Ondanks meerdere pogingen is het niet gelukt om SepF uit te schakelen, maar werk door de groep van Joe McCormick heeft laten zien dat in elk geval in hun genetische achtergrond deze mutanten wel levensvatbaar zijn en een sporulatiedeficiëntie vertonen die vergelijkbaar is met de *ftsZ* mutant (Joe McCormick, ongepubliceerde data). Dit suggereert dat SepF nodig is voor de lokalisatie van FtsZ zowel als voor de polymerisatie, omdat het fenotype extremer is dan dat van *ssgB* mutanten (die nog steeds af en toe een septum produceren). Met andere woorden, terwijl SsgB FtsZ rekruteert en FtsZ filamentvorming stimuleert (Willemse *et al.*, 2011), is SepF essentieel voor FtsZ polymerisatie.

Naast s*epF* zelf heeft *Streptomyces* nog twee *sepF*-achtige genen, SCO1749 en SCO5967, die respectievelijk coderen voor SflA en SflB (voor 'SepF-like' eiwitten). Onze studies laten zien dat SflA en SflB een andere rol hebben dan SepF, uitschakelen van *sflAB* leidt tot vertakking van sporenketens. Omgekeerd leidt de overexpressie van SflA of SflB tot een blokkade van de ontwikkeling, waardoor het lijkt alsof ze negatieve regulatoren zijn van de ontwikkeling van streptomyceten. De data kunnen ook verklaard worden door een afname van tipgroei van de luchthyfen: deletie leidt dan tot meer vertakking, daarentegen leidt overexpressie tot een geblokkeerde vertakking. Verder verliezen de *sflA*- en *sflB*-overexpressie stammen de mogelijkheid om zich aan de oppervlakte van de voedingsboden te hechten, wat wederom een effect op vertakking suggereert, al is dit gerelateerd aan vegetatieve hyfen (er werden geen luchthyfen gevormd door deze kolonies). Er moet daarbij aangetekend worden dat het gen *divIVA,* waarvan het genproduct essentieel is voor de (tip-)groei (Flärdh, 2003), slechts twee genen stroomafwaarts van *sepF* ligt. Samenvattend doen onze data vermoeden dat SflA en SflB de vertakking van *Streptomyces* hyfen controleren. We kunnen echter niet uitsluiten dat deze effecten direct of indirect gereguleerd worden via SepF. SflB interacteert direct met SepF in two-hybrid studies en lokaliseert zeer verassend in een ladderachtig patroon behalve dicht bij de celwand waar de septumvorming geïnitieerd wordt. SflB en SepF zouden dus heterodimeren kunnen vormen, die misschien gericht zijn op de

remming van SepF. Verder lokaliseert SflA langs de laterale membraan van de luchthyfen. Gedetailleerdere image-analyse is nodig, maar tot nu toe is een model waarbij SflA en SflB samen de vroegtijdige polymerisatie van SepF op alle andere plaatsen dan de septum positie voorkomen – en zo vroegtijdige deling voorkomen – het meest waarschijnlijk. Dat laat zien dat er naast positieve controle van celdeling (middels SsgAB) wellicht ook een negatief regulatiesysteem is. Als laatste, de rol van SflAB op zowel deling als vertakking kan verklaard worden door een enkele manier van regulatie als SepF verantwoordelijk is voor de lokalisatie en/of functie van DivIVA. Er zijn op dit moment geen verdere data die dit speculatieve model ondersteunen.

Als het septum eenmaal gevormd is door het divisoom, wat ook in *Streptomyces* erg geconserveerd is (Flärdh and van Wezel, 2003; Jakimowicz and van Wezel, 2012; McCormick, 2009), gaat de celdeling voort en wordt er een dikke celwand gevormd. Peptidoglycansynthese bestaat uit een aantal stadia (recent gereviewed in (Pinho *et al.*, 2013)): de biosynthese van de celwandbouwstenen UDP-*N*-acetylmuraminezuur (UDP-MurNAc) en UDP-*N*-acetylglucosamine (UDP-GlcNAc); het toevoegen van een pentapeptideketen aan UDP-MurNAc om UDP-MurNAc pentapeptide te vormen; en het koppelen van het MurNAc pentapeptide aan bactoprenol om zo lipid I te vormen, waarna de koppeling van GlcNAc resulteert in de PG precursor lipid II; deze wordt daarna over de membraan getransporteerd door FtsW (Mohammadi *et al.*, 2011). Streptomyceten moeten zorgen dat er op tijd genoeg PG bouwstenen in de cel aanwezig zijn die nodig zijn voor septum- en sporenwandsynthese. Als je kijkt naar de hoeveelheid PG bouwstenen die daarvoor nodig zijn, dan worden ze waarschijnlijk *in situ* gesynthetiseerd of uit afbraak gevormd, in plaats van ter plekke gebracht door lange afstandstransport. Onze data suggereren dat YlmD en YlmE, die vergelijkingen vertonen met respectievelijk een laccase-domein eiwit en met alanine racemase, een rol spelen in het onderhouden van de voorraad PG-bouwstenen (Hoofdstuk IV). De D-alanine dimeer D-Ala-D-Ala, geproduceerd door het enzym D-Ala-D-Ala ligase (Ddl), is de laatste eenheid van de pentapeptide keten van het UDP-MurNAc-pentapeptide en het racemase domein in YlmE wijst op een rol in de synthese van PG-bouwstenen. YlmE heeft echter geen aantoonbare racemase-activiteit, hetgeen doet vermoeden we dat het óf een andere functie heeft óf een cofactor of partner nodig heeft om goed te kunnen functioneren. Toch leidt de deletie van *ylmD* of *ylmE* tot een sporulatiedefect, met mislokalisatie van de peptidoglycan- en celwandsynthese in *ylmD* mutanten en vooral in *ylmE* mutanten. Verder kan een hoge concentraties D-Ala de sporulatie herstellen van *ylmE* mutanten en was tevens de gevoeligheid voor het antibioticum D-cycloserine hoger. Dat

laatste is typerend voor alanine racemasemutanten (Caceres *et al.*, 1997; Noda *et al.*, 2004; Peteroy *et al.*, 2000). Daarom moet het sporulatiedefect in de *ylmE* mutanten waarschijnlijk toch tenminste deels toe worden geschreven aan een tekort aan D-alanine.

Een ander aan de celdeling gerelateerde gencluster is ontdekt door sequencen van het genoom van een hypersporulerende mutant van de streptomycineproducent *Streptomyces griseus*. SNP-analyse liet een mutatie zien waardoor het 7^{e} codon van *lcmA* in een stopcodon was veranderd, hetgeen ook consequenties heeft voor de erop volgende genen in het *lcmABC* cluster (Hoofdstuk V). De orthologen in *S. coelicolor* zijn SCO1385-SCO1387 en die liggen in *B. subtilis* naast het celdelingsgen *divIB* in het *dcw* cluster. Dit suggereert dus een relatie met celdeling. Mutatie en/of deletie van de *lcm* genen, die allemaal voor membraaneiwitten coderen, resulteerde in sporen met een dunnere sporenwand en een (vermoedelijk als gevolg daarvan) toegenomen hittegevoeligheid, vooral voor mutanten met de nonsensemutatie *lcmA** of mutanten die het hele *lcmABC* cluster missen. De mutanten lieten een versnelde groei zien op vaste voedingsbodems, misschien omdat de dunnere sporenwand tot snellere ontkieming leidt. Eenzelfde relatie tussen sporenwanddikte en ontkieming was eerder waargenomen in mutanten die *crp* missen, voor het cAMP-receptor eiwit (Piette *et al.*, 2005). LcmA, LcmB en LcmC lokaliseren allemaal op of rond het septum tijdens de celdeling en mutanten hebben veel vaker onvolledige septa dan de oorspronkelijke stam. Dit is in lijn met een rol voor de Lcm-eiwitten bij de laatste stadia van sporenvorming. Het is goed om op te merken dat er een fylogenetische link is tussen de *lcm* genen en het glycine afbreeksysteem (gcv) in veel bacteriën. Vandaar dat sporenextracten zijn geanalyseerd met NMR, wat liet zien dat er belangrijke verschillen zijn qua metabolietprofielen tussen de *lcmABC* mutanten en de oorspronkelijke stam, maar juist weer niet in glycine-ophoping. De precieze gevolgen van de metabole veranderingen in de sporen zijn nog onduidelijk.

Als laatste werd de genetische oorzaak voor een andere reeds lang bekende mutant van *S. griseus* NRRL B2682, namelijk de AFN stam die niet of nauwelijks het hormoonachtige signaalmolecuul A-factor aanmaakt (Biró *et al.*, 2000). Al meer dan 40 jaar is *S. griseus* een model organisme voor signalering via de γ-butyrolactone (GBL) A-factor (Khokhlov *et al.*, 1973). A-factor werkt door aan het A-factor receptoreiwit ArpA te binden, hetgeen zorgt voor het opheffen van de rem door ArpA op de transcriptie van *adpA* (Ohnishi *et al.*, 1999; Ohnishi *et al.*, 2005). AdpA op zijn beurt activeert dan de transcriptie van genen betrokken bij de ontwikkeling en bij het secundaire metabolisme (Ohnishi *et al.*, 1999; Ohnishi *et al.*, 2005). Sequentie-analyse van *S. griseus*

AFN liet zien dat in deze mutant het codon van Trp881 van *afsR* veranderd is in een stopcodon (Hoofdstuk VI). AfsR, dat gefosforyleerd wordt door de belangrijke celcyclus serine/threonine kinase AfsK was al eerder bestudeerd en is waarschijnlijk betrokken bij de relatie tussen de ontwikkeling en de antibioticumproductie tijdens de groei op glucose (Umeyama *et al.*, 1999). Wij vonden een sterke directe relatie tussen AfsR expressie enerzijds en koloniegrootte en streptomycine productie anderzijds, waarbij grote kolonies en versnelde luchthyfenvorming samen met verhoogde streptomycineproductie relateerde aan kolonies met extra kopieën van *afsR*. Dit lijkt in tegenstelling met eerder gepubliceerde data (Umeyama *et al.*, 1999). Helaas was de originele *afsR* mutant van *S. griseus* niet te achterhalen en daarom kon de data niet vergeleken worden. Echter, A-factor productie was niet beïnvloed in ofwel een *afsR* mutant ofwel een stam waarin de AFN-afgeleide nonsense mutatie was ingebracht, hetgeen suggereert dat AfsR een rol heeft die onafhankelijk is van de A-factor signaalcascade.

Toekomstig werk

Tijdens dit werk zijn vele nieuwe bij de celdeling betrokken genen geïdentificeerd, waarbij deletie vaak resulteerde in pleiotrope defecten in sporulatie en sporen maturatie. Dit opent vele deuren voor verder onderzoek. Hoewel de fenotypische veranderingen soms drastisch zijn is het niet altijd makkelijk om de onderliggende moleculaire basis te begrijpen. SepG controleert sporulatiespecifieke celdeling, vermoedelijk door SsgB aan de membraan te koppelen, maar de rol van SepG in nucleoïde condensatie is nog onverklaarbaar. *In vivo* en *in vitro* interactie studies, zoals FRET studies om de interactie met de membraan te bekijken, en two-hybrid en pull-down experimenten om interactiepartners te vinden, kunnen verder inzicht verschaffen in de werking van SepG als ook hoe de celdeling is gereguleerd. Het verassende en tot nu toe onverklaarde effect van de SepF-achtige eiwitten op de groei van de luchthyfen en ook de vertakking verdient zeker verdere aandacht; colocalisatie en live-imaging met SepF, SflA, SflB, DivIVA en FtsZ zouden hun rol in tipgroei en sporulatie vervolgens kunnen ophelderen. Biochemische studies aan de ring-vorming van SepF en de Sfl-eiwitten zouden duidelijk moeten maken of er inderdaad heterocomplexen gevormd worden en wat de affiniteit voor elkaar is, dit om het model te valideren waarbij de Sfl-eiwitten de activiteit van SepF remmen.

Ondanks de vele genetische, biochemische en celbiologische experimenten en hun belangrijke rol bij de celwandsynthese, is het tot nog toe onduidelijk

hoe YlmD en YlmE precies werken. Momenteel wordt in samenwerking met Raffaella Tassoni en Marcellus Ubbink (Instituut voor Chemie, Universiteit Leiden) ligandinteractie studies gedaan met gezuiverd YlmD en YlmE, om te trachten de substraten voor deze eiwitten te achterhalen. Qua Lcm eiwitten zullen onder meer live-imaging technieken (FRET) meer inzicht moeten geven in hoe de Lcm eiwitten *in vivo* met elkaar interacteren en hoe ze relateren aan de septumsynthese. Ook de veranderingen in het sporenmetabolome zijn nog onverklaard. Tenslotte, de waargenomen relatie tussen AfsR expressie, koloniegrootte en secundair metabolisme (*in casu* de streptomycineproductie) is opvallend. Omdat een *afsR** mutatie in de oorspronkelijke *S. griseus* stam niet in een blokkade van A-factor productie resulteerde, dat wil zeggen geen AFN fenotype gaf, ligt het voor de hand dat er een tweede mutatie naast *afsR** gezocht zal moeten worden.

Dit promotieonderzoek begon vanuit het perspectief dat, naast hun duidelijke fundamentele belang, de studie naar nieuwe celdelingseiwitten ook nieuwe ideeën kan opleveren voor de toekomstige ontwikkeling van industriële stammen, vergelijkbaar met eerder toepassingen van de celdelingsactivator SsgA. Veel streptomyceten vormen grote myceliumklonten die nadelig zijn voor groei en productie in de fermentor en hoge expressie van SsgA leidt tot fragmentatie van het mycelium, hetgeen voordelig is voor de productiviteit. Het werk beschreven in dit proefschrift heeft vooral nieuwe inzichten in de celdeling opgeleverd, met name door het karakteriseren van een aantal genen die in nagenoeg alle Gram-positieve bacteriën dichtbij *ftsZ* in de *dcw* cluster liggen. Dit heeft niet alleen ons begrip van de celdeling in *Streptomyces* vergroot, maar biedt tevens nieuwe perspectieven voor onderzoek aan celdeling in vele andere bacteriën. Daarmee zal het werk beschreven in dit proefschrift een basis kunnen vormen voor toekomstig onderzoek naar de bacteriële celdeling.

References

Abeles, A. L., Friedman, S. A. and Austin, S. J. (1985) Partition of unit-copy miniplasmids to daughter cells. *J Mol Biol* **185**: 261-272.

Adamidis, T. and Champness, W. (1992) Genetic analysis of *absB*, a *Streptomyces coelicolor* locus involved in global antibiotic regulation. *J Bacteriol* **174**: 4622-4628.

Adams, D. W. and Errington, J. (2009) Bacterial cell division: assembly, maintenance and disassembly of the Z ring. *Nat Rev Microbiol* **7**: 642-653.

Anuchin, A. M., Goncharenko, A. V., Demidenok, O. I. and Kaprelyants, A. S. (2011) Histone-like proteins of bacteria (review). *Appl Biochem Microbiol* **47**: 580-585.

Atsushi, M., Soon-Kwang, H., Hiroshi, I., Sueharu, H. and Teruhiko, B. (1994) Phosphorylation of the AfsR protein involved in secondary metabolism in *Streptomyces* species by a eukary otic-type protein kinase. *Gene* **146**: 47-56.

Barák, I. and Wilkinson, A. J. (2007) Division site recognition in *Escherichia coli* and *Bacillus subtilis*. *FEMS Microbiol Rev* **31**: 311-326.

Beall, B. and Lutkenhaus, J. (1989) Nucleotide sequence and insertional inactivation of a *Bacillus subtilis* gene that affects cell division, sporulation, and temperature sensitivity. *J Bacteriol* **171**: 6821-6834.

Bennett, J. A., Aimino, R. M. and McCormick, J. R. (2007) *Streptomyces coelicolor* genes *ftsL* and *divIC* play a role in cell division but are dispensable for colony formation. *J Bacteriol* **189**: 8982-8992.

Bennett, J. A. and McCormick, J. R. (2001) Two new loci affecting cell division identified as suppressors of an *ftsQ*-null mutation in *Streptomyces coelicolor* A3(2). *FEMS Microbiol Lett* **202**: 251-256.

Bennett, J. A., Yarnall, J., Cadwallader, A. B., Kuennen, R., Bidey, P., Stadelmaier, B. and McCormick, J. R. (2009) Medium-dependent phenotypes of *Streptomyces coelicolor* with mutations in *ftsI* or *ftsW*. *J Bacteriol* **191**: 661-664.

Bernhardt, T. G. and de Boer, P. A. J. (2005) SlmA, a nucleoid-associated, FtsZ binding protein required for blocking septal ring assembly over chromosomes in *E. coli*. *Mol Cell* **18**: 555-564.

Bi, E. F. and Lutkenhaus, J. (1991) FtsZ ring structure associated with division in *Escherichia coli*. *Nature* **354**: 161-164.

Bibb, M. J. (2005) Regulation of secondary metabolism in streptomycetes. *Curr Opin Microbiol* **8**: 208-215.

Bibb, M. J., Janssen, G. R. and Ward, J. M. (1985) Cloning and analysis of the promoter region of the erythromycin resistance gene (*ermE*) of *Streptomyces erythraeus. Gene* **38**: 215-226.

Bierman, M., Logan, R., O'Brien, K., Seno, E. T., Nagaraja Rao, R. and Schoner, B. E. (1992) Plasmid cloning vectors for the conjugal transfer of DNA from *Escherichia coli* to *Streptomyces* spp. *Gene* **116**: 43-49.

Bigot, S., Saleh, O. A., Lesterlin, C., Pages, C., El Karoui, M., Dennis, C., Grigoriev, M., Allemand, J.-F., Barre, F.-X. and Cornet, F. (2005) KOPS: DNA motifs that control *E. coli* chromosome segregation by orienting the FtsK translocase. *EMBO J* **24**: 3770-3780.

Birkó, Z., Bialek, S., Buzás, K., Szájli, E., Traag, B. A., Medzihradszky, K. F., Rigali, S., Vijgenboom, E., Penyige, A., Kele, Z., van Wezel, G. P. and Biró, S. (2007) The secreted signaling protein Factor C triggers the A-factor response regulon in *Streptomyces griseus*: overlapping signaling routes. *Mol Cell Proteomics* **6**: 1248-1256.

Birkó, Z., Swiatek, M., Szájli, E., Medzihradszky, K. F., Vijgenboom, E., Penyige, A., Keseru, J., van Wezel, G. P. and Biró, S. (2009) Lack of A-factor production induces the expression of nutrient scavenging and stress-related proteins in *Streptomyces griseus*. *Mol Cell Proteomics* **8**: 2396-2403.

Biró, S., Birkó, Z. and Wezel, G. P. v. (2000) Transcriptional and functional analysis of the gene for factor C, an extracellular signal protein involved in cytodifferentiation of *Streptomyces griseus. Antonie Van Leeuwenhoek* **78**: 277-285.

Blatch, G. L. and Lässle, M. (1999) The tetratricopeptide repeat: a structural motif mediating protein-protein interactions. *Bioessays* **21**: 932-939.

Bramkamp, M. and van Baarle, S. (2009) Division site selection in rod-shaped bacteria. *Curr Opin Microbiol* **12**: 683-688.

Breakefield, X. O. and Landman, O. E. (1973) Temperature-sensitive divisionless mutant of *Bacillus subtilis* defective in the initiation of septation. *J Bacteriol* **113**: 985-998.

Burgis, N. E. and Cunningham, R. P. (2007) Substrate specificity of RdgB protein, a deoxyribonucleoside triphosphate pyrophosphohydrolase. *J Biol Chem* **282**: 3531-3538.

Burton, B. M., Marquis, K. A., Sullivan, N. L., Rapoport, T. A. and Rudner, D. Z. (2007) The ATPase SpoIIIE transports DNA across fused septal membranes during sporulation in *Bacillus subtilis*. *Cell* **131**: 1301-1312.

Caceres, N., Harris, N., Wellehan, J., Feng, Z., Kapur, V. and Barletta, R. (1997) Overexpression of the D-alanine racemase gene confers resistance to D-cycloserine in *Mycobacterium smegmatis. J Bacteriol* **179**: 5046-5055.

Ceci, P., Cellai, S., Falvo, E., Rivetti, C., Rossi, G. L. and Chiancone, E. (2004) DNA condensation and self-aggregation of *Escherichia coli* Dps are coupled phenomena related to the properties of the N-terminus. *Nucleic Acids Res* **32**: 5935-5944.

Cha, J. and Stewart, G. (1997) The divIVA minicell locus of *Bacillus subtilis. J Bacteriol* **179**: 1671-1683.

Chater, K. and Losick, R. (1997) *Bacteria as multicellular organisms,* p. 149-182. UK: Oxford University Press.

Chater, K. F. (1972) A morphological and genetic mapping study of white colony mutants of *Streptomyces coelicolor. J Gen Microbiol* **72**: 9-28.

Chiancone, E. and Ceci, P. (2010) The multifaceted capacity of Dps proteins to combat bacterial stress conditions: Detoxification of iron and hydrogen peroxide and DNA binding. *Biochim Biophys Acta* **1800**: 798-805.

Cho, H., McManus, H. R., Dove, S. L. and Bernhardt, T. G. (2011) Nucleoid occlusion factor SlmA is a DNA-activated FtsZ polymerization antagonist. *Proc Natl Acad Sci USA* **108**: 3773-3778.

Claessen, D., Rozen, D. E., Kuipers, O. P., Søgaard-Andersen, L. and van Wezel, G. P. (2014) Bacterial solutions to multicellularity: a tale of biofilms, filaments and fruiting bodies. *Nat Rev Microbiol* **12**: 115-124.

Claus, H. (2003) Laccases and their occurrence in prokaryotes. *Arch Microbiol* **179**: 145-150.

Colson, S., Stephan, J., Hertrich, T., Saito, A., van Wezel, G. P., Titgemeyer, F. and Rigali, S. (2007) Conserved *cis*-acting elements upstream of genes composing the chitinolytic system of streptomycetes are DasR-responsive elements. *J Mol Microbiol Biotechnol* **12**: 60-66.

Colson, S., van Wezel, G. P., Craig, M., Noens, E. E. E., Nothaft, H., Mommaas, A. M., Titgemeyer, F., Joris, B. and Rigali, S. (2008) The chitobiose-binding protein, DasA, acts as a link between chitin utilization and morphogenesis in *Streptomyces coelicolor. Microbiology* **154**: 373-382.

Colwell, C. A. (1946) Small colony variants of *Escherichia coli. J Bacteriol* **52**: 417-422.

Dame, R. T. (2005) The role of nucleoid-associated proteins in the organization and compaction of bacterial chromatin. *Mol Microbiol* **56**: 858-870.

de Boer, P. A. J. (2010) Advances in understanding *E. coli* cell fission. *Curr Opin Microbiol* **13**: 730-737.

de Boer, P. A. J., Crossley, R. and Rothfield, L. (1992) The essential bacterial cell-division protein FtsZ is a GTPase. *Nature* **359**: 254-256.

Dedrick, R. M., Wildschutte, H. and McCormick, J. R. (2009) Genetic interactions of *smc*, *ftsK*, and *parB* genes in *Streptomyces coelicolor* and their developmental genome segregation phenotypes. *J Bacteriol* **191**: 320-332.

Del Sol, R., Mullins, J. G. L., Grantcharova, N., Flärdh, K. and Dyson, P. (2006) Influence of CrgA on

assembly of the cell division protein FtsZ during development of *Streptomyces coelicolor*. *J Bacteriol* **188**: 1540-1550.

Donachie, W. D. (1993) The cell cycle of *Escherichia coli*. *Annu Rev Microbiol* **47**: 199-230.

Drlica, K. and Rouviere-Yaniv, J. (1987) Histonelike proteins of bacteria. *Microbiol Rev* **51**: 301-319.

Duman, R., Ishikawa, S., Celik, I., Strahl, H., Ogasawara, N., Troc, P., Löwe, J. and Hamoen, L. W. (2013) Structural and genetic analyses reveal the protein SepF as a new membrane anchor for the Z ring. *Proc Natl Acad Sci USA* **110**: E4601-E4610.

Erickson, H. (1995) FtsZ, a prokaryotic homolog of tubulin? *Cell* **80**: 367-370.

Errington, J., Daniel, R. A. and Scheffers, D.-J. (2003) Cytokinesis in bacteria. *Microbiol Mol Biol Rev* **67**: 52-65.

Eswaramoorthy, S., Gerchman, S., Graziano, V., Kycia, H., Studier, F. W. and Swaminathan, S. (2002) Structure of a yeast hypothetical protein selected by a structural genomics approach. *Acta Crystallogr Sect D Biol Crystallogr* **59**: 127-135.

Facey, P. D., Hitchings, M. D., Saavedra-Garcia, P., Fernandez-Martinez, L., Dyson, P. J. and Del Sol, R. (2009) *Streptomyces coelicolor* Dps-like proteins: differential dual roles in response to stress during vegetative growth and in nucleoid condensation during reproductive cell division. *Mol Microbiol* **73**: 1186-1202.

Fedoryshyn, M., Welle, E., Bechthold, A. and Luzhetskyy, A. (2008) Functional expression of the Cre recombinase in actinomycetes. *Appl Microbiol Biotechnol* **78**: 1065-1070.

Fiebig, A., Keren, K. and Theriot, J. A. (2006) Fine-scale time-lapse analysis of the biphasic, dynamic behaviour of the two *Vibrio cholerae* chromosomes. *Mol Microbiol* **60**: 1164-1178.

Flärdh, K. (2003a) Essential role of DivIVA in polar growth and morphogenesis in *Streptomyces coelicolor* A3(2). *Mol Microbiol* **49**: 1523-1536.

Flärdh, K. (2003b) Growth polarity and cell division in *Streptomyces*. *Curr Opin Microbiol* **6**: 564-571.

Flärdh, K. and Buttner, M. J. (2009) *Streptomyces* morphogenetics: dissecting differentiation in a filamentous bacterium. *Nat Rev Microbiol* **7**: 36-49.

Flärdh, K. and van Wezel, G. P. (2003) Cell division during growth and development in *Streptomyces*. *Recent Res Dev Bacteriol* **1**: 71-90.

Fleming, T. C., Shin, J. Y., Lee, S.-H., Becker, E., Huang, K. C., Bustamante, C. and Pogliano, K. (2010) Dynamic SpoIIIE assembly mediates septal membrane fission during *Bacillus subtilis* sporulation. *Genes Dev* **24**: 1160-1172.

Floriano, B. and Bibb, M. (1996) *afsR* is a pleiotropic but conditionally required regulatory gene for antibiotic production in *Streptomyces coelicolor* A3(2). *Mol Microbiol* **21**: 385-396.

Fuller, R. S., Funnell, B. E. and Kornberg, A. (1984) The DnaA protein complex with the *E. coli* chromosomal replication origin (*oriC*) and other DNA sites. *Cell* **38**: 889-900.

Girard, G., Traag, B. A., Sangal, V., Mascini, N., Hoskisson, P. A., Goodfellow, M. and van Wezel, G. P. (2013) A novel taxonomic marker that discriminates between morphologically complex actinomycetes. *Open Biol* **3**: 130073.

Goehring, N. W. and Beckwith, J. (2005) Diverse paths to midcell: assembly of the bacterial cell division machinery. *Curr Biol* **15**: R514-R526.

Goosen, N. and Putte, P. (1995) The regulation of transcription initiation by integration host factor. *Mol Microbiol* **16**: 1-7.

Grant, R. A., Filman, D. J., Finkel, S. E., Kolter, R. and Hogle, J. M. (1998) The crystal structure of Dps, a ferritin homolog that binds and protects DNA. *Nat Struct Biol* **5**: 294-303.

Grantcharova, N., Lustig, U. and Flärdh, K. (2005) Dynamics of FtsZ assembly during sporulation in *Streptomyces coelicolor* A3(2). *J Bacteriol* **187**: 3227-3237.

Graumann, P. L. (2001) SMC proteins in bacteria: condensation motors for chromosome segregation?

Biochimie **83**: 53-59.

Gueiros-Filho, F. J. and Losick, R. (2002) A widely conserved bacterial cell division protein that promotes assembly of the tubulin-like protein FtsZ. *Genes Dev* **16**: 2544-2556.

Hale, C. A. and de Boer, P. A. J. (1997) Direct Binding of FtsZ to ZipA, an essential component of the septal ring structure that mediates cell division in *E. coli. Cell* **88**: 175-185.

Hale, C. A., Meinhardt, H. and de Boer, P. A. (2001) Dynamic localization cycle of the cell division regulator MinE in *Escherichia coli*. *EMBO J* **20**: 1563-1572.

Hall, W. H. and Spink, W. W. (1947) *In vitro* sensitivity of *Brucella* to streptomycin: development of resistance during streptomycin treatment. *Exp Biol Med* **64**: 403-406.

Hamoen, L. W., Meile, J.-C., de Jong, W., Noirot, P. and Errington, J. (2006) SepF, a novel FtsZ-interacting protein required for a late step in cell division. *Mol Microbiol* **59**: 989-999.

Harry, E., Monahan, L. and Thompson, L. (2006) Bacterial cell division: the mechanism and its precison. *Int Rev Cytol* **253**: 27-94.

Häussler, S., Lehmann, C., Breselge, C., Rohde, M., Classen, M., Tümmler, B., Vandamme, P. and Steinmetz, I. (2003) Fatal outcome of lung transplantation in cystic fibrosis patients due to small-colony variants of the *Burkholderia cepacia* complex. *Eur J Clin Microbiol Infect Dis* **22**: 249-253.

Hempel, A. M., Cantlay, S., Molle, V., Wang, S.-B., Naldrett, M. J., Parker, J. L., Richards, D. M., Jung, Y.-G., Buttner, M. J. and Flärdh, K. (2012) The Ser/Thr protein kinase AfsK regulates polar growth and hyphal branching in the filamentous bacteria *Streptomyces*. *Proc Natl Acad Sci USA* **109**: E2371-E2379.

Higo, A., Hara, H., Horinouchi, S. and Ohnishi, Y. (2012) Genome-wide distribution of AdpA, a global regulator for secondary metabolism and morphological differentiation in *Streptomyces*, revealed the extent and complexity of the AdpA regulatory network. *DNA Res* **19**: 259-273.

Hirano, S., Tanaka, K., Ohnishi, Y. and Horinouchi, S. (2008) Conditionally positive effect of the TetR-family transcriptional regulator AtrA on streptomycin production by *Streptomyces griseus*. *Microbiology* **154**: 905-914.

Hirano, T. (2002) The ABCs of SMC proteins: two-armed ATPases for chromosome condensation, cohesion, and repair. *Genes Dev* **16**: 399-414.

Hirano, T. (2006) At the heart of the chromosome: SMC proteins in action. *Nat Rev Mol Cell Biol* **7**: 311-322.

Hishinuma, F., Izaki, K. and Takahashi, H. (1969) Effets of glycine and D-amino acids on growth of various microorganisms. *Agric Biol Chem* **33**: 1577-1586.

Hols, P., Defrenne, C., Ferain, T., Derzelle, S., Delplace, B. and Delcour, J. (1997) The alanine racemase gene is essential for growth of *Lactobacillus plantarum. J Bacteriol* **179**: 3804-3807.

Hong, S. K., Kito, M., Beppu, T. and Horinouchi, S. (1991) Phosphorylation of the AfsR product, a global regulatory protein for secondary-metabolite formation in *Streptomyces coelicolor* A3(2). *J Bacteriol* **173**: 2311-2318.

Hopwood, D. A. (2007) *Streptomyces in nature and medicine: the antibiotic makers.* New York: Oxford University Press.

Horinouchi, S. (2002) A microbial hormone, A-factor, as a master switch for morphological differentiation and secondary metabolism in *Streptomyces griseus. Front Biosci* **7**: 2045-2057.

Horinouchi, S. and Beppu, T. (2007) Hormonal control by A-factor of morphological development and secondary metabolism in *Streptomyces*. *Proc Japan Acad, Ser B Phys Biol Sci* **83**: 277-295.

Horinouchi, S., Kumada, Y. and Beppu, T. (1984) Unstable genetic determinant of A-factor biosynthesis in streptomycin-producing organisms: cloning and characterization. *J Bacteriol* **158**: 481-487.

Ishikawa, S., Kawai, Y., Hiramatsu, K., Kuwano, M. and Ogasawara, N. (2006) A new FtsZ-interacting

protein, YlmF, complements the activity of FtsA during progression of cell division in *Bacillus subtilis*. *Mol Microbiol* **60**: 1364-1380.

Ito, T., Iimori, J., Takayama, S., Moriyama, A., Yamauchi, A., Hemmi, H. and Yoshimura, T. (2013) Conserved pyridoxal protein that regulates Ile and Val metabolism. *J Bacteriol* **195**: 5439-5449.

Jacob, F., Brenner, S. and Cuzin, F. (1963) On the Regulation of DNA Replication in bacteria. *Cold Spring Harbor Symp Quant Biol* **28**: 329-348.

Jakimowicz, D., Chater, K. and Zakrzewska-Czerwińska, J. (2002) The ParB protein of *Streptomyces coelicolor* A3(2) recognizes a cluster of *parS* sequences within the origin-proximal region of the linear chromosome. *Mol Microbiol* **45**: 1365-1377.

Jakimowicz, D., Gust, B., Zakrzewska-Czerwińska, J. and Chater, K. F. (2005) Developmental-stage-specific assembly of ParB complexes in *Streptomyces coelicolor* hyphae. *J Bacteriol* **187**: 3572-3580.

Jakimowicz, D., Majka, J., Messer, W., Speck, C., Fernandez, M., Cruz Martin, M., Sanchez, J., Schauwecker, F., Keller, U., Schrempf, H. and Zakrzewska-Czerwińska, J. (1998) Structural elements of the *Streptomyces oriC* region and their interactions with the DnaA protein. *Microbiology* **144**: 1281-1290.

Jakimowicz, D. and van Wezel, G. P. (2012) Cell division and DNA segregation in *Streptomyces*: how to build a septum in the middle of nowhere? *Mol Microbiol* **85**: 393-404.

Jellema, R., Brown, S., Tauler, R. and Walczak, B. (2009) *Comprehensive chemometrics, chemical and biochemical data analysis,* p. 85-108. Oxford: Elsevier.

Jiang, H. and Kendrick, K. E. (2000) Characterization of *ssfR* and *ssgA*, two genes involved in sporulation of *Streptomyces griseus*. *J Bacteriol* **182**: 5521-5529.

Johnson, R. C., Bruist, M. F. and Simon, M. I. (1986) Host protein requirements for in vitro site-specific DNA inversion. *Cell* **46**: 531-539.

Kabeya, Y., Nakanishi, H., Suzuki, K., Ichikawa, T., Kondou, Y., Matsui, M. and Miyagishima, S.-y. (2010) The YlmG protein has a conserved function related to the distribution of nucleoids in chloroplasts and cyanobacteria. *BMC Plant Biol* **10**: 57.

Kaguni, J. M. (2006) DnaA: controlling the initiation of bacterial DNA replication and more. *Annu Rev Microbiol* **60**: 351-375.

Karimova, G., Pidoux, J., Ullmann, A. and Ladant, D. (1998) A bacterial two-hybrid system based on a reconstituted signal transduction pathway. *Proc Natl Acad Sci USA* **95**: 5752-5756.

Katayama, T., Ozaki, S., Keyamura, K. and Fujimitsu, K. (2010) Regulation of the replication cycle: conserved and diverse regulatory systems for DnaA and *oriC*. *Nat Rev Microbiol* **8**: 163-170.

Kato, J.-y., Funa, N., Watanabe, H., Ohnishi, Y. and Horinouchi, S. (2007) Biosynthesis of γ-butyrolactone autoregulators that switch on secondary metabolism and morphological development in *Streptomyces*. *Proc Natl Acad Sci USA* **104**: 2378-2383.

Kawamoto, S. and Ensign, J. C. (1995) Isolation of mutants of *Streptomyces griseus* that sporulate in nutrient rich media: cloning of DNA fragments that suppress the mutations. *Actinomycetologica* **9**: 124-135.

Kawamoto, S., Watanabe, H., Hesketh, A., Ensign, J. C. and Ochi, K. (1997) Expression analysis of the *ssgA* gene product, associated with sporulation and cell division in *Streptomyces griseus*. *Microbiology* **143**: 1077-1086.

Keijser, B. J. F., Noens, E. E., Kraal, B., Koerten, H. K. and van Wezel, G. P. (2003) The *Streptomyces coelicolor ssgB* gene is required for early stages of sporulation. *FEMS Microbiol Lett* **225**: 59-67.

Khodakaramian, G., Lissenden, S., Gust, B., Moir, L., Hoskisson, P. A., Chater, K. F. and Smith, M. C. M. (2006) Expression of Cre recombinase during transient phage infection permits efficient marker removal in *Streptomyces*. *Nucleic Acids Res* **34**: e20.

Khokhlov, A. S., Anisova, L. N., Tovarova, I. I., Kleiner, E. M., Kovalenko, I. V., Krasilnikova, O. I.,

Kornitskaya, E. Y. and Pliner, S. A. (1973) Effect of A-factor on the growth of asporogenous mutants of *Streptomyces griseus*, not producing this factor. *Z Allg Mikrobiol* **13**: 647-655.

Kieser, T., Bibb, M. J., Buttner, M. J., Chater, K. F. and Hopwood, D. A. (2000) *Practical Streptomyces genetics.* John Innes Foundation.

Kikuchi, G., Motokawa, Y., Yoshida, T. and Hiraga, K. (2008) Glycine cleavage system: reaction mechanism, physiological significance, and hyperglycinemia. *Proc Japan Acad, Ser B Phys Biol Sci* **84**: 246-263.

Kim, H. K., Choi, Y. H. and Verpoorte, R. (2010) NMR-based metabolomic analysis of plants. *Nat Protoc* **5**: 536-549.

Kim, M.-J., Nihira, T. and Choi, S.-U. (2012) Cloning and characterization of *afsR* homologue regulatory gene from *Streptomyces acidiscabies* ATCC 49003. *J Korean Soc Appl Biol Chem* **55**: 663-668.

Kim, Y., Maltseva, N., Dementieva, I., Collart, F., Holzle, D. and Joachimiak, A. (2006) Crystal structure of hypothetical protein YfiH from *Shigella flexneri* at 2 Å resolution. *Proteins: Struct Funct Bioinform* **63**: 1097-1101.

Kois, A., Swiatek, M., Jakimowicz, D. and Zakrzewska-Czerwińska, J. (2009) SMC protein-dependent chromosome condensation during aerial hyphal development in *Streptomyces*. *J Bacteriol* **191**: 310-319.

Kolodkin-Gal, I., Romero, D., Cao, S., Clardy, J., Kolter, R. and Losick, R. (2010) D-amino acids trigger biofilm disassembly. *Science* **328**: 627-629.

Kopeloff, N. (1934) Dissociation and filtration of *Lactobacillus Acidophilus. J Infect Dis* **55**: 368-379.

Kurmayer, R., Christiansen, G. and Chorus, I. (2003) The abundance of microcystin-producing genotypes correlates positively with colony size in *Microcystis* sp. and determines its microcystin net production in Lake Wannsee. *Appl Environ Microbiol* **69**: 787-795.

Larson, J. L. and Hershberger, C. L. (1986) The minimal replicon of a streptomycete plasmid produces an ultrahigh level of plasmid DNA. *Plasmid* **15**: 199-209.

Lee, P.-C., Umeyama, T. and Horinouchi, S. (2002) *afsS* is a target of AfsR, a transcriptional factor with ATPase activity that globally controls secondary metabolism in *Streptomyces coelicolor* A3(2). *Mol Microbiol* **43**: 1413-1430.

Leonard, A. C. and Grimwade, J. E. (2010) Regulating DnaA complex assembly: it is time to fill the gaps. *Curr Opin Microbiol* **13**: 766-772.

Leonard, T. A., Butler, P. J. and Löwe, J. (2005a) Bacterial chromosome segregation: structure and DNA binding of the Soj dimer--a conserved biological switch. *EMBO J* **24**: 270-282.

Leonard, T. A., Møller-Jensen, J. and Löwe, J. (2005b) Towards understanding the molecular basis of bacterial DNA segregation. *Philos Trans R Soc Lond, Ser B: Biol Sci* **360**: 523-535.

Liu, G., Chater, K. F., Chandra, G., Niu, G. and Tan, H. (2013) Molecular regulation of antibiotic biosynthesis in *Streptomyces*. *Microbiol Mol Biol Rev* **77**: 112-143.

Livny, J., Yamaichi, Y. and Waldor, M. K. (2007) Distribution of centromere-like *parS* sites in bacteria: insights from comparative genomics. *J Bacteriol* **189**: 8693-8703.

Lutkenhaus, J. (2007) Assembly dynamics of the bacterial MinCDE system and spatial regulation of the Z ring. *Annu Rev Biochem* **76**: 539-562.

MacNeil, D. J., Gewain, K. M., Ruby, C. L., Dezeny, G., Gibbons, P. H. and Maeneil, T. (1992) Analysis of *Streptomyces avermitilis* genes required for avermectin biosynthesis utilizing a novel integration vector. *Gene* **111**: 61-68.

Mahr, K., van Wezel, G. P., Svensson, C., Krengel, U., Bibb, M. J. and Titgemeyer, F. (2000) Glucose kinase of *Streptomyces coelicolor* A3(2): large-scale purification and biochemical analysis. *Antonie Van Leeuwenhoek* **78**: 253-261.

Majka, J., Jakimowicz, D., Messer, W., Schrempf, H., Lisowski, M. and Zakrzewska-Czerwińska, J. (1999)

Interactions of the *Streptomyces lividans* initiator protein DnaA with its target. *Eur J Biochem* **260**: 325-335.

Majka, J., Zakrzewska-Czerwińska, J. and Messer, W. (2001) Sequence recognition, cooperative interaction, and dimerization of the initiator protein DnaA of *Streptomyces*. *J Biol Chem* **276**: 6243-6252.

Manteca, A., Fernández, M. and Sánchez, J. (2005) A death round affecting a young compartmentalized mycelium precedes aerial mycelium dismantling in confluent surface cultures of *Streptomyces antibioticus*. *Microbiology* **151**: 3689-3697.

Manteca, A., Ye, J., Sánchez, J. and Jensen, O. N. (2011) Phosphoproteome analysis of *Streptomyces* development reveals extensive protein phosphorylation accompanying bacterial differentiation. *J Proteome Res* **10**: 5481-5492.

Marbouty, M., Saguez, C., Cassier-Chauvat, C. and Chauvat, F. (2009) ZipN, an FtsA-like orchestrator of divisome assembly in the model cyanobacterium *Synechocystis* PCC6803. *Mol Microbiol* **74**: 409-420.

Margolin, W. (2005) FtsZ and the division of prokaryotic cells and organelles. *Nat Rev Mol Cell Biol* **6**: 862-871.

Marston, A. L. and Errington, J. (1999) Selection of the midcell division site in *Bacillus subtilis* through MinD-dependent polar localization and activation of MinC. *Mol Microbiol* **33**: 84-96.

Marston, A. L., Thomaides, H. B., Edwards, D. H., Sharpe, M. E. and Errington, J. (1998) Polar localization of the MinD protein of *Bacillus subtilis* and its role in selection of the mid-cell division site. *Genes Dev* **12**: 3419-3430.

Mason, J. M. and Setlow, P. (1987) Different small, acid-soluble proteins of the alpha/beta type have interchangeable roles in the heat and UV radiation resistance of *Bacillus subtilis* spores. *J Bacteriol* **169**: 3633-3637.

Mazza, P., Noens, E. E., Schirner, K., Grantcharova, N., Mommaas, A. M., Koerten, H. K., Muth, G., Flärdh, K., van Wezel, G. P. and Wohlleben, W. (2006) MreB of *Streptomyces coelicolor* is not essential for vegetative growth but is required for the integrity of aerial hyphae and spores. *Mol Microbiol* **60**: 838-852.

McBride, M. J. and Ensign, J. C. (1987) Metabolism of endogenous trehalose by *Streptomyces griseus* spores and by spores or cells of other actinomycetes. *J Bacteriol* **169**: 5002-5007.

McCormick, J. R. (2009) Cell division is dispensable but not irrelevant in *Streptomyces*. *Curr Opin Microbiol* **12**: 689-698.

McCormick, J. R. and Losick, R. (1996) Cell division gene *ftsQ* is required for efficient sporulation but not growth and viability in *Streptomyces coelicolor* A3(2). *J Bacteriol* **178**: 5295-5301.

McCormick, J. R., Su, E. P., Driks, a. and Losick, R. (1994) Growth and viability of *Streptomyces coelicolor* mutant for the cell division gene *ftsZ*. *Mol Microbiol* **14**: 243-254.

Merrick, M. J. (1976) A morphological and genetic mapping study of bald colony mutants of *Streptomyces coelicolor*. *J Gen Microbiol* **96**: 299-315.

Milligan, D. L., Tran, S. L., Strych, U., Cook, G. M. and Krause, K. L. (2007) The alanine racemase of *Mycobacterium smegmatis* is essential for growth in the absence of D-alanine. *J Bacteriol* **189**: 8381-8386.

Mingorance, J., Tamames, J. and Vicente, M. (2004) Genomic channeling in bacterial cell division. *J Mol Recognit* **17**: 481-487.

Miroux, B. and Walker, J. E. (1996) Over-production of proteins in *Escherichia coli*: mutant hosts that allow synthesis of some membrane proteins and globular proteins at high levels. *J Mol Biol* **260**: 289-298.

Misra, G., Rojas, E. R., Gopinathan, A. and Huang, K. C. (2013) Mechanical consequences of cell-wall turnover in the elongation of a Gram-positive bacterium. *Biophys J* **104**: 2342-2352.

Mistry, B. V., Del Sol, R., Wright, C., Findlay, K. and Dyson, P. (2008) FtsW is a dispensable cell division protein required for Z-ring stabilization during sporulation septation in *Streptomyces coelicolor. J Bacteriol* **190**: 5555-5566.

Miyakawa, Y. and Komano, T. (1981) Study on the cell cycle of *Bacillus subtilis* using temperature-sensitive mutants. *Mol Gen Genet* **181**: 207-214.

Mohammadi, T., van Dam, V., Sijbrandi, R., Vernet, T., Zapun, A., Bouhss, A., Diepeveen-de Bruin, M., Nguyen-Distèche, M., de Kruijff, B. and Breukink, E. (2011) Identification of FtsW as a transporter of lipid-linked cell wall precursors across the membrane. *EMBO J* **30**: 1425-1432.

Mohr, S. C., Sokolov, N. V., He, C. M. and Setlow, P. (1991) Binding of small acid-soluble spore proteins from *Bacillus subtilis* changes the conformation of DNA from B to A. *Proc Natl Acad Sci USA* **88**: 77-81.

Morris, J. F., Barnes, C. G. and Sellers, T. F. (1943) An outbreak of typhoid fever due to the small colony variety of *Eberthella typhosa*. *American journal of public health and the nation's health* **33**: 246-248.

Morton, H. E. and Shoemaker, J. (1945) The identification of *Neisseria gonorrhoeae* by means of bacterial variation and the detection of small colony forms in clinical material. *J Bacteriol* **50**: 585-587.

Motamedi, H., Shafiee, A. and Cai, S.-J. (1995) Integrative vectors for heterologous gene expression in *Streptomyces* spp. *Gene* **160**: 25-31.

Murphy, L. D. and Zimmerman, S. B. (1997) Isolation and characterization of spermidine nucleoids from *Escherichia coli*. *J Struct Biol* **119**: 321-335.

Murray, H. and Errington, J. (2008) Dynamic control of the DNA replication initiation protein DnaA by Soj/ParA. *Cell* **135**: 74-84.

Nair, S. and Finkel, S. E. (2004) Dps protects cells against multiple stresses during stationary phase. *J Bacteriol* **186**: 4192-4198.

Nilsson, L., Vanet, A., Vijgenboom, E. and Bosch, L. (1990) The role of FIS in trans activation of stable RNA operons of *E. coli. EMBO J* **9**: 727-734.

Noda, M., Kawahara, Y., Ichikawa, A., Matoba, Y., Matsuo, H., Lee, D.-G., Kumagai, T. and Sugiyama, M. (2004) Self-protection mechanism in D-cycloserine-producing *Streptomyces lavendulae*. Gene cloning, characterization, and kinetics of its alanine racemase and D-alanyl-D-alanine ligase, which are target enzymes of D-cycloserine. *J Biol Chem* **279**: 46143-46152.

Noens, E. E. (2007) Control of sporulation-specific cell division in *Streptomyces coelicolor*. In: Leiden University.

Noens, E. E., Mersinias, V., Traag, B. A., Smith, C. P., Koerten, H. K. and van Wezel, G. P. (2005) SsgA-like proteins determine the fate of peptidoglycan during sporulation of *Streptomyces coelicolor. Mol Microbiol* **58**: 929-944.

Noens, E. E., Mersinias, V., Willemse, J., Traag, B. A., Laing, E., Chater, K. F., Smith, C. P., Koerten, H. K. and van Wezel, G. P. (2007) Loss of the controlled localization of growth stage-specific cell-wall synthesis pleiotropically affects developmental gene expression in an *ssgA* mutant of *Streptomyces coelicolor*. *Mol Microbiol* **64**: 1244-1259.

Ohnishi, Y., Ishikawa, J., Hara, H., Suzuki, H., Ikenoya, M., Ikeda, H., Yamashita, A., Hattori, M. and Horinouchi, S. (2008) Genome sequence of the streptomycin-producing microorganism *Streptomyces griseus* IFO 13350. *J Bacteriol* **190**: 4050-4060.

Ohnishi, Y., Kameyama, S., Onaka, H. and Horinouchi, S. (1999) The A-factor regulatory cascade leading to streptomycin biosynthesis in *Streptomyces griseus* : identification of a target gene of the A-factor receptor. *Mol Microbiol* **34**: 102-111.

Ohnishi, Y., Yamazaki, H., Kato, J.-Y., Tomono, A. and Horinouchi, S. (2005) AdpA, a central transcriptional regulator in the A-factor regulatory cascade that leads to morphological development and secondary metabolism in *Streptomyces griseus*. *Biosci, Biotechnol, Biochem* **69**: 431-439.

Pedulla, M. L. and Hatfull, G. F. (1998) Characterization of the *mIHF* gene of *Mycobacterium smegmatis*. *J Bacteriol* **180**: 5473-5477.

Pedulla, M. L., Lee, M. H., Lever, D. C. and Hatfull, G. F. (1996) A novel host factor for integration of mycobacteriophage L5. *Proc Natl Acad Sci USA* **93**: 15411-15416.

Percudani, R. and Peracchi, A. (2003) A genomic overview of pyridoxal-phosphate-dependent enzymes. *EMBO reports* **4**: 850-854.

Peteroy, M., Severin, A., Zhao, F., Lopatin, U., Scherman, H., Harvey, B., Hatfull, G. F., Patrick, J., Connell, N. D., Rosner, D., Lopatin, U. R. I., Belanger, A. and Brennan, P. J. (2000) Characterization of a *Mycobacterium smegmatis* mutant that is simultaneously resistant to D-cycloserine and vancomycin. *American society for microbiology* **44**: 1701-1704.

Pichoff, S. and Lutkenhaus, J. (2002) Unique and overlapping roles for ZipA and FtsA in septal ring assembly in *Escherichia coli*. *EMBO J* **21**: 685-693.

Piette, A., Derouaux, A., Gerkens, P., Noens, E. E. E., Mazzucchelli, G., Vion, S., Koerten, H. K., Titgemeyer, F., De Pauw, E., Leprince, P., van Wezel, G. P., Galleni, M. and Rigali, S. (2005) From dormant to germinating spores of *Streptomyces coelicolor* A3(2): new perspectives from the crp null mutant. *J Proteome Res* **4**: 1699-1708.

Pinho, M. G., Kjos, M. and Veening, J.-W. (2013) How to get (a)round: mechanisms controlling growth and division of coccoid bacteria. *Nat Rev Microbiol* **11**: 601-614.

Plocinski, P., Ziolkiewicz, M., Kiran, M., Vadrevu, S. I., Nguyen, H. B., Hugonnet, J., Veckerle, C., Arthur, M., Dziadek, J., Cross, T. A., Madiraju, M. and Rajagopalan, M. (2011) Characterization of CrgA, a new partner of the *Mycobacterium tuberculosis* peptidoglycan polymerization complexes. *J Bacteriol* **193**: 3246-3256.

Pogliano, K., Harry, E. and Losick, R. (1995) Visualization of the subcellular location of sporulation proteins in *Bacillus subtilis* using immunofluorescence microscopy. *Mol Microbiol* **18**: 459-470.

Pope, M. K., Green, B. D. and Westpheling, J. (1996) The *bld* mutants of *Streptomyces coelicolor* are defective in the regulation of carbon utilization, morphogenesis and cell-cell signalling. *Mol Microbiol* **19**: 747-756.

Price, B., Adamidis, T., Kong, R. and Champness, W. (1999) A *Streptomyces coelicolor* antibiotic regulatory gene, *absb*, encodes an RNase III homolog. *J Bacteriol* **181**: 6142-6151.

Proctor, R. A., von Eiff, C., Kahl, B. C., Becker, K., McNamara, P., Herrmann, M. and Peters, G. (2006) Small colony variants: a pathogenic form of bacteria that facilitates persistent and recurrent infections. *Nat Rev Microbiol* **4**: 295-305.

Radkov, A. D. and Moe, L. A. (2014) Bacterial synthesis of D-amino acids. *Appl Microbiol Biotechnol* **98**: 5363-5374.

Ragkousi, K., Cowan, A. E., Ross, M. A. and Setlow, P. (2000) Analysis of nucleoid morphology during germination and outgrowth of spores of *Bacillus* species. *J Bacteriol* **182**: 5556-5562.

Raskin, D. M. and de Boer, P. A. J. (1997) The MinE ring: an FtsZ-independent cell structure required for selection of the correct division site in *E. coli*. *Cell* **91**: 685-694.

RayChaudhuri, D. (1999) ZipA is a MAP-Tau homolog and is essential for structural integrity of the cytokinetic FtsZ ring during bacterial cell division. *EMBO J* **18**: 2372-2383.

RayChaudhuri, S., Conrad, J., Hall, B. G. and Ofengand, J. (1998) A pseudouridine synthase required for the formation of two universally conserved pseudouridines in ribosomal RNA is essential for normal growth of *Escherichia coli*. *RNA* **4**: 1407-1417.

Rodrigues, C. D. and Harry, E. J. (2012) The Min system and nucleoid occlusion are not required for identifying the division site in *Bacillus subtilis* but ensure its efficient utilization. *PLoS Genet* **8**: e1002561.

Rohde, M. (1999) Small-colony variants of *Pseudomonas aeruginosa* in cystic fibrosis. *Clin Infect Dis* **29**: 621-625.

Romberg, L. and Levin, P. A. (2003) Assembly dynamics of the bacterial cell division protein FtsZ: poised at the edge of stability. *Annu Rev Microbiol* **57**: 125-154.

Romero A, D., Hasan, A. H., Lin, Y.-F., Kime, L., Ruiz-Larrabeiti, O., Urem, M., Bucca, G., Mamanova, L., Laing, E. E., van Wezel, G. P., Smith, C. P., Kaberdin, V. R. and McDowall, K. J. (2014) A comparison of key aspects of gene regulation in *Streptomyces coelicolor* and *Escherichia coli* using nucleotide-resolution transcription maps produced in parallel by global and differential RNA-sequencing. *Mol Microbiol* **94**: 963-987.

Rowland, S. L., Errington, J. and Wake, R. G. (1995) The *Bacillus subtilis* cell-division 135–137° region contains an essential orf with significant similarity to *murB* and a dispensable *sbp* gene. *Gene* **164**: 113-116.

Ruban-Ośmiałowska, B., Jakimowicz, D., Smulczyk-Krawczyszyn, A., Chater, K. F. and Zakrzewska-Czerwińska, J. (2006) Replisome localization in vegetative and aerial hyphae of *Streptomyces coelicolor. J Bacteriol* **188**: 7311-7316.

Salerno, P., Larsson, J., Bucca, G., Laing, E., Smith, C. P. and Flärdh, K. (2009) One of the two genes encoding nucleoid-associated HU proteins in *Streptomyces coelicolor* is developmentally regulated and specifically involved in spore maturation. *J Bacteriol* **191**: 6489-6500.

Sambrook, J., Fritsch, E. and Maniatis, T. (1989) *Molecular cloning: a laboratory manual.* New York: Cold spring harbor laboratory press.

Scheffers, D.-J. and Pinho, M. G. (2005) Bacterial cell wall synthesis: new insights from localization studies. *Microbiol Mol Biol Rev* **69**: 585-607.

Scholefield, G., Errington, J. and Murray, H. (2012) Soj/ParA stalls DNA replication by inhibiting helix formation of the initiator protein DnaA. *EMBO J* **31**: 1542-1555.

Schwedock, J., McCormick, J. R., Angert, E. R., Nodwell, J. R. and Losick, R. (1997) Assembly of the cell division protein FtsZ into ladder-like structures in the aerial hyphae of *Streptomyces coelicolor*. *Mol Microbiol* **25**: 847-858.

Setlow, B., McGinnis, K. A., Ragkousi, K. and Setlow, P. (2000) Effects of major spore-specific DNA binding proteins on *Bacillus subtilis* sporulation and spore properties. *J Bacteriol* **182**: 6906-6912.

Sevcikova, B. and Kormanec, J. (2003) The *ssgB* gene, encoding a member of the regulon of stress-response sigma factor σ^H, is essential for aerial mycelium septation in *Streptomyces coelicolor* A3(2). *Arch Microbiol* **180**: 380-384.

Shapiro, J. A. (1988) Bacteria as multicellular organisms. *Sci Am* **258**: 82-89.

Strunnikov, A. V. (2006) SMC complexes in bacterial chromosome condensation and segregation. *Plasmid* **55**: 135-144.

Studier, F. W. and Moffatt, B. A. (1986) Use of bacteriophage T7 RNA polymerase to direct selective high-level expression of cloned genes. *J Mol Biol* **189**: 113-130.

Stutzman-Engwall, K. J., Otten, S. L. and Hutchinson, C. R. (1992) Regulation of secondary metabolism in *Streptomyces* spp. and overproduction of daunorubicin in *Streptomyces peucetius*. *J Bacteriol* **174**: 144-154.

Suzuki, H., Takahashi, S., Osada, H. and Yoshida, K.-I. (2011) Improvement of transformation efficiency by strategic circumvention of restriction barriers in *Streptomyces griseus*. *J Microbiol Biotechnol* **21**: 675-678.

Świątek, M. A. (2012) Global control of development and antibiotic production by nutrient-responsive signalling pathways in *Streptomyces.* In: Leiden University.

Świątek, M. A., Gubbens, J., Bucca, G., Song, E., Yang, Y.-H., Laing, E., Kim, B.-G., Smith, C. P. and van Wezel, G. P. (2013) The ROK family regulator Rok7B7 pleiotropically affects xylose utilization, carbon catabolite repression, and antibiotic production in *Streptomyces coelicolor. J Bacteriol* **195**: 1236-1248.

Świątek, M. A., Tenconi, E., Rigali, S. and van Wezel, G. P. (2012) Functional analysis of the N-acetylglucosamine metabolic genes of *Streptomyces coelicolor* and role in control of development and antibiotic production. *J Bacteriol* **194**: 1136-1144.

Tamames, J., González-Moreno, M. a., Mingorance, J., Valencia, A. and Vicente, M. (2001) Bringing gene order into bacterial shape. *Trends Genet* **17**: 124-126.

Tanaka, A., Takano, Y., Ohnishi, Y. and Horinouchi, S. (2007) AfsR recruits RNA polymerase to the *afsS* promoter: a model for transcriptional activation by SARPs. *J Mol Biol* **369**: 322-333.

Tezuka, T. and Ohnishi, Y. (2014) Two glycine riboswitches activate the glycine cleavage system essential for glycine detoxification in *Streptomyces griseus*. *J Bacteriol* **196**: 1369-1376.

Tonthat, N. K., Arold, S. T., Pickering, B. F., Van Dyke, M. W., Liang, S., Lu, Y., Beuria, T. K., Margolin, W. and Schumacher, M. A. (2011) Molecular mechanism by which the nucleoid occlusion factor, SlmA, keeps cytokinesis in check. *EMBO J* **30**: 154-164.

Traag, B. A. and van Wezel, G. P. (2008) The SsgA-like proteins in actinomycetes: small proteins up to a big task. *Antonie Van Leeuwenhoek* **94**: 85-97.

Treuner-Lange, A., Aguiluz, K., van der Does, C., Gomez-Santos, N., Harms, A., Schumacher, D., Lenz, P., Hoppert, M., Kahnt, J., Munoz-Dorado, J. and Sogaard-Andersen, L. (2013) PomZ, a ParA-like protein, regulates Z-ring formation and cell division in *Myxococcus xanthus*. *Mol Microbiol* **87**: 235-253.

Trun, N. J. and Marko, J. F. (1998) Architecture of a bacterial chromosome. *ASM News* **64**: 276-283.

Umeyama, T., Lee, P.-C. C., Ueda, K. and Horinouchi, S. (1999) An AfsK/AfsR system involved in the response of aerial mycelium formation to glucose in *Streptomyces griseus*. *Microbiology* **145. 9**: 2281-2292.

van De Putte, P., van Dillewijn, J. and Rörsch, A. (1964) The selection of mutants of *Escherichia coli* with impaired cell division at elevated temperature. *Mutat Res* **1**: 121-128.

van Dissel, D., Claessen, D. and van Wezel, G. P. (2014) Morphogenesis of *Streptomyces* in submerged cultures. *Adv Appl Microbiol* **89**: 1-45.

van Wezel, G. P., Krabben, P., Traag, B. A., Keijser, B. J. F., Kerste, R., Vijgenboom, E., Heijnen, J. J. and Kraal, B. (2006) Unlocking *Streptomyces* spp. for use as sustainable industrial production platforms by morphological engineering. *Appl Environ Microbiol* **72**: 5283-5288.

van Wezel, G. P., Mahr, K., König, M., Traag, B. A., Pimentel-Schmitt, E. F., Willimek, A. and Titgemeyer, F. (2005) GlcP constitutes the major glucose uptake system of *Streptomyces coelicolor* A3(2). *Mol Microbiol* **55**: 624-636.

van Wezel, G. P. and McDowall, K. J. (2011) The regulation of the secondary metabolism of *Streptomyces*: new links and experimental advances. *Nat Prod Rep* **28**: 1311-1333.

van Wezel, G. P., Meulen, J. v. d., Taal, E., Koerten, H. and Kraal, B. (2000a) Effects of increased and deregulated expression of cell division genes on the morphology and on antibiotic production of streptomycetes. *Antonie Van Leeuwenhoek* **78**: 269-276.

van Wezel, G. P., van der Meulen, J., Kawamoto, S., Luiten, R. G., Koerten, H. K. and Kraal, B. (2000b) *ssgA* is essential for sporulation of *Streptomyces coelicolor* A3(2) and affects hyphal development by stimulating septum formation. *J Bacteriol* **182**: 5653-5662.

Vara, J., Lewandowska-Skarbek, M., Wang, Y. G., Donadio, S. and Hutchinson, C. R. (1989) Cloning of genes governing the deoxysugar portion of the erythromycin biosynthesis pathway in *Saccharopolyspora erythraea* (*Streptomyces erythreus*). *J Bacteriol* **171**: 5872-5881.

Varshavsky, A. J., Nedospasov, S. A., Bakayev, V. V., Bakayeva, T. G. and Georgiev, G. P. (1977) Histone-like proteins in the purified *Escherichia coli* deoxyribonucleoprotein. *Nucleic Acids Res* **4**: 2725-2746.

Viollier, P. H., Thanbichler, M., McGrath, P. T., West, L., Meewan, M., McAdams, H. H. and Shapiro, L. (2004) Rapid and sequential movement of individual chromosomal loci to specific subcellular

locations during bacterial DNA replication. *Proc Natl Acad Sci USA* **101**: 9257-9262.

Vögtil, M., Chang, P.-C. and Cohen, S. N. (1994) *afsR2*: a previously undetected gene encoding a 63-amino-acid protein that stimulates antibiotic production in *Streptomyces lividans. Mol Microbiol* **14**: 643-653.

Vollmer, W., Blanot, D. and de Pedro, M. a. (2008) Peptidoglycan structure and architecture. *FEMS Microbiol Rev* **32**: 149-167.

von Eiff, C., Becker, K., Metze, D., Lubritz, G., Hockmann, J., Schwarz, T. and Peters, G. (2001) Intracellular persistence of *Staphylococcus aureus* small-colony variants within keratinocytes: a cause for antibiotic treatment failure in a patient with darier's disease. *Clin Infect Dis* **32**: 1643-1647.

Vrancken, K. and Anné, J. (2009) Secretory production of recombinant proteins by *Streptomyces*. *Future Microbiol* **4**: 181-188.

Wang, L., Yu, Y., He, X., Zhou, X., Deng, Z., Chater, K. F. and Tao, M. (2007) Role of an FtsK-like protein in genetic stability in *Streptomyces coelicolor* A3(2). *J Bacteriol* **189**: 2310-2318.

Webb, C. D., Graumann, P. L., Kahana, J. A., Teleman, A. A., Silver, P. A. and Losick, R. (1998) Use of time-lapse microscopy to visualize rapid movement of the replication origin region of the chromosome during the cell cycle in *Bacillus subtilis. Mol Microbiol* **28**: 883-892.

Wecke, J., Perego, M. and Fischer, W. (2009) D-alanine deprivation of *Bacillus subtilis* teichoic acids is without effect on cell growth and morphology but affects the autolytic activity. *Microb Drug Resist* **2**: 123-129.

Wietzorrek, A. and Bibb, M. (1997) A novel family of proteins that regulates antibiotic production in streptomycetes appears to contain an OmpR-like DNA-binding fold. *Mol Microbiol* **25**: 1181-1184.

Wildermuth, H. and Hopwood, D. (1970) Septation during sporulation in *Streptomyces coelicolor. J Gen Microbiol* **60**: 51-59.

Willemse, J., Borst, J. W., de Waal, E., Bisseling, T. and van Wezel, G. P. (2011) Positive control of cell division: FtsZ is recruited by SsgB during sporulation of *Streptomyces*. *Genes Dev* **25**: 89-99.

Willemse, J. and van Wezel, G. P. (2009) Imaging of *Streptomyces coelicolor* A3(2) with reduced autofluorescence reveals a novel stage of FtsZ localization. *PloS one* **4**: e4242.

Wolański, M., Donczew, R., Kois-Ostrowska, A., Masiewicz, P., Jakimowicz, D. and Zakrzewska-Czerwinska, J. (2011a) The level of AdpA directly affects expression of developmental genes in *Streptomyces coelicolor*. *J Bacteriol* **193**: 6358-6365.

Wolański, M., Jakimowicz, D. and Zakrzewska-Czerwińska, J. (2014) Fifty years after the replicon hypothesis: cell-specific master regulators as new players in chromosome replication control. *J Bacteriol* **196**: 2901-2911.

Wolański, M., Jakimowicz, D. and Zakrzewska-Czerwinska, J. (2012) AdpA, key regulator for morphological differentiation regulates bacterial chromosome replication. *Open Biol* **2**: 120097.

Wolański, M., Wali, R., Tilley, E., Jakimowicz, D., Zakrzewska-Czerwinska, J. and Herron, P. (2011b) Replisome trafficking in growing vegetative hyphae of *Streptomyces coelicolor* A3(2). *J Bacteriol* **193**: 1273-1275.

Woldringh, C. L., Mulder, E., Huls, P. G. and Vischer, N. (1991) Toporegulation of bacterial division according to the nucleoid occlusion model. *Res Microbiol* **142**: 309-320.

Wolf, S. G., Frenkiel, D., Arad, T., Finkel, S. E., Kolter, R. and Minsky, A. (1999) DNA protection by stress-induced biocrystallization. *Nature* **400**: 83-85.

Wu, L. J. and Errington, J. (2004) Coordination of cell division and chromosome segregation by a nucleoid occlusion protein in *Bacillus subtilis. Cell* **117**: 915-925.

Wu, L. J. and Errington, J. (2012) Nucleoid occlusion and bacterial cell division. *Nat Rev Microbiol* **10**: 8-12.

Xu, Q., Traag, B. A., Willemse, J., McMullan, D., Miller, M. D., Elsliger, M.-A., Abdubek, P., Astakhova, T., Axelrod, H. L., Bakolitsa, C., Carlton, D., Chen, C., Chiu, H.-J., Chruszcz, M., Clayton, T., Das, D., Deller, M. C., Duan, L., Ellrott, K., Ernst, D., Farr, C. L., Feuerhelm, J., Grant, J. C., Grzechnik, A., Grzechnik, S. K., Han, G. W., Jaroszewski, L., Jin, K. K., Klock, H. E., Knuth, M. W., Kozbial, P., Krishna, S. S., Kumar, A., Marciano, D., Minor, W., Mommaas, A. M., Morse, A. T., Nigoghossian, E., Nopakun, A., Okach, L., Oommachen, S., Paulsen, J., Puckett, C., Reyes, R., Rife, C. L., Sefcovic, N., Tien, H. J., Trame, C. B., van den Bedem, H., Wang, S., Weekes, D., Hodgson, K. O., Wooley, J., Deacon, A. M., Godzik, A., Lesley, S. A., Wilson, I. A. and van Wezel, G. P. (2009) Structural and functional characterizations of SsgB, a conserved activator of developmental cell division in morphologically complex actinomycetes. *J Biol Chem* **284**: 25268-25279.

Yang, Y.-H., Song, E., Willemse, J., Park, S.-H., Kim, W.-S., Kim, E.-j., Lee, B.-R., Kim, J.-N., van Wezel, G. P. and Kim, B.-G. (2012) A novel function of *Streptomyces* integration host factor (sIHF) in the control of antibiotic production and sporulation in *Streptomyces coelicolor*. *Antonie Van Leeuwenhoek* **101**: 479-492.

Yokoyama, E., Doi, K., Kimura, M. and Ogata, S. (2001) Disruption of the *hup* gene encoding a histone-like protein HSl and detection of HSl2 of *Streptomyces lividans*. *Res Microbiol* **152**: 717-723.

Yu, X.-C., Weihe, E. K. and Margolin, W. (1998) Role of the C Terminus of FtsK in *Escherichia coli* chromosome segregation. *J Bacteriol* **180**: 6424-6428.

Zakrzewska-Czerwińska, J., Jakimowicz, D., Zawilak-Pawlik, A. and Messer, W. (2007) Regulation of the initiation of chromosomal replication in bacteria. *FEMS Microbiol Rev* **31**: 378-387.

CURRICULUM VITAE

Le Zhang was born on the 19th of December 1983 in Xi'an, China. In 2002, she graduated from affiliated middle school of Xi'an Electronic Science and Technology University in Shaanxi, China. Between 2002 and 2006 she studied at Northwest University in China, obtaining a Bachelor of Biotechnology. During 2007-2009 she studied at Wageningen University (the Netherlands), where she obtained a Master degree in Cellular/Molecular Biotechnology. In 2009, she completed an internship at Unilever R&D (Vlaardingen, the Netherlands) under the supervision of Dr. Gabriele Gross. In the autumn of 2009 she started as a PhD student at Leiden University, working in the Molecular Biotechnology group under the supervision of Prof. Dr. Gilles van Wezel. Here she performed studies on *Streptomyces* for identification and characterization of morphogenes. The work done as a PhD student is presented in this thesis. During this time, she attended a short-term study trip in the group of Prof. Dr. Yasuo Ohnishi at Tokyo University (Japan). She also participated two international conferences (4th ASM Conference in Montreal, Canada and ISBA17 in Aydin, Turkey) and presented her work there. Currently, she is continuing in the laboratory of Gilles van Wezel as a postdoctoral researcher, on the synthetic biology and genomics of antimicrobial peptides.